Development of a Thermostable Tuberculosis Vaccine Candidate Suitable for Pulmonary Delivery through Particle Engineering

by

Mellissa Gomez

A thesis submitted in partial fulfillment of the requirements for the degree of

Master of Science

Department of Mechanical Engineering
University of Alberta

Abstract

Tuberculosis (TB) is a preventable and curable highly infectious respiratory disease that is responsible for the deaths of approximately 1.5 million people every year. However, vaccination programs are hindered by refrigeration requirements for vaccines during transportation and storage. Additionally, research has shown that administration of vaccines via inhalation may be more effective at conferring protection against respiratory illnesses. A promising subunit TB vaccine candidate, ID93+GLA-SE, consisting of an antigen, ID93, and adjuvant system, GLA-SE, has been developed; however, the vaccine candidate is stable only under refrigeration. This thesis details how particle engineering via spray drying was implemented to convert ID93+GLA-SE into a thermostable, inhalable dry powder format suitable for global health applications.

First, ID93+GLA-SE was converted into a thermostable dry powder composed of many microparticles via spray drying. *In silico* modelling was used to develop an appropriate formulation and calculate spray drying processing parameters to effectively encapsulate and stabilize the vaccine nanoemulsion droplets within a trehalose matrix. A one-year stability study was conducted, with powders held at multiple temperatures up to 40 °C. Physical stability of the powder was assessed in terms of particle morphology, moisture content, and solid state. Vaccine chemical properties were assessed in terms of nanoemulsion droplet size, adjuvant system concentration, antigen presence, pH, and osmolality. Results showed that overall physical stability was maintained for all storage temperatures. Nanoemulsion droplet size, oil component of the adjuvant system, pH, and osmolality were within the preset stability criteria. Similarly, the antigen was shown to be present even after one year of storage at 40 °C. The agonist showed 17-25% and 56-58% loss after 13.5 months of storage at 25 and 40 °C, respectively; however, high temperature degradation results were comparable to a lyophilized presentation of the vaccine candidate.

Second, an inhalable presentation of the spray-dried vaccine was investigated. Leucine, pullulan, and trileucine were explored as dispersibility enhancing agents. Six inhalable candidates were designed and spray-dried. The aerosol performance results showed that the leucine- and trileucine-containing candidates improved aerosol performance (32% and 33-34% lung dose, respectively) as compared to a formulation without a dispersibility enhancer (18% lung dose). The pullulan-containing candidates did not improve the aerosol performance significantly (19-25% lung dose). Chemical analysis indicated that the leucine- and pullulan-containing formulations did not effectively preserve vaccine integrity. These results established trileucine as the lead dispersibility enhancing agent.

Third, the lead inhalable vaccine candidate containing trileucine was spray-dried and placed on a seven-month stability study at storage temperatures up to 50 °C. A trileucine-free version of the formulation was also spray-dried and included in the study for comparison. The physical stability of both powder formulations was assessed in terms of particle morphology, solid state, moisture content, and aerosol performance. Results showed that both spray-dried formulations maintained particle morphology, solid state, and moisture content for the duration of the stability study at all temperatures. However, aerosol performance for the trileucine-free vaccine powder decreased when it was stored at high temperatures. By comparison, the trileucine-containing formulation was shown to maintain aerosol performance even after high-temperature storage.

Finally, due to the overall success in spray drying the ID93+GLA-SE vaccine candidate, preclinical trials with mice were planned to assess immunogenicity and protective efficacy. The preclinical trials were designed to evaluate administration of the inhalable candidate through both the intranasal and pulmonary routes. The spray-dried inhalable vaccine was adapted to be suitable for inhalation by mice in order to complete these trials. Two formulations were developed, one

designed for deposition in the nose only, and the other designed for deposition in the nose and lungs. Characterization confirmed that the mouse-inhalable vaccine candidates retained key vaccine properties post-spray drying. An aerosol delivery system was also designed and characterized for use in the preclinical trials for both administration routes. Processing conditions were optimized such that approximately 10% and 44% of the maximum possible dose could be delivered, respectively. However, results showed that even with optimized parameters, the system would be unable to deliver the target powder dose without placing restrained mice under considerable stress. It is recommended that the antigen and agonist concentrations be increased to achieve target delivered dose.

Preface

The research detailed in this thesis was part of a research collaboration with the Infectious Disease Research Institute, led by Dr. Christopher Fox, with Professor Reinhard Vehring as the lead collaborator at the University of Alberta.

Chapter 2 of this thesis is a paper manuscript titled "Microparticle Encapsulation of Subunit Tuberculosis Vaccine Candidate containing Adjuvants via Spray Drying," submitted for publication under the authorship of Mellissa Gomez, Michelle Archer, David Barona, Hui Wang, Mani Ordoubadi, Shabab Bin Karim, Nicholas B. Carrigy, Zheng Wang, Joseph McCollum, Chris Press, Alana Gerhardt, Christopher B. Fox, Ryan M. Kramer, and Reinhard Vehring. I was responsible for experimental design, data collection, data analysis, and manuscript composition. Michelle Archer assisted with experimental design, data collection, and data analysis and contributed to manuscript edits. David Barona assisted with experimental design, provided advice during concept development, and contributed to manuscript edits. Hui Wang assisted with data collection, data analysis, and contributed to manuscript edits. Mani Ordoubadi assisted with concept development, experimental design, and contributed to manuscript edits. Shabab Bin Karim assisted with data collection, data analysis, and contributed to manuscript edits. Zheng Wang assisted with data collection, data analysis, and contributed to manuscript edits. Nicholas Carrigy assisted with concept development, experimental design, data collection, and contributed to manuscript edits. Joseph McCollum assisted with data collection, data analysis, and contributed to manuscript edits. Chris Press assisted with data collection, data analysis, and contributed to manuscript edits. Alana Gerhardt assisted with data collection, data analysis, and contributed to manuscript edits. Ryan Kramer and Christopher Fox were supervisory authors who were involved

with concept formation, discussion of results, and manuscript edits. Reinhard Vehring was the supervisory author at the University of Alberta and was involved in concept formation, discussion of results, and manuscript composition. Leanne Millburn assisted with preliminary data collection and Tony Phan assisted with material preparation. Larry Wolfraim contributed to manuscript edits.

Chapter 3 of this thesis is a paper manuscript titled "Formulation development for a spray-dried, inhalable tuberculosis vaccine," submitted for publication under the authorship of Mellissa Gomez, Joseph McCollum, Hui Wang, Mani Ordoubadi, Chester Jar, Nicholas B. Carrigy, David Barona, Isobel Tetreau, Michelle Archer, Alana Gerhardt, Chris Press, Ryan M. Kramer, Christopher B. Fox, and Reinhard Vehring. I was responsible for experimental design, data collection, data analysis, and manuscript composition. Joseph McCollum assisted with data collection, data analysis, and contributed to manuscript edits. Hui Wang assisted with concept development, experiment design, and contributed to manuscript edits. Mani Ordoubadi assisted with concept development, experiment design, data collection, and contributed to manuscript edits. Chester Jar assisted with data collection, data analysis and contributed to manuscript edits. Nicholas Carrigy assisted with concept development, experimental design, and contributed to manuscript edits. David Barona assisted with concept development and contributed to manuscript edits. Isobel Tetreau assisted with data analysis and contributed to manuscript edits. Michelle Archer assisted with concept development, data analysis, and contributed to manuscript edits. Chris Press assisted with data collection, data analysis, and contributed to manuscript edits. Alana Gerhardt assisted with data collection, data analysis, and contributed to manuscript edits. Ryan Kramer and Christopher Fox were supervisory authors who were involved with concept formation, discussion of results, and manuscript edits. Reinhard Vehring was the supervisory author at the University of Alberta and was involved in concept formation, discussion of results, and manuscript composition.

I was responsible for experiment design, data collection, data analysis, and chapter composition of the work detailed in Chapter 4. Shital Bachchhav assisted with data collection and data analysis. Isobel Tetreau assisted with data collection and data analysis. Reinhard Vehring was involved in concept formation and discussion of results.

For the work discussed in Chapter 5, I was responsible for apparatus design, experimental design, data collection, data analysis, and chapter composition. Hui Wang and David Barona assisted with apparatus design. Mani Ordoubadi provided advice on experimental design. Shital Bachchhav assisted with data collection. Nicholas Carrigy assisted with apparatus design, experimental design, data collection, and data analysis. Joe McCollum, Alana Gerhardt, and Chris Press assisted with data collection and data analysis. Philip Kuehl provided advice on apparatus design and experimental design. Ryan Kramer and Christopher Fox were supervisory authors who were involved with concept formation, and discussion of results. Reinhard Vehring was the supervisory author at the University of Alberta and was involved in concept formation and discussion of results. As this chapter focused on preparation for preclinical trials but did not actually include working with mice, no ethics approval was needed.

This work is dedicated to my loving parents, Joseph Gomez and Evelyn Gomez, and my dear brother, Jacob Gomez. Thank you for all your support throughout the years; this achievement is as much yours as it is mine.

Acknowledgments

This work could not have been accomplished without the help and guidance of many wonderful people. I would like to thank my supervisor, Professor Reinhard Vehring, for the opportunities and experiences I have been granted as a graduate student with his research group. I am truly grateful for his guidance and for the chance to learn from someone I admire greatly. To my brilliant colleagues, the other members of the Particle Engineering Group, thank you so much for your support and insight throughout the good, the bad, and the strange data. I have no doubt that each of you will change the world. To Luba Slabyj, thank you for all your hard work editing my writing from moderately legible to a manuscript that does the research justice. Finally, I would like to thank our collaborators at the Infectious Disease Research Institute. It has been my pleasure working on this worthwhile and challenging project with you all, and I hope the opportunity arises to work with you again.

The work detailed in this thesis was supported by federal funds from the National Institute of Allergy and Infectious Diseases, National Institutes of Health, Department of Health and Human Services, under Contract HHSN272201400041C.

Table of Contents

List of Tables

List of Figures

Chapter 1. Introduction

1.1. Overview of tuberculosis and intervention strategies

Pandemics caused by highly infectious respiratory illnesses are one of the greatest threats facing the modern world. The infectious disease tuberculosis (TB), caused by infection with *Mycobacterium tuberculosis*, is one such respiratory illness. An estimated 10 million people worldwide contracted TB in 2018, with approximately 1.2 million HIV-negative people dying of the disease (World Health Organization 2019). TB infections are concentrated in population-dense developing nations located in South-East Asia, Africa, and the Western Pacific. The disease is transmitted primarily through the air as droplets; thus, the primary site of infection is the lungs. Fortunately, treatment is available to combat TB infections.

Treatment of TB has been studied extensively. The current recommended treatment consists of four first-line drugs: isoniazid, rifampicin, ethambutol, and pyrazinamide. This relatively inexpensive treatment plan is six months long and has been reported by the World Health Organization (WHO) to have an 85% treatment success rate (World Health Organization 2019). Several drug treatment plans also exist for the treatment of latent TB infections. However, there has been a rise in the prevalence of rifampicin-resistant and multidrug-resistant strains of TB. In 2018, approximately half a million new cases of rifampicin-resistant or multidrug-resistant TB appeared (World Health Organization 2019). The treatment of these drug-resistant strains is significantly more costly and requires the use of second-line drugs that are more toxic. The treatment success of multi-drug resistant strains of TB is much lower, reportedly only 56% globally

(World Health Organization 2019). Therefore, prevention of disease progression via extensive vaccination is one of the best tools available to combat TB.

The bacille Calmette-Guerin (BCG) vaccine is the only approved TB vaccine available. However, despite widespread use, the BCG vaccine is not without significant drawbacks. The efficacy of BCG vaccine varies with geographical location, with lower effectiveness demonstrated in areas with a high occurrence of nontuberculous mycobacterium (Andersen and Doherty 2005, Brandt, et al. 2002). The BCG vaccine provides protection against TB for infants and children but does not effectively confer protection against TB for adolescents and adults. Additionally, studies have reported that the BCG vaccine is only effective for up to 20 years (Andersen and Doherty 2005), and the BCG vaccine does not prevent latent TB from becoming active (World Health Organization 2019). These issues with the BCG vaccine have decreased the effectiveness of the WHO's TB prevention strategy. To this end, many alternative vaccines are being developed to act as a booster or eventual replacement for the BCG vaccine. One such vaccine candidate is an adjuvanted subunit vaccine developed by the Infectious Disease Research Institute.

The vaccine candidate ID93+GLA-SE is formulated as a subunit vaccine consisting of an antigen, ID93, and an adjuvant system, GLA-SE. The adjuvant system is formulated as a nanoemulsion, in which squalene comprises the oil component and is stabilized in nanodroplets of approximately 90 nm in diameter using DMPC as an emulsifier, with a synthetic TLR4 agonist, GLA, present at the oil-water interface. The vaccine candidate did not induce any adverse systemic reactions when administered to humans (Penn-Nicholson, et al. 2018). A Phase I clinical trial demonstrated the necessity of the complex GLA-SE adjuvant system as higher immune responses were generated when it was administered with the ID93 antigen as compared to ID93 alone (Coler, Day, et al.

2018). Subunit vaccines are generally safer than live attenuated vaccines, such as the BCG vaccine, as subunit vaccines rely on the detection of bacterium proteins rather than on a self-replicating mechanism to induce immunity. Additionally, a study reported that vaccination with a subunit vaccine conferred a similar level of protection against TB challenge in both naïve mice and mice exposed to nontuberculous mycobacteria, whereas the BCG vaccine was unable to induce significant protection against TB challenge in the latter mouse population (Brandt, et al. 2002). The vaccine candidate ID93+GLA-SE has shown promising results; however, like most liquid vaccines, the formulation needs to be kept refrigerated in order to maintain its efficacy.

The required refrigeration during transportation and storage is commonly referred to as the "cold chain". However, maintaining the cold chain throughout distribution is not feasible in countries with unstable or limited electrical and transportation infrastructure. Thus, the cold chain requirement limits the accessibility of vital vaccines. Overall vaccine wastage has been reported by the WHO to be approximately 50% globally (World Health Organization 2005) and exposure to heat or freezing contributes to this wastage. In addition to improving accessibility of a given vaccine, improved thermostability can reduce resource burden and thus improve accessibility of temperature-sensitive vaccines. Modelling of six vaccines in Niger's vaccine supply chain showed that making even just one vaccine thermostable improved accessibility of all vaccines due to alleviation of supply chain bottlenecks and reduced use of temperature-controlled storage and transportation resources (Lee, Cakouros, et al. 2012). Similarly, modelling of a vaccine supply chain found that the cost of replacing the current BCG vaccine with a thermostable version was cost-effective in terms of medical costs and productivity losses averted, even when the vaccine

price was increased three-fold (Lee, Wedlock, et al. 2017). One method of improving thermostability of a liquid product is through stabilizing the formulation in a dry powder form.

1.2. Spray drying as a method of encapsulating complex formulations

Methods of desiccation to convert a liquid into a dry product include lyophilization – commonly known as freeze drying, spray drying, spray freeze drying, and foam drying (Chen, et al. 2016, Shetty, Cipolla, et al. 2020). Lyophilization is performed by adding stabilizing excipients to the formulation and subsequently freezing the liquid formulation. The frozen liquid is then sublimed out, leaving a dry 'cake'. Lyophilization has been widely used for stabilization of formulations for eventual reconstitution and subsequent parenteral administration (Chen, et al. 2016). As the process results in a lyophilized cake, the product must undergo secondary processing if the intent is to produce an inhalable product. Lyophilization has been used to address vaccine wastage by conferring stability on vaccines such as the oral polio vaccine, BCG vaccine, and measles vaccine, to name a few, so that they can be exposed to freezing temperatures (World Health Organization 2005, World Health Organization (WHO) 2006). However, many vaccines are considered "freeze-sensitive" and cannot be frozen (World Health Organization (WHO) 2006). An alternative to lyophilization that does not require freezing of the formulation is spray drying. Spray drying is a desiccation method that consists of atomizing the liquid formulation into a drying gas medium which dries the droplets into a dry powder composed of many particles. These particles are then separated from the flow for collection. Spray drying is a method commonly used to produce powders suitable for inhalation (Shetty, Cipolla, et al. 2020). Spray freeze drying is a method that involves aspects of both the spray drying and lyophilization processes. The spray freeze-drying process involves the atomization of a liquid formulation into a cryogenic medium, forming frozen

droplets. These frozen droplets are then sublimed in order to remove the ice, leaving behind porous particles (Chen, et al. 2016). This method is useful for forming inhalable powders from heat-sensitive formulations. Foam drying consists of boiling the liquid formulation under reduced pressure and then rapidly evaporating the water in order to leave a solid foam structure. Lyophilization (Lovalenti, et al. 2016), spray freeze drying (Murugappan, et al. 2013), and foam drying (Lovalenti, et al. 2016, Ohtake, Martin, et al. 2011) have all been previously investigated as methods to convert liquid vaccines into a dry product.

Previous work has been done to develop a lyophilized version of the ID93+GLA-SE vaccine candidate. The lead lyophilized vaccine candidate was stabilized using a trehalose and tris excipient system, with less than 10% antigen and agonist loss after three months (Kramer, et al. 2018). The lead candidate was also shown to induce some antibody responses in mice after storage at 50 °C for three months. Due to this success in lyophilizing the vaccine candidate, spray drying was assessed as an alternative method of desiccation. Spray drying was chosen because it is potentially a more cost-effective method of conferring thermostability.

As discussed in Chapter 2, spray drying of emulsions has been conducted primarily for preservation in the food industry. A key consideration with spray drying of emulsions is the prevention of the emulsion droplets from evaporating during the spray drying process. Another important consideration is ensuring that the emulsion droplets are encapsulated within the particles rather than accumulating on the particle surface. Surface oil is likely to degrade more quickly than encapsulated oil and may contribute to particle fusing. Multiple factors, such as choice of encapsulating material, temperature, and feed concentration, are important to increasing encapsulation efficiency (Arpagaus, et al. 2018). In addition to high encapsulation efficiency, the

dispersed phase diameter of vaccines formulated as emulsions must be preserved in order to be recognized by antigen-presenting cells (Kunda, et al. 2015). Fusing of emulsion droplets into large diameter droplets increases the risk of embolisms when parenterally injected (Koster, et al. 1996). There has been some success in recent years in spray drying of vaccines formulated as emulsions. Table 1 lists several studies investigating spray drying of dispersion-based vaccines.

Table 1 List of recent studies on spray drying vaccines formulated as dispersions

Disease	Vaccine	Excipient System	Reference
Vesicular stomatitis virus, Influenza, Adenovirus	VSVGFP, Influenza mNeon, AdHu5GFP	Mixtures of trehalose, mannitol, dextran, and lactose	(Toniolo, et al. 2019)
Whooping cough	OmPV	Trehalose	(Kanojia, Raeven, et al. 2018)
Tuberculosis	H56/CAF01	Trehalose	(Thakur, et al. 2018)
Pneumonia	PspA4Pro	Leucine	(Kunda, et al. 2015)
Influenza	A/PR8/34	Trehalose	(Kanojia, Willems, et al. 2016)

1.3. Stabilization through modification of operating parameters and formulations

Conferment of spray-dried powder stability can be achieved by modifying processing parameters as well as the formulation composition (Shetty, Cipolla, et al. 2020). Calculation of the appropriate processing parameters is a crucial step to achieving a successful spray-dried product and requires careful consideration of the formulation structure. For instance, high temperatures and atomization can lead to degradation of heat-sensitive and shear-sensitive components. The process should be designed such that the biologic is kept away from the air-water interface. Exposure to the drying air can lead to heat-related degradation; however, the droplet temperature is much lower than the drying temperature. Additionally, it is critical to keep the biological components away from the surface of the dried particle. Exposure at the particle surface indicates that the biologic is not safely encapsulated within the particle and is instead exposed to the environment. As well, it has been found that the mobility near the surface of amorphous materials is higher than the bulk mobility (Yu 2016). Therefore, increased stability is expected when the biologic is kept from the particle

surface. Component distribution can be predicted using material engineering models. Models can also be used to calculate appropriate processing parameters to reduce residual moisture content within the powders. Excess moisture can lead to physical and chemical instability as well as degradation of aerosol performance (Chen, et al. 2016).

In order to achieve long-term stability of the vaccine candidate, the antigen, ID93, the agonist, GLA, and the nanoemulsion, GLA-SE, must all be stabilized. ID93 is a protein, GLA is a synthetic lipid, and the adjuvant system's membrane is composed primarily of the phospholipid DMPC. As will be further discussed in Chapter 2, the non-reducing disaccharide trehalose was chosen as the main stabilizing excipient. Trehalose is an attractive stabilizer for several reasons: trehalose has a high glass transition temperature (T_g) of approximately 110 °C when dry (Chen, Fowler and Toner 2000), low toxicity (Richards, et al. 2002), high solubility (Lammert, Schmidt and Day 1998), and great effectiveness as a glass stabilizer of both proteins (Richards, et al. 2002) and phospholipid membranes (Lambruschini, et al. 2000, Pereira and Hunenberger 2006).

There are two main theories regarding stabilization of both proteins and phospholipid membranes: water replacement theory and vitrification theory. Water replacement theory suggests that hydrogen bonds formed by the lipid membrane or protein with water in a solution are replaced during drying with hydrogen bonds formed with the hydroxyl group of the stabilizer. The replacement of hydrogen bonds preserves the native conformation and thus prevents changes in structure. This replacement is especially critical for proteins as non-native proteins are more likely to undergo noncovalent aggregation than are native proteins (Roberts 2006). Vitrification theory suggests that the protein or lipid structure is immobilized within a rigid, amorphous matrix. Entrapment reduces molecular mobility of the protein and the lipid structures. This fact is

especially crucial for stabilization of proteins as reducing molecular mobility slows down degradation mechanisms such as denaturation. Vitrification also creates a barrier between adjacent lipid membranes, preventing fusion due to trehalose acting as an obstacle between membranes. These mechanisms are not mutually exclusive, though it is not simple to determine which plays a stronger role. Further discussion on water replacement theory and vitrification theory can be found elsewhere (Mensink, et al. 2017, Grasmeijer, et al. 2013, Carrigy and Vehring, Engineering stable spray-dried biologic powder for inhalation 2019).

Another key mechanism in the stabilization of phospholipid membranes is the depression of the phase transition temperature (T_m) (Ingvarsson, Yang, et al. 2011, Pereira and Hunenberger 2006). At temperatures below the T_m, the phospholipid membrane is predominantly in the gel state, where the hydrocarbon chains are aligned nearly perpendicular to the layer and fully extended, leading to closely ordered packing (Eze 1991). At temperatures above the T_m, the phospholipids exist predominantly in the liquid crystalline state, where the hydrocarbon chains are mobile. Typically, T_m of a lipid dried without a stabilizer is much higher than the T_m when fully hydrated. Therefore, stabilizers are required to prevent increase in T_m and the subsequent phase transition of the membrane during the dehydration and rehydration process. However, the presence of other molecules in the membrane can affect T_m. Trehalose has been shown to depress the T_m of phospholipids during dehydration, thus maintaining the liquid crystalline phase of the membrane even on rehydration (Crowe, Carpenter and Crowe, The role of vitrification in anhydrobiosis 1998). Phospholipid phase change has been shown to lead to membrane destabilization on rehydration (Crowe, Hoekstra and Crowe, Membrane phase transitions are responsible for imbibitional damage in dry pollen 1989).

Trehalose is an especially effective glass stabilizer due to its small size, high T_g, and lack of reducing groups. The molecular weight of sugars has an effect on the ability of the sugar to stabilize proteins, as the smaller the sugar, the closer the sugar can pack together to match to the complex shape of a given protein (Tonnis, et al. 2015). As well, it was found that smaller sugars are able to form more hydrogen bonds with a protein. The improved ability to form hydrogen bonds is related to the size of the sugars as smaller molecules are less affected by steric hindrance. A high T_g is beneficial as both the water replacement and vitrification mechanisms of stabilization are reliant on the stabilizing excipient maintaining an amorphous solid state. At temperatures above the T_g, the glass material properties undergo a reversible change from brittle properties to rubber-like properties. Change from a rigid matrix to a rubbery state affects the ability of the sugar to immobilize the encapsulated components. Additionally, at temperatures above T_g, the material may begin crystallizing. Formation of crystals can induce shear stresses on the encapsulated components and causes the loss of hydrogen bonds with the components. The loss of interaction negatively impacts the preservation of protein and lipid membrane structure. Another benefit of using trehalose is that, as a non-reducing sugar, Maillard Browning is avoided. Maillard Browning is a cascade of reactions that occurs between a protein and the aldehyde or ketone group of a reducing sugar and leads to covalent aggregation and thus chemical degradation (Mensink, et al. 2017). As well, trehalose has been found to provide strong stabilization of spray-dried liposomes due to its ability to form stronger hydrogen bonds than other sugars (Toniolo, et al. 2019).

1.4. Particle engineering to make inhalable delivery an accessible route of administration

Direct delivery to the lungs may induce greater immunity against respiratory illnesses as the local immune response is generated at the primary site of infection. Common aerosol pulmonary

delivery devices include nebulizers, metered dose inhalers, and dry powder inhalers (DPI). Nebulizers convert a liquid product into a fine mist that can be inhaled. One benefit of this device is that it can be used by any age group because it relies on passive inhalation (Geller 2005). Metered dose inhalers contain a pressurized formulation wherein the pharmaceutical is suspended within propellent. Administration requires actuation of the device while inhaling. These devices are small and portable; however, the required coordination renders administration difficult (Geller 2005). Additionally, the propellants used within these devices may be contributing to climate change. DPIs contain dry powder within a capsule. On actuation the capsule is opened, and powder is dispersed into the lungs through patient inspiration. Several advantages of DPIs are the lack of propellent, ease of handling, high portability, and high potential for storage stability (Chen, et al. 2016). However, as the powder delivery is reliant on a high inspiration rate to disperse the powders, this device is not recommended for infants and those with poor lung function.

Dry powders must have certain characteristics to be suitable for inhalable delivery. For instance, the powder must be able to deposit in the lung. There are several factors affecting deposition, including airway geometry, particle size, and inhalation rate (Darquenne 2012). The powder must also be able to be dispersed; otherwise the powder may deposit in the extrathoracic region. Therefore, two key characteristics for inhalable powders are appropriate particle size and reduced cohesiveness of the powder. Both of these can be conferred through particle engineering through modification of the formulation and processing parameters. One method to reduce powder cohesiveness is to add dispersibility enhancing agents. These agents can reduce the powder cohesiveness through a variety of mechanisms, which are discussed in greater detail in Chapter 3. Additionally, the presence of another component, such as a dispersibility enhancing agent, on the

surface of particles acts to keep the biologic away from the surface. These surface-enriched components also function as a particle "coating". Since surface diffusion of amorphous solids is much higher than the bulk diffusion, surface coating can improve stability (Yu 2016). However, these agents are only effective if they accumulate on the surface. Particle engineering techniques can be used to predict the required mass fraction and processing parameters that will lead to surface accumulation of the agent.

1.5. Evaluation of vaccine efficacy through animal models

Preclinical trials must be completed to assess viability of a pharmaceutical product. These trials are carried out on animal models in order to assess safety, immunogenicity, and protective efficacy of the formulation. Both immunogenicity and protective efficacy tests may be necessary to properly assess the potential of a drug product. Animal immunogenicity experiments involving comparison of BCG administration through either parenteral injection or inhalation found that the latter route induced a lower overall immune response; however, the protective efficacy tests found that administration via inhalation conferred greater protection against a TB challenge (Verreck, et al. 2017). Types of animal models commonly used for TB preclinical trials include mice, guinea pigs, and non-human primates. Mice are useful for initial trials due to their small size, quick growth time and availability. Guinea pigs are larger than mice; however, they are especially useful for TB research as their immune response to TB infection includes the formation of granulomas to contain the bacteria, much like the human immune response does. Non-human primates offer the best approximation of human immune system response; however, trials employing them are significantly more expensive to conduct than trials using rodent models.

As discussed in Chapter 5, there are several methods of delivering a dry powder aerosol to mice, including insufflation, whole body exposure, and nose-only exposure. The last of these provides the best approximation of airway deposition through passive inhalation while minimizing product losses. Commercial nose-only exposure systems and aerosol generators for preclinical animal models exist; however, these products are very costly. Custom aerosol delivery systems can be designed instead for laboratory experiments. However, due to the obvious differences in physiology, formulations designed for human inhalation must be modified to be suitable for respiratory delivery to mice. Additionally, the aerosol delivery system must be characterized to optimize the dosing efficiency to mice while ensuring that the mice are not placed under excessive stress during aerosol dosing due to intolerable aerosol concentration or long exposure times.

This thesis investigates the stabilization of the TB vaccine candidate ID93+GLA-SE in a dry powder suitable for either reconstitution or inhalable delivery via spray drying. Production of a thermostable format and the development of an inhalable route of delivery improves the accessibility of a formulation. Both these goals were targeted with the intent of reducing global TB incidence rates. The work presented also includes the design of a dry powder presentation and an aerosol delivery system suitable for preclinical mouse studies on the spray-dried ID93+GLA-SE vaccine candidate. This thesis presents work that has been prepared for publication and additional work that has yet to be published.

Chapter 2. Microparticle encapsulation of subunit tuberculosis vaccine candidate containing nanoemulsion adjuvants via spray drying

2.1. Introduction

An important aspect of disease control is intervention by inducing widespread protective immunity through vaccination. Liquid pharmaceutical formulations, such as vaccines, usually must be kept refrigerated during transportation and storage in order to maintain their efficacy. Widespread global immunization is limited because vaccines often require refrigeration to remain effective (World Health Organization (WHO) 2006). Exposure to higher temperatures can lead to loss of efficacy of the active pharmaceutical ingredient and the possible formation of unsafe byproducts. Eliminating the refrigeration requirement would facilitate greater global distribution through cost reduction of storage and transportation. This would be especially beneficial towards interventions for diseases that are prevalent in population-dense locations that lack the required infrastructure to maintain refrigeration. Thermostability can be improved by converting a liquid product into a dry form that can be rehydrated for administration as needed. Desiccation processing methods, such as spray drying, have been widely used in the food processing, chemical, and pharmaceutical industries to preserve temperature-sensitive components (Carrigy and Vehring 2019). Spray drying produces a dry powder made up of microparticles through the drying of atomized droplets via a drying gas. Once the solvent has evaporated, the dried particles are separated from the drying gas, e.g. via a cyclone.

Thermostability of vaccines can be improved by stabilization via spray drying. Experimental dry powder vaccines have been developed for the intervention of measles (Argarkhedkar, et al. 2014),

influenza (Sou, et al. 2015, Kanojia, Willems, et al. 2016, Toniolo, et al. 2019, Zhu, et al. 2014), anthrax (Jones, et al. 2017), herpes (LeClair, et al. 2019), whooping cough (Kanojia, Raeven, et al. 2018), and tuberculosis (Jin, et al. 2010, Thakur, et al. 2018). The immunogenicity of spray-dried vaccines can be maintained provided an appropriate stabilizing system and drying conditions are used. Successfully stabilized dry powder vaccines have been reported to elicit similar immunogenicity profiles as their liquid counterparts after reconstitution when administered in animal models (Argarkhedkar, et al. 2014, Sou, et al. 2015, Zhu, et al. 2014, Kanojia, Raeven, et al. 2018). Ideally, a simple formulation is used to improve stability, however, multiple stabilizers may be required for biologics that are difficult to stabilize (Carrigy, Liang, et al. 2019).

A disease whose eradication would be greatly advanced with the existence of a thermostable vaccine is tuberculosis (TB). The World Health Organization has noted that TB is the leading cause of death from a single infectious agent, having caused an estimated 1.5 million deaths in 2018. Approximately 1 in 4 people globally is infected with latent TB, wherein the immune response has not eliminated the pathogen and instead has contained it within granulomas (Flynn and Chan 2001). Ten percent of those with latent TB are expected to develop active TB within their lifetime (World Health Organization 2019, World Health Organization 2018). There is currently no vaccine that is fully effective in preventing either TB incidence or latent TB becoming active in adults (World Health Organization 2019). Due to these significant drawbacks to the current intervention strategy, an alternative TB vaccine must be developed. The WHO has explicitly noted that new TB vaccines must improve upon the current BCG vaccine with demonstrated efficacy in adolescent and adult subjects with and without latent tuberculosis, and must be safe for all subjects, including those with suppressed immune systems (World Health

Organization 2018). Subunit vaccines typically have better safety profiles than live attenuated vaccines; however, they often do not elicit strong immune responses on their own. Thus, if administered via parenteral injection, an adjuvant may be required to stimulate a robust immune response (Reed, et al. 2009).

A vaccine candidate under development by the Infectious Disease Research Institute, ID93+GLA-SE, is a subunit TB vaccine based on a recombinant protein, ID93, and a nanoemulsion adjuvant system, GLA-SE. ID93 is composed of four *Mycobacterium tuberculosis* genes, Rv3619, Rv1813, Rv3620, and Rv2608, all associated with virulence or latency. These antigens were chosen on the basis of a comprehensive study identifying which antigens stimulate a strong cell mediated immune response (Bertholet, Ireton and Kahn, et al. 2008). The adjuvant system is formulated as a nanoemulsion and is comprised of glucopyranosyl lipid A (GLA), a synthetic Toll-like receptor 4 agonist, and a squalene oil-in-water stable emulsion (SE). Development and characterization of the GLA-SE system is discussed elsewhere (Coler, Bertholet, et al. 2011). The ID93+GLA-SE vaccine candidate has shown promising preclinical and clinical results. Preclinical trials in mice, guinea pigs and nonhuman primates showed that administration of ID93+GLA-SE induced antigen-specific T-cell immune responses and significantly reduced viable bacteria in the lung after challenge with both TB and a multi-drug resistant strain of TB (Bertholet, Ireton and Ordway, et al. 2010), and clinical testing has confirmed the benefit of GLA-SE in enhancing antigen-specific immune responses (Coler, Day, et al. 2018). The current adjuvanted ID93 vaccine candidate has been administered in clinical studies in a two-vial system consisting of rehydrated lyophilized ID93 and the liquid adjuvant, which are mixed prior to administration (Kramer, et al. 2018). The two-vial presentation is designed for short-term stability to support point-of-care

mixing and immunization. However, a single vial presentation with long-term thermostability would require a different approach since a liquid ID93+GLA-SE sample experienced greater than 50% decrease in GLA concentration when stored at 25 °C for three months (Orr, Kramer, et al. 2014).

To improve thermal stability, a liquid product may be converted into a dry version through processing methods such as lyophilization or spray drying. Lyophilization, also known as freeze-drying, removes water by freezing the product and then removing the ice through sublimation, leaving behind a dry 'cake'. A previous study investigated lyophilization of the ID93+GLA-SE vaccine in a single vial as a method of improving thermal stability (Orr, Kramer, et al. 2014). Reconstitution of the lyophilized vaccine showed that physicochemical characteristics, such as ID93 and GLA integrity, were maintained. Further formulation development led to several lyophilized vaccine candidates (Kramer, et al. 2018), which were stable after three months' storage at 37 °C and still elicited immune response in mice after storage at 50 °C for three months. The best-performing candidate utilized a trehalose-Tris excipient system to stabilize the vaccine (Kramer, et al. 2018) and is currently undergoing a Phase I clinical trial (Infectious Disease Research Institute 2019). Success in lyophilization of the ID93+GLA-SE vaccine led to consideration of spray drying as an alternative technique to produce a dry vaccine product. Spray drying is more cost-effective than lyophilization as it is a faster, more scalable process with reduced operation and installation costs (Schwartzbach 2011, Kanojia, ten Have, et al. 2017). Nevertheless, there are technical difficulties associated with spray drying the ID93+GLA-SE formulation. One challenge is due to the structure of the ID93+GLA-SE vaccine as a nanoemulsion with a phospholipid emulsifier. Its emulsion droplets must be encapsulated with high efficiency

within particles during the spray drying. Another challenge is to stabilize both the ID93 and GLA-SE active components of the vaccine within the dry powder for long-term room temperature stability. Both challenges must be overcome to produce a successful spray-dried vaccine powder.

Stabilization requires an appropriate stabilizer and optimal spray drying conditions to ensure that desiccation does not lead to losses or changes in vaccine component structure. There has been successful stabilization via spray drying of vaccines formulated as dispersions. Enveloped viral vector vaccines (Toniolo, et al. 2019), an outer membrane vesicle vaccine (Kanojia, Raeven, et al. 2018), and a subunit vaccine consisting of an antigen and liposomal adjuvant system (Thakur, et al. 2018) have all been stabilized through spray drying with the disaccharide trehalose as an excipient. Trehalose acted as a glass stabilizer to stabilize both the protein and lipid components of the vaccines in order to create a successful dry powder product. Trehalose is a commonly used glass stabilizer due to its high glass transition temperature, high solubility (Lammert, Schmidt and Day 1998), low toxicity (Richards, et al. 2002), and ability to act as both a protein (Grasmeijer, et al. 2013) and liposome (Ingvarsson, Yang, et al. 2011) stabilizer during spray drying. The glass transition temperature (T_g) can be defined as the temperature at which the brittle properties of an amorphous material undergo a reversible change to more rubber-like ones. Glass stabilizers are hypothesized to physically stabilize proteins during drying and storage through two main mechanisms: water replacement and vitrification (Carrigy and Vehring 2019, Grasmeijer, et al. 2013, Ohtake and Wang 2011, Tonnis, et al. 2015). Water replacement theory states that biologic structure is maintained in water through hydrogen bonding. During drying, the hydrogen bonds between the water and the biologic are replaced by hydrogen bonds with the glass stabilizer. To inhibit protein denaturing, the glass stabilizer must be capable of forming many hydrogen bonds

and maintain an amorphous state in order to match the biologic structure (Carrigy and Vehring 2019, Grasmeijer, et al. 2013). Vitrification theory states that the biologic is rendered immobile within a glassy matrix (Carrigy and Vehring, Engineering stable spray-dried biologic powder for inhalation 2019, Grasmeijer, et al. 2013). Protein stability is largely dependent on the molecular mobility of the stabilizer at temperatures near the glass transition temperature (Carrigy and Vehring 2019, Grasmeijer, et al. 2013). It has been reported that glass stabilizers also stabilize the phospholipid layer of liposomes through both the water replacement and vitrification mechanisms (Ingvarsson, Yang, et al. 2011). The hydrogen bond replacement occurs between the stabilizer's hydroxyl groups and the phosphate groups of the liposomes' lipid head groups (Ingvarsson, Yang, et al. 2011). As with the stabilization of proteins, it is critical that the stabilizer be amorphous such that the hydroxyl groups are able to orient themselves into the required bond with the lipid head group without changing the liposome structure. Trehalose is reported to be an effective stabilizer for phospholipid membranes as it forms stronger hydrogen bonds with phosphate groups than other stabilizers, such as mannitol (Toniolo, et al. 2019). Vitrification stabilizes the liposomes by rendering them immobile and by creating a barrier between adjacent liposomes, thus inhibiting liposome fusion (Ingvarsson, Yang, et al. 2011).

In this paper, we stabilize the tuberculosis subunit vaccine ID93+GLA-SE via spray drying using trehalose as a stabilizer. A successful spray-dried ID93+GLA-SE product must stabilize the ID93 protein and GLA long-term as well as encapsulate the GLA-SE nanoemulsion droplets with high efficiency. An *in-silico* engineering approach was used to calculate spray drying process parameters based on material properties to minimize vaccine component losses. The resulting

powder was placed on stability study at various temperatures for a year and analyzed to assess both the physical stability of the powder and the chemical stability of the vaccine components.

2.2. Materials and Methods

2.2.1. Materials

Trehalose dihydrate (CAS 6138-23-4; Fisher Scientific Ottawa, ON, Canada) with a purity of 98% was used as the excipient for spray drying. Tris(hydroxymethyl)aminomethane (Tris) (CAS 77-86-1; Sigma Aldrich, Oakville, ON, Canada) and hydrochloric acid (CAS 7647-01-0; Sigma Aldrich, Oakville, ON, Canada) were used as a buffer system. Formulations were made with HPLC grade water (CAS 7732-18-5; Fisher Scientific Ottawa, ON, Canada).

The ID93 antigen and GLA-SE adjuvant components of the vaccine were produced separately. The construction, expression, and purification of the ID93 recombinant fusion protein has been described previously (Bertholet, Ireton and Ordway, et al. 2010). Briefly, ID93 was expressed in *E. coli*, purified under denaturing conditions by chromatography, and analyzed by SDS-PAGE. ID93 protein was stored in aliquots of 1.2 mg/mL at -80 °C prior to use. GLA-SE was formulated with squalene droplets and dimyristoyl-sn-glycero-3-phosphocholine (DMPC) as an emulsifier. Manufacture of the GLA-SE generally followed the same procedure as described in Orr et al. (Orr, Kramer, et al. 2014), except that the oil phase in the present work included the addition of α-tocopherol (0.05% w/v) and glycerol and buffer were omitted from the aqueous phase. GLA-SE nanoemulsions with a squalene concentration of 10% v/v and GLA concentration of 50 µg/mL were stored in a refrigerator prior to use. The initial emulsion droplet size was determined to be 90.6 nm in diameter, with a polydispersity index of 0.06.

Two formulations were prepared for spray drying: an adjuvant system-only formulation and a formulation containing both the antigen and adjuvant system. The former will hereafter be referred to as spray-dried trehalose+GLA-SE (SD-TG) and the latter as spray-dried trehalose+GLA-SE+ID93 (SD-TGI). The adjuvant system-only formulation was investigated for applications where different antigens can be added to the dose after reconstitution of the adjuvant system. The feedstock was prepared by first dissolving trehalose to 200 mg/mL and Tris to 40 mM in HPLC grade water. This solution was then pH adjusted to a pH of 7.5±0.1 using hydrochloric acid. A separate solution of GLA-SE or GLA-SE+ID93 was diluted with water to twice the working concentration (4% [v/v] squalene, 20 µg/mL GLA; 8 µg/mL ID93). The trehalose-Tris solution and the nanoemulsion were then mixed in a 1:1 ratio such that the final concentrations, summarized in Table 2, were achieved. A lyophilized vaccine candidate of ID93+GLA-SE was established in prior stabilization work and used in this study for comparison (Kramer, et al. 2018). It utilized an excipient combination of 10% trehalose (w/v) and 20 mM Tris buffered to a pH of 7.5.

Table 2 Final concentration of the main components in the adjuvant-only SD-TG and antigen-containing SD-TGI feedstock formulations

Component	Feedstock Concentration	
	SD-TG	**SD-TGI**
Trehalose	100 mg/mL	100 mg/mL
Tris (buffer)	2.42 mg/mL (20 mM)	2.42 mg/mL (20 mM)
Squalene	17.2 mg/mL	17.2 mg/mL
GLA	10 µg/mL	10 µg/mL
ID93	-	4 µg/mL

2.2.2. Theory

Particle Design

Use of a glass stabilizer is required to stabilize both the ID93 protein and the GLA-SE nanoemulsion droplets. Trehalose was chosen as the glass stabilizing excipient for this study due to its relatively high T_g and demonstrated ability to stabilize spray-dried proteins and lipid-based dispersions. A relatively high solute concentration (100 mg/mL) of the excipient was chosen. Increasing the solids content increases the generated particle size. Larger particles have a lower surface-to-volume ratio, which increases the probability for nanoemulsion droplets to be embedded within the particle. This is because a lower surface area will decrease availability for the droplets to accumulate on the surface. Increased encapsulating agent concentration supports an earlier shell formation (Wang, Che, et al. 2015), thus trapping the nanoemulsion droplets within the interior of the forming particle. Additionally, Carrigy et al. (Carrigy, Liang, et al. 2019) previously demonstrated that spray drying 100 mg/mL trehalose concentration provided better stabilization to phages than 20 mg/mL trehalose.

An amorphous solid phase is desired in order to promote stabilization of the antigen, agonist, and phospholipid membrane of the adjuvant system. Studies on the lyophilization of the GLA-SE vaccine have shown that crystalline lyophilisate increased GLA-SE emulsion droplet size after reconstitution (Kramer, et al. 2018). Amorphous trehalose microparticles can be designed to be stable for storage at a specific temperature by ensuring low molecular mobility. With a low molecular mobility, the amorphous structure will maintain its shape as a brittle glass. The molecular mobility of these materials is a function of the storage temperature (Zhou, et al. 2000). Storage at or below the Kauzmann temperature—that is, the temperature at which the molecular

mobility is insignificant—maximizes physical stability. The Kauzmann temperature is approximately 50 K below the glass transition temperature, T_g, for pharmaceutical powders (Hoe, et al. 2014). The success criteria for the lyophilized formulation was long-term stability at 37 °C. Hence, the T_g of the spray-dried powder must be ≥ 88 °C. As described by the Gordon-Taylor equation (Gordon and Taylor 1952), T_g for sugar-water mixtures can be determined based on their mass fractions and an empirical parameter k. Chen et al. (Chen, Fowler and Toner 2000) modelled the trehalose-water glass transition curve as a function of powder moisture content by fitting literature data to the Gordon-Taylor equation. For low water content systems, a k of 5.9 was determined based on a trehalose T_g of 387.1 K (Chen, Fowler and Toner 2000, Crowe, Reid and Crowe 1996) and a water T_g of ~138 K (Chen, Fowler and Toner 2000). For a spray-dried powder with a T_g greater than or equal to 88 °C, the moisture content of the spray-dried trehalose powder must not exceed 2-3%. The moisture sorption isotherm of trehalose indicates that subjecting trehalose powder to 10% relative humidity (RH) leads to an approximate 2-3% moisture content (Iglesias, Chirife and Buera 1999, Roe and Labuza 2005). Therefore, in order to obtain a T_g greater than or equal to 88 °C, the relative humidity at the collection point of the spray dryer must be less than 10%. Additionally, some level of moisture content may be necessary for protein stability as over-drying may lead to increased degradation (Mensink, et al. 2017).

Another critical processing parameter is the spray dryer outlet temperature. This must be much lower than the T_g to prevent powder adhesion to the dryer surfaces and crystallization of the resulting powder. Furthermore, a relatively low inlet drying gas temperature of 65 °C was chosen in order to prevent possible evaporation of the nanoemulsion droplets during the spray drying process and the deactivation of GLA and ID93. Experiments involving twin fluid atomizers to

spray dry oil-in-water emulsions reported that a high air-liquid-ratio will decrease the emulsion size distribution (Munoz-Ibanez, et al. 2015). An air-liquid ratio of 8 was selected in order to minimize any changes to the emulsion droplet structure during the atomization step of spray drying.

Particle Formation and Structure

The encapsulation of very small particles or droplets within a protective material via spray drying has been summarized elsewhere (Arpagaus, et al. 2018). This process, known as microencapsulation or nanoencapsulation via spray drying, has been studied for the main uses of protecting the encapsulated product from the surrounding environment, encapsulating a toxic product, or controlling the rate of release of the encapsulated product. Spray drying has been shown to successfully encapsulate food ingredients (Encina, Vergara, et al. 2016, Sarkar, et al. 2016, Pang, et al. 2017) as well as lipid-based drug delivery systems (Re 2006) as dry emulsions. Briefly, oil-in-water emulsions can be spray-dried to produce a powder containing the encapsulated droplets. The properties of these particles are dependent on the processing parameters, as well as on the properties of both the encapsulated ingredient and the encapsulating agent. The resulting particles can be spherical or irregular, and the droplets can be encapsulated as singular droplets or as multiple droplets embedded in a continuous matrix of the encapsulating agent (Arpagaus, et al. 2018).

Wang et al. (Wang, Che, et al. 2015) investigated the particle surface formation mechanics of algae oil containing emulsion droplets drying on a glass filament. The study summarized the drying process of emulsions into three stages. The first stage consisted of constant-rate drying before initial particle shell formation where the emulsion droplets are evenly distributed through the

aqueous phase. The second phase consisted of the initial shell formation where a soft outer layer forms due to saturation of the components on the droplet surface. The final stage was defined as the thickening of the fully formed shell. These stages summarized Wang et al.'s (Wang, Che, et al. 2015) findings on the general formation mechanics of spray-dried emulsions; however, the distribution of components and the particle morphology are also dependent on the material properties and processing conditions of the spray dryer. Appropriate processing conditions, such as drying temperature, is contingent on the properties of the given formulation. A sufficiently high temperature must be used to form a thin shell around the drying droplets early in the drying process in order to entrap the emulsion droplets and obtain a high encapsulation efficiency. However, the temperature must also be low enough to prevent possible evaporation of emulsion droplets or inactivation of temperature-sensitive components (Ziaee, et al. 2019). Encapsulation efficiency, defined here as the mass of the dispersed phase retained within the powder after spray drying, has been reported to increase with the concentration of the encapsulating agent (Gharsallaoui, et al. 2007, Linke, Balke and Kohlus 2018). An encapsulated ingredient to encapsulating agent ratio of 1:4 is often used in the spray drying of emulsions in order to obtain a high encapsulation efficiency (Jafari, et al. 2008, Encina, Marquez-Ruiz, et al. 2018, Bringas-Lantigua, et al. 2011). These findings can be applied to the encapsulation of vaccines formulated as dispersions via spray drying.

Based on Wang et al.'s findings, a high encapsulation efficiency is obtained when the first stage is short enough for the initial shell formation to occur quickly. An early shell formation will prevent the emulsion droplets from reaching the surface of the drying droplet and thus be lost during the evaporative process. Droplet drying time, τ_D, can be approximated using Eq. 1, where

d_0 is the initial droplet diameter and κ is the evaporation rate (Vehring, Pharmaceutical Particle Engineering via Spray Drying 2008).

$$\tau_D = \frac{d_0^2}{\kappa} \quad \textbf{1}$$

In order to predict the shell formation process, a particle formation model that describes the radial distribution of components within the atomized droplets during the drying process was used, in which a dimensionless Peclet number, *Pe*, was defined as Eq. 2, where D_i refers to the diffusion coefficient of component i and κ stands for the evaporation rate of the solvent (Vehring, Foss and Lechuga-Ballesteros 2007). Therefore, *Pe* is a parameter affected by both material properties of the components and processing parameters and can be used to predict final particle morphology (Vehring, Foss and Lechuga-Ballesteros 2007).

$$Pe_\mathrm{i} = \frac{\kappa}{8D_\mathrm{i}} \quad \textbf{2}$$

For the nanoemulsion system studied in this case, the nanoemulsion droplets can be treated as nanoparticles, assuming they remain stable in an aqueous dispersion. The diffusion coefficient of nanoparticles can be approximated through the Stokes-Einstein equation, given in Eq. 3, where *D* is the diffusion coefficient for the emulsion droplet, k_B is Boltzmann's constant, T is temperature, μ is viscosity, and d_h is hydrodynamic diameter. From this equation it is apparent that larger nanoparticles and nanodroplets will have a low diffusion coefficient, typically much lower than that of dissolved molecules, leading to a much larger *Pe*.

$$D = \frac{k_\mathrm{B}T}{3\pi\mu d_h} \quad \textbf{3}$$

In general, for a component with low *Pe*, material migration of the given component inside of an atomized droplet is quick relative to the speed of the receding droplet surface (Vehring, Foss and Lechuga-Ballesteros 2007). Hence, solutes with a low *Pe* distribute evenly in the atomized droplet during evaporation, typically forming spherical, solid particles if they do not crystallize. For components with very large *Pe*, such as nanoemulsion droplets, the diffusion is slow compared to the evaporation rate, rendering the component effectively immobile, and thus the component will accumulate near the surface as the atomized droplet dries. Using the particle formation model, it is possible to manipulate the distribution of the main components trehalose and the nanoemulsion droplets within the spray-dried powder.

The *Pe* for trehalose was designed to be approximately 1 in order to achieve a successfully spray-dried powder. The trehalose must be evenly distributed in order to increase coverage of the nanoemulsion droplets to facilitate stabilization during the drying process. The diffusion coefficient for trehalose in water at 100 mg/ml is 5×10^{-10} m^2/s (Vehring, Foss and Lechuga-Ballesteros 2007). For a *Pe*=1 for trehalose, based on Eq. 2, the evaporation rate must be 4×10^{-9} m^2/s. The GLA-SE droplet size has been measured as approximately 92 nm (Kramer, et al. 2018). The diffusion coefficient of GLA-SE nanoemulsion droplets with a diameter of 92 nm has been measured via dynamic light scattering as 5.3×10^{-12} m^2/s (data not shown). For a theoretical evaporation rate of 4×10^{-9} m^2/s, the *Pe* of the nanoemulsion droplets is ~ 95. The nanoemulsion droplets are expected to accumulate near the surface of the atomized droplet. At a very high *Pe*, the nanoemulsion droplets are expected to accumulate and possibly coalesce near the surface due to the force from the receding particle surface and convective flux of water towards the surface.

Based on similar studies, trehalose is expected to form solid, spherical amorphous particles when spray-dried (Vehring, Foss and Lechuga-Ballesteros 2007, Wang, Nobes and Vehring 2019).

2.2.3. Methods

Spray Drying

Spray drying was conducted using a custom research spray dryer (Ivey, et al. 2016) with a twin fluid atomizer operated at an air-liquid ratio of 8, which corresponds to an atomized droplet diameter of approximately 9 μm (Hoe, et al. 2014). The outlet humidity target was less than 10% RH to achieve a T_g greater than 88 °C. A spray dryer process mass and energy balance model (Ivey and Vehring 2010) was used to determine processing conditions to achieve an outlet temperature of 36 °C and outlet RH of 7%. The feedstock was supplied to the atomizer at a rate of 0.6 mL/min using a peristaltic pump (Model 77200-60; Cole-Parmer, Montreal, QC, Canada). The atomized droplets dried in an air flow rate of 200 SLPM, where the drying gas temperature at the inlet was 65 °C. Dry particles were separated from the air by a cyclone, and powder was collected in glass jars. These jars were sealed and stored in an environmental chamber set to 25 °C and 7% RH until powder packaging.

Stability Study

The design targets for the spray-dried formulation required that the vaccine concentration and integrity be retained post-spray drying and that the powder maintains stability for at least three months at 40 °C. Stability of the spray-dried powder was assessed using the following acceptance criteria: no particle fusing or crystallization, emulsion droplet size change less than or equal to 50%, polydispersity index less than 0.2, squalene content loss less than or equal to 20%, GLA

content loss less than or equal to 20%, and ID93 is present. Similar criteria were used previously for the assessment of lyophilized candidates (Kramer, et al. 2018).

The powders were stored at -20 °C, 2-8 °C, 25 °C, and 40 °C. The stability arm was chosen for 40 °C rather than 37 °C as recommended by the International Council for Harmonization of Technical Requirements for Pharmaceuticals for Human Use (ICH) guidelines for pharmaceutical stability studies (International Conference On Harmonisation Of Technical Requirements For Registration Of Pharmaceuticals For Human Use 2003). Similarly, time points were chosen based on the ICH guidelines. Characterization tests for chemical stability of the reconstituted powder were conducted at the beginning of the study, and then at multiple time points after storage at two weeks, one month, two months, three months, six months, nine months, and 13.5 months. Similarly, characterization tests for physical stability of the dry powder were conducted at the beginning of the study, and after one month, three months, and twelve months of storage. The final chemical characterization timepoint was originally planned for the same date; however, due to equipment repairs the chemical and colloidal characterization for the 12-month time point was delayed and characterization was completed 13.5 months after the initial timepoint.

Dry Powder Packaging for Stability Study

Spray-dried powder will equilibrate to the new water activity when placed in an environment with a different RH than its initial value (Waterman and MacDonald 2010). Desiccants, such as silica gel, are hygroscopic agents that can be used to modify or buffer the RH within a closed package. Chemical degradation due to a change in RH has been shown to be mitigated by the inclusion of desiccant within the package (Waterman and MacDonald 2010). Desiccants can be equilibrated to the desired moisture content when placed in an environmental chamber at the desired RH value

(Carrigy and Vehring, Engineering stable spray-dried biologic powder for inhalation 2019). The time required to equilibrate is influenced by several factors, such as the difference in RH value and temperature and the permeability of the packaging seals.

A packaging process involving the use of desiccants was utilized to prevent moisture uptake in the powder during temperature-controlled storage of the stability study. Packaging preparation involved placing silica gel pouches into an environmental chamber set to 25 °C and 7% RH for 3-4 days in order to equilibrate the desiccant to the outlet RH of the spray dryer. An equal number of silica gel pouches were equilibrated to 0% RH in a regulated glove box over the same time period. The packaging process took place within a custom glovebox set to 0% RH. The powder was aliquoted into low bind snap cap tubes (Product Z768820; Sigma Aldrich, Oakville, ON, Canada). The powder-containing tubes were then placed into an aluminum bag, along with a 7% RH desiccant pouch to prevent powder moisture changes. However, moisture transfer rates through the seals increase with a larger difference between the environments. To counteract this, the aluminum bag was then double heat-sealed and placed into another aluminum bag, along with a 0% RH desiccant pouch to minimize the moisture difference between the innermost package and the external environment. This external bag was also double heat-sealed and labelled. A simplified schematic summarizing the configuration is shown in Figure 1.

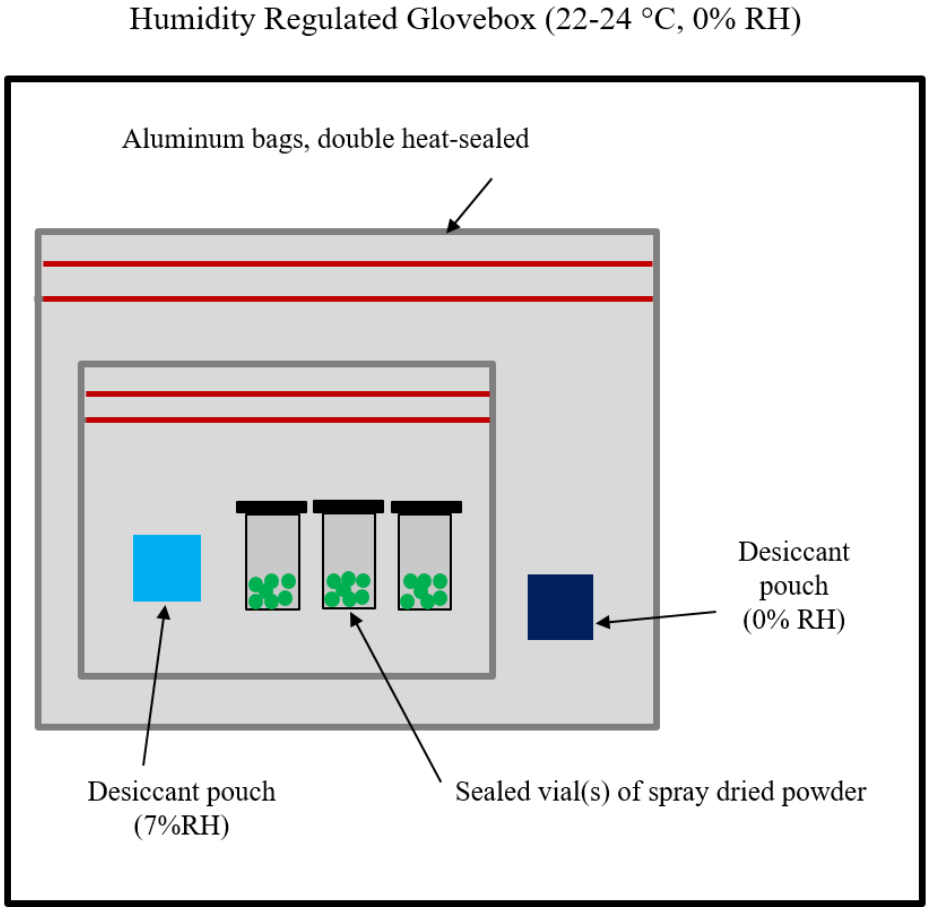

Figure 1 Simplified schematic for packaging protocol to ensure powder moisture content control during long-term powder storage

Dry Powder Characterization

Field Emission Scanning Electron Microscopy (Zeiss Sigma FE-SEM; Carl Zeiss, Oberkochen, Germany) was used to determine whether powder morphology changed over time. Powder samples were dispersed directly onto aluminum SEM stubs (Product 16111; Ted Pella, Inc.; Redding, CA, USA) and pressed against the surface of the stub to intentionally produce cracked particles for imaging. To prevent damage to the electron microscope, these samples were placed in a desiccator connected to an in-house vacuum system for 2-4 days to remove the exposed nanoemulsion droplets. Subsequently, the samples were sputtered with a coating of 80% gold and 20% palladium

(Leica ACE600 Carbon/Metal Coater; Concord, ON, Canada) to a thickness of 10-15 nm. Images ranging from magnifications of 500 to 20000× were taken at a working distance of 5.3-6.3 mm using an accelerating voltage of 3-4 kV.

The solid phase of the powder was monitored by Raman spectroscopy to assess whether or not the spray-dried powder remained amorphous during storage. A custom dispersive Raman spectroscopy system was utilized for this purpose. The system included a 671 nm diode-pumped solid-state laser (Ventus Solo MPC6000; Laser Quantum, Stockport, UK). A detailed description of a similar apparatus has been published elsewhere. (Wang, Barona, et al. 2017). Samples were placed in a closed sample chamber under nitrogen to prevent moisture exposure. All spectra were measured at a temperature of 22.0-23.0 °C and at less than 5% RH. In addition to measured SD-TG and SD-TGI powder samples, Raman spectra analysis was also conducted on neat amorphous and crystalline trehalose powder samples as references. Similarly, reference spectra were also obtained for liquid samples of squalene and crystalline Tris powder samples. A deconvolution process was used to assess the contributions and solid phase of each component. The deconvolution process is described elsewhere (Vehring 2005).

Karl Fisher Calorimetry (Karl Fisher Coulometric Titrator Model C30; Mettler Toledo; Mississauga, ON, Canada) was used to measure the water content of powder samples by mass. Results were displayed as a percentage based on the measured sample mass. Oven temperature for the method was 110 °C. Moisture content of the powder was determined by measuring and averaging results of two vials of the same powder. Analysis of experiments to determine moisture

content of a HYDRANAL water standard (Honeywell; Mexico City, Mexico) showed that the machine variance was 0.3%.

Reconstituted Powder Characterization

At each stability time point, approximately 108 mg of spray-dried powder was reconstituted with the appropriate volume of freshly dispensed MilliQ water to yield sample concentrations expected in the liquid drug product. The exact reconstitution volume was based off the exact mass of powder in each vial and an empirically determined expansion factor. Each test was performed in triplicate on separate vials of reconstituted powder for the first three months. Remaining timepoints were performed on single vials. Replicates of measurements of the feedstock were made from the same vial. The stability study involved storage of the spray-dried powders at several storage temperatures: -20, 2-8, 25 and 40 °C. For each temperature, at a given time point the powders were reconstituted and assessed for nanoemulsion droplet diameter, polydispersity index, squalene concentration, GLA concentration, ID93 presence, and pH. Unlike other chemical characterization tests, osmolality was only measured initially, after three months, and after 13.5 months for all storage temperatures.

A dynamic light scattering technique (Zetasizer APS; Malvern, UK) was used to measure the mean hydrodynamic diameter and polydispersity index of the nanoemulsion droplets in the liquid formulations reconstituted from spray-dried powders. Polydispersity index of the nanoemulsion droplets was defined as the standard deviation of a given measurement divided by the hydrodynamic diameter, squared. A polydispersity index of less than 0.2 was considered sufficiently monodisperse. Details of the measurement process have been described elsewhere (Chan, et al. 2017). Liquid feedstock measurements were from one sample analyzed three times.

GLA content in the powder was quantified using a reversed-phase HPLC method. Separation of GLA from the sample was performed on an Agilent 1200 series HPLC (Agilent Technologies; Santa Clara, CA, USA) equipped with a silica-based, C18 reversed-phase column (Atlantis T3 Column; Waters; Elstree, UK) with a gradient from 50% mobile phase B to 90% mobile phase B over 18 minutes and a flowrate of 1.0 mL/min. Mobile phase A contained 75:15:10 (v/v/v) methanol:chloroform:water, 1% (v/v) acetic acid, and 20 mM ammonium acetate. Mobile phase B contained 50:50 (v/v) methanol:chloroform, 1% (v/v) acetic acid, and 20 mM ammonium acetate. Samples were diluted 10-fold in mobile phase B, and the injection volume was 100 µL. Column temperature was held constant at 30 °C. A charged aerosol detector (Corona CAD; ESA Biosciences; Chelmsford, MA, USA) was used for analyte detection. A standard curve was prepared from GLA in mobile phase B. The peak heights from the standards were fit with a second order polynomial per the charged aerosol detector manufacturer's directions. Sample analyte concentrations were calculated by interpolation. Liquid feedstock measurements were done in two replicates, each analyzed once.

Squalene content in the powder was quantified using a reversed-phase HPLC method. Separation of squalene from the sample was done with the same equipment and the same mobile phases used for GLA as described above. Samples were diluted 100-fold in mobile phase B, and 10 µL of volume was injected with a gradient from 50% mobile phase B to 90% mobile phase B over 30 minutes and a flowrate of 1.0 mL/min. Column temperature was held constant at 30 °C. The peak area from the standards were fit with a second order polynomial per the charged aerosol detector manufacturer's directions. Sample analyte concentrations were calculated by interpolation. Liquid feedstock measurements were completed in two replicates, each analyzed once.

SDS-PAGE was used to detect the presence of the ID93 protein in the samples. Samples were reduced in LDS buffer (NP0007; Thermo Fisher Scientific, Waltham, MA, USA) spiked with β-Mercaptoethanol to a final concentration of 1.25% (v/v). Samples were heated at 90 °C for 15 minutes and then cooled to room temperature. Once cooled and centrifuged at 2000 rpm for 30 seconds, samples and molecular weight marker (LC5925; Thermo Fisher Scientific, Waltham, MA, USA) were run in 4-20% Tris-Glycine gels (XP04205BOX; Thermo Fisher Scientific, Waltham, MA, USA). Gels were silver stained (PROTSIL1-1KT; Sigma Aldrich, St. Louis, MO, USA) and imaged (AlphaImager EC; Protein Simple, San Jose, CA, USA). At each time point, two SDS-PAGE samples were prepared and analyzed per vial to confirm the presence of the ID93 protein.

Reconstituted powder pH was measured using a pH meter (Orion ROSS Ultra Semi-micro pH Electrode, Thermo Fisher Scientific, Waltham, MA, USA). Liquid feedstock measurements consisted of one sample. Measurements of reconstituted samples were performed in triplicate for the first three months; measurements were performed once for the remaining timepoints.

Osmolality of the reconstituted powder was measured using an osmometer (Model 2020; Advanced instruments, Norwood, MA, USA) to determine if the reconstituted powder was isotonic and suitable for injection. Liquid feedstock measurements consisted of one sample. Measurements of reconstituted samples were performed in triplicate for the first three months; measurements were performed once for the remaining timepoints.

Statistical Analysis

Mean results are reported, and the indicated error is the standard deviation of replicate measurements. Number of replicates for each method are indicated above. A two-tailed student's t-test was used for analysis, where statistically significant differences were reported for $p<0.05$.

2.3. Results

2.3.1. Powder Manufacturing

Process calculations predicted the nominal solids throughput in the spray dryer to be 75 mg/min. During powder manufacturing for the stability study, the actual rate to produce SD-TG and SD-TGI powders was 49 mg/min and 45 mg/min, corresponding to spray drying yields of 65% and 60%, respectively. Considering the relatively small spray drying batch size of 16.4 g and 17.3 g, produced over 5.5 hours and 6.5 hours, respectively, the yield was typical and well within the acceptable range for early development.

The measured properties of the formulations before and after spray drying (post-reconstitution) are shown in Table 3. The target values given are the same as for the lyophilized vaccine product. All measured vaccine properties were well within the target values. Average nanoemulsion droplet size was nearly the same as the liquid vaccine product. Hydrodynamic diameter increased only slightly by 2-3% after spray drying. The polydispersity index of the nanoemulsion droplets did not change significantly ($p>0.05$) over the course of spray drying for either formulation.

Squalene content levels before and after spray drying are very similar, indicating a high encapsulation efficiency. The results show high retention (>90%) of the squalene component for both formulations. The high retention indicates that the evaporation losses during low temperature

spray drying for this system are less than 10%. The GLA content did not change significantly (p>0.05) over the course of spray drying for either formulation, indicating that the GLA component, a synthetic lipid, was successfully stabilized by the trehalose. The retention of GLA content indicates that this component does not degrade over the course of spray drying, which was a concern, as GLA is sensitive to thermal stress (Kramer, et al. 2018). Similarly, ID93 protein was shown to be present in both the liquid and reconstituted formulations. Likewise, the pH did not change significantly (p>0.05) over the course of spray drying for either formulation.

Table 3 Chemical and colloidal properties before and after spray drying for adjuvant-only (SD-TG) and antigen-containing (SD-TGI) formulations.

ID		Nanoemulsion Droplet Diameter (nm)	Polydispersity Index	Squalene Content (mg/mL)	GLA Content (µg/mL)	ID93	pH	Osmolality (mOsmol/kg)
Target		120 ± 40	<0.2	13.6 – 20.5	10 ± 2.5	Present	7.5 – 8.5	315 – 415
SD-TG	Feedstock Liquid	95.3 ± 0.9	0.05 ± 0.04	19.1 ± 0.4	9.2 ± 0.5	N/A	7.62	383
	Reconstituted Powder	96.9 ± 0.2	0.07 ± 0.02	18.8 ± 0.3	9.5 ± 0.4	N/A	7.57 ± 0.04	376 ± 8
SD-TGI	Feedstock Liquid	94.9 ± 0.8	0.06 ± 0.01	18.8 ± 0.3	9.3 ± 0.4	Present	7.56	389
	Reconstituted Powder	97.6 ± 1.1	0.09 ± 0.01	17.3 ± 0.6	9.0 ± 0.4	Present	7.55 ± 0.01	351 ± 8

2.3.2. Physicochemical Stability

Particle Morphology

The SEM images for the spray-dried SD-TG and SD-TGI formulations are shown in Figure 2. Analysis of the SEM images indicates that spray drying the formulations produced a polydisperse powder sample with microparticles ranging in geometric diameter from ~1-20 μm. These images show that the spray-dried microparticles were spherical with surfaces ranging from smooth to slightly dimpled. The spray-dried powders containing the emulsion droplets were relatively flowable and easy to handle. The similarity of the microparticles from the SD-TG and SD-TGI formulations indicates that the presence of the protein ID93 does not affect the particle morphology. Microparticles of neat trehalose spray-dried from a 100 mg/mL aqueous solution under the same processing conditions are also shown in Figure 2 for comparison. The trehalose particles have an outer particle morphology very similar to those of the SD-TG and SD-TGI formulation, that is, spherical particles with smooth or slightly dimpled surfaces and a similar geometric diameter. Spray-dried bacteriophage encapsulated in trehalose (Carrigy, Liang, et al. 2019, Vandenheuvel, et al. 2014) and outer membrane vesicle pertussis vaccine spray-dried with trehalose (Kanojia, Raeven, et al. 2018) produced particles with a similar exterior morphology. These particles, composed mainly of trehalose, were also spherical, had a similar geometric diameter range and exhibited a smooth or dimpled surface.

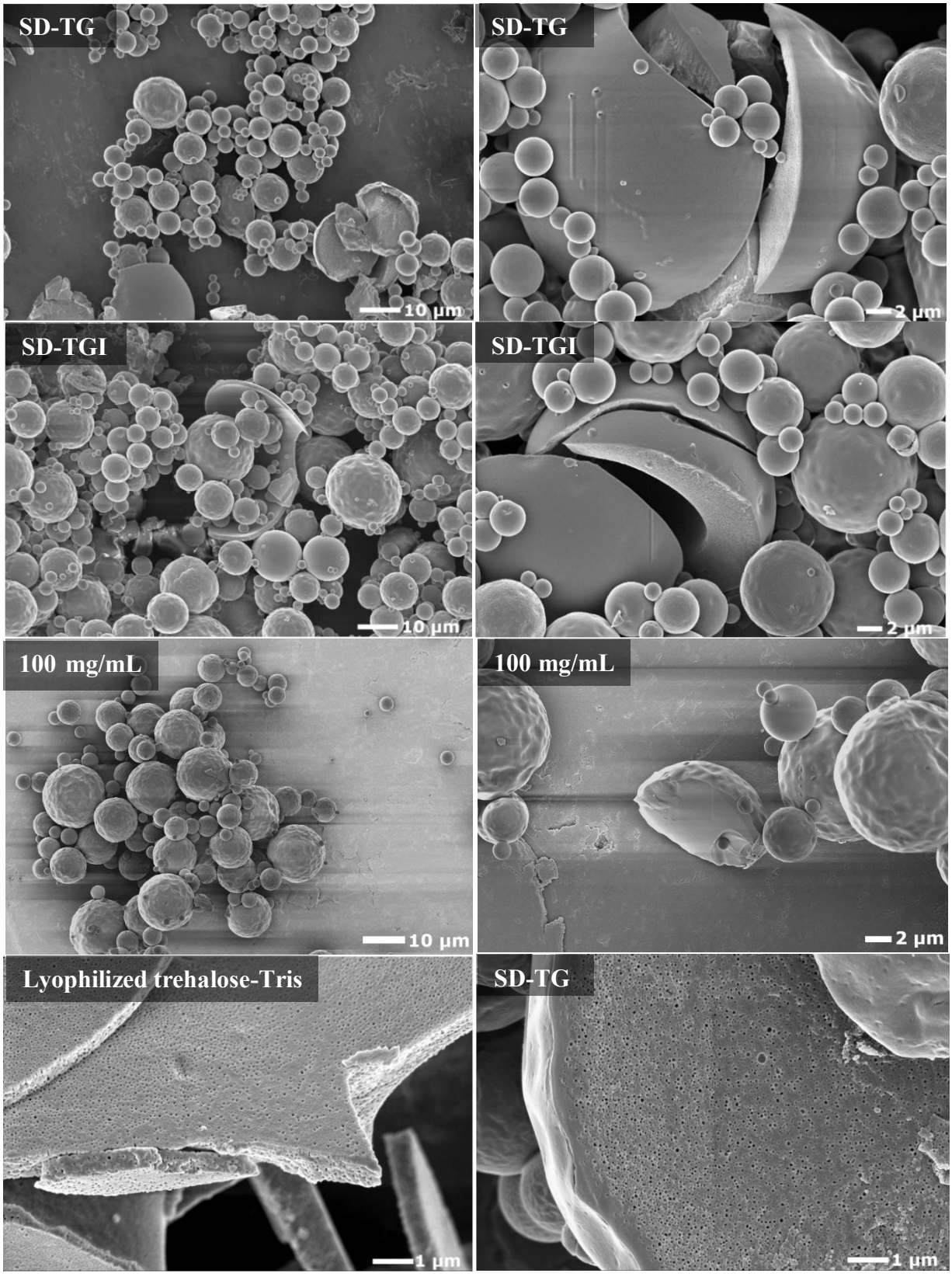
SD-TG
10 µm
SD-TG
2 µm
SD-TGI
10 µm
SD-TGI
2 µm
100 mg/mL
10 µm
100 mg/mL
2 µm
Lyophilized trehalose-Tris
1 µm
SD-TG
1 µm

Figure 2 Comparison of morphology for the adjuvant-only SD-TG formulation, antigen-containing SD-TGI formulation, spray-dried trehalose and the lyophlized vaccine. External morphology of all spray-dried powders shows similar spherical, polydisperse particles that are not fused. Interior structure of the lyophilized vaccine and the spray-dried particles shows similar voids left by the encapsulated emulsion droplets. Scales are provided on the respective images.

SEM images of the cracked microparticles of SD-TG and SD-TGI all show that these particles can be hollow or solid, with a range of shell thicknesses within a given sample. The images show that the interior structure of this shell differs from particles formed with spray-dried trehalose. Trehalose particles show a solid interior whereas the interior of the SD-TG and SD-TGI particles appears to be foam-like with numerous voids within the trehalose matrix. These voids observed in the SEM images of SD-TG and SD-TGI also appear in images of the lyophilized trehalose-Tris formulation (Figure 2). The geometric diameter of these voids appears to be approximately the same as that of the nanoemulsion droplet hydrodynamic diameter. It can be concluded that these voids are left behind by nanoemulsion droplets that evaporated during the imaging preparation process. Higher magnification images of the surface (not shown) show comparatively few of these voids on the surface of the particle.

Similar interior morphologies have been shown in SEM images particles generated by emulsion encapsulation via spray drying of isoeugenol in a glucose syrup matrix (Krogsgard Nielsen, et al. 2016), spray drying of D-Limonene emulsion with different combinations of the excipients gum arabic, maltodextrin, and trehalose (Paramita, et al. 2010), and spray drying of fish oil in a whey protein isolate matrix (Wang, Liu, et al. 2019). The particles in the latter paper are especially like the particles shown in this study. Both studies generated intact thin-shelled particles with the

emulsion droplets embedded within the particle wall. A central void was also found in the particles generated in a study on surface formation of drying emulsions (Wang, Che, et al. 2015).

There appears to be a slight gradient in nanoemulsion droplet distribution within the particle, with a higher concentration of droplets closer to the surface of the particle than to the center, as demonstrated by the cracked SD-TG microparticle in Figure 2. As per the theoretical particle formation theory calculations previously discussed, the *Pe* number of the nanoemulsion droplets is >>1 and the *Pe* of trehalose is ≈1. Theory suggests that the nanoemulsion droplets accumulated near the surface of the drying droplet because the nanoemulsion droplets were unable to diffuse to the centre faster than the particle was forming. The lack of visual nanoemulsion droplet aggregation and relatively even distribution in the SD-TG and SD-TGI particles suggests that an appropriate drying temperature was chosen.

Similar SEM images of the powder samples were taken over the course of the stability study. Figure 3 shows the SD-TGI formulation after three months' and twelve months' storage at 40 °C. A lower magnification view, shown in Figure 3a, shows that the sample stored at 40 °C has maintained overall exterior particle structure even after twelve months of storage. Smaller particles may experience some bridging, as shown by the smaller particles attaching to the larger particles. As shown in Figure 3b, the interior structure of the particle is also maintained after storage at 40 °C, as the voids left by the nanoemulsion droplets are clearly distinct. Cavities within the central void are too large to be nanoemulsion droplets; they may be caused by ruptured nanoemulsion droplets, which led to the pockmarked inner surface. The pockmarked inner surface was not consistently exhibited in cracked particles. The morphology for the samples stored at lower

temperatures also displayed a maintenance of interior and exterior particle structure over twelve months of storage. No particle bridging was apparent in the samples stored at lower temperatures.

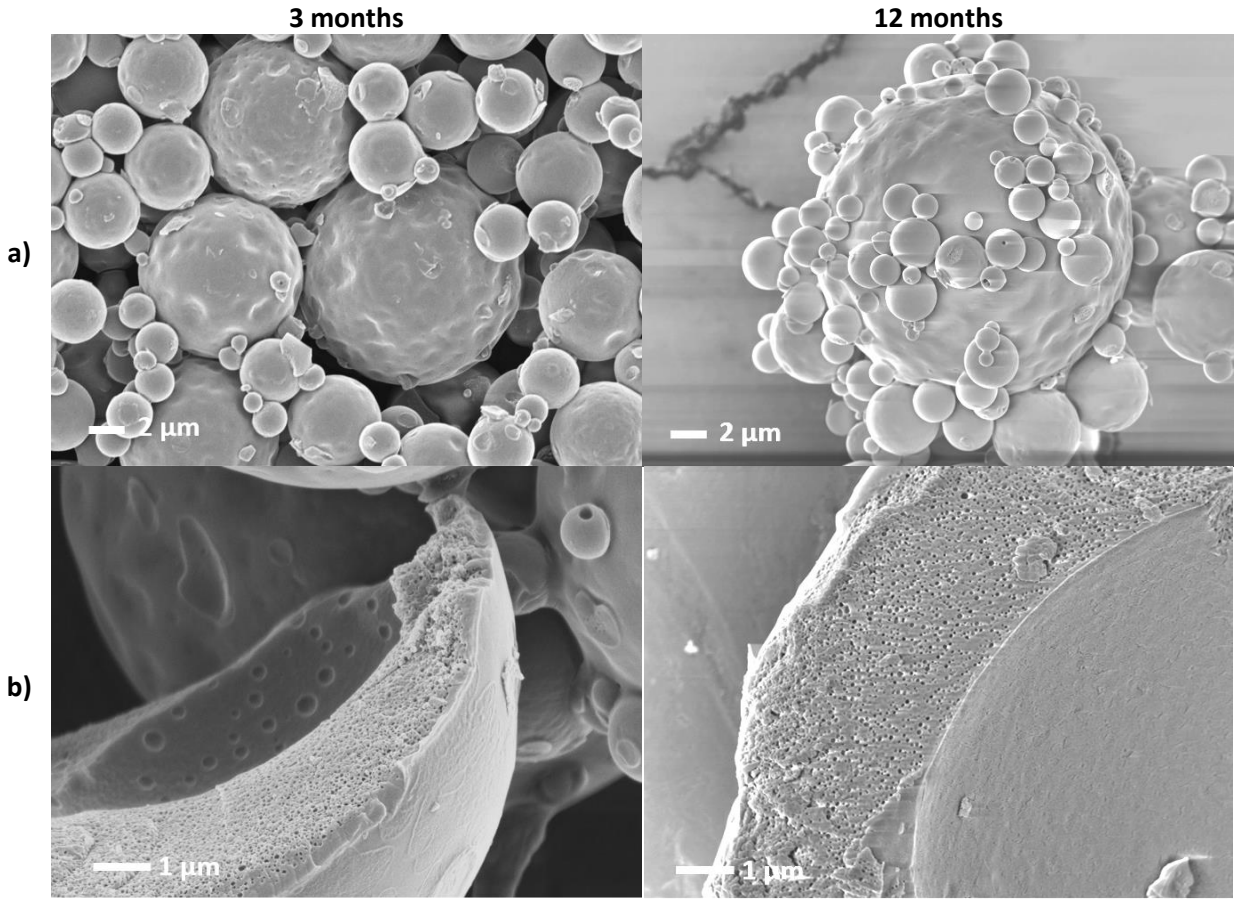

Figure 3 SEM images of antigen-containing SD-TGI powder after three months and twelve months of storage at 40 °C indicating a) sample maintains external morphology after accelerated storage, b) interior particle structure is maintained. Scales are provided on the respective images.

Powder Moisture Content

Maintenance of moisture content is critical to avoid lowering of the T_g, which would result in powder crystallization. Crystallization of amorphous spray-dried powder will inactivate the biological components (Carrigy and Vehring 2019). The moisture content of the powder by wet basis after manufacture was measured to be 2.6 ± 0.1% in this study. Moisture content of the SD-TGI powder over twelve months of storage is shown in Figure 4. The moisture content after twelve months of storage at 2-8, 25, and 40 °C was 2.5%, 2.1%, and 1.8%, respectively. This lack of moisture uptake signifies that the implemented packaging system is very robust.

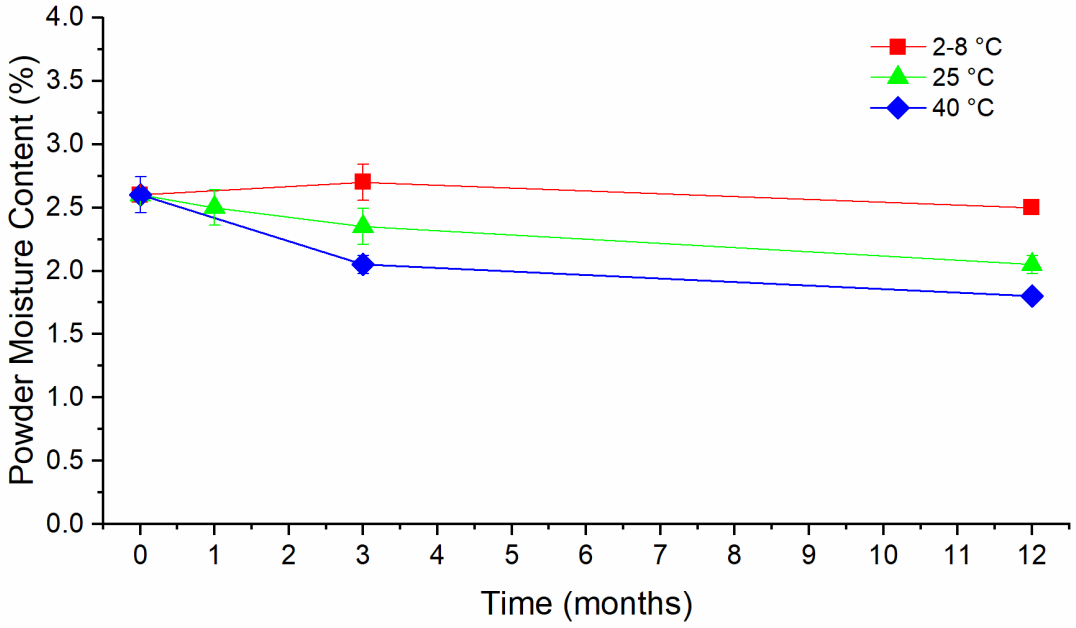

Figure 4 Graph indicating the powder moisture content of the antigen-containing SD-TGI powder sample after twelve months of storage at 2-8, 25, and 40 °C. The minimal change at each temperature arm of the stability study indicates that the moisture content of the powder is preserved and the robustness of the implemented packaging system.

Solid State Analysis

Raman spectroscopy analysis was completed on SD-TG and SD-TGI powders at various time points during the stability study in order to confirm the presence of initially formulated components within the sample and to determine any changes in solid phase. Sample spectra for SD-TG powder obtained at timepoint 0, as well as reference spectra for amorphous trehalose, squalene, crystalline Tris, and crystalline trehalose, are shown in Figure 5. The ID93 protein and GLA contributions were not considered due to their low mass fraction.

Inspection of the sample spectra showed the trehalose component to be completely amorphous. This is evidenced by the presence of amorphous trehalose characteristic peaks at 425, 460, 560, 865, 935, and 1145 cm^{-1} in the sample and further supported by the lack of crystalline trehalose characteristic peaks at approximately 395, 455, 695, 980, and 1235 cm^{-1}, to cite a few examples. The squalene in the sample was identified by its characteristic peak appearing at 1400 cm^{-1}. The solid phase of trehalose is further confirmed by the low normalized intensity of the residual spectrum, shown in Figure 5. The residual spectrum was obtained by subtracting the reference spectra for amorphous trehalose (mass fraction 81%), squalene (mass fraction 14%) and Tris (mass fraction 2%) from the sample spectrum. Similar analysis was completed on the SD-TGI powder (not shown), also confirming the amorphous structure of the trehalose component and the presence of squalene and Tris buffer in the sample. It is expected that SD-TG and SD-TGI have similar results, as the only difference in formulation between the samples is the presence of ID93 in the latter.

Sample spectra for SD-TGI at time point 0 and after twelve months of storage at 2-8, 25, and 40 °C are shown in Figure 6. The residual spectrum after subtracting the SD-TGI spectrum collected

after twelve months at 40 °C from the timepoint 0 spectrum is also shown in Figure 6. The subtracted spectrum of the most extreme storage condition from the initial spectra was extremely low. The spectra for all storage temperatures were very similar, indicating that the solid phase of the powder had not measurably changed over the course of the stability study. Indeed, deconvolution of the SD-TG and SD-TGI spectra collected at different points of the stability study confirmed that all samples showed presence of squalene and Tris, and that trehalose remained amorphous. This ties into the moisture content data, in that if moisture content did not rise, it is unlikely that the trehalose crystallized as the T_g was theoretically >88 °C.

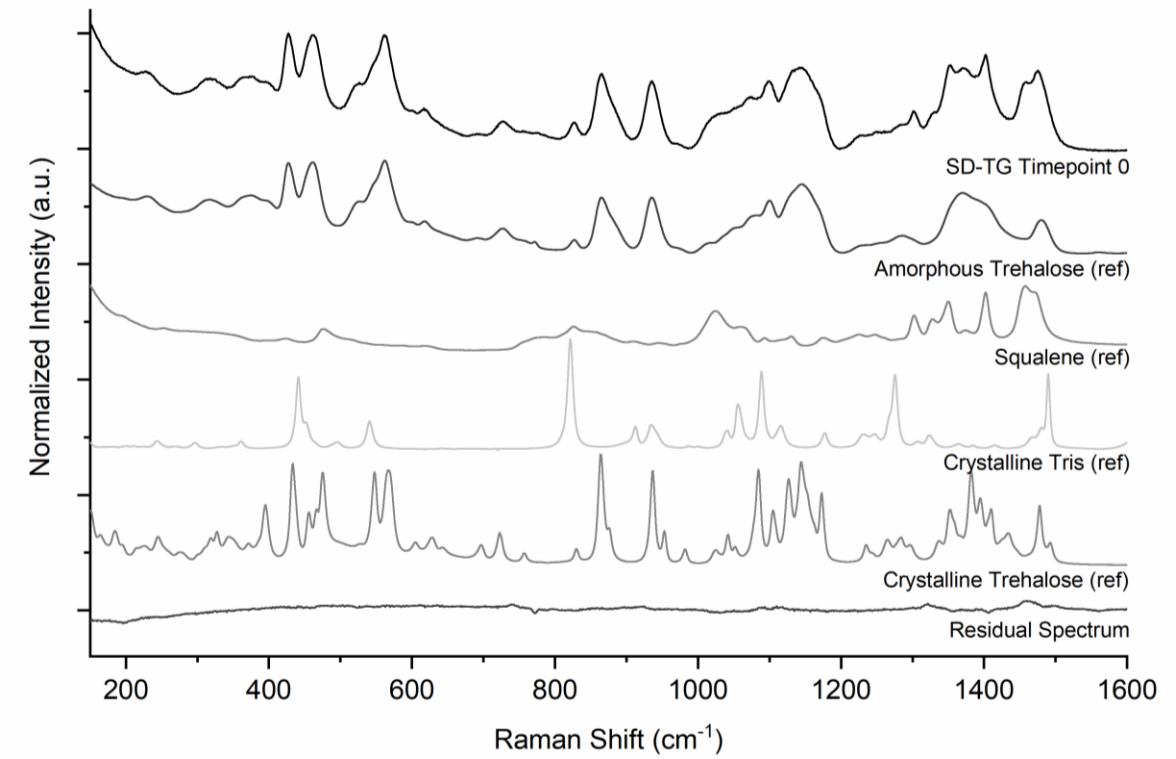

Figure 5 Normalized Raman spectrum of the adjuvant-only SD-TG powder sample, and reference spectra of amorphous trehalose, squalene, Tris, and crystalline trehalose. Also shown is the normalized residual spectrum, obtained by subtracting individual component contributions from the raw measured SD-TG spectrum.

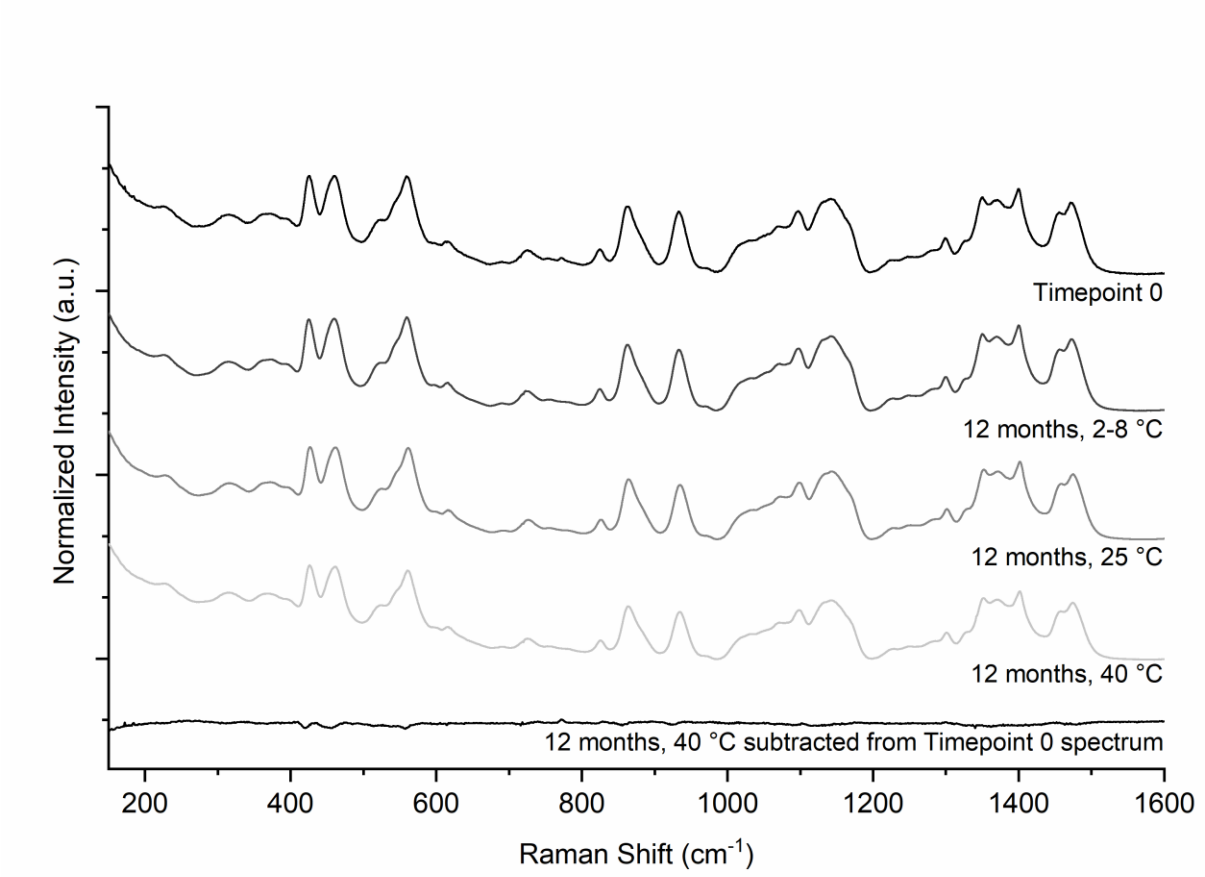

Figure 6 Normalized Raman spectra of the antigen-containing SD-TGI powder formulation, shown after twelve months of storage at 2-8, 25, and 40 °C, and at time point 0. All samples shown were normalized according to the peak at 460 cm^{-1}. Also shown is residual spectrum obtained from subtracting the twelve-month, 40 °C spectrum from the spectrum obtained at time point 0. The residual spectrum indicates that the SD-TGI powder stored for twelve months at 40 °C does not undergo any solid phase changes.

Emulsion Droplet Size and Distribution

Properties of the emulsion droplet size of the GLA-SE vehicle over 13.5 months of the stability study are shown in Figure 7. The changes are all within the pre-determined target stability criteria mentioned above; that is, <50% change in droplet size; and polydispersity index <0.2 after three months' storage at 40 °C. Both the initial change in emulsion diameter and the subsequent size change over storage are important in evaluating a spray-dried emulsion. After three months' storage, droplet size increased only 1-3% for the SD-TG formulation. Similarly, droplet size increased only 2-4% for the SD-TGI formulation. The polydispersity index did not change significantly over the course of three months at any given storage temperature (p>0.05). The nearly constant droplet diameter and polydispersity index indicates that the nanoemulsion droplets did not coalesce or shrink during the three-month storage or on reconstitution, even at the highest temperature of 40°C, proving that the nanoemulsion droplets were well protected by the trehalose stabilizer as designed.

Nanoemulsion droplet diameter for all samples after 13.5 months was within -4 to 2% of the initial measurement. These results show that even after long term storage the powder is well within the <50% change in diameter stability criteria. Similarly, the polydispersity index is below 0.2 after 13.5 months of storage. Low measured polydispersity index indicates that the nanoemulsion droplet diameter distribution remains relatively monodisperse over the course of the stability study.

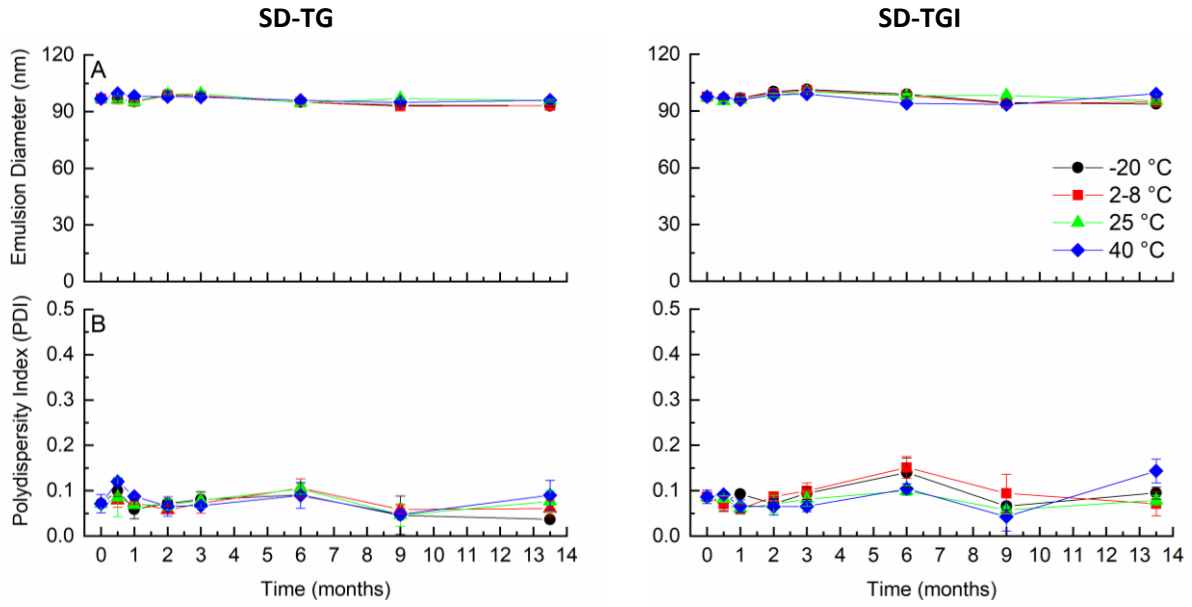

Figure 7 Plots showing A) nanoemulsion droplet diameter size and B) polydispersity index of droplets for the reconstituted adjuvant-only SD-TG powder (left) and reconstituted antigen-containing SD-TGI powder (right) stored over 13.5 months at the indicated temperatures. Legend indicates the storage temperatures for the powder. Parameters are within targets over time at all temperatures. Error bars indicate the standard deviation of three measurements.

Squalene Content

Squalene retention of the SD-TG and SD-TGI powders over 13.5 months of the stability study are shown in Figure 8. The changes are all within the pre-determined target <20% loss for squalene content defined previously. Squalene content was preserved after three months at high temperature storage, with 84% retention for the SD-TG formulation and 91% retention for the SD-TGI formulation, when compared to the initial measurement. After 13.5 months of storage, the squalene content for the SD-TG formulation was 83% to 89% retained. Similarly, after 13.5 months of storage, the squalene content for the SD-TGI formulation was 91 to 94% retained. Squalene content analysis for both formulations shows a similar pattern where the squalene loss trend among all storage temperatures are similar, but appears to increase with increasing temperature. Squalene loss appears to occur over the first three months of storage and then remains relatively constant afterwards for a given storage temperature. Reported increases in squalene content may be due to assay variability.

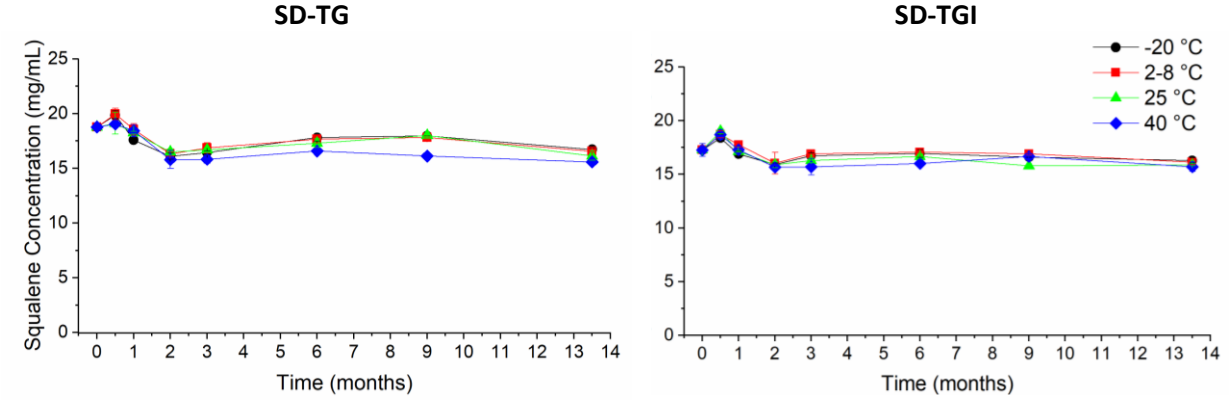

Figure 8 Plots showing squalene content of the reconstituted adjuvant-only SD-TG powder (left) and reconstituted antigen-containing SD-TGI powder (right) stored over 13.5 months at the indicated temperatures. Legend indicates the storage temperatures for the powder. Parameters are within targets over time at all temperatures, indicating that the squalene component of the vaccine is stabilized within the dry powder. Error bars indicate the standard deviation of three measurements.

GLA Content

The pre-determined target stability criteria for the agonist GLA was <20% loss of GLA after three months' storage at 40 °C. GLA retention of the SD-TG and SD-TGI powders over 13.5 months of the stability study are shown in Figure 9. GLA retention is high for storage at -20 and 2-8 °C after three months for both powders (87-93% retained). A decrease of GLA concentration of 40% for the SD-TG formulation and 43% for SD-TGI formulation stored at 40 °C for three months was observed.

After 13.5 months of storage, the GLA content for the SD-TG and SD-TGI formulation remained stable when stored at -20 and 2-8 °C (92-98% retained). Retention of GLA for the SD-TG and SD-TGI formulations stored at 25 °C was 83% and 75%, respectively. Both the formulations underwent 56-58% loss in GLA after storage at 40 °C for 13.5 months

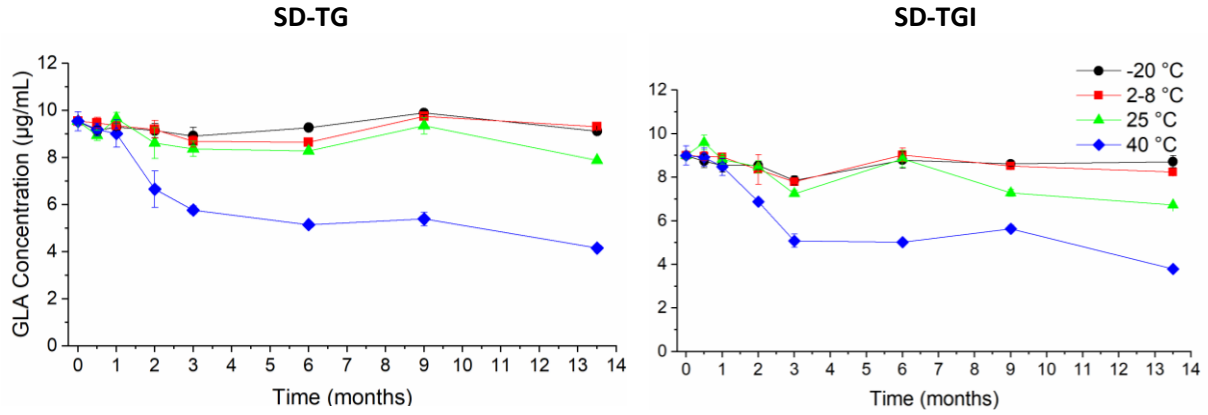

Figure 9 Plots showing GLA content of the reconstituted adjuvant-only SD-TG powder (left) and reconstituted antigen-containing SD-TGI powder (right) stored over 13.5 months at the indicated temperatures. Legend indicates the storage temperatures for the powder. Error bars indicate the standard deviation of three measurements.

ID93 Content

SDS-PAGE results of the samples after three months and 13.5 months of storage were compared to an ID93 control and a two-vial ID93+GLA-SE control. Oil smear shown at the top of the gel was due to GLA-SE (Schwartz, et al. 2017). The presence of the ID93 band in all samples, shown in Figure 10 and Figure 11, confirms that ID93 is present at all storage temperatures after three months and 13.5 months, respectively. The results indicate that the ID93 protein survives in the spray-dried powder over 13.5 months of storage even at temperatures up to 40 °C. All samples showed similar band intensity to the control at timepoint 0, after two weeks, one month and two months of storage (data not shown). The reduced intensity of the band in the 25 and 40 °C samples as compared to the control may suggest that there is some loss in ID93 protein after three months' storage.

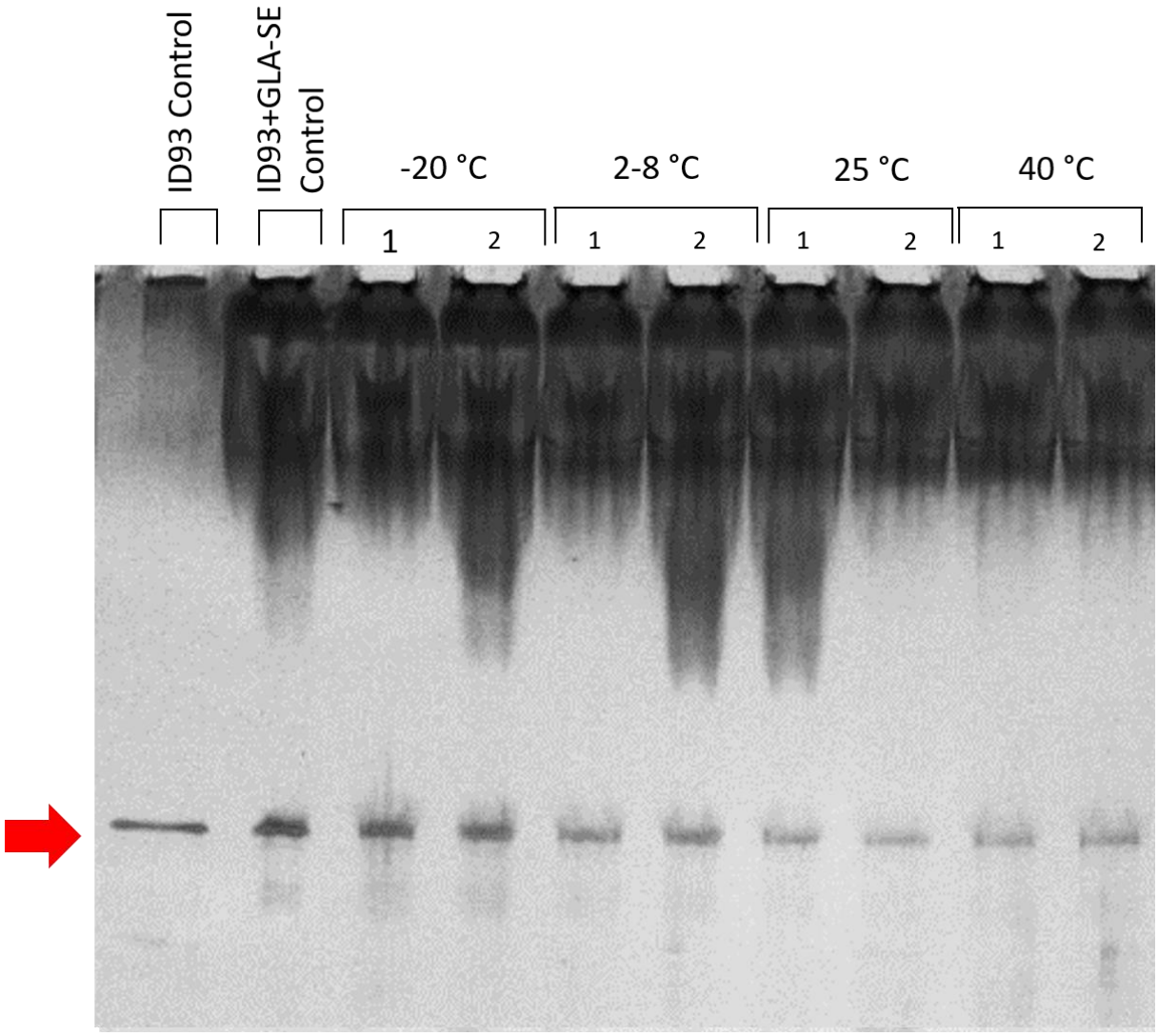

Figure 10 SDS-PAGE results of SD-TGI powder after three months' storage at temperatures -20, 2-8, 25, and 40 °C. ID93 and ID93+GLA-SE control samples are shown for comparison. Results shown are from a single run. The red arrow points to the ID93 protein band.

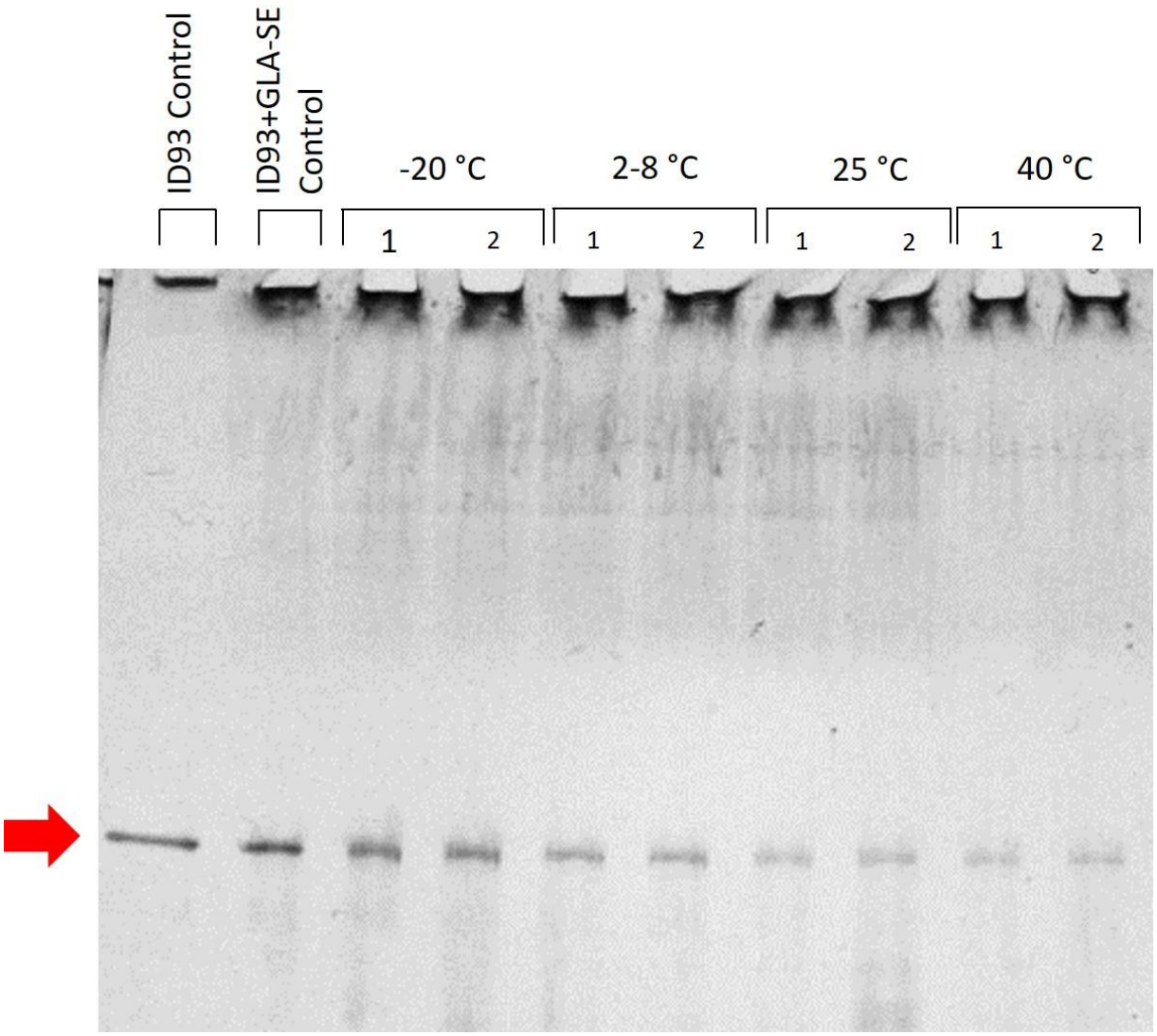

Figure 11 SDS-PAGE results of SD-TGI powder after 13.5 months' storage at temperatures -20, 2-8, 25, and 40 °C. ID93 and ID93+GLA-SE control samples are shown for comparison. Results shown are from a single run. The red arrow points to the ID93 protein band.

pH and Osmolality

A previous study found that increased aggregation of ID93 occurs at and below neutral pH (Kramer, et al. 2018). Formulating the vaccine at pH 7.5 or 8 minimizes aggregation and maximizes the temperature at which unfolding occurs (Kramer, et al. 2018). Overall, pH of the reconstituted liquid trended slightly downward over time for all temperatures. After three months of storage, the greatest pH change was 0.07- 0.16 pH units; comparatively, the lead lyophilized vaccine candidates stored at 37 °C for three months showed similar pH decreases of less than 0.12 pH units (Kramer, et al. 2018). The pH of the liquid, two-vial and lyophilized proof-of-concept samples exhibited pH decreases of ≥0.2 pH units. Thus, the spray-dried formulations appear to offer greater protection against pH change than the liquid vaccine presentations and similar protection as the lead lyophilized candidates. After storage for 13.5 months at -20, 2-8, and 25 °C, the greatest pH change in the spray-dried powders was 0.1 pH units. Somewhat greater pH decrease (0.3 pH units) was evident in reconstituted SD-TG and SD-TGI powders after storage at 40 °C for 13.5 months.

Osmolality was monitored through the stability study to ensure that the reconstituted formulation is isotonic and suitable for injection. Osmolality changed only slightly after 13.5 months for all samples. For the SD-TG sample, osmolality increased 0.4% for the samples stored at 40 °C and decreased by 1-3% for the samples stored at -20, 2-8, and 25 °C. Osmolality of the SD-TGI powder increased 1-5%. The osmolality of all samples remained within the 300±100 mOsmol/kg target.

2.4. Discussion

This study reports the development of a thermostable presentation of an adjuvanted subunit TB vaccine candidate via spray drying. Spray drying a vaccine into a dry powder form can greatly improve long term stability over its liquid counterpart; however, loss of efficacy can occur due to suboptimal formulation and processing parameters, causing loss or structural change of the vaccine components (Ingvarsson, Schmidt, et al. 2013). Our results showed that spray drying of the ID93+GLA-SE vaccine candidate with trehalose as a stabilizer successfully preserved all vaccine components. The nanoemulsion droplets maintained their size on reconstitution after spray drying. The lack of membrane fusing suggests that the chosen processing parameters effectively facilitated the stabilization at the phospholipid monolayer membrane of the GLA-SE nanoemulsion droplets within trehalose matrix. The overall preservation of nanoemulsion droplet diameter is critical as it is has been shown that smaller nanoemulsion droplets are more stable over time than large ones (Fox, et al. 2008). Additionally, the ID93+GLA-SE vaccine candidate targets uptake by dendritic cells to induce immunity and particle size is known to influence dendritic cell uptake.

The maintenance of droplet size shows that the shearing forces on the formulation due to the twin fluid atomizer were not sufficient to cause droplet size change. Similar preservation of membrane integrity was achieved by Kanoija et al.'s (Kanojia, Raeven, et al. 2018) spray drying of outer membrane vesicle pertussis vaccine. Their study also used trehalose as a stabilizing excipient and found that vesicle size before and after spray drying was approximately 130 nm. Conversely, spray drying of H56/CAF01, which was formulated as a liposomal dispersion, resulted in size change of the CAF01 adjuvant (Thakur, et al. 2018). H56/CAF01 was also spray-dried with trehalose, further indicating that stabilization must also consider the processing parameters rather than just the

stabilizing excipient. Similarly, the method of manufacture plays a role in preserving phospholipid membrane integrity. Spray drying the vaccine showed little change in GLA-SE droplet diameter; however, after lyophilization, GLA-SE diameter increased 31% and 18% for trehalose-containing and sucrose-containing lead candidates, respectively (Kramer, et al. 2018). The discrepancy in diameter changes for the formulations with similar excipients but differing manufacturing methods indicates that there are additional stresses in the lyophilization process that may cause the nanoemulsion droplets to coalesce.

In additional to nanoemulsion droplet size preservation, results show that a high encapsulation of squalene within the spray-dried particles was achieved, suggesting that trehalose was an appropriate choice of wall material for this vaccine candidate. High retention of GLA further signifies that trehalose provided suitable protection during desiccation. Preservation of these components over spray drying was a concern as both need to be stabilized during the desiccation process. The chosen drying temperature was clearly not too high as the integrity of these components was preserved. For the chosen drying gas temperature, the droplet temperature was predicted to be near the wet bulb temperature, i.e. approximately 28 °C. Protection of these components against desiccation stress is likely due to glass stabilization by trehalose. Similar stabilizing performance was shown in the lyophilization study, where GLA concentration did not significantly decrease below the target after lyophilization for any of the samples (Kramer, et al. 2018).

High encapsulation efficiencies via spray drying have been previously achieved for nanoemulsions at the 100 nm scale. Nanoemulsions containing the drug tioconazole were formulated with a mean size of 182 nm and spray-dried using lactose as an excipient (Ribeiro, et al. 2016). The authors

reported that nanoemulsion size was preserved and that there was no loss of drug over the spray drying process. Successful encapsulation of H56/CAF0, a TB liposomal vaccine candidate at the nano-scale within trehalose microparticles has been demonstrated by Thakur et al. (Thakur, et al. 2018). The size of the tested liposomal dispersions ranged from approximately 370-770 nm. Encapsulation efficiency was not directly measured; however, similar immunogenicity profiles were elicited from the reconstituted vaccine as compared to the liquid formulation. The similarly generated immune responses suggest that a high amount of the active ingredient was encapsulated within the particles.

The ID93+GLA-SE vaccine candidate is formulated as a nanoemulsion with a phospholipid membrane. The successful stabilization of this candidate with trehalose is consistent with the stabilization of the phospholipid based vaccines via spray drying. Kanoija et al. (Kanojia, Willems, et al. 2016) spray-dried several formulations of an influenza vaccine with trehalose as an excipient and held the powder at 60 °C for three months. For all tested formulations, greater than 86% of the antigen was retained after the stability study. Conversely, the liquid influenza vaccine when stored under the same conditions lost all antigenicity after only 5 days. However, appropriate stabilizer is dependent on the structure of the vaccine. Toniolo et al. (Toniolo, et al. 2019) spray-dried enveloped and non-enveloped viral vaccines using combinations of trehalose, mannitol, dextran, and lactose as stabilizers and stored the powders at 37 °C. The thermostability of the spray-dried vaccines was improved over the liquid vaccine, with up to 50% titer remaining for certain vaccine and excipient formulations after 30 days. Titer for the liquid vaccine was reduced to 0 after only 15 days when stored under the same conditions. The different types of vaccines had different levels of titer remaining for the same processing conditions and stabilizer used. The enveloped viral

vaccines had different levels of stabilization success but showed a similar trend in titer loss as compared to the non-enveloped vaccine. Trehalose and trehalose mixtures stabilized the enveloped vaccines best, whereas the non-enveloped viral vaccine was best stabilized by the mannitol-dextran mixture. Given such differences, the optimal formulation depends on the vaccine type.

However, success of long-term vaccine stabilization is also dependent on the spray drying parameters. Analysis of HSV-2 vaccine spray-dried with either trehalose or sucrose as the stabilizing excipient under various processing conditions after storage at 45 °C over 10 days showed differences in activity loss among samples (LeClair, et al. 2019). Trehalose-containing HSV-2 powders exhibited suitable thermostability. Sucrose was not as effective as a stabilizer. The HSV-2 vaccine powders stabilized with sucrose had a large range of activity loss depending on the spray drying parameters used, indicating that the processing conditions will affect the long-term stabilization of the vaccine. To this end, this study also assessed the long-term stability of the spray-dried SD-TG and SD-TGI powders to determine if processing conditions and trehalose were appropriate for conferring thermostability.

A protective packaging method was necessary to effectively evaluate the stability of dry powders. This study showed that moisture content of the spray-dried vaccine powder remained low over throughout the stability study for all storage temperatures. Proper packaging method likely conferred protection of powders against moisture uptake. Proper packaging is required to preserve powder integrity, as shown for spray-dried anthrax vaccine powders held at 25 and 40 °C for three months (Jones, et al. 2017), where the moisture content of the anthrax vaccine powders was within 0.5% of initial measurement after three months of storage due to the use of an effective packaging method. Similarly, Price et al. (Price, et al. 2020) stored spray-dried BCG vaccine powders at

different temperatures up to one year. The vaccine powders were stored in either a scintillation vial or a protective packaging system that utilized desiccant, reactive oxygen species scavengers, and inert gas. Powders stored at 40 °C without humidity protection showed significant titer losses.

The long-term stability study results showed that the spray-dried powders maintained amorphous structure for all storage temperatures over one year. The extremely low normalized residual spectrum of the 40 °C SD-TGI sample after one year storage subtracted from the timepoint 0 spectra indicates that the two samples are remarkably similar and therefore the solid phase of the powder has been maintained over this period, even with the added thermal stress placed on the powder. As shown in these results, trehalose, when stored dry, does not crystallize. This was also shown for spray-dried anthrax vaccine powders using a packaging system including desiccant (Jones, et al. 2017). These powders also used trehalose as the main stabilizing excipient. The moisture content of the powders remained close to the initial measurement, and the powders remained amorphous. Vandenheuval et al. (Vandenheuvel, et al. 2014) spray-dried bacteriophages in trehalose powders and stored them at 4 and 25 °C at 0 and 54% RH. They found that phage was inactivated due to the crystallization of amorphous trehalose. This result is due to the storage of unprotected trehalose-based powders at high humidity. The spray-dried SD-TG and SD-TGI powders did not crystallize in this study, indicating that the packing system effectively protected the powders from crystallization caused by exposure to high humidity.

Suboptimal encapsulation of the emulsion resulting from inappropriate processing parameters can lead to accumulation of emulsion droplets on the surface of the particle (Jones, et al. 2013). Particles with a high surface oil content were reported to have small protrusions on the outer

surface (Jones, et al. 2013) or exhibit a pockmarked surface (Wang, Che, et al. 2015, Jones, et al. 2013). The studies suggested that the protrusions are caused by the covered oil droplets and the pockmarks are from the surface oil droplets rupturing, leaving behind small craters in the outer particle wall. As neither of these surface morphologies is seen in either of the SD-TG or the SD-TGI particles SEM, it appears that no nanoemulsion droplets accumulated directly on the outer surface. Additionally, images of the particles obtained over the course of the stability study showed that interior and exterior morphology was overall preserved. Some bridging was shown between the small particles of the spray-dried vaccine powder stored at 40 °C. However, bridging is to be expected after long term storage at high temperatures. Particle fusing among smaller particles was also shown in spray-dried HAC1 vaccine with trehalose after storage for three months at 50 °C (Zhu, et al. 2014). Bridging between particles is due to transition to a more energy favorable state through surface area reduction. This bridging is facilitated by increased molecular mobility due to increased temperature. However, the overall lack of particle fusing, shape change, and maintenance of internal structure indicates physical stability was achieved. Physical stability at a higher temperature over twelve months is a strong indicator of long-term physical stability at room temperature.

Reported nanoemulsion droplet diameter change after 13.5 months of storage was within a few percent of the initial measurement for all storage temperatures. These results can be compared to a stability study completed on the liquid single-vial presentation, the two vial clinical presentation, the proof of concept lyophilized candidate, as well as the lead lyophilized candidates (Kramer, et al. 2018). Compared to three-month stability studies at 37 °C conducted on lead lyophilized candidates and liquid single-vial presentation, the spray-dried powders have a comparable or better

performance regarding droplet size change (Kramer, et al. 2018). Additionally, the droplet diameter of the spray-dried candidates undergo less change than the 2-vial clinical presentation and the proof-of-concept lyophilized candidate (Kramer, et al. 2018). The droplet size of the 2-vial clinical presentation increased to over 240 nm, and the droplet size of the lyophilized proof-of-concept candidate increased to over 200 nm after three months' storage at 37 °C. It is apparent that the spray-dried powders have greatly improved the thermostability of the ID93+GLA-SE vaccine candidate. Emulsion diameter results combined with the results of particle morphology, moisture content, and solid-state analysis further indicate that the powder is well-stabilized physically by trehalose. Mlalila et al.'s (Mlalila, et al. 2014) experiments of spray drying w/o/w methyltestoterone emulsion droplets initially showed similar preservation of droplet diameter immediately after spray drying. However, after one month of storage in a desiccator the nanoemulsion droplet sizes increased by a factor of 2-8. In this particular case, the stabilizer of stearic acid was unable to prevent droplets from aggregating. By contrast, our study shows that trehalose was an effective stabilizer of the vaccine's phospholipid membrane and offered significant thermal protection. Pereira and Hünenberger (Pereira and Hunenberger 2006) showed that the bilayer structure of DPPC liposomes in water was thermally disrupted at 475 K, but the structure was preserved when trehalose was added to the solution.

High levels of squalene were retained after 13.5 months of storage, even at high temperatures. Approximately 40% GLA losses were shown in the samples stored at 40 °C after three months of storage, failing the target stability criteria. However, this result is comparable to the reported GLA loss in the lyophilized proof-of-concept formulation. When stored at 37 °C for three months, the lyophilized proof-of-concept formulation exhibited a decrease of 48% in GLA concentration

(Kramer, et al. 2018). GLA loss for the lead lyophilized candidates and two-vial clinical presentation ranged from no losses up to 36% loss in content (Kramer, et al. 2018). The spray-dried formulations perform comparably to the proof-of-concept lyophilized formulation. The lead lyophilized candidates generally outperform the spray-dried formulations in terms of GLA retention. However, these lead candidates were developed and tested after an extensive design-of-experiments approach. The spray-dried candidates in this paper are a first iteration and clearly exhibit some improved protection against degradation as compared to the liquid vaccine. Approximately 40% of the GLA content was retained after storage at the most extreme condition, whereas all GLA was degraded when stored as a liquid product at similar temperatures (Kramer, et al. 2018). Degradation of GLA was shown to increase with increasing temperature storage. Approximately 80% of GLA was retained for the spray-dried samples stored at room temperature after 13.5 months. This is to be expected as GLA similarly showed temperature-influenced degradation in the lyophilized candidates (Kramer, et al. 2018). The presence of antigen ID93 was confirmed after 13.5 months of storage at all temperatures. These results indicate that spray drying the ID93+GLA-SE vaccine candidate conferred some level of thermostability in terms of chemical preservation.

Squalene loss and GLA degradation did not exhibit a linear pattern over time. Squalene and GLA degradation appeared to have occurred primarily during the first three months of the stability study. Measured content for the remaining timepoints appear to be either relatively constant or decreasing slightly. Powder crystallization may lead to loss of stabilizing hydrogen bonds with the phosphate head groups of the GLA-SE membrane. However, characterization of the physical stability of the powder indicates that the powder remains amorphous and that therefore GLA is not degrading due

to crystallization of the powder. Air-dried enveloped viral vaccines stabilized in trehalose-pullulan films exhibited a similar degradation pattern of initially rapid loss followed by a period of gradual loss (Leung, et al. 2019). It was suggested that this degradation pattern indicates the existence of multiple degradation mechanisms.

2.5. Conclusion

A subunit vaccine candidate containing a nanoemulsion adjuvant system with trehalose and Tris buffer as additional excipients was spray-dried and the stability of the dry powder product was evaluated over one year. Two formulations were tested for stability: (1) the oil-in-water nanoemulsion adjuvant system, and (2) the oil-in-water adjuvant system with the protein antigen. *In-silico* formulation and process development were utilized, significantly reducing the required amount of empirical work. This approach is especially prudent for work that involves highly complicated formulations. To the authors' best knowledge, these are the first published results regarding the stabilization of a subunit vaccine formulated as a nanoemulsion at the 100-nm diameter scale using trehalose via spray drying and showing long-term stability potential.

These results are especially meaningful in light of global health applications as refrigeration infrastructure required for vaccine distribution is not always available. Because our dry power is stable at a wide temperature range, it alleviates the necessity for such refrigeration infrastructure. The dry powder product was physically stable after twelve months of storage at a high temperature up to 40 °C, suggesting that the product is physically stable for long-term storage under ambient temperature. Besides, formulating the vaccine as a dry powder and reconstituting as needed will significantly reduce the costs associated with transport and storage. In comparison to the lyophilization treatment of these biological formulations, which has been proven to be a beneficial

method of storage (Kramer, et al. 2018), spray drying presents a promising alternative with its potentially lower processing cost and improved scalability (Schwartzbach 2011). The increased production capability of spray drying can be utilized to stockpile larger amounts of thermostable vaccine for pandemic situations. Moreover, spray-dried vaccines have the potential to be administered directly by inhalation without the need for reconstitution (Argarkhedkar, et al. 2014).

Comparison of the formulation feedstock and the reconstituted spray-dried powder showed that the integrity of the emulsion was maintained for both size and squalene concentration. The agonist was shown to have a similar concentration and the antigen presence was confirmed post-spray drying. The preservation of physicochemical properties upon reconstitution strongly suggests that the efficacy of the vaccine is preserved over the course of spray drying. These spray-dried powders were then assessed for stability over one year, up to a temperature of 40 °C, through characterization of the reconstituted powder and the dry powder itself. The results showed that the powders maintained physical stability for all temperatures after one year. Powder stability at one year at a higher temperature suggests long-term stability at room temperature. Physicochemical characterization for both formulations, at all temperatures, showed that the average nanoemulsion droplet size and polydispersity did not change appreciably; they performed significantly better than a lyophilized proof-of-concept and on par with the lead lyophilized candidates (Kramer, et al. 2018). Agonist preservation was on par with the proof-of-concept lyophilized version (Kramer, et al. 2018). After being held for three months up to 50 °C, immune cell production for the lyophilized vaccine was maintained whereas the liquid vaccine lost most of its immunogenicity under the same conditions. Immunogenicity studies have not been carried out on the spray-dried vaccine; however,

the spray-dried vaccine appears to be comparable to the lyophilized vaccine in terms of biophysical characterization.

This study showed that integrity of both the biologic and the adjuvant system was preserved over the spray drying process. Given the small scale, the efficiency of encapsulation and preservation of the nanoemulsion droplets is especially notable. The dry powder version of oil-in-water adjuvant systems can be combined with subunit vaccines for other diseases. Further formulation development must be conducted to improve long term chemical stability. Spray drying, unlike lyophilization, allows for the engineering of properties such as particle size and flowability. These properties open doors to other delivery routes, such as pulmonary and intranasal, rather than intramuscular injections. The demonstrated preservation of the physical state of the spray-dried powder suggests that it will maintain aerosol performance even after long-term storage at high temperatures.

2.6. References

Argarkhedkar, Sharad, Prasad S. Kulkarni, Scott Winston, Robert Sievers, Rajeev M. Dhere, Bhagwat Gunale, Ken Powell, Paul a. Rota, Mark Papania, and MDVP author group. 2014. "Safety and immunogenicity of dry powder measles vaccine administered by inhalation: A randomized controlled Phase 1 clinical trial." *Vaccine* 32: 6791-6797. doi:10.1016/j.vaccine.2014.09.071.

Arpagaus, Cordin, Andreas Collenburg, David Rutti, Elham Assadpour, and Seid Mahdi Jafari. 2018. "Nano spray drying for encapsulation of pharmaceuticals." *International Journal of Pharmaceutics* 546: 194-214. doi:10.1016/j.ijpharm.2018.05.037.

Bertholet, Sylvie, Gregory C. Ireton, Diane J. Ordway, Hillarie Plessner Windish, Samuel O. Pine, Maria Kahn, Tony Phan, et al. 2010. "A defined tuberculosis vaccine candidate boosts BCG and protects against multidrug-resistant Mycobaterium tuberculosis." *Science Translational Medicine* 2 (53): 53-74. doi:10.1126/scitranslmed.3001094.

Bertholet, Sylvie, Gregory C. Ireton, Maria Kahn, Jeffrey Guderian, Raodoh Mohamath, Nicole Stride, Elsa M. Laughlin, et al. 2008. "Identification of human T cell antigens for the development of vaccines against Mycobacterium tuberculosis." *Journal of Immunology* 181 (11): 7948-7957. doi:10.4049/jimmunol.181.11.7948.

Bringas-Lantigua, Madai, Idalmis Exposito-Molina, Gary A. Reineccius, Orestes Lopez-Hernandez, and Jorge A. Pino. 2011. "Influence of spray-dryer air temperatures on encapsulated mandarin oil." *Drying Technology* 29: 520-526. doi:10.1080/07373937.2010.513780.

Carrigy, Nicholas B. , Lu Liang, Hui Wang, Samuel Kariuki, Tobi E. Nagel, Ian F. Connerton, and Reinhard Vehring. 2019. "Trileucine and pullulan improve anti-Campylobacter bacteriophage stability in

engineered spray-dried microparticles." *Annals of Biomedical Engineering* 48: 1169-1180. doi:10.1007/s10439-019-02435-6.

Carrigy, Nicholas B., and Reinhard Vehring. 2019. "Engineering stable spray-dried biologic powder for inhalation." In *Pharmaceutical Inhalation Aerosol Technology (3rd ed.)*, edited by A. J. Hickey and S. da Rocha, 291-326. Boca Raton: CRC Press.

Chan, Michelle Y., Quinton M. Dowling, Sandra J. Sivananthan, and Ryan M. Kramer. 2017. "Particle sizing of nanoparticle adjuvant formulations by dynamic light scattering (DLS) and nanoparticle tracking analysis (NTA)." *Methods in Molecular Biology* 1494: 239-252. doi:10.1007/978-1-4939-6445-1_17.

Chen, Tani, Alex Fowler, and Mehmet Toner. 2000. "Literature review: supplemented phase diagram of the trehalose-water binary mixture." *Cryobiology* 40 (3): 277-282.

Coler, Rhea N., Sylvie Bertholet, Magdalini Moutaftsi, Jeff A. Guderian, Hillarie Plessner Windish, Susan L. Baldwin, Elsa M. Laughlin, et al. 2011. "Development and characterization of synthetic glucopyranosyl lipid adjuvant system as a vaccine adjuvant." *Public Library of Science One* 6 (1): e16333. doi:10.1371/journal.pone.0016333.

Coler, Rhea N., Tracey A. Day, Ruth Ellis, Franco M. Piazza, Anna Marie Beckmann, Julie Vergara, Tom Rolf, et al. 2018. "The TLR-4 agonist adjuvant, GLA-SE, improves magnitude and quality of immune responses elicited by the ID93 tuberculosis vaccine: first-in-human trial." *Nature Partner Journals* 3 (34). doi:10.1038/s41541-018-0057-5.

Crowe, Lois M., David S. Reid, and John H. Crowe. 1996. "Is trehalose special for preserving dry biomaterials?" *Biophysical Journal* 71: 2087-2093.

Encina, Cristian, Cristina Vergara, Begona Gimenez, Felipe Oyarzun-Ampuero, and Paz Robert. 2016. "Conventional spray-drying and future trends for the microencapsulation of fish oil." *Trends in Food Science & Technology* 56: 46-60.

Encina, Cristian, Gloria Marquez-Ruiz, Francisca Holgado, Begona Gimenez, Cristina] Vergara, and Paz Robert. 2018. "Effect of spray-drying with organic solvents on the encapsulation, release and stability of fish oil." *Food Chemistry* 263: 283-291. doi:https://doi.org/10.1016/j.foodchem.2018.05.026.

Flynn, JoAnne L., and John Chan. 2001. "Immunology of Tuberculosis." *Annual Review of Immunology* 19 (1): 93-129.

Fox, Christopher B., Ryan C. Anderson, Timothy S. Dutill, Yasuyuki Goto, Steven G. Reed, and Thomas S. Vedvick. 2008. "Monitoring the effects of component structure and source on formulation stability and adjuvant activity of oil-in-water emulsions." *Colloids and Surfaces B; Biointerfaces* 65: 98-105.

Gharsallaoui, Adem, Gaelle Roudaut, Odile Chambin, Andree Voilley, and Remi Saurel. 2007. "Applications of spray-drying in microencapsulation of food ingedients: An overview." *Food Research International* 2007: 1107-1121.

Gordon, Manfred, and James S. Taylor. 1952. "Ideal copolymers and the second-order transitions of synthetic rubbers. i. non-crystalline copolymers." *Journal of Applied Chemistry* 2 (9): 493-500.

Grasmeijer, N., M. Stankovic, H. de Waard, H. W. Frijlink, and W. L. J. Hinrichs. 2013. "Unraveling protein stabilization mechanisms: vitrification and water replacement in a glass transition temperature controlled system." *Biochimica et Biophysica Acta* 1834 (4): 763-769. doi:10.1016/j.bbapap.2013.01.020.

Hoe, Susan, James W. Ivey, Mohammed A. Boraey, Abouzar Shamsaddini-Shahrbabak, Emadeddin Javaheri, Matinkhoo Sadaf, Warren H. Finlay, and Reinhard Vehring. 2014. "Use of a fundamental approach to spray-drying formulation design to facilitate the development of multi-component dry powder aerosols for respiratory drug delivery." *Pharmaceutical Research* 32 (2): 449-465.

Iglesias, Hector A., Jorge Chirife, and Maria P. Buera. 1999. "Adsorption isotherm of amorphous trehalose." *Journal of the Science of Food and Agriculture* 75 (2): 183-186.

Infectious Disease Research Institute. 2019. "Identifier: NCT03722472, Phase 1 Clinical Trial of Single-Vial ID93 + GLA-SE in Healthy Adults." *U.S. National Library of Medicine Clinical Trials Registry.* September 3. Accessed April 23, 2020. https://clinicaltrials.gov/ct2/show/NCT03722472?term=id93&draw=2&rank=1.

Ingvarsson, Pall Thor, Mingshi Yang, Hanne Morck Nielsen, Jukka Rantanen, and Camilla Foged. 2011. "Stabilization of liposomes during spray drying." *Expert Opinion on Drug Delivery* 8 (3): 375-388. doi:10.1517/17425247.2011.553219.

Ingvarsson, Pall Thor, Signe Tandrup Schmidt, Dennis Christensen, Niels Bent Larsen, Wouter Leonardus Joseph Hindrichs, Peter Andersen, Jukka Rantanen, Hanne Morck Nielson, Mingshi Yang, and Camilla Foged. 2013. "Designing CAF-adjuvanted dry powder vaccines: Spray drying preserves the adjuvant activity of CAF01." *Journal of Controlled Release* 167: 256-264. doi:10.1016/j.jconrel.2013.01.031.

International Conference On Harmonisation Of Technical Requirements For Registration Of Pharmaceuticals For Human Use. 2003. *ICH Harmonised Tripartite Guideline - Stability Testing of New Drug Substances and Products Q1A(R2).* ICH.

Ivey, James W., and Reinhard Vehring. 2010. "The use of modeling in spray drying of emulsions and suspensions accelerates formulation and process development." *Computers and Chemical Engineering* 34: 1036-1040. doi:10.1016/j.compchemeng.2010.02.031.

Ivey, James, Pallavi Bhambri, David Lewis, Tayna Church, Warren Finlay, and Reinhard Vehring. 2016. "Dried corticosteroid particle formation from evaporating monodisperse propellant solution droplets." *AAPS Annual Meeting and Exposition.* Denver.

Jafari, Seid Mahdi, Elham Assadpoor, Yinghe He, and Bhesh Bhandari. 2008. "Encapsulation efficiency of food flavours and oils during spray drying." *Drying Technology* 26 (7): 816-835.

Jin, Tom H., Eric Tsao, Jaap Goudsmit, Veerabadran Dheenadhayalan, and Jerald Sadoff. 2010. "Stabilizing formulations for inhalable powders of adenovirus 35-vectored tuberculosis (TB) vaccine (AERAS-402)." *Vaccine* 28: 4639-4375. doi:10.1016/j.vaccine.2010.04.059.

Jones, Jim R., Dominic Prime, Mark C. Leaper, David J. Richardson, Chris D. Rielly, and Andrew G. F. Stapley. 2013. "Effect of processing variables and bulk composition on the surface composition of spray dried powders of a model food system." *Journal of Food Engineering* 118: 19-30.

Jones, R. Mark, Michael Burke, Devon Dubose, Jessica A. Chichester, Slobodanka Manceva, April Horsey, Stephen J. Streatfield, Jeff Breit, and Vidadi Yusibov. 2017. "Stability and pre-formulation development of a plant-produced anthrax vaccine candidate." *Vaccine* 35: 5463-5470. doi:10.1016/j.vaccine.2016.12.009.

Kanojia, Gaurav, Geert-Jan Willems, Henderik W. Frijlink, Gideon F. A. Kersten, Peter C. Soema, and Jean-Pierre Amorij. 2016. "A design of experiment approach to predict product and process parameters for a spray-dried influenza vaccine." *International Journal of Pharmaceutics* 511: 198-1111. doi:10.1016/j.ijpharm.2016.08.022.

Kanojia, Gaurav, Rene H. M. Raeven, Larissa van der Maas, Tim H. E. Bindels , Elly van Riet, Bernard Metz, Peter C. Soema, et al. 2018. "Development of a thermostable spray dried outer membrane vesicle pertussis vaccine for pulmonary immunization." *Journal of Controlled Release* 286: 167-178. doi:10.1016/j.jconrel.2018.07.035.

Kanojia, Gaurav, Rimko ten Have, Peter C. Soema, Henderik Frijlink, Pierre Amorij, and Gideon Kersten. 2017. "Developments in forumulation and delivery of spray dried vaccines." *Human Vaccines & Immunotherapeutics* 13 (10): 2364-2378. doi:10.1080/21645515.2017.1356952.

Kramer, Ryan M., Michelle C. Archer, Natasha Dubois, Natasha Dubois Cauwelaert, Elyse A. Beebe, Po-wei D. Huang, Quinton M. Dowling, et al. 2018. "Development of a thermostable nanoemulsion adjuvanted vaccine against tuberculosis using a design-of-experiments approach." *International Journal of Nanomedicine* 13: 3689-3711.

Krogsgard Nielsen, Christina, Jorgen Kjems, Tina Mygind, Torben Snabe, Karin Schwarz, Yvonne Serfert, and Rikke Louise Meyer. 2016. "Enhancing the antibacterial efficacy of isoeugenol by emulsion encapsulation." *International Journal of Food Microbiology* 229: 7-14.

Lammert, Amy M., Shelly J. Schmidt, and Gary A. Day. 1998. "Water activity and solubility of trehalose." *Food Chemistry* 61 (1): 139-144.

LeClair, Daniel A., Lillian Li, Nausheen Rahman, Emily D. Cranston, Zhou Xing, and Michael R. Thompson. 2019. "Stabilization of HSV-2 viral candidate by spray drying." *International Journal of Pharmaceutics* 569: 1-10. doi:10.1016/j.ijpharm.2019.118615.

Leung, Vincent, Jonathan Mapletoft, Ali Zhang, Amanda Lee, Fatemeh Vahedi, Marianne Chew, Alexandra Szewczyk, et al. 2019. "Thermal stabilization of viral vaccines in low-cost sugar films." *Scientific Reports* 9 (7631).

Linke, Annika, Tobias Balke, and Reinhard Kohlus. 2018. "Identification of key factors determining the surface oil concentration of encapsulated lipid particles produced by spray drying." *21st International Drying Symposium*. Valencia, Spain. doi:http://dx.doi.org/10.4995/ids2018.2018.7739.

Mensink, Maarten A., Henderik W. Frijlink, Kees van der Voort Maarschalk, and Wouter L. J. Hinrichs. 2017. "How sugars protect proteins in the solid state and during drying (review): Mechanisms of stabilization in relation to stress conditions." *European Journal of Pharmaceutics and Biopharmaceutics* 114: 288-295.

Mlalila, Nichrous, Hulda Swai, Lonji Kalombo, and Askwar Hilonga. 2014. "Effects of spray-drying on w/o/w multiple emulsions prepared from a stearic acid matrix." *Nanotechnology, Science and Applications* 7: 105-112. doi:10.2147/NSA.S72083.

Munoz-Ibanez, Marta, Christiane Azagoh, Bipro Nath Dubey, Elisabeth Dumoulin, and Christelle Turchiuli. 2015. "Changes in oil-in-water emulsion size distribution during the atomization step in spray-drying encapsulation." *Journal of Food Engineering* 167: 122-132.

Ohtake, Satoshi, and John Wang. 2011. "Trehalose: current use and future applications." *Journal of Pharmaceutical Sciences* 100 (6): 2020-2053.

Orr, Mark T., Ryan M. Kramer, Lucien V. Barnes, Quinton M. Dowling, Anthony L. Desbien, Elyse A. Beebe, John D. Laurance, et al. 2014. "Elimination of the cold-chain dependence of a nanoemulsion adjuvant vaccine against tuberculois by lyophilization." *Journal of Controlled Release* 10 (177): 20-26. doi:10.1016/j.jconrel.2013.12.025.

Pang, Yuqi, Xu Duan, Guangyue Ren, and Wenchao Liu. 2017. "Comparative study on different drying methods of fish oil microcapsules." *Journal of Food Quality* 1-7. doi:10.1155/2017/1612708.

Paramita, V., K. Iida, H. Yoshii, and T. Furuta. 2010. "Effect of additives on the morphoolgy of spray-dried powder." *Drying Technology* 28 (3): 323-329. doi:10.1080/07373931003627098.

Pereira, Cristina S., and Philippe H. Hunenberger. 2006. "Interaction of the sugars trehalose, maltose and glucose with a phospholipid bilayer: a comparative molecular dynamics study." *The Journal of Physical Chemistry* 110 (31): 15572-15581. doi:10.1021/jp060789l.

Price, Dominique N., Nitesh K. Kunda, Rajaun Ellis, and Pavan Muttil. 2020. "Design and optimization of a temperature-stable dry powder BCG vaccine." *Pharmaceutical Research* 37 (11): 1-14. doi:10.1007/s11095-019-2739-8.

Re, Maria-Ines. 2006. "Formulating Drug Delivery Systems by Spray Drying." *Drying Technology* 24: 433-446.

Reed, Steven G., Sylvie Bertholet, Rhea N. Coler, and Martin Friede. 2009. "New horizons in adjuvants for vaccine development." *Trends in Immunology* 30 (1): 23-32. doi:10.1016/j.it.2008.09.006.

Ribeiro, Roseane Fagundes, Mariana Heldt Motta, Andreia Pisching Garcia Harter, Fernanda Cramer Flores, Ruy Carlos Ruver Beck, Scheila Rezende Schaffazick, and Cristiane de Bona da Silva. 2016. "Spray-dried powders improve the controlled relase of antifungal tioconazole-loaded polymeric nanocapsules compared to with lyophilized products." *Materials Science and Engineering C* 59: 875-884.

Richards, A. B., S. Krakowka, L. B. Dexter, H. Schmid, A. P. M. Wolterbeek, D. H. Waalkens-Berendsen, A. Shigoyuki, and M. Kurimoto. 2002. "Trehalose: a review of properties, history of use and human tolerance, and results of multiple safety studies." *Food and Chemical Toxicology* 40: 871-898.

Roe, K. D., and T. P. Labuza. 2005. "Glass transition and crystallization of amorphous trehalose-sucrose mixtures." *International Journal of Food Properties* 8 (3): 559-574.

Sarkar, Anwesha, Judith Arfsten, Pierre-Alain Golay, Simone Acquistapace, and Emmanuel Heinrich. 2016. "Microstructure and long-term stability of spray dried emulsions with ultra-high oil content." *Food Hydrocolloids* 52: 857-867.

Schwartz, Alicia M., Michelle Y. Chan, Dawn M. Fedor, and Sandra J. Sivananthan. 2017. "Staining and transfer techniques for SDS-PAGE Gels to minimize oil-in-water emulsion adjuvant interference." In *Vaccine Adjuvants. Methods in Molecular Biology, vol 1494*, 273-283. New York: Humana Press. doi:10.1007/978-1-4939-6445-1_20.

Schwartzbach, Henrik. 2011. "Achieving aseptic drying with spray drying technologies." *Pharmaceutical Technology Europe* 23 (9).

Sou, Tomas, David A. V. Morton, Mark Williamson, Els N. Meeusen, Lisa M. Kaminskas, and Michelle P. McIntosh. 2015. "Spray-dried influenza antigen with trehalose and leucine produces an aerosolizable powder vaccine formulation that induces strong systemic and mucosal immunity after pulmonary administration." *Journal of Aerosol Medicine and Pulmonary Drug Delivery* 28 (5): 361-371. doi:10.1089/jamp.2014.1176.

Thakur, Aneesh, Pall Thor Ingvarsson, Signe Tandrup Schmidt, Fabrice Rose, Peter Andersen, Dennis Christensen, and Camilla Foged. 2018. "Immnological and physical evaluation of the multistage tuberculosis subunit vaccine candidate H56/CAF01 formulated as a spray dried powder." *Vaccine* 36: 3331-3339. doi:10.1016/j.vaccine.2018.04.055.

Toniolo, Steven P., Sam Afkhami, Ahmad Mahmood, Cecile Fradin, Brian D. Lichty, Matthew S. Miller, Zhou Xing, Emily D. Cranston, and Michael R. Thompson. 2019. "Excipient selection for thermally stable enveloped and non-enveloped viral vaccine platforms in dry powders." *International Journal of Pharmaceutics* 561: 66-73. doi:10.1016/j.ijpharm.2019.02.035.

Tonnis, W. F., M. A. Mensink, A. de Jager, K. van der Voort Maarschalk, H. W. Frijlink, and W. L. Hinrichs. 2015. "Size and molecular flexibility of sugars determine the storage stability of freeze-dried proteins." *Molecular Pharmaceutics* 12: 684-694. doi:10.1021/mp500423z.

Vandenheuvel, Dieter, Joke Meesus, Rob Lavigne, and Guy Van den Mooter. 2014. "Instability of bacteriophages in spray-dried trehalose powders is caused by crystallization of the matrix." *International Journal of Pharmaceutics* 472: 202-205.

Vehring, Reinhard. 2008. "Pharmaceutical Particle Engineering via Spray Drying." *Pharmaceutical Research* 25 (5): 999-1022. doi:10.1007/s11095-007-9475-1.

Vehring, Reinhard. 2005. "Red-excitation dispersive Raman spectroscopy is a suitable technique for solid-state analysis of respirable pharmaceutical powders." *Applied Spectroscopy* 59 (3): 286-292.

Vehring, Reinhard, Willard R. Foss, and David Lechuga-Ballesteros. 2007. "Particle formation in spray drying." *Aerosol Science* 38: 728-746.

Wang, Hui, David Barona, Sulayman Oladepo, Lisa Williams, Susan Hoe, David Lechuga-Ballesteros, and Reinhard Vehring. 2017. "Macro-Raman spectroscopy for bulk composition and homogeneity analysis of multi-component pharmaceutical powders." *Journal of Pharmaceutical and Biomedical Analysis* 141: 180-191.

Wang, Hui, David S. Nobes, and Reinhard Vehring. 2019. "Particle Surface Roughness Improves Colloidal Stability of Pressured Pharmaceutical Suspensions." *Pharmaceutical Research* 36 (43). doi:https://doi.org/10.1007/s11095-019-2572-0.

Wang, Yang, Liming Che, Nan Fu, Xiao Dong Chen, and Cordelia Selomulya. 2015. "Surface formation phenomena of DHA-containing emulsion during convective droplet drying." *Journal of Food Engineering* 150: 50-61.

Wang, Yang, Wenjie Liu, Xiao Dong Chen, and Cordelia Selomulya. 2019. "Micro-encapsulation and stabilization of DHA containing fish oil in protein-based emulsion through mono-disperse droplet spray dryer." *Journal of Food Engineering* 175: 74-84.

Waterman, Kenneth C., and Bruce C. MacDonald. 2010. "Package selection for moisture protection for solid, oral drug products." *Journal of Pharmaceutical Sciences* 99 (11): 4437-4452. doi:10.1002/jps.22161.

World Health Organization (WHO). 2006. "Temperature sensitivity of vaccines." August. Accessed April 17, 2020. doi:WHO/IVB/06.10.

World Health Organization. 2019. *Global Tuberculosis Report.* Geneva: World Health Organization. https://www.who.int/tb/publications/global_report/en/.

World Health Organization. 2018. *WHO Preferred Product Characteristics for New Tuberculosis Vaccines.* Geneva: World Health Organization.

Zhou, Deliang, Geoff G.Z. Zhang, Devalina Law, David J.W. Grant, and Eric A. Schmitt. 2000. "Physical stability of amorphous pharmaceuticals: Importance of configurational thermodynamic quantities and molecular mobility." *Journal of Pharmaceutical Sciences* 91 (8): 1863-1872.

Zhu, Changcheng, Yoko Shoji, Michael Burke, Caitlin E. Hartman, Jessica A. Chichester, Jeff Breit, Vidadi Yusibov, Dexiang Chen, and Manjari Lal. 2014. "Stabilization of HAC1 Influenza Vaccine by Spray Drying." *Pharmaceutical Research* 31: 3006-3018. doi:10.1007/s11095-014-1394-3.

Ziaee, Ahmad, Ahmad B. Albadarin, Luis Padrela, Tim Femmer, Emmet O'Reilly, and Gavin Walker. 2019. "Spray drying of pharmaceuticals and biopharmaceuticals: Critical parameters and experimental process optimization approaches." *European Journal of Pharmaceutical Sciences* 127: 300-318.

Chapter 3. Formulation development for a spray-dried, inhalable tuberculosis vaccine

3.1. Introduction

Spray drying is a method of desiccating a liquid product into a dry powder composed of many small particles. Briefly, a liquid feedstock is atomized into small droplets during spray drying. These droplets, containing dissolved or suspended solids, evaporate within a drying gas into particles. The particles are then separated from the flow, e.g. with a cyclone. Spray drying is commonly used in the food processing and pharmaceutical industries to encapsulate an active component into a dry powder and thus protect it from potentially harmful environmental conditions, such as high humidity and temperature (Carrigy and Vehring 2019). Spray drying has been previously used to improve the stability of experimental vaccines using the disaccharide trehalose as a stabilizer (LeClair, et al. 2019, Jones, et al. 2017, Toniolo, et al. 2019, Kanojia, Willems, et al. 2016). Spray drying also allows for engineering of the resulting particles for specific properties, making them suitable for intranasal or pulmonary routes via inhalation (Kunda, et al. 2015, Sou, et al. 2015, Price, et al. 2020). Both the improvement of thermostability and the development of an inhalable route of delivery are useful for vaccines as these properties address the elimination of cold-chain requirements and the development of additional routes of administration, respectively.

Preclinical trials have been promising. However, as dry powder vaccination via inhalation is an emerging field, clinical trials are limited. The first inhalable dry powder vaccine for pulmonary delivery, a measles vaccine, completed Phase I clinical trials in 2013 (Argarkhedkar, et al. 2014).

Further work is warranted because there are many benefits to developing alternative administration routes to injection. The general advantages of respiratory drug delivery include convenience, reduced chance of adverse systemic reactions, and smaller amounts of drug required due to direct targeting. Compared to injectable delivery, the use of a non-invasive route of administration reduces the chance of needlestick injuries, and with that reduces the transmission of blood-borne illnesses such as HIV. It also eliminates needle waste. As well, mucosal immunization through inhalable delivery is potentially more effective at conferring protection than parenteral injection against respirable diseases, such as tuberculosis (TB) (Aguilo, et al. 2016). Additionally, injectable delivery of a reconstituted vaccine requires sterile water, a commodity that is taken for granted in developed nations.

TB is a disease caused by *Mycobacterium tuberculosis* infection. TB is the leading cause of death from a single infectious agent, and approximately 10 million people contracted TB in 2018 (World Health Organization 2019). TB is transmitted through air as droplets, making the lungs the primary infection site (Flynn, Chan and Llin 2011). Currently, the bacille Calmette-Guérin (BCG) vaccine is the only licensed TB vaccine. BCG is administered via injection as part of standard childhood immunization programs in many countries (World Health Organization 2019). Due to the widespread use of BCG, any improvement in efficacy would have a large impact. To this end, administration routes alternative to injection have been investigated for BCG. Research involving animal models have reported that the BCG vaccine provides better protection against TB when administered to the respiratory system directly rather than through injection (Chen, et al. 2004, Derrick, et al. 2014, Aguilo, et al. 2016, Verreck, et al. 2017). Aguilo et al. (Aguilo, et al. 2016) demonstrated that intranasal delivery of BCG, but not subcutaneous delivery, conferred protection

against pulmonary TB in TB-susceptible mice. Verreck et al. (Verreck, et al. 2017) suggested that pulmonary immunization results in a more reliably protective local immune response. Recently, Price et al. (Price, et al. 2020) spray-dried the BCG vaccine into a thermostable presentation designed for inhalable dry powder delivery. Mouse immunization studies showed that the liquid BCG vaccine, the reconstituted freshly spray-dried BCG vaccine, and the reconstituted spray-dried BCG vaccine stored at 25 °C for two years had no significant difference in induced cytokine response in mice. However, despite the effort in improving the efficacy of BCG vaccine via different routes of delivery, the vaccine carries several limitations. It has demonstrated variable efficacy in humans based on geography (0-80%) (Andersen and Doherty 2005), confers only limited protection to adults (World Health Organization 2019), is unsafe for immunocompromised infants (Hesseling, et al. 2009), and is not effective in preventing latent TB from becoming active (World Health Organization 2019). Alternative vaccines for TB are being developed to address these shortcomings.

One such vaccine candidate is ID93+GLA-SE, an adjuvanted subunit vaccine comprised of a recombinant fusion antigen, ID93, and an adjuvant system, GLA-SE. The main components of the adjuvant system consist of synthetic TLR4 agonist glucopyranosyl lipid A (GLA), squalene nanodroplets, and DMPC as an emulsifier. ID93+GLA-SE has shown promising results in animal models (Bertholet, Ireton and Ordway, et al. 2010) and has progressed to Phase II clinical testing (World Health Organization 2019). Conversion of this vaccine to a thermostable presentation has been explored, as per WHO guidelines, to focus on thermostable options for promising candidates (World Health Organization (WHO) 2006, World Health Organization 2018). Both lyophilization (Kramer, et al. 2018, Orr, Kramer, et al. 2014) and spray drying have been investigated and found

to confer thermostability using trehalose as a stabilizing excipient. The lyophilized vaccine candidate is currently undergoing a Phase I clinical trial (Infectious Disease Research Institute 2019). Spray drying is considered more scalable than lyophilization, potentially has lower processing costs (Langford, et al. 2018, McAdams, Chen and Kristensen 2012), and also allows for the manipulation of morphology and structure of the final particle product.

Respiratory delivery of an aerosolized powder occurs through nasal or pulmonary routes, each with an optimum particle size range for the most effective drug delivery. Drug particles or drug sprays are usually delivered locally during nasal administration whereas the active components for pulmonary delivery must surpass the upper extrathoracic airways before it can deposit in either the targeted trachea-bronchia region or the targeted alveolar region (Finlay 2019). Therefore, successful pulmonary delivery requires smaller particles (1-5 μm) than for nasal delivery (~20 μm) and much more flowable drug particles that need to be carefully designed (Kanojia, ten Have, et al. 2017, Bahamondez-Canas and Cui 2018, Hickey, et al. 2016, Shang, et al. 2015). In addition, to achieve successful lung deposition, particles must also not get stuck in the delivery device, nor be exhaled out. Therefore, the formulation development for pulmonary delivery can be much more challenging. Two of the most important factors that need to be considered during dry powder formulation development are the aerodynamic particle size and dispersibility of the powder (Usmani, Biddiscombe and Barnes 2005). However, delivery devices, such as dry powder inhalers (DPI), are usually unable to fully disperse the powder to the appropriate size as individual particles will naturally form aggregates due to the intrinsic cohesiveness of the powder. The addition of larger carrier particles is a traditional method to reduce powder retention within DPIs. However, added carriers should be used only for potent actives as they reduce the drug load per inhaled dose.

Instead, particle engineering can be used to improve powder dispersibility through reduction of cohesive forces between particles. Cohesiveness reduction can be accomplished through the addition to the formulation of dispersibility enhancing agents. This paper investigates the use of leucine, pullulan, and trileucine as dispersibility enhancing agents.

Leucine is an amino acid that has been proposed in combination with trehalose as a system to stabilize biologics (Leung, et al. 2018). The leucine component of spray-dried formulations has been designed to form a fully crystalline, rugose outer shell to improve the dispersibility of a powder (Feng, et al. 2011, Li, et al. 2016). Addition of 10-20% leucine has also been shown to protect aerosol performance against moisture-induced decline (Li, et al. 2016). An influenza vaccine has been previously stabilized via spray drying in a 90% trehalose - 10% leucine excipient system, where the resulting powder was fully amorphous and all vaccine components were preserved (Sou, et al. 2015). Pullulan is a polysaccharide that has been used in the food drying industry and pharmaceutical industry to improve thermostability. Films formed from drying pullulan with trehalose have been reported to improve the thermostability of live-attenuated or inactivated viral vaccines for up to 12 weeks at 40 °C (Leung, et al. 2019). The pullulan and trehalose system was shown to improve long-term thermostability of the vaccines over trehalose alone. Spray-dried pullulan and trehalose systems have also been reported to stabilize bacteriophages (Carrigy, Liang, et al. 2019). Under normal spray drying conditions, both pullulan and trehalose remain amorphous (Carrigy, Ordoubadi, et al. 2019). Trileucine is a tripeptide that has been shown to form an amorphous layer on spray-dried particles under normal spray drying conditions (Vehring 2008). The formation of a trileucine layer reduced particle cohesiveness and thus improved aerosol performance (Lechuga-Ballesteros, et al. 2008). The addition of trileucine

as an outer layer has also been shown to improve the stability of trehalose microparticles suspended in HFA227ea propellant (Wang, Nobes and Vehring 2019) and the stability of spray-dried bacteriophages (Carrigy, Liang, et al. 2019).

Improved thermostability and development of an inhalable route would be especially beneficial for intervention of TB. This paper studies three dispersibility enhancers: leucine, pullulan and trileucine, for producing spray-dried ID93+GLA-SE powder suitable for inhalation. Success of the inhalable candidates was assessed in terms of aerosol performance and preservation of vaccine integrity after spray drying. Characterization of vaccine integrity included testing for changes in emulsion size distribution, squalene and GLA content, and presence of ID93.

3.2. Materials and Methods

3.2.1. Chemicals

Trehalose dihydrate with a purity of 98% was used as the primary stabilizing excipient for spray drying (CAS 6138-23-4; Fisher Scientific Ottawa, ON, Canada). L-Leucine with a purity of 99% (CAS 61-90-5; Fisher Scientific Ottawa, ON, Canada), pullulan (CAS 9057-02-7; Alfa Aesar, Tewksbury, MA, USA), and trileucine with a purity of ≥90% (CAS 10329-75-6; Sigma Aldrich, Oakville, ON, Canada) were investigated as dispersibility enhancing materials. Tris(hydroxymethyl)aminomethane (Tris) (CAS 77-86-1; Sigma Aldrich, Oakville, ON, Canada) and hydrochloric acid (CAS 7647-01-0; Sigma Aldrich, Oakville, ON, Canada) were used as a buffer system to adjust the pH of the feedstock prior to spray drying. Formulations were made using HPLC grade water (CAS 7732-18-5; Fisher Scientific Ottawa, ON, Canada) or deionized water. The ID93 antigen and GLA-SE adjuvant system were formulated separately; manufacturing of these components has been described in Chapter 2.

3.2.2. Formulation Composition

Six formulations were assessed as inhalable vaccine candidates. The feedstock composition and the projected material composition of the final dried particles are given in Table 4. Concentrations for several of the main components, including trehalose, GLA-SE, ID93, and Tris buffer, were kept constant for all the formulated liquid feedstocks, as listed in the table.

ID93 protein was stored at a concentration of 1.2 mg/mL at -80 °C prior to use. GLA-SE nanoemulsions with a squalene concentration of 10% v/v and GLA concentration of 50 µg/mL were stored in a refrigerator prior to use. All formulation processes began with preparation of 4

mg/ml Tris. The Tris solution was then pH adjusted by addition of hydrochloric acid to a pH of 7.5±0.1. Preliminary work found that the buffer system had no apparent effect on particle morphology. For each formulation, the trehalose and relevant dispersibility enhancing agent were dissolved in water into buffered Tris solution. Once fully dissolved, GLA-SE was added to the solution and gently mixed. ID93 was added last to the feedstock to minimize potential protein binding to container surfaces.

Table 4 Formulation parameters and designed particle composition by mass of the human inhalable vaccine candidates.

Component\Formulation	T	T20Leu	T10Pul	T20Pul	T3Tri	T6Tri
Feedstock Composition (mg/mL)						
Leucine	-	10.0	-	-	-	-
Pullulan	-	-	4.5	10.5	-	-
Trileucine	-	-	-	-	1.3	2.6
Trehalose	33.3	33.3	33.3	33.3	33.3	33.3
Tris (buffer)	0.807	0.807	0.807	0.807	0.807	0.807
Squalene	5.73	5.73	5.73	5.73	5.73	5.73
DMPC	1.27	1.27	1.27	1.27	1.27	1.27
GLA	0.0033	0.0033	0.0033	0.0033	0.0033	0.0033
ID93	0.0013	0.0013	0.0013	0.0013	0.0013	0.0013
Total Feed Concentration	41.1	51.1	45.6	51.6	42.4	43.7
Particle Composition (w/w)						
Leucine	-	20%	-	-	-	-
Pullulan	-	-	10%	20%	-	-
Trileucine	-	-	-	-	3%	6%
Trehalose	81%	65%	73%	65%	78%	76%
Tris (buffer)	2%	2%	2%	2%	2%	2%
Squalene	14%	11%	12%	11%	14%	13%
DMPC	3%	2%	3%	2%	3%	3%
GLA	0.01%	0.01%	0.01%	0.01%	0.01%	0.01%
ID93	0.003%	0.003%	0.003%	0.003%	0.003%	0.003%

3.2.3. Spray Drying

Spray drying parameters were chosen in order to minimize potential antigen or agonist losses during processing based on previous work involving spray drying ID93+GLA-SE, as detailed in Chapter 2. A custom research spray dryer (Ivey, et al. 2016) with a twin fluid atomizer was utilized to conduct the spray drying. Use of a twin-fluid atomizer has been reported to significantly reduce degradation of a shear- and temperature-sensitive protein during the atomization step as compared to use of a vibrating mesh atomizer (Grasmeijer, Tiraboschi, et al. 2019, Carrigy, Liang, et al. 2019). The atomizer was operated at an air-liquid ratio of 8, corresponding to a mass median initial droplet diameter of approximately 9 µm. Characterization of the atomizer is described elsewhere (Hoe, et al. 2014).

A relatively low drying gas temperature of 65 °C was utilized in order to minimize temperature-dependent degradation. The other spray drying parameters were calculated using a mass and energy balance model (Ivey and Vehring 2010) to achieve an outlet humidity of less than 10% relative humidity and low outlet temperature. A low outlet humidity was targeted to achieve a low (2-3%) powder moisture content as over-drying can also lead to protein degradation. A low outlet temperature was needed to limit the temperature the powder was exposed to during cyclone collection. The feedstock was supplied to the atomizer at a rate of 0.6 mL/min using a peristaltic pump (Model 77200-60; Cole-Parmer, Montreal, QC, Canada), and the drying gas flow rate was set to 200 SLPM, leading to a low outlet temperature of approximately 36 °C. Powders were stored under dry conditions prior to characterization.

3.2.4. Particle Design

Respirable Range

Particles with an aerodynamic diameter of 10 μm and greater are expected to deposit prior to the upper respiratory tract (McAdams, Chen and Kristensen 2012), whereas particles 0.5 μm and smaller are expected to be exhaled out (Darquenne 2012). Respirable particle size range is generally accepted to be 1-5 μm. However, producing small particles close to the low end of the size range (~ 1 μm) requires much longer production time and particle aggregation becomes more significant at smaller particle sizes, which is detrimental to the powder dispersibility. On the other hand, larger particles approaching 5 μm will lead to a lower drug delivery efficiency to the deep lung. Therefore, the target particle aerodynamic diameter range for this study was chosen to be 3-4 μm.

The range in feedstock concentration to produce particles within the target size range was calculated using Eq. 4, where, d_{a}, is the aerodynamic diameter, ρ_{P} is the particle density, $\rho^{*}$is the reference density (1000 kg/m^3), c_{F} is the feedstock concentration, and d_{D} is the diameter of the droplets (Vehring 2008). Further details on the derivation of this equation can be found elsewhere (Vehring 2008).

$$d_a = \sqrt[6]{\frac{\rho_{\mathrm{P}}}{\rho^*}}\sqrt[3]{\frac{c_{\mathrm{F}}}{\rho^*}}d_{\mathrm{D}} \qquad \mathbf{4}$$

Morphology analysis in Chapter 2 has shown that spray drying the ID93+GLA-SE vaccine produces particles with varying shell thicknesses. Material density of this formulation was estimated to be 1438 kg/m^3. Assuming the average particle contains 30% interior void space, the particle density was approximated to be 1007 kg/m^3. Initial droplet diameter was predicted to be

9 μm based on the processing conditions. Based on these assumptions, the concentration of the feedstock must be between 36.9-87.5 mg/mL to achieve a particle size between 3 and 4 μm.

Selection of Excipients to Improve Powder Dispersibility

Aerodynamic particle size is a strong indicator of a powder's ability to deposit within the lung. Therefore, dispersing particle aggregates into primary particles is essential; otherwise, aggregated small particles will behave aerodynamically as larger particles and potentially deposit prior to the lung. However, passive delivery devices, such as DPIs, can only provide limited dispersing force as they rely solely on the patients' inhalation flow to de-aggregate the loaded powder dosages. Thus, it is necessary to reduce intrinsic powder cohesiveness to improve the dispersibility. Powder cohesiveness can be described in terms of the contact mechanics between adjacent particles. Based on theoretical cohesion models, e.g. the Li-DMT model (Li , Rudolph and Peukert 2006), the force of cohesion between two particles, F_c, can be reduced by lowering the surface energy, decreasing the deformability of the surface, and decreasing the contact area.

The excipients investigated in this study, leucine, pullulan, and trileucine, were expected to reduce the force of cohesion between particles. The component mass fraction for all investigated dispersibility enhancing agents in this study was limited to a maximum of 20% in order to maximize the adjuvant dose in the powder. Leucine was chosen as it has been reported to change the surface morphology of spray-dried particles through formation of a crystalline surface layer. Increasing leucine concentration changes particle surface from a smooth morphology to solid particles with corrugated surfaces (Feng, et al. 2011, Li, et al. 2016). Additional increases in leucine concentration further changes particle morphology to rugose hollow particles. The increased surface roughness due to crystal surface asperities is expected to increase the effective

radius of the particles and reduce effective contact area between particles. Additionally, the formation of a crystalline outer layer is expected to reduce the deformability of the surface as compared to an amorphous particle surface. Feng et al. (Feng, et al. 2011) reported that, for their given spray drying parameters, 25% leucine mass fraction in a leucine-trehalose system was required to achieve complete crystallinity of leucine. Thus, a mass fraction of 20% leucine was chosen for the T20Leu formulation to promote crystal growth in order to improve powder dispersibility.

Pullulan was chosen as it has been shown to introduce particle folding in pullulan-trehalose systems (Carrigy, Ordoubadi, et al. 2019). Depending on orientation, particle effective radius may increase, and effective contact area may decrease. Carrigy et al. (Carrigy, Ordoubadi, et al. 2019) reported that the formation of folded, irregularly shaped particles increases with increasing pullulan concentration, and 10% pullulan mass fraction in a pullulan-trehalose system slightly improved aerosol performance as compared to a trehalose-only formulation. Based on these results, a mass fraction of 10% pullulan was chosen for the T10Pul formulation in order to modify the surface morphology to promote improved dispersibility. Due to the reported increase in particle folding with increased pullulan content, a mass fraction of 20% pullulan for the T20Pul formulation was also investigated.

Trileucine was chosen as it has been reported to form highly wrinkled particle surfaces with increasing trileucine concentration, and has been shown to decrease the surface energy of spray-dried particles (Lechuga-Ballesteros, et al. 2008, Wang, Nobes and Vehring 2019). Highly rugose particle surface morphologies are expected to decrease contact area between particles, and reduced surface energy is expected to reduce the force of cohesion between particles. Wang et al. (Wang,

Nobes and Vehring 2019) demonstrated that at 1.0% mass fraction of trileucine in trileucine-trehalose systems the particle morphology appears rugose. Particle surface rugosity was improved greatly when the trileucine mass fraction was increased to 5.0%. Due to trileucine solubility limitations, 6% trileucine by mass for the T6Tri formulation was chosen for investigation in this study. 6%, a relatively high mass fraction, was chosen in order to promote increased particle surface rugosity and thus reduce particle cohesion. A lower mass fraction of 3% for the T3Tri formulation was also investigated in this study to determine if a similar performance could be obtained with a formulation with lower excipient costs.

Particle Formation Model

Previous studies have reported the mass fractions of leucine, pullulan, and trileucine required to induce surface morphology changes. However, these studies utilized different spray drying processing conditions. Change in processing conditions will affect the distribution of components within a drying droplet. A simple particle formation model (Boraey and Vehring 2014) was used to predict drying time and component distribution of the investigated formulations to verify that the dispersibility agents will form a shell on the particle exterior for the given spray drying parameters.

As the droplet dries, the radial concentration gradient of the formulation components is controlled by two mechanisms: the receding droplet surface and the diffusion of solutes from the surface towards the center of the droplet (Boraey and Vehring 2014, Vehring, Foss and Lechuga-Ballesteros 2007). The former mechanism will increase surface concentration whereas the latter will decrease surface concentration. This relationship can be described by the dimensionless Péclet number, Pe. The Péclet number is the ratio of the evaporation rate, κ, and the diffusion coefficient,

D, of a component *i*, as seen in Eq. 5. For a Pe close to 1 or smaller, the material will be able to diffuse quickly relative to receding droplet surface and thus will be evenly distributed. For a large Pe, the component is expected to be relatively immobile and therefore accumulate near the droplet surface.

$$Pe_i = \frac{\kappa}{8D_i} \quad \textbf{5}$$

Pe can be used to determine the surface enrichment of a given component. Surface enrichment is the surface concentration of a component, $c_{\mathrm{s},i}$, relative to its mean concentration within the droplet, $c_{\mathrm{m},i}$. Surface enrichment for a component with a *Pe* smaller than 20 can be approximated using Eq. 6 (Vehring, Pharmaceutical Particle Engineering via Spray Drying 2008), in which the steady state surface enrichment value, E_{ss}, assumes that the solute concentration within the droplet changes at the same rate as the mean concentration.

$$E_{\mathrm{ss}} = \frac{c_{\mathrm{s},i}}{c_{\mathrm{m},i}} \approx 1 + \frac{Pe_i}{5} + \frac{Pe_i^2}{100} - \frac{Pe_i^3}{4000} \quad \textbf{6}$$

Steady state surface enrichment for *Pe* values larger than 20 can be approximated using Eq. 7 (Boraey and Vehring 2014). Further discussion on Pe and surface enrichment can be found elsewhere (Boraey and Vehring 2014).

$$E_{\mathrm{ss}} \approx \frac{Pe_i}{3} + 0.363 \quad \textbf{7}$$

E_{ss} was used to approximate the time when a particle shell will form. The time at which shell formation is expected to start for components that do not crystallize is the time it takes a component to reach a concentration at the surface equivalent to its true density, $\tau_{\mathrm{t},i}$. The time at which shell formation is expected to start for components that do crystallize is the time that the component

reaches critical supersaturation at the surface, $\tau_{s,i}$. The $\tau_{t,i}$, is given in Eq. 8, where $C_{0,i}$ is the initial concentration of component i and $\rho_{t,i}$ stands for its material true density, and τ_D is the droplet drying time. As the formulations investigated contain multiple components, true density of a mixture, $\rho_{t,mix}$, was calculated and substituted for $\rho_{t,i}$. The calculation of $\rho_{t,mix}$ is described elsewhere (Carrigy, Ordoubadi, et al. 2019). The $\tau_{s,i}$ is given in Eq. 9, where $C_{sol,i}$ is the solubility of component i.

$$\tau_{t,i} = \tau_D \left[1 - \left(\frac{C_{0,i}}{\rho_{t,i}} E_i\right)^{\frac{2}{3}}\right] \quad \textbf{8}$$

$$\tau_{s,i} = \tau_D \left[1 - \left(\frac{C_{0,i}}{C_{sol,i}} E_i\right)^{\frac{2}{3}}\right] \quad \textbf{9}$$

The evaporation rate of a pure water droplet at the drying gas temperature, 65 °C, is 3.7×10^{-9} m^2/s (Vehring, Foss and Lechuga-Ballesteros 2007). The diffusion coefficient of pullulan was approximated to be 2.8×10^{-11} m^2/s (Carrigy, Ordoubadi, et al. 2019). The diffusion coefficient for trehalose in water, D_{tre}, was calculated to be 3×10^{-10} m^2/s using Eq. 10 (Grasmeijer, Frijlink and Hinrichs 2016), where w_s is the mass fraction of solute and T is droplet temperature in K, i.e. 301 K. This equation was obtained by fitting an equation to experimental data of trehalose diffusion in aqueous solutions (Ekdawi-Sever and de Pablo 2003).

$$D_{tre} = \frac{5\times10^8}{e^{-13(w_s)^{1.1}}} e^{-1500\frac{e^{1.9\cdot w_s}}{T}} \quad \textbf{10}$$

Diffusion coefficients for other solutes were approximated based on molecular size using the Einstein-Stokes equation. The GLA-SE nanoemulsion droplets were considered as a component for the sake of diffusion calculations. The diffusion coefficient of the nanoemulsion droplets has been previously approximated to be 5.3×10^{-12} m^2/s using the Einstein-Stokes equation, assuming that the nanoemulsion droplets remain stable as an aqueous dispersion and can be treated as nanoparticles.

The size of a peptide was approximated based on its mass using Eq. 11, assuming the peptide is in the shape of a sphere (Erickson 2009). Eq. 11 determines $R_{\min}$ of a peptide, the minimum radius of a sphere that could contain its mass. $R_{\min}$ is given in nm and M is the molecular weight of the peptide, given in Da. The diffusion coefficient for leucine was approximated to be 6.3×10^{-10} m^2/s and the diffusion coefficient for trileucine was approximated to be 4.5×10^{-10} m^2/s.

$$R_{\min} = 0.066M^{1/3} \quad \textbf{11}$$

Distribution calculations for ID93 were not conducted as previous work has reported that an estimated 96% of the antigen is associated with the adjuvant (Orr, Fox, et al. 2013). The literature values for the density and solubility of the given components are summarized in Table 5. Table 5 also shows the calculated Pe and E_{ss} for each component.

Non-crystallizing components with a Pe near 1 and high solubility, such as trehalose, are expected to form solid particles later in the droplet lifetime with even component distribution. The Pe of both pullulan and the GLA-SE emulsion droplets was much greater than 1, suggesting that these components will accumulate near the surface of the drying droplet. In Chapter 2, encapsulation of the vaccine candidate with trehalose via spray drying showed that the GLA-SE droplets are

distributed throughout the trehalose matrix, with increasing radial concentration towards the particle surface.

Table 5 Density and solubility values from literature, and calculated *Pe* and E_{ss} for the main components of the spray-dried inhalable vaccine candidates.

Component	Density (kg/m^3)	Solubility (mg/mL)	Pe_i	$E_{ss,i}$	References
Trehalose	1580	690	1.4	1.3	(Wang, Nobes and Vehring, 2019), (Grasmeijer, Frijlink and Hinrichs, 2016)
Leucine	1293	23	0.7	1.1	(Sigma-Aldrich 2020)
Pullulan	1850	Variable	17	6.1	(Sangon Biotech 2018), (Leathers 2003)
Trileucine	1250	6.8	1	1.2	(Carrigy, Liang, et al. 2019), (Lechuga-Ballesteros, et al. 2008)
GLA-SE	N/A	N/A	90	30	N/A

A summary of the calculated particle formation parameters is given in Table 6, with calculations based on the values given in Table 5. These simplified calculations assume constant Pe to provide an estimated timeline of the drying processes without looking into the detailed droplet drying steps. For example, formation of crystals will increase the Pe due to increasing component size, which will further facilitate surface enrichment. Similarly, increasing viscosity near the droplet surface due to increasing solute concentration over time will increase the Pe and thus facilitate shell formation. This particle formation model also neglects the effect of surface activity. Inclusion of these considerations results in very complex models that are outside the scope of this study.

Time to true density was calculated for trehalose and pullulan as neither are crystallizing systems under normal spray drying conditions. As leucine was expected to crystallize, time to saturation was calculated. For trileucine, the phase separation is not fully understood at this time, however, previous studies have shown that it forms a shell soon after reaching saturation (Carrigy, Liang, et

al. 2019, Wang, Nobes and Vehring 2019, Carrigy and Vehring 2019). For this reason, the time to saturation was calculated for trileucine.

It is apparent that the trehalose will reach the true density of the given mixture relatively late (>90%) in the droplet lifetime for all formulations. The calculations predict that leucine reaches critical saturation relatively early (37.2%) in the droplet lifetime and therefore forms an outer shell composed of growing crystals. Pullulan was predicted to reach true density close to the same time as trehalose (93.0% and 87.9%), which suggests that the outer surface of these particles may be composed of both pullulan and trehalose. The model predicts that trileucine will accumulate on the surface and form a shell early in the drying process due to relatively short time to reach saturation (62.3% and 40.2%). Therefore, the model predicts that the chosen mass fractions are likely to result in partial to total particle surface coverage with the dispersibility enhancing agents for the given spray drying parameters.

Table 6 Feed concentrations of each component, true density, and normalized time for each component to reach true density or saturation for each inhalable vaccine formulation. Abbreviations: tre – trehalose, leu – leucine, pull – pullulan, tri – trileucine.

Formulation	$C_{0,\mathrm{tre}}$ (mg/mL)	$C_{0,\mathrm{leu}}$ (mg/mL)	$C_{0,\mathrm{pull}}$ (mg/mL)	$C_{0,\mathrm{tri}}$ (mg/mL)	$\rho_{\mathrm{t,mix}}$ (kg/m^3)	$\frac{\tau_{\mathrm{t,tre}}}{\tau_{\mathrm{D}}}$	$\frac{\tau_{\mathrm{s,leu}}}{\tau_{\mathrm{D}}}$	$\frac{\tau_{\mathrm{t,pull}}}{\tau_{\mathrm{D}}}$	$\frac{\tau_{\mathrm{s,tri}}}{\tau_{\mathrm{D}}}$
T	33.3	-	-	-	1438	90.3%	-	-	-
T20Leu	33.3	10	-	-	1411	90.2%	37.2%	-	-
T10Pul	33.3	-	4.5	-	1473	90.5%	-	93.0%	-
T20Pul	33.3	-	10.5	-	1510	90.6%	-	87.9%	-
T3Tri	33.3	-	-	1.3	1428	90.3%	-	-	62.3%
T6Tri	33.3	-	-	2.6	1425	90.3%	-	-	40.2%

3.2.5. Dry Powder Characterization

Field Emission Scanning Electron Microscopy (Zeiss Sigma FE-SEM; Carl Zeiss, Oberkochen, Germany) was used to determine particle morphology for the inhalable vaccine candidates. Powder samples were mounted either directly onto aluminum SEM stubs (Product 16111; Ted Pella, Inc.; Redding, CA, USA) or onto carbon tape placed over the stubs. The former method included scraping the powder against the stubs in order to intentionally crack particles open to view the interior structure. The latter method was implemented to avoid intentional destruction of the particles in order to view the exterior structure. These samples were placed in a desiccator connected to an in-house vacuum system for 1-4 days to remove the exposed nanoemulsion droplets and prevent damage to the electron microscope. Following desiccation, the samples were sputtered with a coating of 80% gold and 20% palladium (Leica ACE600 Carbon/Metal Coater; Concord, ON, Canada) to a thickness of 10-15 nm or with a coating of gold (Denton Vacuum Desk II Sputter Coater; Denton, Moorestown, NJ, USA) to a thickness of approximately 16 nm. Images ranging from magnifications of 500 to 25000× were taken at a working distance of 5.4-6.8 mm using an accelerating voltage of 4-5 kV.

The solid phase of the powder was assessed by Raman spectroscopy to determine powder crystallinity for each spray-dried formulation using a custom dispersive Raman spectroscopy system. This system was used in Chapter 2 to monitor solid phase of spray-dried ID93+GLA-SE over time; a detailed description of a similar apparatus has been published elsewhere (Wang, Barona, et al. 2017). All spectra were measured at a temperature of 22.0-23.0 °C and at less than 3% RH to prevent moisture exposure. Raman spectrum analysis was also conducted on crystalline trehalose, crystalline leucine, raw crystalline trileucine, crystalline Tris, and raw pullulan as references. Similarly, spray-dried trehalose and spray-dried trileucine were analyzed as amorphous references. Reference spectra were also obtained for a liquid sample of squalene. The amorphous leucine spectrum was obtained by subtracting the water spectrum from a concentrated aqueous leucine solution (20 mg/mL) spectrum. It has been previously demonstrated that spectra of amorphous solids are similar to a concentrated aqueous solution of the solid (Vehring, Red-excitation dispersive Raman spectroscopy is a suitable technique for solid-state analysis of respirable pharmaceutical powders 2005).

Lung deposition was measured *in vitro* using a Next Generation Impactor (NGI) (Copley Scientific; Nottingham, UK) with an Alberta Idealized Throat (AIT) attachment. The AIT mimics the general geometry of a human mouth-throat (Zhang, Gilbertson and Finlay 2007). Grgic et al. (Grgic, Finlay and Heenan 2004) established that particle deposition using the model is in agreement with human experimental extrathoracic deposition data. A simplified schematic of this set up is shown in Figure 12.

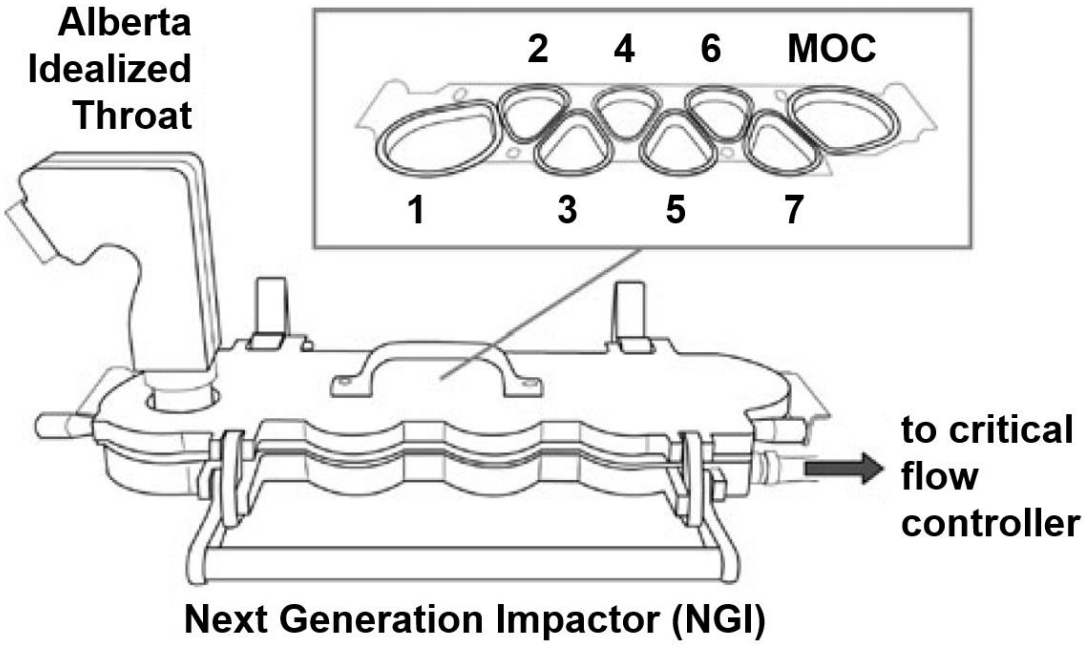

Figure 12 *In vitro* aerosol performance testing apparatus (Hoe, et al. 2014). The Alberta Idealized Throat was utilized to obtain a reasonable approximation of vaccine powder deposition in the human oral cavity and pharynx (mouth-throat) region. The Next Generation Impactor consists of seven stages and a micro-orifice collector (MOC) for assessment of particle size distribution.

A commercial low resistance DPI (Seebri Breezhaler, Novartis International AG; Basel, Switzerland) was used to deliver the powder. The DPI has been characterized elsewhere (Pavkov, et al. 2010). The DPI was connected to the throat model using a custom 3D-printed mouthpiece adapter. A similar set up was used in Hoe et al. (Hoe, et al. 2014) and Carrigy et al. (Carrigy, Ordoubadi, et al. 2019). Inhalation flow rate was simulated via a critical flow controller (Critical Flow Controller Model TPK 2000, Copley Scientific Limited; Nottingham, UK) connected to a vacuum pump (Maxima M16C, Fisher Scientific; Ottawa, ON, Canada). This set up was utilized to obtain an assessment of loss due to extrathoracic powder deposition under normal use. A similar procedure was followed as given in Carrigy et al. (Carrigy, Ordoubadi, et al. 2019). Prior to the experiment, the impactor stages, the micro-orifice collector (MOC) and the interior of the throat

model were coated with silicone spray (Molykote 316 Silicone Release Spray, Dow Corning Corporation; Midland, MI, USA) to mitigate particle bounce (Zhou, Sun and Cheng 2011). Powder was manually loaded into size 3 hydroxypropyl methylcellulose capsules (Quali-V-1; Qualicaps, Inc., Madrid, Spain) in a dry glovebox. Each capsule contained 41 ± 9 mg of powder. Actuation and inhalation was performed using three capsules in succession to obtain sufficient mass on the impactor stages and MOC for gravimetric analysis. Inhalation was simulated at an inspiratory flow rate of 100 L/min over 2.4 seconds to achieve 4 L of air withdrawal as per the USP 601 monograph (United States Pharmacopeia 2017). Experiments were performed in triplicate and conducted under ambient conditions. A two-tailed student's t-test was used for analysis, where statistically significant differences were reported for $p<0.05$.

All gravimetric measurements were conducted with a microbalance (ME204E, Mettler Toledo; Mississauga, ON, Canada). Capsules were weighed before and after powder loading to determine the mass of powder added. The DPI containing the loaded capsule was measured before and after actuation to determine the emitted dose, defined as the percentage of loaded mass that exited the inhaler. Lung dose was defined as the percentage of loaded mass that penetrated the throat model. Lung dose was calculated as the total powder deposition on the impactor stages relative to the loaded powder mass. Powder deposition was determined gravimetrically by measuring the stages before and after the experiment run. Correlation of mass distribution to particle size was based on stage cutoff diameters at 100 L/min flow rate, as determined elsewhere (Marple, et al. 2003).

Mass median aerodynamic diameter, $d_{a,50}$, and geometric standard deviation, σ_g, of the deposited powder was calculated by fitting the data to a cumulative lognormal distribution function (Carrigy,

Ordoubadi, et al. 2019). In this case, $d_{a,50}$ and σ_g measured are for the powder that has deposited within the impactor, not the size distribution of the spray-dried formulations themselves. Real-time sampling during production to obtain the $d_{a,50}$ and σ_g of the spray-dried formulations could not be completed due to equipment issues. Data fitting was done using the MATLAB (MathWorks Inc., Natick, MA, USA) "Curve Fitting" application. For a given stage, the cutoff diameter was plotted as the upper size limit for each bin, and the deposition fraction for each bin was calculated with respect to the total amount of powder deposited on the stages.

As previously indicated, inhalable aerosols can be administered through the intranasal or pulmonary route. The spray-dried powders investigated in this study were designed for delivery to the lungs through inhalation past the mouth. Powders designed for intranasal delivery through the nose would have to be assessed for deposition through other methods; however, this model can be used to provide an indication of powder dispersibility for a given formulation.

3.2.6. Reconstituted Powder Characterization

All samples were reconstituted to the feedstock concentrations with freshly dispensed MilliQ water for analysis. Nanoemulsion droplet diameter, polydispersity index, squalene concentration, GLA concentration, and ID93 presence were evaluated in the reconstituted powders. Similar experimental techniques as detailed in Chapter 2 were used to assess retention of vaccine components in spray-dried powder.

Mean hydrodynamic diameter and polydispersity of the nanoemulsion droplets in liquid formulations were measured using a dynamic light scattering technique (Zetasizer APS; Malvern, Worcestershire, UK). Polydispersity index was calculated as the standard deviation of the

measured size distribution divided by the mean hydrodynamic diameter, squared Details of the measurement process have been described elsewhere (Chan, et al. 2017). Reported average and standard deviation measurements for each sample are from the same sample analyzed 3 times.

Squalene content was quantified using a reverse phase HPLC method. Separation of squalene from sample was performed on an Agilent 1200 HPLC (1200 HPLC; Agilent Technologies; Santa Clara, CA, USA) equipped with a silica-based, C18 reversed-phase column (Atlantis T3 Column; Waters; Elstree, UK). Column temperature was held constant at 30 °C and analyte detection was accomplished using a charged aerosol detector (Corona CAD; ESA Biosciences; Chelmsford, MA, USA). Mobile phase A contained 75:15:10 (v/v/v) methanol:chloroform:water, 1% (v/v) acetic acid, and 20 mM ammonium acetate and mobile phase B contained 50:50 (v/v) methanol:chloroform, 1% (v/v) acetic acid, and 20 mM ammonium acetate. Samples were diluted in mobile phase B and injected with a gradient over 30 minutes. Squalene content was quantified by peak area. Concentration measurements were made by interpolation of a curve generated from standards fitted with a second order polynomial. Reported average and standard deviation measurements for each formulation are from two separately prepared HPLC samples.

GLA content was also quantified using a reverse phase HPLC method, in which separation of GLA from sample was done with the same equipment and the same mobile phases. Samples were diluted in mobile phase B and injected with a gradient over 18 minutes. Column temperature was held constant at 30 °C. GLA content was quantified by peak height. Concentration measurements were made by interpolation of a curve generated from standards fitted with a second order polynomial.

Reported average and standard deviation measurements for each formulation are from two separately prepared HPLC samples.

Due to insolubility in the HPLC buffers, samples that contained pullulan were diluted with the appropriate volume of mobile phase B, capped, and then centrifuged on an EZ-2 Mk2 centrifugal evaporator (Genevac LTD, Ipswich, England) for 20 minutes on the low boiling point setting with a maximum temperature set to 35°C. A 200 uL aliquot of sample was transferred to a new HPLC vial and then injected as normal. An internal standard containing either GLA or squalene was included to ensure no analyte loss upon centrifugation or transfer. Care was used not to disturb the pullulan pellet upon transfer.

The presence of ID93 in formulated samples was determined using SDS-PAGE. Gel samples were prepared by mixing 4X LDS Buffer (Thermo Fisher Scientific, Waltham, MA, USA) spiked with 5% (v/v) β-Mercaptoethanol, a 20% (w/v) sodium dodecyl sulfate solution (Thermo Fisher Scientific, Waltham MA, USA), and formulated sample in a 1:2:1 ratio. Prepared samples were heated in an 85°C water bath for 15 minutes, and then left to cool in a room temperature water bath. A precast, 4-20% Tris-Glycine SDS-PAGE gel (Thermo Fisher Scientific, Waltham, MA, USA) was prepared according to manufacturer's instructions for denaturing gel electrophoresis using Tris-Glycine SDS Running Buffer (Thermo Fisher Scientific, Waltham, MA, USA) and the recommended gel tank and power supply (Thermo Fisher Scientific, Waltham, MA, USA). Cooled gel samples were centrifuged at 2000 RPM in a benchtop centrifuge (Thermo Fisher Scientific, Waltham, MA, USA) for 2 minutes to collect the sample, and then briefly vortexed prior to loading onto the prepared gel. Mark12 ladder (data not shown) (Thermo Fisher Scientific, Waltham, MA, USA) was diluted 1:4 with freshly dispensed MilliQ water and also run on the gel as a molecular

weight marker to confirm the expected migration of ID93 through the gel. The gel was run at 180V for 65 minutes, and then stained overnight using Sypro Ruby stain (Thermo Fisher Scientific, Waltham, MA, USA) according to the manufacturer's instructions. Stained gels were imaged using a gel imaging system (ChemiDoc; Bio-Rad, Mississauga, ON, Canada) employing the manufacturer's settings for Sypro Ruby stain. Duplicate gels were run to confirm the presence or absence of the ID93 monomer band.

3.3. Results and Discussion

3.3.1. Particle Morphology

SEM images of the inhalable vaccine candidates are shown in Figure 13. The spray-dried T formulation particles visually appear to be within respirable range. The particles' surface ranges from smooth to slightly dimpled, which was consistent with work shown in Chapter 2 and spray-dried bacteriophages encapsulated in trehalose (Carrigy, Liang, et al. 2019, Vandenheuvel, et al. 2014). The smooth disaccharide particle surface is undesirable in terms of powder dispersibility as smooth surfaces are more cohesive than rugose surfaces. Interior analysis of cracked particles revealed the presence of many small voids. These voids are caused by the encapsulated nanoemulsion droplets within the amorphous trehalose matrix. Results shown in Chapter 2 have indicated that the nanoemulsion droplets appear to be distributed along a gradient within the dry particle, with a higher concentration towards the particle surface. Particle interiors feature either a large central void or many central voids (not shown) and exhibit a range of shell thicknesses.

Like the T formulation, the spray-dried T20Leu particles also appear to be within respirable range. Unlike the T formulation, T20Leu particle surfaces were rough, with many surface asperities. These surface asperities are likely individual leucine crystals. Similar surface morphology has been produced in spray-dried crystalline leucine and trehalose systems (Feng, et al. 2011, Carrigy, Liang, et al. 2019). The presence of leucine crystals at the particle surface was also predicted by the particle formation model; the formulation was designed such that leucine reached saturation on the surface early in the droplet evaporation process, providing the necessary time to form a shell on the surface before trehalose. Crystal size is related to how much time is available for crystallization; hence earlier leucine saturation at the surface will lead to larger crystals (Carrigy

and Vehring 2019). A rugose crystalline leucine surface layer is expected to improve powder dispersibility. Analysis of the cracked particle suggests that the T20Leu particles are composed of a trehalose core that transitioned into a crystalline leucine surface layer. Like the T particles, the nanoemulsion droplets are encapsulated within the spray-dried T20Leu particles.

Both the pullulan-containing formulations, T10Pul and T20Pul, produced dimpled particles which appear to be within respirable range. Increased number and depth of dimples was shown with increasing pullulan concentration. The surface particle morphology and increasing dimpling shown with increasing pullulan content were consistent with studies involving spray drying of trehalose-pullulan systems (Carrigy, Ordoubadi, et al. 2019). The dimpled morphology was not seen in the T particles, suggesting that the particle formation model correctly predicted that pullulan would enrich the surface. However, the particle surface appears to still be smooth even with the addition of pullulan. The smoothness of the particle surfaces is expected to promote powder cohesiveness. Interior particle morphology showed that the nanoemulsion droplets are encapsulated within the particle wall for both the pullulan containing formulations. Cracked particles appeared to be hollow, with a range of shell thicknesses (not shown). Unlike the T20Leu formulation, it was difficult to visually determine the presence or location of a radial pullulan-trehalose transition. The lack of a clear transitional layer was expected as trehalose and pullulan are amorphous materials with no discernible visual difference at the given magnification.

The spray-dried formulations containing trileucine, T3Tri and T6Tri, produced highly folded particle surfaces, with increased wrinkles exhibited with increased trileucine concentration. Exterior particle morphology was consistent with previous work on spray-dried trileucine-trehalose systems, which produced particles with low particle density, i.e. containing interior or

exterior void space, or both (Carrigy, Liang, et al. 2019, Wang, Nobes and Vehring, Particle Surface Roughness Improves Colloidal Stability of Pressured Pharmaceutical Suspensions 2019). Increased corrugation of particles with increasing trileucine concentration had also been demonstrated in other systems (Lechuga-Ballesteros, et al. 2008). The trileucine layer at the surface of the particles was predicted by the particle formation model as the time for trileucine saturation preceded time for trehalose precipitation. Folded surface morphology was due to the formation of a trileucine shell early in the particle formation process (Wang, Nobes and Vehring 2019). The particles collapsed due to the lack of early shell mechanical strength during the drying process and thus appear rugose. Increased trileucine concentration led to earlier shell formation; thus, the formulation with higher trileucine content showed particles with increased levels of folding, as designed. The T6Tri formulation's cracked particle image indicated that the nanoemulsion droplets were encapsulated within the particle. A cracked particle could not be found for the T3Tri formulation; however, the interior morphology was expected to be similar to T6Tri interior morphology due to formulation similarity. Trileucine mass fraction in both the T3Tri and T6Tri formulations was low, which increased the probability of trehalose surrounding the nanoemulsion droplets. The stabilization via mostly trehalose instead of encapsulation within an excipient mixture may have contributed to the improved preservation of vaccine integrity compared to the other dispersibility enhancing agents.

The trileucine containing formulations appear to produce large particles that are outside the intended size range. However, morphology analysis indicates that these particles are thin-shelled and hollow; therefore, the aerodynamic diameter of the particles is much smaller than the geometric diameter. These geometrically large yet thin-shelled hollow particles suggest low

density and increased effective geometric particle diameter. Powders composed of geometrically large particles are easier to disperse as the aerodynamic forces, which act to disperse the powder during inhalation, increase with increasing particle diameter (Finlay 2019). Additionally, the designed wrinkled surface morphology due to trileucine surface accumulation decreases contact area between particles, theoretically improving powder dispersibility. Accumulation of trileucine on the particle surface is also expected to reduce surface energy. Previously, increased trileucine content has been shown to improve powder dispersibility through reduction of particle surface energy even when particle morphology was no longer changing with increasing concentration (Lechuga-Ballesteros, et al. 2008).

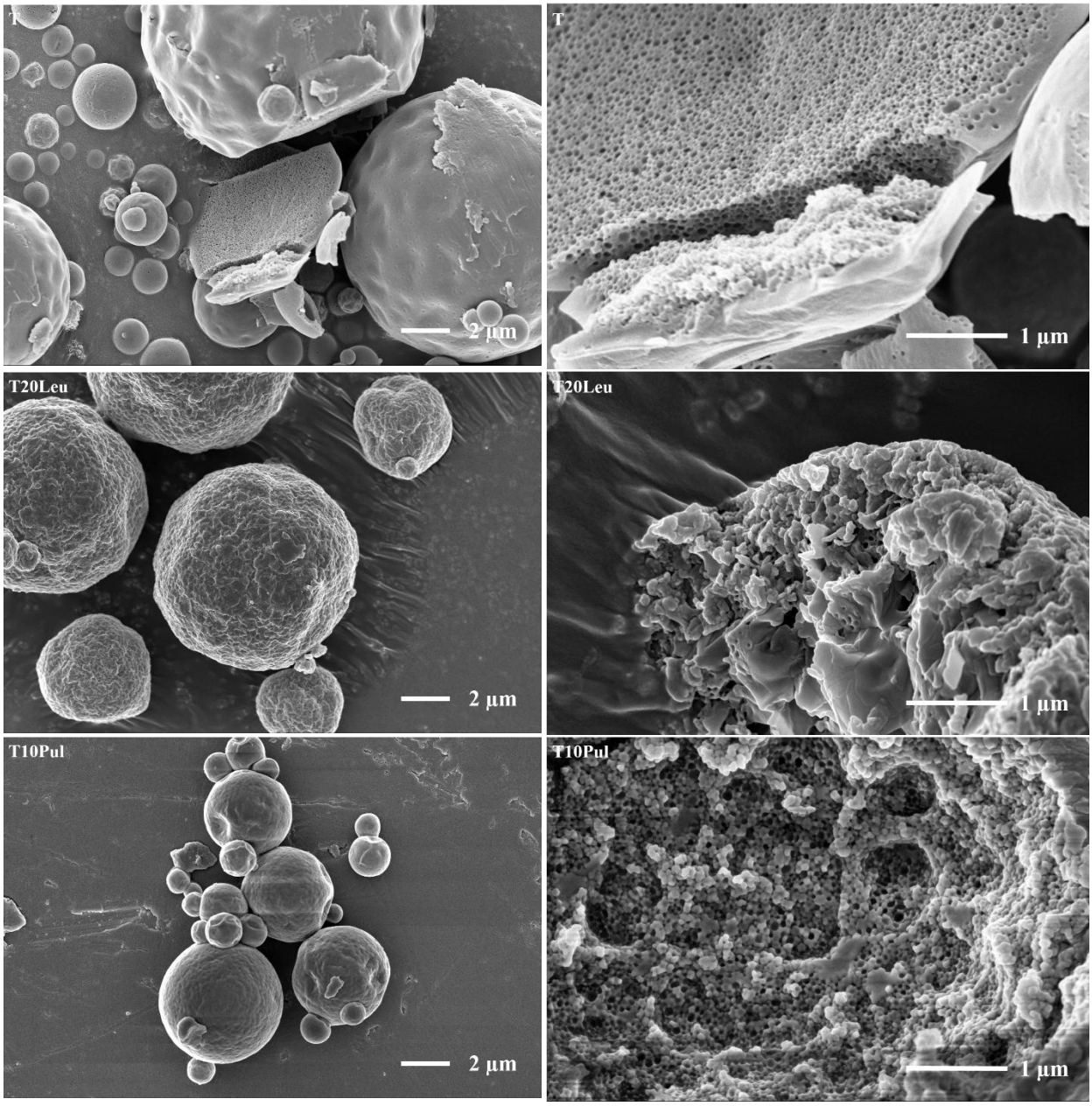
T
2 µm
T
1 µm
T20Leu
2 µm
T20Leu
1 µm
T10Pul
2 µm
T10Pul
1 µm

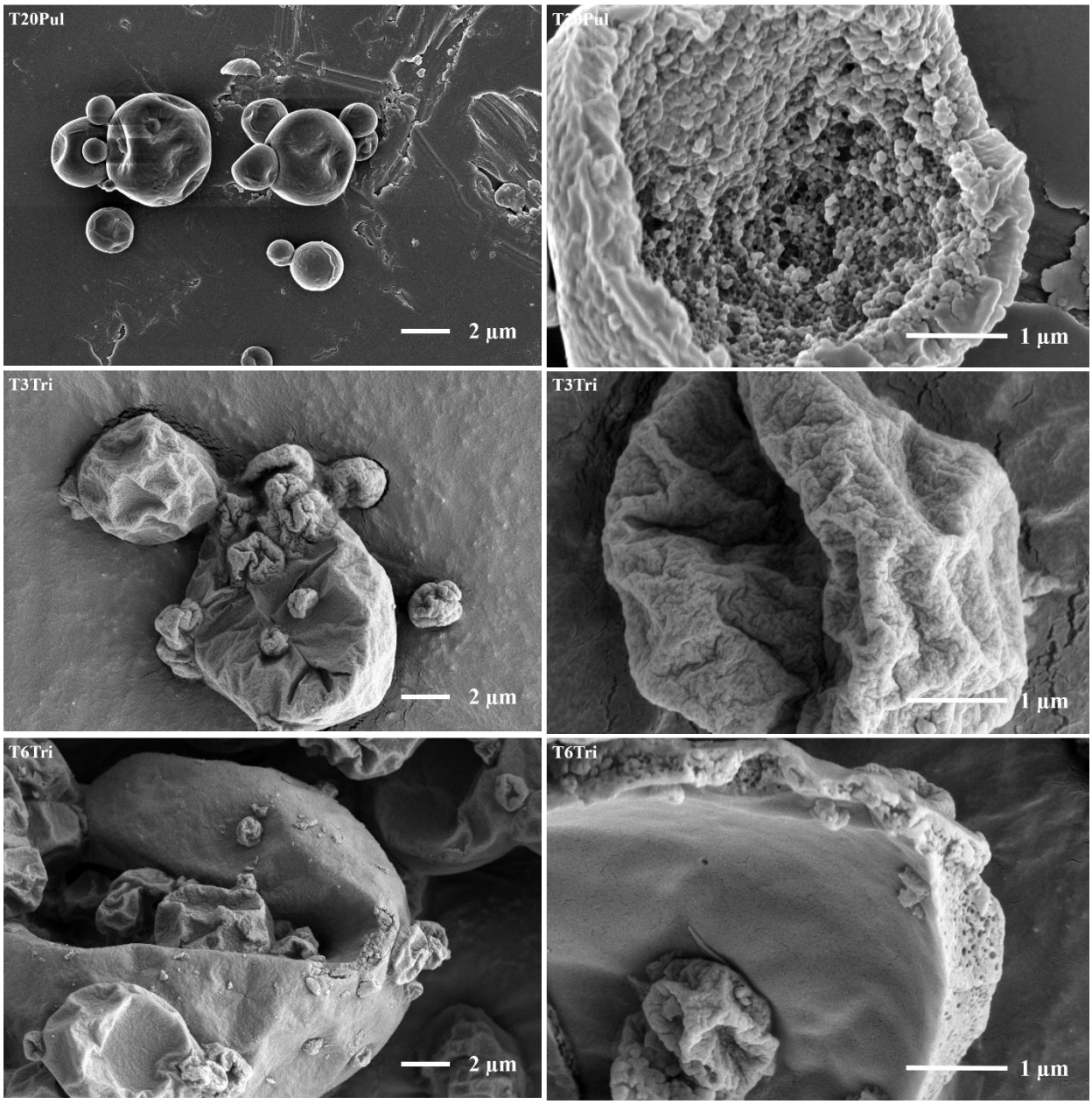

Figure 13 Low (left) and high (right) magnification SEM images of the inhalable vaccine candidates T, T20Leu, T10Pul, T20Pul, T3Tri, and T6Tri from top to bottom. SEM images showed that exterior particle morphologies vary based on excipient combination. Images of cracked particles indicate the encapsulation of vaccine nanoemulsion droplets. Scale bars are shown on respective images.

3.3.2. Crystallinity Analysis

The Raman spectra of the inhalable vaccine candidates were analyzed to determine the solid phase of the spray-dried powder. The reference spectra for amorphous and crystalline trehalose, squalene, amorphous and crystalline leucine, pullulan, and amorphous and crystalline trileucine are shown in Figure 14. The ID93 and GLA contributions were not considered due to their low mass fraction. The Raman spectra for the inhalable vaccine candidates are shown in Figure 15. The residual spectrum after partial deconvolution is given under the respective formulation. Partial deconvolution was completed by subtracting the amorphous trehalose, squalene, and Tris reference spectra for all inhalable candidates. Additionally, for the formulations with dispersibility enhancing agents, crystalline leucine, pullulan, and amorphous trileucine reference spectra were subtracted from the T20Leu, T10Pul and T20Pul, and T3Tri and T6Tri formulations, respectively. Details on the deconvolution process are discussed elsewhere (Vehring 2005).

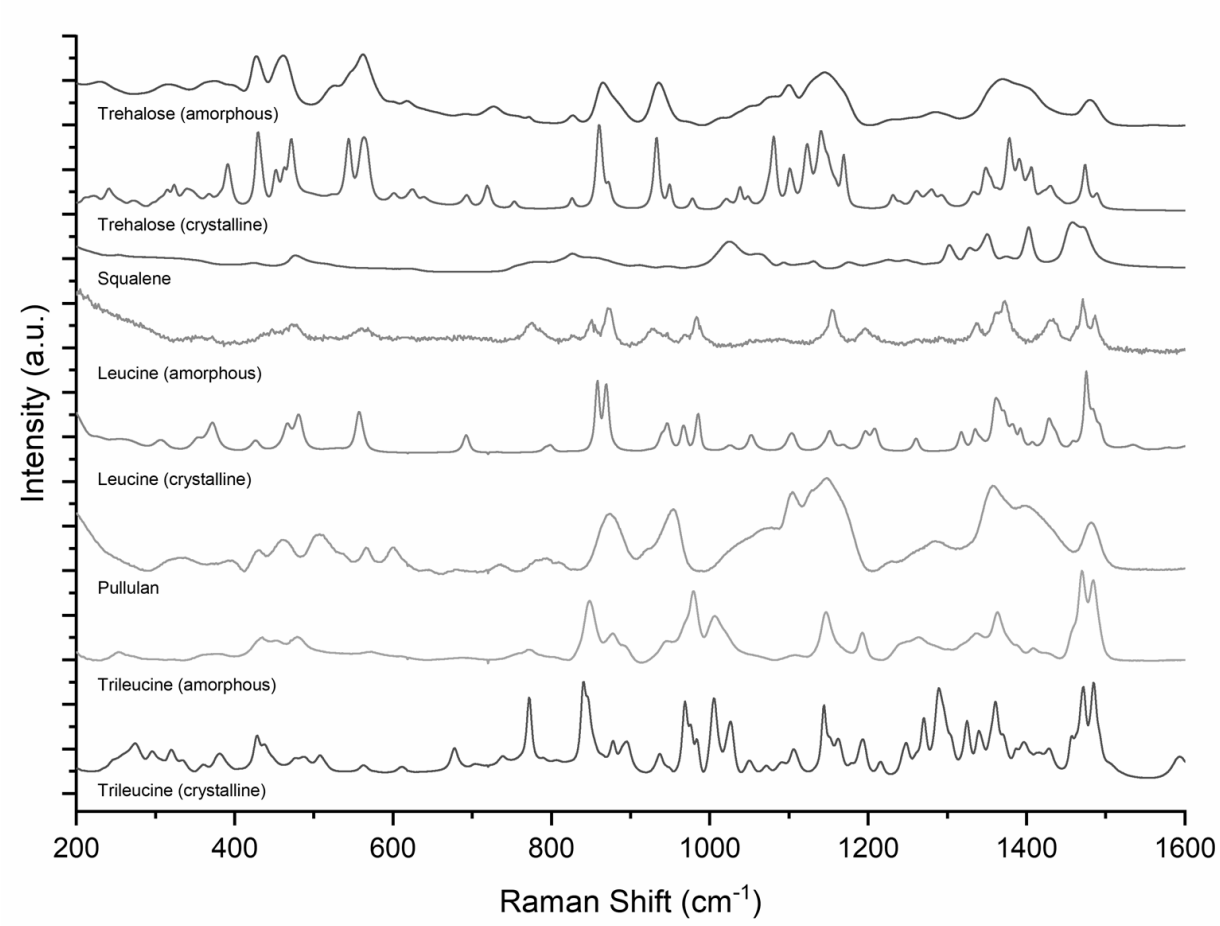

Figure 14 Reference spectra for the main components of the inhalable vaccine candidates: trehalose, squalene, leucine, pullulan, and trileucine. Amorphous and crystalline reference spectra are shown where applicable.

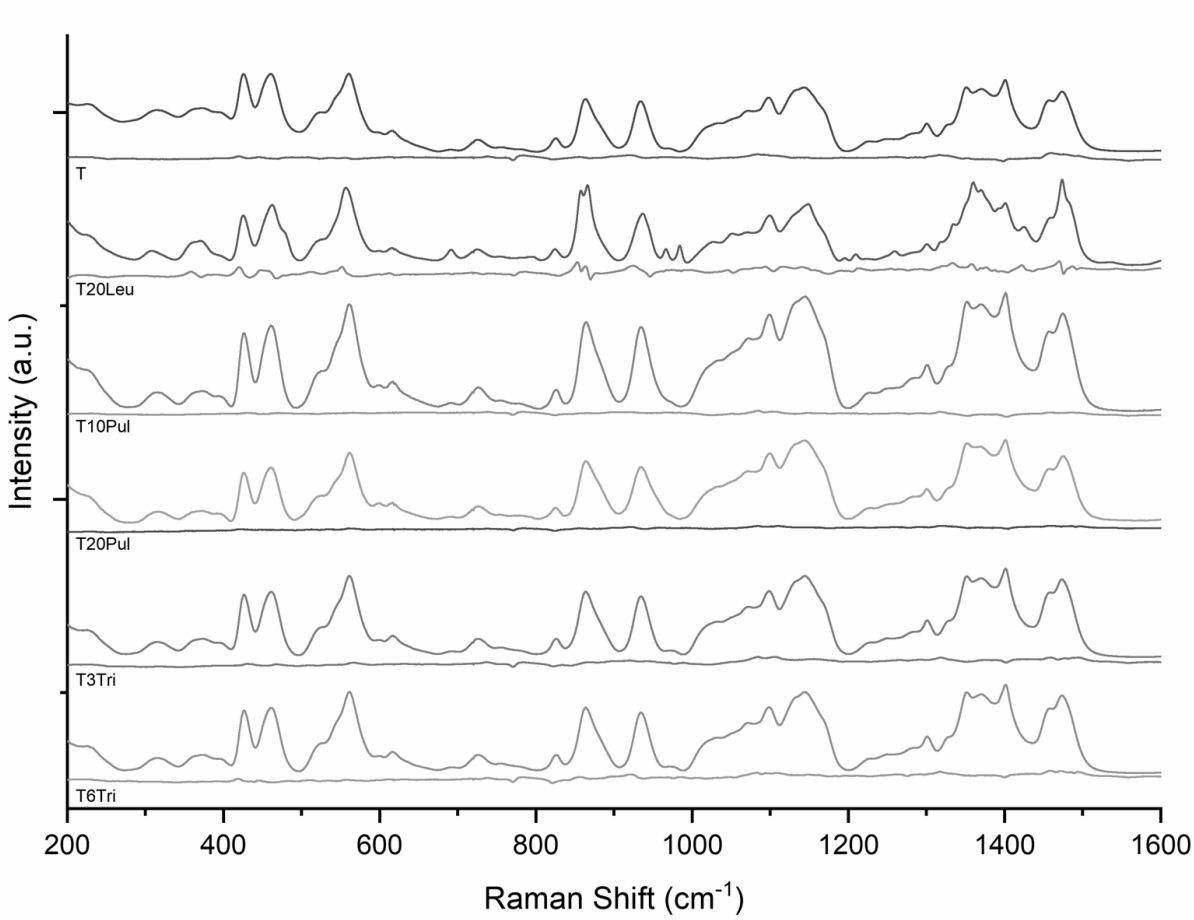

Figure 15 Raman spectra of spray-dried inhalable vaccine candidates. Respective residual spectra are given underneath the given inhalable candidate sample spectra. Primarily amorphous structure is shown in all candidates, as indicated by the relatively low intensity residual spectra. The leucine-containing T20Leu formulation was the only spectrum that exhibited some crystalline peaks. Peaks shown in the residual spectrum for the T20Leu formulation suggest that the leucine component was mostly crystalline.

Deconvolution indicated that the trehalose component of all formulations was completely amorphous, as expected. The amorphous trehalose spectrum dominated the sample spectra as trehalose was the most abundant component in all formulations, with a designed mass fraction of 65-81%. All spray-dried vaccine powders, except for the T20Leu formulation, exhibit fully amorphous spectra, as indicated by the relatively low intensity residual spectra. The T20Leu spectrum features several crystalline leucine peaks, most noticeably at 966 and 984 cm^{-1}. The

T20Leu formulation was designed to have a crystalline outer leucine layer, whereas all other formulations utilized dispersibility enhancing agents that were predicted to form an amorphous shell. These results provide additional evidence that the surface asperities shown in T20Leu morphology analysis are leucine crystals. Further spectral deconvolution indicated the presence of leucine in its amorphous state, which is consistent with the findings of other studies (Feng, et al. 2011). This study considered formulations with dispersibility enhancing agents ≤20% by mass fraction in order to maximize the adjuvant dose in the powder. However, Feng et al. (Feng, et al. 2011) previously established that a critical crystallization time for the given system must be surpassed in order for the leucine component to be completely crystalline. Leucine crystallinity can be improved by increasing the crystallization time, for example by either increasing the mass fraction or feed concentration.

3.3.3. Nanoemulsion Size Distribution

The vaccine nanoemulsion droplets' average diameter in the liquid formulation and reconstituted spray-dried powder are compared in Figure 16. Acceptable emulsion diameter range (80-160 nm) are represented by dashed red lines. The acceptance criteria are the same as those given in Chapter 2. It is apparent that all formulations except T20Leu preserve emulsion diameter post-spray drying.

The trehalose control and both trileucine-containing formulations showed less than an 8% increase in emulsion diameter. These formulations had the highest relative mass fraction of trehalose, where trehalose composed 76-81% of the dry particles. High trehalose mass fraction increases the probability that the nanoemulsion droplets are surrounded by trehalose rather than other excipients. Similarly, results shown in Chapter 2 of the spray-dried trehalose formulation at a higher feedstock concentration indicated a low increase in emulsion diameter of only 2-3%.

The T20Leu formulation's measured emulsion droplet diameter was the largest, increasing 145% to 225 nm. The significant increase in droplet diameter strongly suggests that leucine promotes instability of the GLA-SE membrane. The exhibited increase in emulsion diameter outside the acceptance limit removes the T20Leu candidate from consideration for further development. Crystallinity analysis results have shown that the leucine component in the T20Leu candidate is mostly crystalline. Studies on the lyophilization of the vaccine have shown that crystalline lyophilisate increased the GLA-SE particle size after reconstitution (Kramer, et al. 2018). However, particle size analysis on a similar spray-dried formulation containing only 5% leucine mass fraction also showed an increase in emulsion droplet diameter from 94 nm to 178 nm on reconstitution (data not shown). It is highly likely that the leucine component of this spray-dried formulation with such a low leucine mass fraction (<10%) is primarily amorphous, according to Feng et al.'s work (Feng, et al. 2011). Therefore, crystallization of leucine may not be the only mechanism which destabilizes the GLA-SE membranes. It has been established that leucine molecules are able to penetrate DMPC monolayers in aqueous solutions (Nakagaki and Okamura 1982). Penetration of the lipid layer by an amino acid has been previously reported to cause membrane destabilization on dehydration and subsequent reconstitution (Chen, et al. 2011). Despite the similar molecular structure of leucine and trileucine, the trileucine-containing formulations did not exhibit a large increase in emulsion diameter.

Spray drying the pullulan-containing formulations led to an increase in emulsion droplet diameter of 28% and 53%, for T10Pul and T20Pul, respectively. The increase in diameter for the T10Pul formulation is comparable to the increase in GLA-SE diameter of the lyophilized vaccine (Kramer, et al. 2018). Increasing pullulan concentration appears to cause greater increase in nanoemulsion

droplet diameter on reconstitution. The particle formation model predicted that pullulan enriches the surface, however, the time to true density occurs near the same time for the trehalose component. Particle morphology of these formulations suggests that the particles are likely composed of a pullulan and trehalose mixture, as there is no clear distinction between the pullulan and trehalose layers. This distribution of components increases the likelihood of the emulsion droplets becoming encapsulated by pullulan, or a pullulan and trehalose mixture during drying. Addition of pullulan to stabilizing excipients has been previously shown to increase emulsion droplet size on reconstitution (Bakry, et al. 2016).

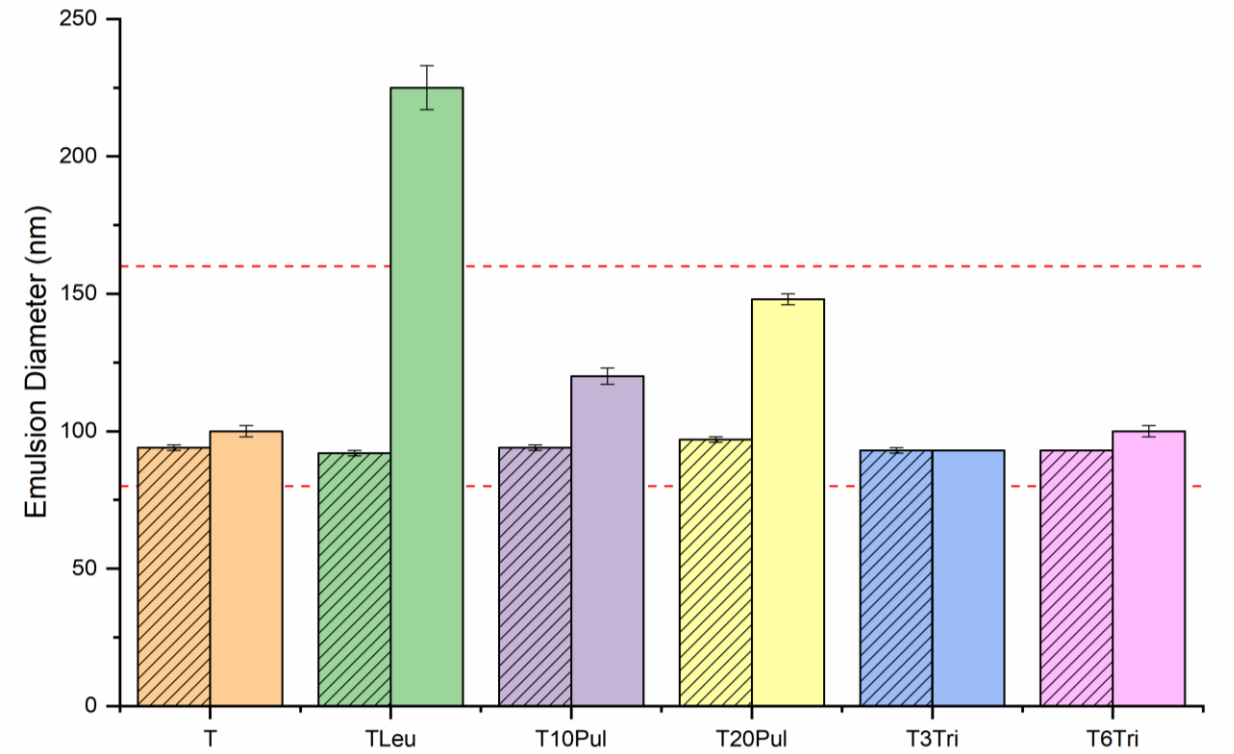

Figure 16 Droplet diameter of the nanoemulsion before and after spray drying. Addition of pullulan appears to increase the average droplet diameter slightly. Inclusion of leucine greatly increased the droplet diameter. Trehalose-only and trileucine-containing formulations preserved the droplet diameter. Striped bars represent measurements on the liquid feedstock formulations. Solid bars represent measurements on the reconstituted spray-dried powders. Error bars represent the standard deviation of three measurements. Dashed red lines indicate the acceptance limits.

The polydispersity index of the nanoemulsion droplets in the liquid formulation and the reconstituted spray-dried powder for all inhalable vaccine candidates is shown in Figure 17. Maximum acceptable polydispersity index is represented by the dashed red line. The results show that spray drying increased the polydispersity index of all inhalable vaccine candidates. This result is to be expected as some of the dispersed nanoemulsion droplets will inevitably collide and merge into larger ones during the spray drying process, causing the size distribution to deviate from perfect monodispersity. However, the measured polydispersity index of all formulations, except for the T20Leu candidate, was within the preset target criteria (<0.2). Increased polydispersity index further suggests that leucine destabilized the emulsion membrane.

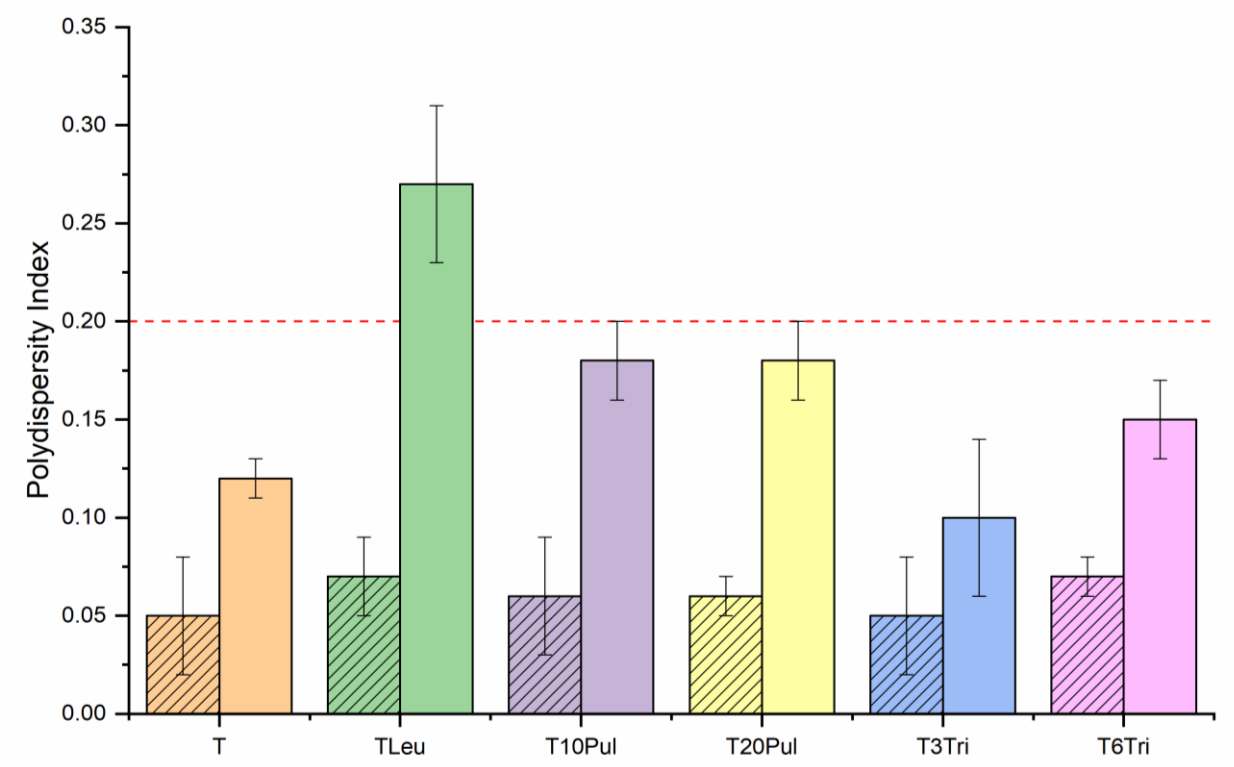

Figure 17 Polydispersity index before and after spray drying for the inhalable vaccine candidates. The graph indicates that the polydispersity index increased for all formulations after spray drying. The leucine-containing formulation had a polydispersity index greater than 0.2 post-spray drying. Striped bars represent measurements on the liquid feedstock formulations. Solid bars represent

measurements on the reconstituted spray-dried powders. Error bars represent the standard deviation of three measurements. Dashed red line indicates the acceptance limit.

3.3.4. Squalene and GLA Content

Comparison of squalene and GLA content between the feedstock and the reconstituted spray-dried powder for all inhalable candidates is shown in Table 7. Target content values are also given. No decrease in squalene content was detectable for any formulation, suggesting successful encapsulation of nanoemulsion droplets during spray drying. Therefore, addition of the chosen dispersibility enhancing agents did not have a negative effect on encapsulation efficiency. The same processing conditions were used for a first candidate of the T formulation that was formulated at a higher feedstock concentration. Previously, it was suggested that a higher feedstock concentration may increase encapsulation efficiency as a higher feedstock concentration will increase particle size and thus increase the chances for nanoemulsion droplets to be embedded in the particle. The successful retention of squalene indicates that the employed processing conditions were applicable at lower feedstock concentration for the different formulations. Reported higher values in squalene content after spray drying may be due to assay variability.

Table 7 Measured squalene and GLA content before and after spray drying for all inhalable candidates. All values are within the preset target conditions.

Formulations	Squalene Concentration (mg/mL)		GLA Concentration (µg/mL)	
	Liquid	Reconstituted Powder	Liquid	Reconstituted Powder
Target	4.53 - 6.83		2.50 - 4.17	
T	6.31 ± 0.12	6.27 ± 0.07	3.72 ± 0.08	3.77 ± 0.00
T20Leu	6.11 ± 0.06	6.35 ± 0.14	3.57 ± 0.02	3.73 ± 0.07
T10Pul	5.71 ± 0.08	6.10 ± 0.07	3.66 ± 0.02	3.77 ± 0.05
T20Pul	5.93 ± 0.07	6.21 ± 0.08	3.73 ± 0.01	3.83 ± 0.02
T3Tri	6.21 ± 0.02	6.42 ± 0.10	3.67 ± 0.02	3.83 ± 0.05
T6Tri	6.37 ± 0.11	6.89 ± 0.07	3.64 ± 0.04	3.52 ± 0.12

Similarly, it is apparent that no decrease in GLA content was detected for any formulation. Previously, it has been shown that GLA is relatively small, with a molecular weight of 1.76 kDA (Coler, Bertholet, et al. 2011), and exists at the emulsion droplet interface with the phosphate group towards the aqueous interface. The majority of the agonist (95%) resides in the squalene phase (Anderson, et al. 2010). Stabilization of GLA and subsequent desiccation protection during spray drying was expected to be due primarily to hydrogen bonds formed between the phosphate group and trehalose (Ingvarsson, Yang, et al. 2011, Pereira and Hunenberger 2006). The successful retention of GLA over spray drying suggests that the addition of the chosen dispersibility enhancing agents did not interfere with GLA stabilization via trehalose. Reported higher values in GLA content after spray drying may be due to assay variability.

3.3.5. ID93 Retention

ID93 presence was measured using SDS-PAGE analysis. Stained gels of the inhalable vaccine candidates and a control are shown in Figure 18. The ID93 band was present in all formulations with the exception of those that contained pullulan. This suggests that the addition of leucine or trileucine did not interfere with the stabilization of the antigen by trehalose during desiccation. Leucine alone has previously been demonstrated to be compatible with spray-dried BCG vaccine (Price, et al. 2020).

The absence of an ID93 band in the T10Pul and T20Pul formulations shows that the addition of pullulan negatively affects the formulations' ability to stabilize the ID93 protein, thus eliminating these formulations from consideration as inhalable candidates. Results were repeated for the pullulan-containing formulations (not shown) to confirm the absence of the ID93 band. The pullulan-trehalose excipient system was expected to stabilize the protein. Air dried pullulan tablets

have been shown to stabilize the proteins luciferase (24 kDa) and human serum albumin (66.5 kDa) (Jahanshahi-Anbuhi, et al. 2016). Similarly, the protein β-galactosidase (520 kDa) was stabilized in mixtures of pullulan and trehalose through freeze drying (Teekamp, et al. 2017). Tonnis et al.'s (Tonnis, et al. 2015) study on freeze drying of proteins stabilized in sugars of different size and molecular flexibility demonstrated that the smallest sugar tested, trehalose, was the most effective stabilizer of proteins. However, the results showed that combinations of a disaccharide and a polysaccharide were also able to stabilize the proteins, albeit to a lower degree, as the addition of a small disaccharide was suggested to counteract the steric hindrance associated with a polysaccharide, such as pullulan. However, pullulan alone is not an effective stabilizer of vaccines. Pullulan alone has been shown to offer poor protection against desiccation for HSV-2 vaccine, with significant loss in titer on drying and complete loss after only a week of storage at room temperature (Leung, et al. 2019). Similarly, spray drying of bacteriophage showed significantly higher titer loss due to processing for pullulan alone as compared to a pullulan and trehalose excipient system (Carrigy, Liang, et al. 2019). The molecular size of sugars affects the stabilization ability of proteins during spray drying and smaller molecules are better able to stabilize proteins (Grasmeijer, et al. 2013). Pullulan has a molecular mass of 115 kDa (Carrigy, Liang, et al. 2019) and ID93 protein has a similar molecular mass of 93 kDa (Bertholet, Ireton and Ordway, et al. 2010). By contrast, trehalose has a much smaller molecular mass of 0.342 kDa, allowing the trehalose molecules to closely interact with the irregular protein structure. In the present study, due to the similar molecular mass, the ID93 protein may have accumulated on the particle surface with pullulan. This would result in ID93 primarily encapsulated in a pullulan

matrix instead of trehalose where, based on literature, the ID93 protein would not be well-protected against desiccation stress.

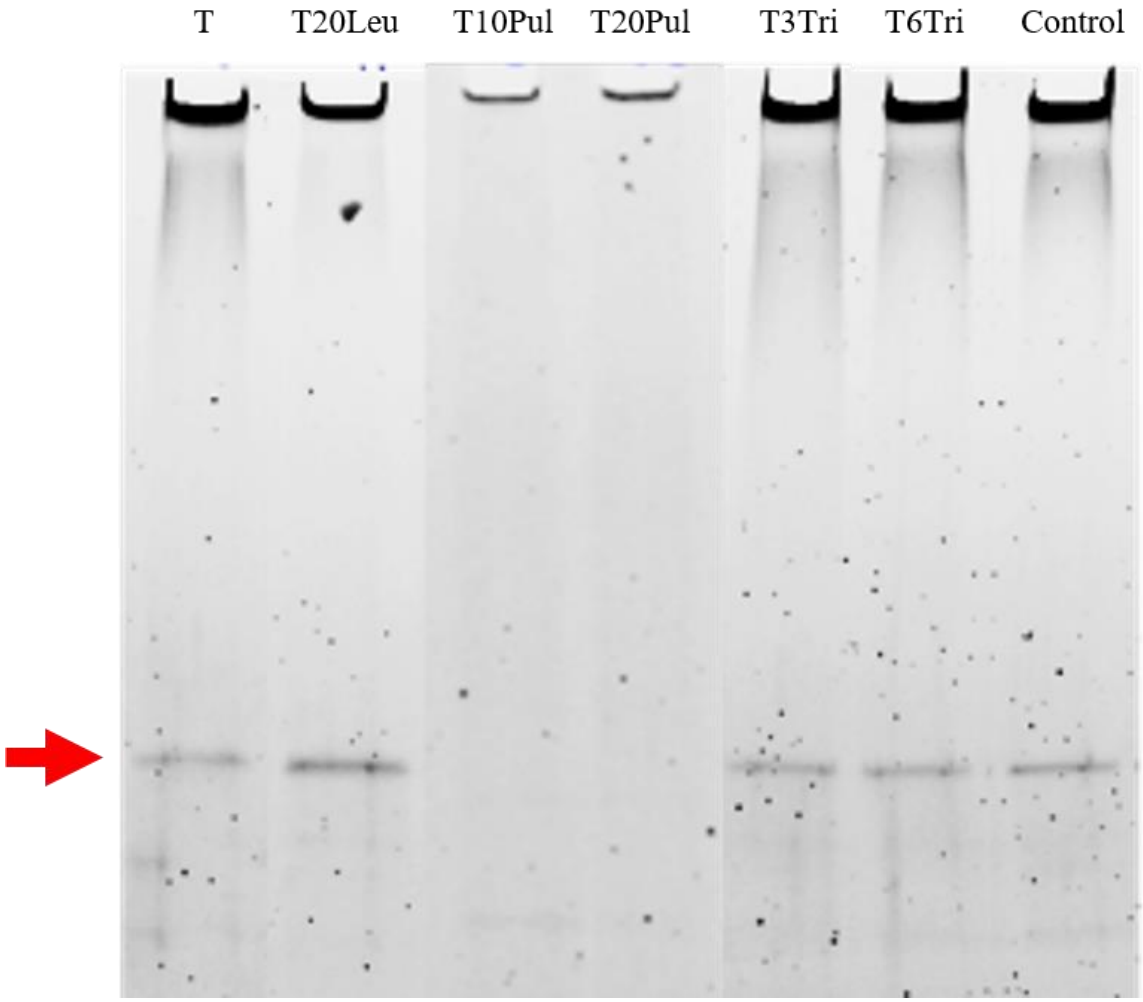

Figure 18 SDS-PAGE analysis for ID93 presence based on existence and location of band. Analysis was completed on all inhalable vaccine candidates. SDS-PAGE analysis for a control ID93+GLA-SE formulation has been provided in the last lane for comparison. It is apparent that the band is present for all formulations except the ones containing pullulan.

3.3.6. Aerosol Performance

Successful respiratory pharmaceutical delivery requires an that appropriate dose be delivered to the lung and that the powder deposits in the appropriate region of the lung. Aerosol performance

and size distribution of a powder are useful measures of suitability for respiratory delivery. Table 8 compares the inhalable vaccine candidates' overall aerosol performance and size distribution of the lung dose, that is, the powder which penetrated the throat model and deposited within the impactor. Mass distribution of each candidate, shown in Figure 19, was used to calculate size distribution. The bracketed $d_{a,50}$ values are greater than the minimum particle size expected to deposit on Stage 1 (6.12 μm). The larger value indicates that these powders experienced greater deposition in the throat and on the first stage of the impactor due to significant particle aggregation.

Emitted dose for all inhalable candidates ranged from 84-97%. These results are very high for an experimental dry powder formulation, even outperforming some commercial DPI products (de Boer, et al. 2017). However, the candidates exhibited markedly different performances in terms of lung dose.

Table 8 Emitted dose, lung dose, and particle size analysis of the deposited powder for all inhalable vaccine candidates after aerosol performance experiments. Emitted dose was defined as the mass of powder that has left the DPI, and lung dose was defined as the mass of powder that penetrates the throat model. Both parameters are given as a percentage of the powder dose mass loaded into the capsules. Size distribution parameters $d_{a,50}$ and σ_g were calculated via a fit to the cumulative lognormal distribution of the powder that deposited on the impactor stages. Results shown represent the average of triplicate measurements and error bars represent standard deviation. Statistically significant differences relative to the T formulation are marked with an asterisk. Bracketed values are greater than the Stage 1 cutoff diameter.

Formulation	Emitted Dose (% Dose)	Lung Dose (% Dose)	$d_{a,50}$ (μm)	σ_g
T	87 ± 13	18 ± 0.5	5.7 ± 0.8	2.3 ± 0.1
T20Leu	97 ± 3*	32 ± 12	(8.8 ± 2.3)*	2.9 ± 0.6
T10Pul	89 ± 13	25 ± 3	(10.8 ± 0.3)*	2.5 ± 0.3
T20Pul	84 ± 12	19 ± 2	(6.4 ± 0.2)*	2.6 ± 0.3
T3Tri	93 ± 15	34 ± 6*	5.7 ± 0.2	4.2 ± 1.5
T6Tri	96 ± 6	33 ± 6*	5.4 ± 0.2	3.4 ± 0.4*

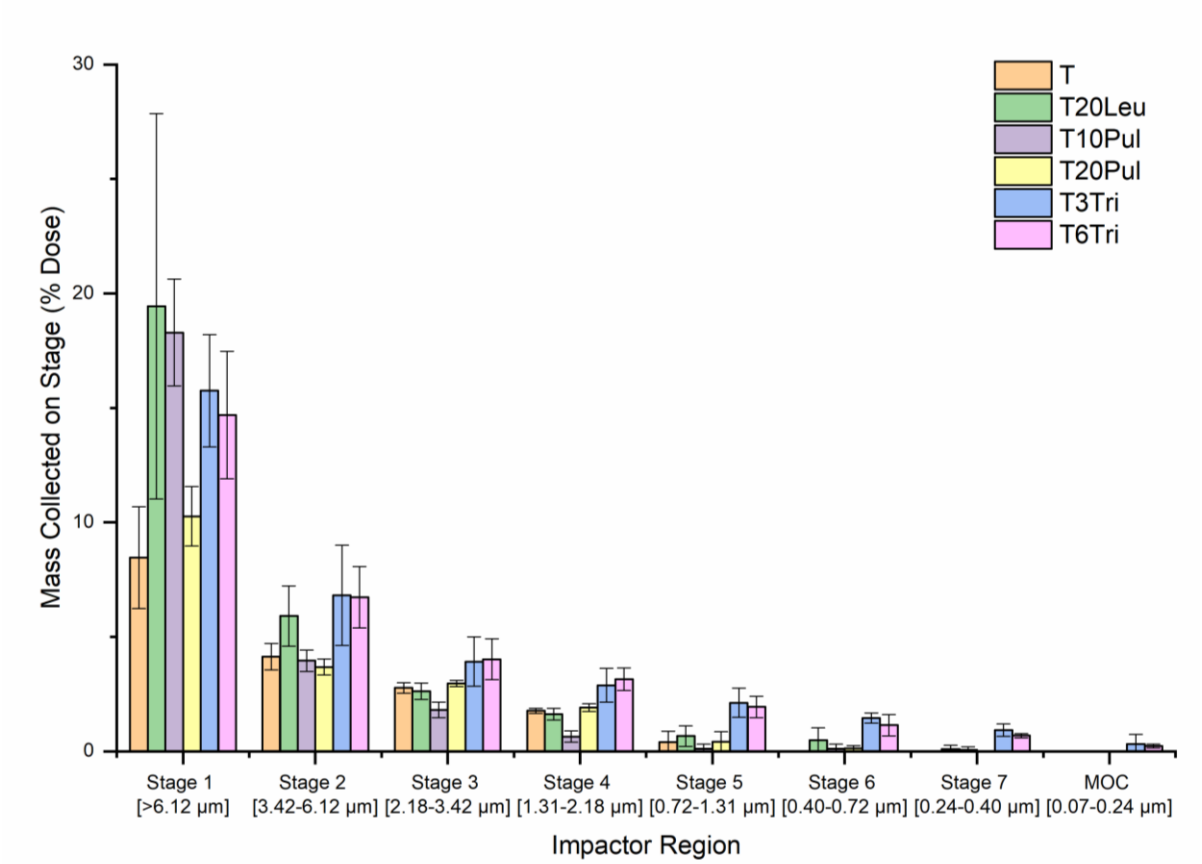

Figure 19 Mass distribution of the inhalable vaccine powder for each formulation. Depth of penetration varied based on formulation composition. The trileucine containing formulations had the greatest penetration, with deposition measured on the micro-orifice collector (MOC) of the impactor. Results shown represent the average of triplicate measurements and error bars represent standard deviation.

The T formulation had the lowest mean lung dose of the investigated candidates. These results are expected as the T formulation did not include any dispersibility enhancing agents. The $d_{a,50}$ of the T formulation was low compared to the other formulations, which would typically suggest that the formulation was well-dispersed. However, as shown in Figure 19, the T formulation deposited the least average amount of mass on Stage 1 as most of the powder aggregates deposited in the throat model instead. The lack of powder deposited on the later stages of the impactor further indicates that the T formulation was not well-dispersed. The low measured $d_{a,50}$ is due to the much higher

level of particle aggregation as compared to the others. The high level of aggregation led to most of the larger aggregates depositing in the throat prior to the impactor stages, as evidenced by the lowest lung dose.

The T20Leu formulation almost doubled lung dose as compared to the T formulation due to the designed crystalline layer of leucine on the surface of the former. As discussed previously, increased rugosity and stiffness of the surface decrease the force of cohesion between particles and therefore make the powder more dispersible. These results showing that a crystalline leucine surface layer increases dispersibility of the powder was consistent with other studies. However, the fact that the measured $d_{\mathrm{a},50}$ was higher than the theoretical values suggests that many particles remained aggregated after exiting the DPI. Feng et al. (Feng, et al. 2011) demonstrated that increasing leucine concentration in spray-dried leucine-trehalose systems improves dispersibility of the powder. Similarly, Arora et al. (Arora, et al. 2016) demonstrated that spray drying the drug voriconazole with 20% leucine increased dispersibility when tested using a similar DPI and NGI set up. Emitted dose for the spray-dried voriconazole formulation without leucine was only 58% but increased to 82% for the formulation containing 20% leucine. However, the dispersibility of a crystalline formulation is not solely dependent on the presence of surface crystals but also on their size and the number density of these surface crystals. Raula et al. (Raula, et al. 2010) coated salbutamol sulphate microparticles with leucine at different saturation levels and assessed dispersibility of the powders using a commercial DPI with a custom inhalation simulator. Morphological analysis found that increasing leucine content led to an increase in size and number density of asperities on the surface of the particles. The leucine coating improved particle dispersity over the uncoated particles, however, the authors found that the emitted dose decreased

with further increasing leucine content. Smaller surface asperities may be more beneficial for improving particle dispersity as larger surface asperities may not reduce contact area and instead introduce mechanical interlocking forces between particles.

The neither of the pullulan-containing T10Pul or T20Pul formulations statistically significantly improved lung dose. The change in surface morphology due to the addition of pullulan did not sufficiently reduce the forces of cohesion between the particles. The particle surface dimples may have been detrimental in the present study due to the polydispersity of the powder. It is possible that the dimples in the larger particles may have provided an area for smaller particles to settle into, increasing the contact area between the two. Similarly, the measured particle sizes, which were larger than the theoretical predictions also suggest a high level of particle aggregation. Particle dimples are shown to a higher extent with increased pullulan concentration, possibly explaining the lower aerosol performance of the T20Pul formulation compared to T10Pul. Previously, it was shown that spray-dried pullulan-trehalose systems at different concentrations either improved or had the same aerosol performance as spray-dried trehalose microparticles (Carrigy, Liang, et al. 2019). Similar to the results shown in this study, the formulation containing 10% pullulan and 90% trehalose by mass improved the aerosol performance compared to spray-dried trehalose alone, however, the 40% pullulan and 60% trehalose formulation had an aerosol performance similar to that of trehalose alone. This suggests a point of diminishing returns for the addition of pullulan to improve powder dispersibility.

It is apparent that the trileucine containing formulations, T3Tri and T6Tri, performed the best out of the tested inhalable vaccine candidates. These formulations were the only ones found to significantly improve the mean lung dose as compared to the T formulation. The measured $d_{\mathrm{a},50}$

for the trileucine-containing formulations was also the lowest out of all inhalable candidates. The average σ_g values of the trileucine-containing formulations were the largest, indicating a wide range in particle size of the deposited powder. The dispersed powder size range is illustrated in Figure 19 where the trileucine-containing formulations were the only candidates to exhibit powder deposition on all NGI stages and the MOC. Altogether, these results indicate that the inclusion of trileucine led to superior ability to disperse the smaller particles in the powder. Based on the high dispersibility potential, the trileucine containing formulations are the only ones which can deliver a portion of the vaccine in the peripheral region of the lung. Differences in the aerosol performance of the T3Tri and the T6Tri formulations were statistically insignificant, suggesting a similar level of trileucine particle surface coverage for both the T3Tri and the T6Tri formulations.

None of the inhalable vaccine candidates was completely dispersed to the predicted primary aerodynamic particle size of 3-4 μm. However, aerosol performance assessment was completed with an unoptimized DPI in this study. As explicitly noted in de Boer et al.'s (de Boer, et al. 2017) review paper on dry powder inhalation, successful pulmonary delivery of vaccines often requires further DPI development to improve efficiency and deep lung delivery. Recently, Sibum et al. (Sibum, et al. 2020) assessed the aerosol performance and stability of isoniazid spray-dried with leucine or trileucine. Their results found that use of the Cyclops DPI over a Twincer DPI improved the emitted dose of the 3% leucine, 5% leucine, and 3% trileucine formulations by approximately 40%, 25%, and 10%, respectively.

3.4. Conclusion

This study demonstrates the use of particle engineering principles in the investigation of various excipients to improve aerosol performance of a complex inhalable vaccine formulation. In this study an excipient system was developed that encapsulated an adjuvanted subunit TB vaccine candidate formulated as a nanoemulsion via spray drying. Promising aerosol performance was achieved by adding a dispersibility enhancer, trileucine, to the formulation. This study also demonstrated the potential of the vaccine to be delivered as a respirable dosage to human lungs via inhalation using a DPI. Published work on spray drying vaccines formulated as lipid-based dispersions has primarily focused on stabilization. To the best of our knowledge, there has not been any published work on successfully stabilizing a vaccine formulated as a nanoemulsion at the 100 nm scale in a spray-dried powder that maintained nanoemulsion size and demonstrated reasonable *in vitro* aerosol performance.

The demonstrated potential for pulmonary vaccine delivery creates options for vaccines, such as the model TB vaccine investigated in this study, to be administered via a route that is alternative to the traditional parenteral injection. Intranasal delivery of the spray-dried vaccine may be possible with adjustments to some particle properties, such as the size of the spray-dried particles, or switching to another delivery device. Administration through inhalation mitigates risks associated with needle delivery such as needlestick injuries, needlestick waste, and transfer of bloodborne illnesses. Nevertheless, more work is needed to further characterize the storage stability of the inhalable spray-dried vaccine. The potential for pulmonary delivery has been demonstrated, however, at this point it is not known which administration route will elicit the strongest immune response for this particular TB vaccine candidate. Preclinical *in vivo* studies

must be completed to compare the effects of vaccine administration via different routes on immunogenicity and efficacy.

3.5. References

Aguilo, Nacho, Samuel Alvarez-Arguedas, Santiago Uranga, Dessislava Marinova, Marta Monzon, Juan Badiola, and Carlos Martin. 2016. "Pulmonary but not subcutaneous delivery of BCG vaccine confers protection to tuberculosis-susceptible mice by an interleukin 17-dependent mechanism." *Journal of Infectious Diseases* 213 (5): 813-839. doi:10.1093/infdis/jiv503.

Andersen, Peter, and Timothy Mark Doherty. 2005. "The success and failure of BCG - implications for a novel tuberculosis vaccine." *Nature Reviews Microbiology* 3: 656-662. doi:10.1038/nrmicro1211.

Anderson, Ryan C., Christopher B. Fox, Timothy S. Dutill, Narek Shaverdian, Tara L. Evers, Garrett R. Poshusta, James Chesko, et al. 2010. "Physicochemical characterization and biological activity of synthetic TLR4 agonist formulations." *Colloids and Surfaces B: Biointerfaces* 75: 123-132.

Argarkhedkar, Sharad, Prasad S. Kulkarni, Scott Winston, Robert Sievers, Rajeev M. Dhere, Bhagwat Gunale, Ken Powell, Paul a. Rota, Mark Papania, and MDVP author group. 2014. "Safety and immunogenicity of dry powder measles vaccine administered by inhalation: A randomized controlled Phase 1 clinical trial." *Vaccine* 32: 6791-6797. doi:10.1016/j.vaccine.2014.09.071.

Arora, Sumit, Mehra Haghi, Paul M. Young, Michael Kappl, Daniela Traini, and Sanyog Jian. 2016. "Highly respirable dry powder inhalable formulation of voriconazole with enhanced pulmonary bioavailability." *Expert Opinion on Drug Delivery* 13 (2): 183-193. doi:10.1517/17425247.2016.1114603 ORIGINAL.

Bahamondez-Canas, Tania F., and Zhengrong Cui. 2018. "Intranasal immunization with dry powder vaccines." *European Journal of Pharmaceutics and Biopharmaceutics* 122: 167-175.

Bakry, Amr M., Zheng Fang, Yingzhou Ni, Hao Cheng, Yong Q. Chen, and Li Liang. 2016. "Stability of tuna oil and tuna oil/peppermint oil blend microencapsulated using whey protein isolate in

combination with carboxymethyl cellulose or pullulan." *Food Hydrocolloids* 60: 559-571. doi:10.1016/j.foodhyd.2016.04.026.

Bertholet, Sylvie, Gregory C. Ireton, Diane J. Ordway, Hillarie Plessner Windish, Samuel O. Pine, Maria Kahn, Tony Phan, et al. 2010. "A defined tuberculosis vaccine candidate boosts BCG and protects against multidrug-resistant Mycobaterium tuberculosis." *Science Translational Medicine* 2 (53): 53-74. doi:10.1126/scitranslmed.3001094.

Boraey, Mohammed A., and Reinhard Vehring. 2014. "Diffusion controlled formation of microparticles." *Journal of Aerosol Science* 67: 131-143.

Carrigy, Nicholas B. , Lu Liang, Hui Wang, Samuel Kariuki, Tobi E. Nagel, Ian F. Connerton, and Reinhard Vehring. 2019. "Trileucine and pullulan improve anti-Campylobacter bacteriophage stability in engineered spray-dried microparticles." *Annals of Biomedical Engineering* 48: 1169-1180. doi:10.1007/s10439-019-02435-6.

Carrigy, Nicholas B., and Reinhard Vehring. 2019. "Engineering stable spray-dried biologic powder for inhalation." In *Pharmaceutical Inhalation Aerosol Technology (3rd ed.)*, edited by A. J. Hickey and S. da Rocha, 291-326. Boca Raton: CRC Press.

Carrigy, Nicholas B., Mani Ordoubadi, Yushan Liu, Omar Melhem, David Barona, Hui Wang, Leanne Milburn, Conor A. Ruzycki, Warren H. Finlay, and Reinhard Vehring. 2019. "Amorphous pullulan trehalose microparticle platform for respiratory delivery." *International Journal of Pharmaceutics* 563: 156-168. doi:10.1016/j.ijpharm.2019.04.004.

Chan, Michelle Y., Quinton M. Dowling, Sandra J. Sivananthan, and Ryan M. Kramer. 2017. "Particle sizing of nanoparticle adjuvant formulations by dynamic light scattering (DLS) and nanoparticle

tracking analysis (NTA)." *Methods in Molecular Biology* 1494: 239-252. doi:10.1007/978-1-4939-6445-1_17.

Chen, Lihao, Jun Wang, Anna Zganiacz, and Zhou Xing. 2004. "Single intranasal mucosal Mycobacterium bovis BCG vaccination confers improved protection compared to subcutaneous vaccination against pulmonary tuberculosis." *Infection and Immunity* 72 (1): 238-246. doi:10.1128/IAI.72.1.238–246.2004.

Chen, Liuhua, Lihua Gan, Mingxian Liu, Rong Fan, Zijie Xu, Hao Zhixian, and Longwu Chen. 2011. "Destabilization of artificial biomembrane induced by the penetration of tryptophan." *Applied Surface Science* 257: 5070-5076. doi:10.1016/j.apsusc.2011.01.023.

Coler, Rhea N., Sylvie Bertholet, Magdalini Moutaftsi, Jeff A. Guderian, Hillarie Plessner Windish, Susan L. Baldwin, Elsa M. Laughlin, et al. 2011. "Development and characterization of synthetic glucopyranosyl lipid adjuvant system as a vaccine adjuvant." *Public Library of Science One* 6 (1): e16333. doi:10.1371/journal.pone.0016333.

Darquenne, Chantal. 2012. "Aerosol deposition in health and disease." *Journal of Aerosol Medicine and Pulmonary Drug Delivery* 25 (3): 140-147. doi:10.1089/jamp.2011.0916.

de Boer, A. H., P. Hagedoorn, M. Hoppentocht, F. Buttini, F. Grasmeijer, and H. W. Frijlink. 2017. "Dry powder inhalation: past, present and future." *Expert Opinion on Drug Delivery* 14 (4): 499-512. doi:10.1080/17425247.2016.1224846.

Derrick, Steven C., Kristopher Kolibab, Amy Yang, and Sheldon L. Morris. 2014. "Intranasal administration of Mycobacterium bovis BCG induces superior protection against aerosol infection with Mycobacterium tuberculosis in mice." *Clinical and Vaccine Immunology* 21 (10): 1443-1451.

Ekdawi-Sever, Nancy, and Juan J. de Pablo. 2003. "Diffusion of sucross and a,a-trehalose in aqueous solutions." *Journal of Physical Chemistry A* 107: 936-943. doi:10.1021/jp020187b.

Erickson, Harold P. 2009. "Size and shape of protein molecules at the nanometer level determined by sedimentation, gel filtration, and electron microscopy." *Biological Procedures Online* 11: 32-51. doi:10.1007/s12575-009-9008-x.

Feng, A. L., M. A. Boraey, M. A. Gwin, P. R. Finlay, P. J. Kuehl, and R. Vehring. 2011. "Mechanistic models facilitate efficient development of leucine containing microparticles for pulmonary drug delivery." *International Journal of Pharmaceutics* 409: 156-163.

Finlay, Warren H. 2019. *The Mechanics of Inhaled Pharmaceutical Aerosols: An Introduction.* 2nd. Academic Press. doi:10.1016/C2018-0-00116-4.

Flynn, Joanne L., J. Chan, and P. L. Llin. 2011. "Macrophages and control of granulomatous inflammation in tuberculosis." *Mucosal Immunology* 4 (3): 271-278. doi:10.1038/mi.2011.14.

Grasmeijer, N., M. Stankovic, H. de Waard, H. W. Frijlink, and W. L. J. Hinrichs. 2013. "Unraveling protein stabilization mechanisms: vitrification and water replacement in a glass transition temperature controlled system." *Biochimica et Biophysica Acta* 1834 (4): 763-769. doi:10.1016/j.bbapap.2013.01.020.

Grasmeijer, Niels, Henderik W. Frijlink, and Wouter L. J. Hinrichs. 2016. "Model to predict inhomogeneous protein-sugar distribution in powders prepared by spray drying." *Journal of Aerosol Science* 101: 22-33. doi:10.1016/j.jaerosci.2016.07.012.

Grasmeijer, Niels, Valeria Tiraboschi, Herman J. Woerdenbag, Henderik W. Frijlink, and Wouter L. J. Hinrichs. 2019. "Identifying critical process steps to protein stability during spray drying using a

vibrating mesh or a two-fluid nozzle." *European Journal of Pharmaceutical Sciences* 128: 152-157.

Grgic, Biljana, Warren H. Finlay, and Anthony Heenan. 2004. "Regional aerosol deposition and flow measurements in an idealized mouth and throat." *Journal of Aerosol Science* 35: 21-32.

Hesseling, A. C., L. F. Johnson, H. Jaspan, M. F. Cotton, A. Whitelaw, H. S. Schaaf, P. E. M. Fine, et al. 2009. "Disseminated bacille Calmette-Guerin disease in HIV-infected South African infants." *Bulletin of the World Health Organization* 87: 505-511. doi:doi:10.2471/BLT.08.055657.

Hickey, A. J., P. G. Durham, A. Dharmadhikari, and E. A. Nardell. 2016. "Inhaled drug treatment for tuberculosis: Past progress and future prospects." *Journal of Controlled Release* 240: 127-134.

Hoe, Susan, James W. Ivey, Mohammed A. Boraey, Abouzar Shamsaddini-Shahrbabak, Emadeddin Javaheri, Matinkhoo Sadaf, Warren H. Finlay, and Reinhard Vehring. 2014. "Use of a fundamental approach to spray-drying formulation design to facilitate the development of multi-component dry powder aerosols for respiratory drug delivery." *Pharmaceutical Research* 32 (2): 449-465.

Infectious Disease Research Institute. 2019. "Identifier: NCT03722472, Phase 1 Clinical Trial of Single-Vial ID93 + GLA-SE in Healthy Adults." *U.S. National Library of Medicine Clinical Trials Registry.* September 3. Accessed April 23, 2020. https://clinicaltrials.gov/ct2/show/NCT03722472?term=id93&draw=2&rank=1.

Ingvarsson, Pall Thor, Mingshi Yang, Hanne Morck Nielsen, Jukka Rantanen, and Camilla Foged. 2011. "Stabilization of liposomes during spray drying." *Expert Opinion on Drug Delivery* 8 (3): 375-388. doi:10.1517/17425247.2011.553219.

Ivey, James W., and Reinhard Vehring. 2010. "The use of modeling in spray drying of emulsions and suspensions accelerates formulation and process development." *Computers and Chemical Engineering* 34: 1036-1040. doi:10.1016/j.compchemeng.2010.02.031.

Ivey, James, Pallavi Bhambri, David Lewis, Tayna Church, Warren Finlay, and Reinhard Vehring. 2016. "Dried corticosteroid particle formation from evaporating monodisperse propellant solution droplets." *AAPS Annual Meeting and Exposition.* Denver.

Jahanshahi-Anbuhi, Sana, Balamurali Kannan, Vincent Leung, Kevin Pennings, Meng Liu, Carmen Carrasquilla, Dawn White, et al. 2016. "Simple and ultrastable all-inclusive pullulan tablets for challenging bioassays." *Chemical Science* 7: 2342-2346. doi:10.1039/c5sc04184h.

Jones, R. Mark, Michael Burke, Devon Dubose, Jessica A. Chichester, Slobodanka Manceva, April Horsey, Stephen J. Streatfield, Jeff Breit, and Vidadi Yusibov. 2017. "Stability and pre-formulation development of a plant-produced anthrax vaccine candidate." *Vaccine* 35: 5463-5470. doi:10.1016/j.vaccine.2016.12.009.

Kanojia, Gaurav, Geert-Jan Willems, Henderik W. Frijlink, Gideon F. A. Kersten, Peter C. Soema, and Jean-Pierre Amorij. 2016. "A design of experiment approach to predict product and process parameters for a spray-dried influenza vaccine." *International Journal of Pharmaceutics* 511: 198-1111. doi:10.1016/j.ijpharm.2016.08.022.

Kanojia, Gaurav, Rimko ten Have, Peter C. Soema, Henderik Frijlink, Pierre Amorij, and Gideon Kersten. 2017. "Developments in forumulation and delivery of spray dried vaccines." *Human Vaccines & Immunotherapeutics* 13 (10): 2364-2378. doi:10.1080/21645515.2017.1356952.

Kramer, Ryan M., Michelle C. Archer, Natasha Dubois, Natasha Dubois Cauwelaert, Elyse A. Beebe, Po-wei D. Huang, Quinton M. Dowling, et al. 2018. "Development of a thermostable nanoemulsion

adjuvanted vaccine against tuberculosis using a design-of-experiments approach." *International Journal of Nanomedicine* 13: 3689-3711.

Kunda, Nitesh K., Iman M. Alfagih, Eliane N. Miyaji, Douglas B. Figueiredo, Viviane M. Goncalves, Daniela M. Ferreira, Sarah R. Dennison, Satyanarayana Somavarapu, Gillian A. Hutcheon, and Imran Y. Saleem. 2015. "Pulmonary dry powder vaccine of pneumococcal antigen loaded nanoparticles." *International Journal of Pharmaceutics* 495 (2): 903-912. doi:10.1016/j.ijpharm.2015.09.034.

Langford, Alex, Bakul Bhatnagar, Robert Walters, Serguel Tchessalov, and Satoshi Ohtake. 2018. "Drying technologies for biopharmaceutical applications: Recent developments and future direction." *Drying Technology* 36 (6): 677-687. doi:10.1080/07373937.2017.1355318.

Leathers, T. D. 2003. "Biotechnical production and applications of pullulan." *Applied Microbiology and Biotechnology* 62: 468-473. doi:10.1007/s00253-003-1386-4.

Lechuga-Ballesteros, David, Chatan Charan, Cheryl L.M. Stults, Cynthia L. Stevenson, Danforth P. Miller, Reinhard Vehring, Vathana Tep, and Mei-Chang Kuo. 2008. "Trileucine Improves Aerosol Performance and Stability of Spray-Dried Powders for Inhalation." *Journal of Pharmaceutical Sciences* 97 (1): 287-302. doi:10.1002/jps.21078.

LeClair, Daniel A., Lillian Li, Nausheen Rahman, Emily D. Cranston, Zhou Xing, and Michael R. Thompson. 2019. "Stabilization of HSV-2 viral candidate by spray drying." *International Journal of Pharmaceutics* 569: 1-10. doi:10.1016/j.ijpharm.2019.118615.

Leung, Sharon S. Y., Thaigarajan Parmasivam, An Nguyen, Thomas Gengenbach, Elizabeth A. Carter, Nicholas B. Carrigy, Hui Wang, et al. 2018. "Effect of storage temperature on the stability of spray

dried bacteriophage powders." *European Journal of Pharmaceutics and Biopharmaceutics* 127: 213-222.

Leung, Vincent, Jonathan Mapletoft, Ali Zhang, Amanda Lee, Fatemeh Vahedi, Marianne Chew, Alexandra Szewczyk, et al. 2019. "Thermal stabilization of viral vaccines in low-cost sugar films." *Scientific Reports* 9 (7631).

Li , Q., V. Rudolph, and W. Peukert. 2006. "London-van der Waals adhesiveness of rough particles." *Powder Technology* 161: 248-255.

Li, Lang, Siping Sun, Thaigarajan Parumasivam, John A. Denman, Thomas Gengenbach, Patricia Tang, Shirui Mao, and Hak-Kim Chan. 2016. "L-Leucine as an excipient against moisture on in vitro aerosolization performances of highly hygroscopic spray-dried powders." *European Journal of Pharmaceutics and Biopharmaceutics* 102: 132-141. doi:10.1016/j.ejpb.2016.02.010.

Marple, Virgil A., Daryl L. Roberts, Francisco J. Romay, Nicholas C. Miller, Keith G. Truman, Michiel Van Oort, Bo Olsson, Michael J. Holroyd, Jolyon P. Mitchell, and Dieter Hochrainer. 2003. "Next Generation Pharmaceutical Impactor (A New Impactor for Pharmaceutical Inhaler Testing) Part 1: Design." *Journal of Aerosol Medicine* 16 (3): 283-299.

McAdams, David, Dexiang Chen, and Debra Kristensen. 2012. "Spray drying and vaccine stabilization." *Expert Review of Vaccines* 11 (10): 1211-1219. doi:10.1586/erv.12.101.

Nakagaki, Masayuki, and Emiko Okamura. 1982. "Penetration leucine and norleucine into lecithin monolayers from underlying aqueous solutions." *Bulletin of the Chemical Society of Japan* 55 (11): 3381-3385. doi:10.1246/bcsj.55.3381.

Orr, Mark T., Christopher B. Fox, Susan L. Baldwin, Sandra J. Sivananthan, Elyse Lucas, Susan Lin, Tony Phan, et al. 2013. "Adjuvant formulation structure and composition are critical for the development of an effective vaccine against tuberculosis." *Journal of Controlled Release* 172: 190-200.

Orr, Mark T., Ryan M. Kramer, Lucien V. Barnes, Quinton M. Dowling, Anthony L. Desbien, Elyse A. Beebe, John D. Laurance, et al. 2014. "Elimination of the cold-chain dependence of a nanoemulsion adjuvant vaccine against tuberculois by lyophilization." *Journal of Controlled Release* 10 (177): 20-26. doi:10.1016/j.jconrel.2013.12.025.

Pavkov, Richard, Stefan Mueller, Katrin Fiebich, Dilraj Singh, Frank Stowasser, Giovanni Pignatelli, Benoit Walter, et al. 2010. "Characteristics of a capsule based dry powder inhaler for the delivery of indacterol." *Current Medial Research and Opinion* 26 (11): 2527-2533.

Pereira, Cristina S., and Philippe H. Hunenberger. 2006. "Interaction of the sugars trehalose, maltose and glucose with a phospholipid bilayer: a comparative molecular dynamics study." *The Journal of Physical Chemistry* 110 (31): 15572-15581. doi:10.1021/jp060789l.

Price, Dominique N., Nitesh K. Kunda, Rajaun Ellis, and Pavan Muttil. 2020. "Design and optimization of a temperature-stable dry powder BCG vaccine." *Pharmaceutical Research* 37 (11): 1-14. doi:10.1007/s11095-019-2739-8.

Raula, Janne, Frank Thielmann, Majid Naderi, Vessa-Pekka Lehto, and Esko I. Kauppinen. 2010. "Investigations on particle surface characteristics vs. dispersion behaviour of L-leucine coated carrier-free inhalable powders." *International Journal of Pharmaceutics* 385: 79-85.

Sangon Biotech. 2018. "Safety Data Sheets: Pullulan." February 6. Accessed April 5, 2020. https://www.sangon.com/productImage/SDS/A506209/A506209_EN_S.pdf.

Shang, Yidan, Jingliang Dong, Kiao Inthavong, and Jiyuan Tu. 2015. "Comparative numerical modeling of inhaled micron-sized particle deposition in human and rate nasal cavities." *Inhalation Toxicology* 27 (13): 694-705.

Sibum, Imco, Paul Hagedoorn, Markus P. G. Kluitman, Martijn Kloezen, Henderik W. Frijlink, and Floris Grasmeijer. 2020. "Dispersity and storage stability optimization of high dose isoniazid dry powder inhalation formulations with L-leucine or trileucine." *Pharmaceutics* 12 (24): 1-14. doi:10.3390/pharmaceutics12010024.

Sigma-Aldrich. 2020. "Safety Data Sheet: L-Leucine." January 15. Accessed April 5, 2020. https://www.sigmaaldrich.com/catalog/product/sigma/l8000?lang=en&region=US.

Sou, Tomas, David A. V. Morton, Mark Williamson, Els N. Meeusen, Lisa M. Kaminskas, and Michelle P. McIntosh. 2015. "Spray-dried influenza antigen with trehalose and leucine produces an aerosolizable powder vaccine formulation that induces strong systemic and mucosal immunity after pulmonary administration." *Journal of Aerosol Medicine and Pulmonary Drug Delivery* 28 (5): 361-371. doi:10.1089/jamp.2014.1176.

Teekamp, Naomi, Yu Tian, Carolina Visser, Peter Olinga, Henderik W. Frijlink, Herman J. Woerdenbag, and Wouter L. J. Hinrichs. 2017. "Addition of pullulan to trehalose glasses improves the stability of beta-galactosidase at high moisture conditions." *Carbohydrate Polymers* 176: 374-380.

Toniolo, Steven P., Sam Afkhami, Ahmad Mahmood, Cecile Fradin, Brian D. Lichty, Matthew S. Miller, Zhou Xing, Emily D. Cranston, and Michael R. Thompson. 2019. "Excipient selection for thermally stable enveloped and non-enveloped viral vaccine platforms in dry powders." *International Journal of Pharmaceutics* 561: 66-73. doi:10.1016/j.ijpharm.2019.02.035.

Tonnis, W. F., M. A. Mensink, A. de Jager, K. van der Voort Maarschalk, H. W. Frijlink, and W. L. Hinrichs. 2015. "Size and molecular flexibility of sugars determine the storage stability of freeze-dried proteins." *Molecular Pharmaceutics* 12: 684-694. doi:10.1021/mp500423z.

United States Pharmacopeia. 2017. "<601> Aerosols, nasal sprays, metered-dose inhalers, and dry powder inhalers."

Usmani, Omar S., Martyn S. Biddiscombe, and Peter J. Barnes. 2005. "Regional lung deposition and bronchodilator response as a function of beta2-agonist particle size." *American Journal of Respiratory and Critical Care Medicine* 172 (12): 1497-1504.

Vandenheuvel, Dieter, Joke Meesus, Rob Lavigne, and Guy Van den Mooter. 2014. "Instability of bacteriophages in spray-dried trehalose powders is caused by crystallization of the matrix." *International Journal of Pharmaceutics* 472: 202-205.

Vehring, Reinhard. 2008. "Pharmaceutical Particle Engineering via Spray Drying." *Pharmaceutical Research* 25 (5): 999-1022. doi:10.1007/s11095-007-9475-1.

Vehring, Reinhard. 2005. "Red-excitation dispersive Raman spectroscopy is a suitable technique for solid-state analysis of respirable pharmaceutical powders." *Applied Spectroscopy* 59 (3): 286-292.

Vehring, Reinhard, Willard R. Foss, and David Lechuga-Ballesteros. 2007. "Particle formation in spray drying." *Aerosol Science* 38: 728-746.

Verreck, Frank A. W., Elma Z. Tchilian, Richard A.W. Vervenne, Claudia C. Sombroek, Ivanela Kondova, Okke A. Eissen, Vinod Sommandas, et al. 2017. "Variable BCG efficacy in rhesus populations: pulmonary BCG provides protection where standard intradermal vaccination fails." *Tuberculosis* 104: 46-57.

Wang, Hui, David Barona, Sulayman Oladepo, Lisa Williams, Susan Hoe, David Lechuga-Ballesteros, and Reinhard Vehring. 2017. "Macro-Raman spectroscopy for bulk composition and homogeneity analysis of multi-component pharmaceutical powders." *Journal of Pharmaceutical and Biomedical Analysis* 141: 180-191.

Wang, Hui, David S. Nobes, and Reinhard Vehring. 2019. "Particle Surface Roughness Improves Colloidal Stability of Pressured Pharmaceutical Suspensions." *Pharmaceutical Research* 36 (43). doi:https://doi.org/10.1007/s11095-019-2572-0.

World Health Organization (WHO). 2006. "Temperature sensitivity of vaccines." August. Accessed April 17, 2020. doi:WHO/IVB/06.10.

World Health Organization. 2019. *Global Tuberculosis Report.* Geneva: World Health Organization. https://www.who.int/tb/publications/global_report/en/.

World Health Organization. 2018. *WHO Preferred Product Characteristics for New Tuberculosis Vaccines.* Geneva: World Health Organization.

Zhang, Yu, Kyle Gilbertson, and Warren H. Finlay. 2007. "In vivo-in vitro comparison of deposition in three mouth-throat models with Qvar and Turbuhaler inhalers." *Journal of Aerosol Medicine* 20: 227-235. doi:10.1089/jam.2007.0584.

Zhou, Yue, Jajie Sun, and Yung-Sung Cheng. 2011. "Comparison of deposition in the USP and physical mouth-throat models with solid and liquid particles." *Journal of Aerosol Medicine and Pulmonary Drug Delivery* 24 (6): 277-284. doi:10.1089/jamp.2011.0882.

Chapter 4. Stability of spray-dried tuberculosis vaccine candidate for respirable delivery

4.1. Introduction

Spray drying is a desiccation process that is commonly used in the food (Gharsallaoui, et al. 2007) and pharmaceutical industries (Re 2006, Ziaee, et al. 2019) to encapsulate and stabilize actives within a dry powder form for later rehydration as needed. Improvement of formulation stability is of particular concern from a global health perspective. Thermostable therapeutics and prophylactics will eliminate the required refrigeration during transportation and storage, known as the cold chain. Limitations due to the inability to maintain the cold chain have led to ineffective distribution, contributing to an estimated 19.4 million infants not receiving basic vaccines in 2018 (World Health Organization 2019). However, thermostability can be conferred through the stabilization of a product within a dry format. Recently, Price et al. (Price, et al. 2020) spray-dried the bacille Calmette-Guérin (BCG) vaccine and showed that the spray-dried vaccine held at 25 °C over 2 years induced similar cytokine responses in mice as the injected liquid version. Improvement of thermostability is especially useful for intervention in highly infectious diseases that are prevalent in developing nations, such as tuberculosis (TB). The need for a thermostable vaccine to prevent TB incidence has grown even more pressing with the increasing prevalence of multiple and extremely drug resistant strains of TB (World Health Organization 2019).

Chapter 3 discusses the work completed to develop an inhalable spray-dried version of the ID93+GLA-SE vaccine candidate. Several excipient combinations were characterized to assess preservation of vaccine components after spray drying and aerosol performance of the dry powder.

The best performing candidates utilized the disaccharide trehalose as a stabilizer and low concentrations of the tripeptide trileucine as a dispersibility enhancing agent. Trileucine has been shown to improve the dispersibility of dry powders for pulmonary delivery (Lechuga-Ballesteros, et al. 2008, Sibum, et al. 2020). An especially attractive feature of trileucine is that, due to its low solubility, only small amounts are required to achieve surface enrichment for the production of rugose particles. As well, trileucine has the potential to improve physical stability of formulations due to its high transition glass temperature (~104 °C) (Lechuga-Ballesteros, et al. 2008). A trileucine and trehalose excipient system has previously been used to stabilize Phage CP30A bacteriophages in a dry powder form (Carrigy, Liang, et al. 2019). The trileucine and trehalose formulation was shown to experience only a 0.6 log titer reduction after processing and storage for one month at room temperature. This was a significant improvement over the stability of the bacteriophages spray-dried with trehalose alone, where 3.9 log reduction was measured under the same conditions. Trileucine has also been shown to protect against moisture-related degradation (Lechuga-Ballesteros, et al. 2008) and aerosol performance losses (Sibum, et al. 2020). A patent on spray-dried oxytocin showed that trileucine also improves stability as compared to the commonly used dispersibility enhancing agent leucine (Fabio, et al. 2018). The data showed that a spray-dried formulation containing 87% trehalose and 10% leucine retained only 51.6% of oxytocin after storage for 32 weeks in heat sealed bags at 40 °C and 75% RH. Conversely, a formulation containing 87% trehalose and 10% trileucine retained 72.4% of oxytocin during storage under the same conditions. Recently, a dry powder formulation containing 35% ribavirin, and 55% trehalose and 10% trileucine as excipients, was administered to healthy subjects via inhalation as part of a Phase I clinical study (Dumont, et al. 2020). The study reported that

administration of single-escalating doses of the formulation was well-tolerated, with no severe adverse events reported.

Development of a dry powder vaccine suitable for pulmonary delivery via inhalation will bypass the risks associated with needle delivery. Storage stability of the formulation must be determined as dry powder vaccines designed for global distribution should be thermostable in order to maximize accessibility. The stability of a spray-dried inhalable version of the ID93+GLA-SE vaccine candidate is evaluated in this chapter. Two formulations were placed on stability study: 1) a version of the thermostable presentation developed in Chapter 2 that was modified to be within respirable range, and 2) the lead inhalable vaccine candidate containing 3% trileucine developed in Chapter 3. The former was included as a control sample. Both spray-dried vaccine powders were stored at multiple temperatures. Stability was assessed in terms of physical stability over time, namely particle morphology, moisture content, solid state of the powder, and aerosol performance. Aerosol performance was assessed using an *in vitro* model including an idealized geometry of the human mouth-throat to obtain a relatively accurate assessment of powder dosing to the lungs.

4.2. Materials and Methods

4.2.1. Materials

Trehalose dihydrate with a purity of 98% was used as the primary stabilizing excipient for spray drying (CAS 6138-23-4; Fisher Scientific Ottawa, ON, Canada), and trileucine with a purity of ≥90% (CAS 10329-75-6; Sigma Aldrich, Oakville, ON, Canada) was utilized as a dispersibility enhancing agent. Tris(hydroxymethyl)aminomethane (Tris) (CAS 77-86-1; Sigma Aldrich, Oakville, ON, Canada) and hydrochloric acid (CAS 7647-01-0; Sigma Aldrich, Oakville, ON,

Canada) were used as a buffer system. Formulations were made using deionized water. The ID93 antigen and GLA-SE adjuvant system were formulated separately; production of these components has been described in Chapter 2.

As discussed in Chapter 2, the vaccine candidate has been successfully spray-dried into a powder with demonstrated long-term stability potential. Following these promising results, several inhalable spray-dried powder candidates were investigated, as detailed in Chapter 3. The results established the best performing candidates to be the T3Tri and the T6Tri formulation. Both formulations exhibited comparable aerosol performance, suggesting that similar levels of trileucine surface coverage were achieved. To minimize costs associated with excipients and maximize vaccine per inhaled dose, the T3Tri formulation was chosen as the lead inhalable candidate. However, this formulation has not been assessed for stability. To this end, two formulations were spray-dried and placed on stability for this study: 1) the formulation with demonstrated thermostability and 2) the formulation with demonstrated aerosol performance. The former was included as a control. For simplicity, the former will be further referred to as the Control formulation, and the latter will be referred to as the Inhalable Vaccine formulation. The formulation parameters of both are detailed in Table 9. The designed particle composition for the formulations are given in terms of mass fraction in Table 10.

Table 9 Formulation parameters of the spray-dried Control and Inhalable Vaccine formulations.

Component	Feedstock Concentration	
	Control	Inhalable Vaccine
Trehalose (mg/mL)	33.3	33.3
Tris (buffer) (mg/mL)	0.8	0.8
Squalene (mg/mL)	5.73	5.73
DMPC (mg/mL)	1.27	1.27
GLA (µg/mL)	3.33	3.33
ID93 (µg/mL)	1.33	1.33
Trileucine (mg/mL)	-	1.3
Total Solid Content (mg/mL)	41	42

Table 10 Designed particle composition by mass of the spray-dried Control and Inhalale Vaccine formulations.

Component	Mass Fraction in Powder	
	Control	Inhalable Vaccine
Trehalose	81%	78%
Tris (buffer)	2%	2%
Squalene	14%	14%
DMPC	3%	3%
GLA	0.01%	0.01%
ID93	0.003%	0.003%
Trileucine	-	3%

Formulation procedure for the stability study candidates in this chapter is similar to the formulation procedures carried out in Chapter 2 and Chapter 3. Briefly, chemical powders were massed and dissolved in a glass beaker using deionized water as a solvent. Once the chemicals were fully dissolved, the solution was pH-adjusted using hydrochloric acid to a pH of approximately 7.5. After pH adjustment, the solutions were syringe-filtered using a sterile filter with a 0.22 µm pore size (GSWP02500; Sigma Aldrich, Oakville, ON, Canada). GLA-SE was then added to the

solution and gently stirred to mix. ID93 was added to the formulation last to minimize ID93 loss due to container binding.

4.2.2. Methods

Spray Drying

As with the work detailed in Chapter 2 and Chapter 3, spray drying was completed using a custom research spray dryer and twin fluid atomizer. Processing conditions for spray drying the stability study candidates were previously calculated in Chapter 2. Production of the Inhalable Vaccine formulation had to be completed in two batches. Both batches of the Inhalable Vaccine formulation were characterized at the initial timepoint to confirm that the batches were similar.

Stability Study

The designed stability study is given in Table 11. The stability study was designed to assess powder stored at 5, 25, 40, and 50 °C. The study was planned such that the batch of powder tested was consistent throughout storage at a given temperature.

Table 11 Stability study design for the Control (C) and Inhalable Vaccine (IV) formulations

Storage Temperature (°C)	Timepoint			
	Timepoint 0 (t0)	1-month	3-month	7-month
5	C IV: Batch 1/2	C IV: Batch 2	C IV: Batch 2	C IV: Batch 2
25		C IV: Batch 1	C IV: Batch 1	C IV: Batch 1
40		C IV: Batch 2	C IV: Batch 2	C IV: Batch 2

50		IV: Batch 2	IV: Batch 2	IV: Batch 2

Dry Powder Packaging for Stability Study

An intensive packaging process was used to protect the spray-dried powder from moisture uptake. This packaging process is described in detail in Chapter 2. A packaging system was utilized in order to assess the powder stability with minimal moisture uptake.

Scanning Electron Microscopy

Assessment of particle morphology change over storage was completed using Field Emission Scanning Electron Microscopy (Zeiss Sigma FE-SEM; Carl Zeiss, Oberkochen, Germany). Two stubs were prepared for SEM analysis for each sample. The first was prepared by adding the powder to a carbon tape-covered aluminum SEM stub (Product 16111; Ted Pella, Inc.; Redding, CA, USA). The second specimen was prepared by mounting powder samples directly onto the aluminum SEM stubs and pressing the powder in order to break open the particles. The first specimen was prepared in order to assess external powder morphology, whereas the second specimen was prepared in order to assess internal powder morphology. These prepared samples were placed in a desiccator connected to an in-house vacuum system for 2-4 days in order to remove exposed nanoemulsion droplets to prevent possible damage to the electron microscope. Then, the samples were sputtered with a coating of 80% gold and 20% palladium (Leica ACE600 Carbon/Metal Coater; Concord, ON, Canada) to a thickness of 10-15 nm. Images ranging from 1000 to 25000× were taken at a working distance of 6.0-6.7 mm using an accelerating voltage of 3.0-4.0 kV.

Moisture Content

Water content of the powders over the course of the stability study was measured through Karl Fisher Calorimetry (Karl Fisher Coulometric Titrator Model C30; Mettler Toledo; Mississauga, ON, Canada). Oven temperature was 110 °C, and results were given as a wet basis percentage based on the measured sample mass. Experiments were completed in duplicate. Calibration with a water standard (Honeywell; Mexico City, Mexico) indicated that the machine variance was ±0.3%.

Raman Spectroscopy

Raman spectroscopy was used to monitor the solid phase of the powder over the course of the stability study. Samples were measured at a temperature of 22.8-23.5 °C and an RH of ≤5.5% to minimize moisture uptake during the sampling process. Raman spectra analysis was also completed on crystalline trehalose, trileucine, and Tris material as references. Similarly, Raman spectra analysis was performed on a liquid sample of squalene as a reference. Reference spectra were also obtained for spray-dried trehalose and spray-dried trileucine. The spray-dried materials were treated as reference amorphous samples as trehalose and trileucine do not crystallize under normal spray drying conditions.

In vitro Aerosol Performance

Aerosol performance of the dry powders was assessed using the method previously described in Chapter 3. Briefly, the aerosol performance of the formulations was evaluated using a commercial dry powder inhaler (DPI) actuated into an Alberta Idealized Throat (AIT) connected to a Next Generation Impactor (NGI). Inhalation was simulated at 100 L/min for 2.4 s to obtain 4 L of inhaled air. Impactor plates and the interior of the AIT were coated with silicone spray (Molykote 316 Silicone Release Spray, Dow Corning Corporation; Midland, MI, USA) to mitigate particle

bounce. Aerosol performance was assessed in terms of emitted dose, total lung dose, and fine particle fraction. Emitted dose was defined as the percentage of the loaded dose that exited the DPI. Total lung dose was defined as the percentage of the loaded dose that penetrated the AIT. Fine particle fraction was defined as the percentage of powder mass that deposited on the plates with a particle size of ≤5 μm, relative to the loaded dose. Measured powder mass distribution on the impactor plates was used to calculate the mass median aerodynamic diameter, $d_{a,50}$, and the geometric standard deviation, σ_g, of the deposited powder by fitting the data to a cumulative lognormal function.

Statistical Analysis

Statistical analysis was completed as detailed in Chapter 2 and Chapter 3. Results are reported as mean ± standard deviation. Statistically significant differences were reported for $p<0.05$, as determined by a two-tailed student's t-test.

4.3. Results and Discussion

4.3.1. Particle Morphology

Particle morphology of the spray-dried Control formulation over the course of the stability study is shown in Figure 21. The exterior morphology indicates that the polydisperse powder consists of spherical particles with relatively smooth surfaces. Analysis of the cracked particles shows that the nanoemulsion droplets are encapsulated within the trehalose matrix. Comparison of the interior and exterior morphologies over time indicates that the physical structure of the particles was preserved even after seven months of storage at temperatures up to 40 °C. These results are

consistent with the morphology results of a similar formulation placed on a stability study, as discussed in Chapter 2.

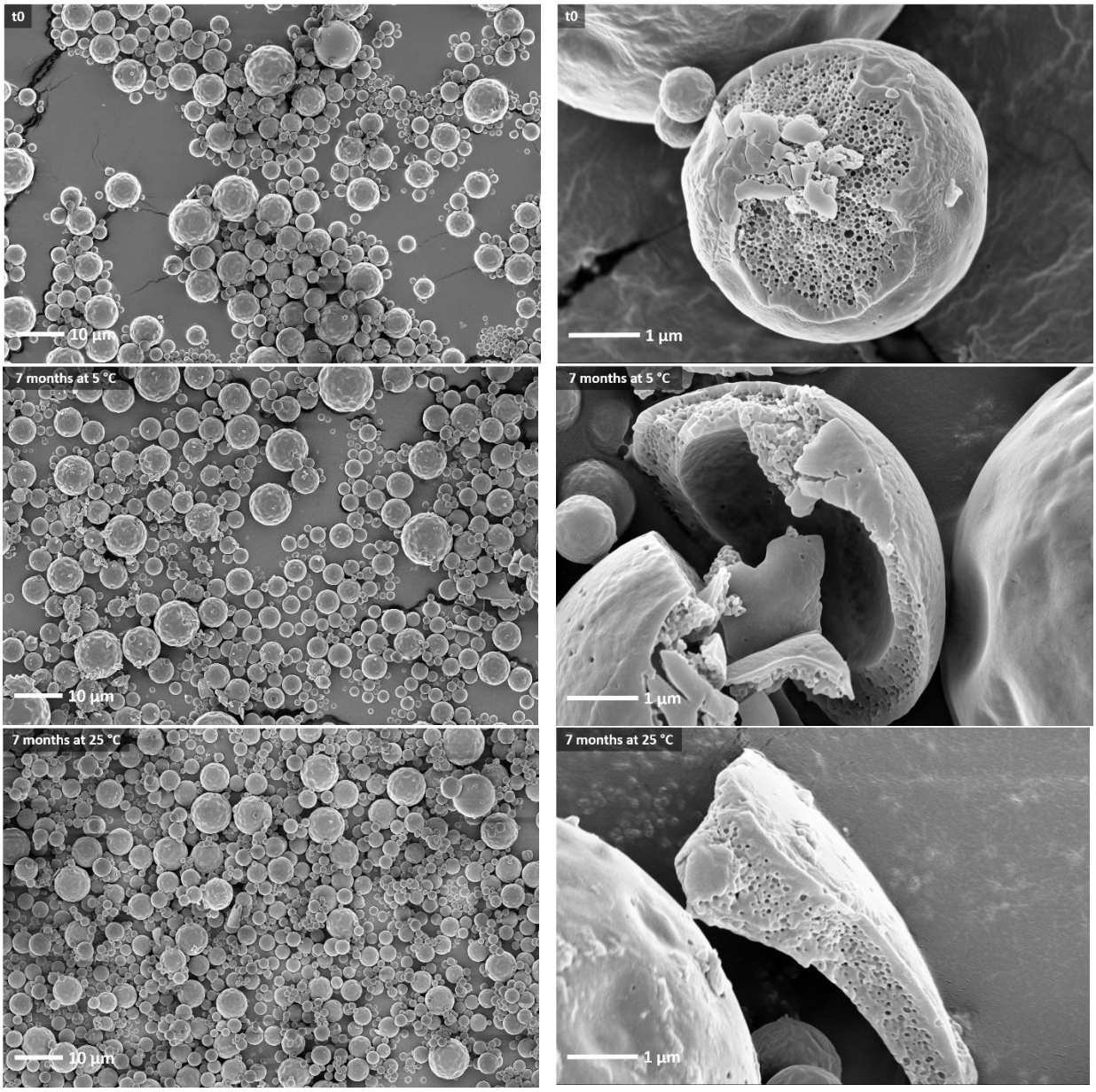

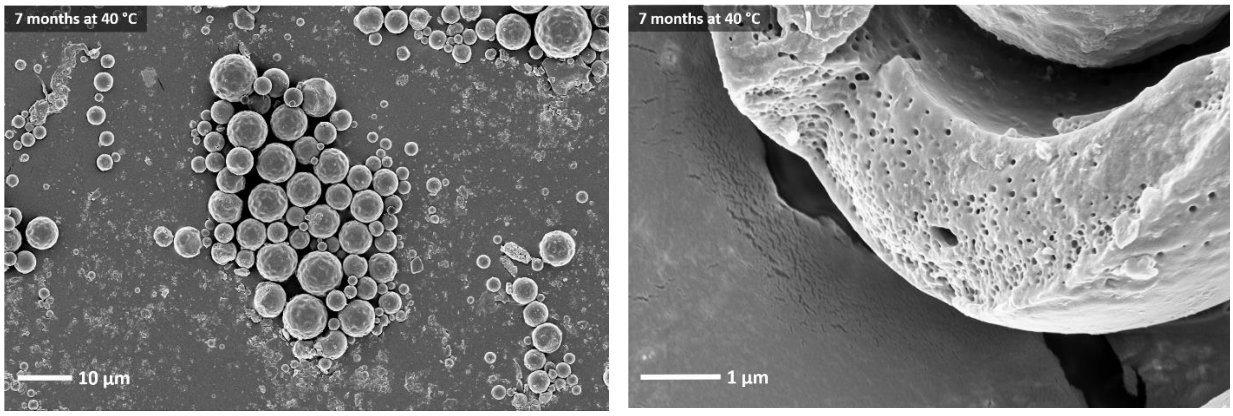

Figure 20 SEM images comparing interior and exterior particle morphology of spray-dried Control formulation at timepoint 0 (t0) and after seven months of storage at 5, 25, and 40 °C. Scale bars are indicated on the respective images.

Particle morphology of the spray-dried Inhalable Vaccine over the course of the stability study is given in Figure 21. Analysis of the spray-dried Inhalable Vaccine at timepoint 0 show highly wrinkled and folded surface morphology. As with the cracked Control particles, analysis of the cracked Inhalable Vaccine particles demonstrates that the nanoemulsion droplets are encapsulated within the particle shell. These results are consistent with the particle morphology of the Vaccine+Trehalose+3% Trileucine discussed in Chapter 3. The folded and corrugated nature of the particles is consistent with morphologies shown in other studies on spray-dried trehalose and trileucine systems (Carrigy, Liang, et al. 2019, Wang, Nobes and Vehring 2019). The morphologies of Batch 1 and Batch 2 at timepoint 0 appear to be identical, suggesting that manufacture of the Inhalable Vaccine is reproducible. Comparison of exterior particle morphologies indicates that these are maintained throughout the stability study at all storage temperatures.

An SEM image of a cracked Inhalable Vaccine particle after seven months of storage at 50 °C is shown in Figure 22. Cracked particles could not be found in the samples stored at other

temperatures for the seven-month timepoint. There is no discernible difference in interior morphology of the sample stored for seven months at 50 °C when compared to the samples imaged at timepoint 0, suggesting that particle structure is maintained even under the harshest storage conditions.

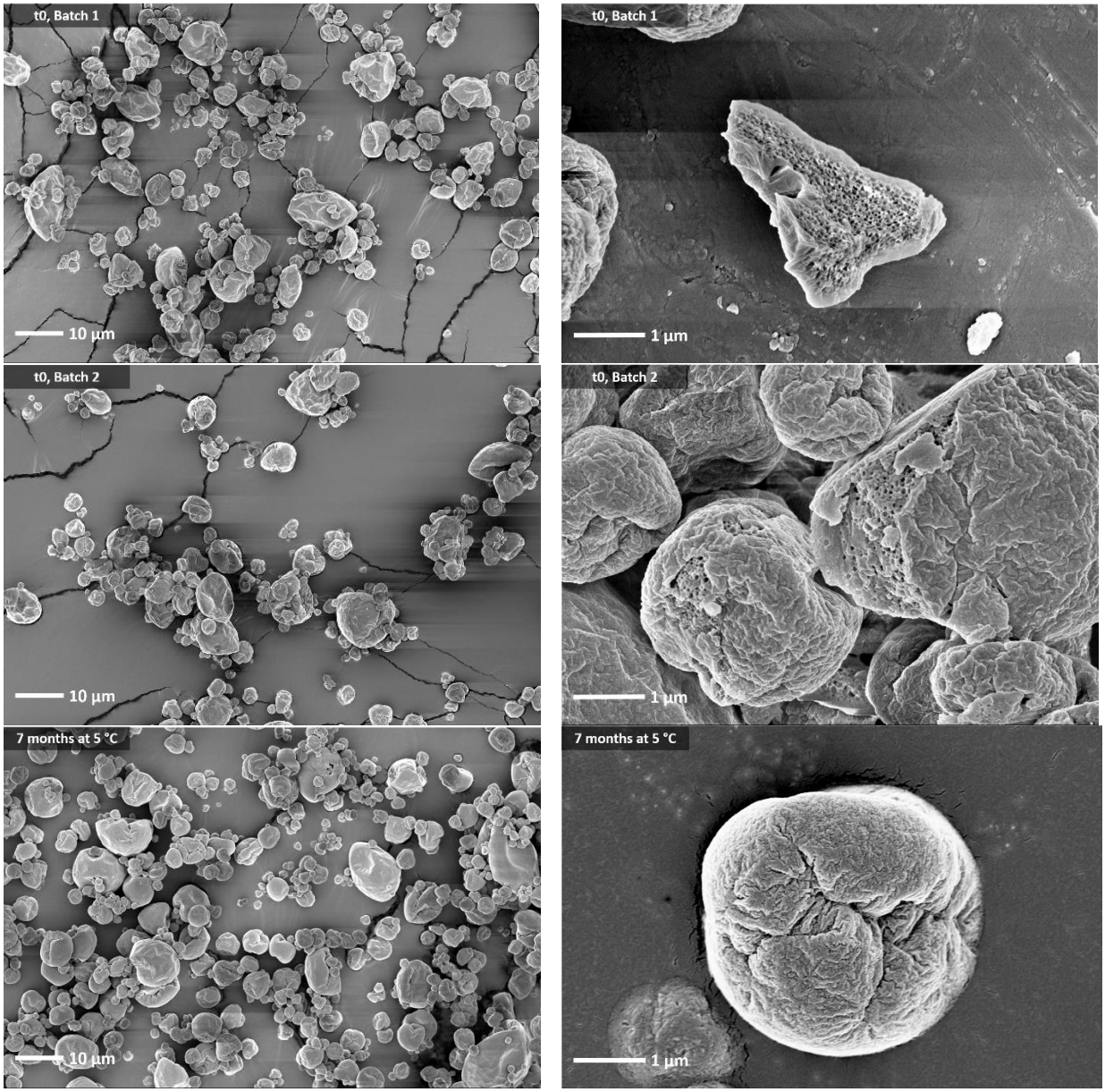

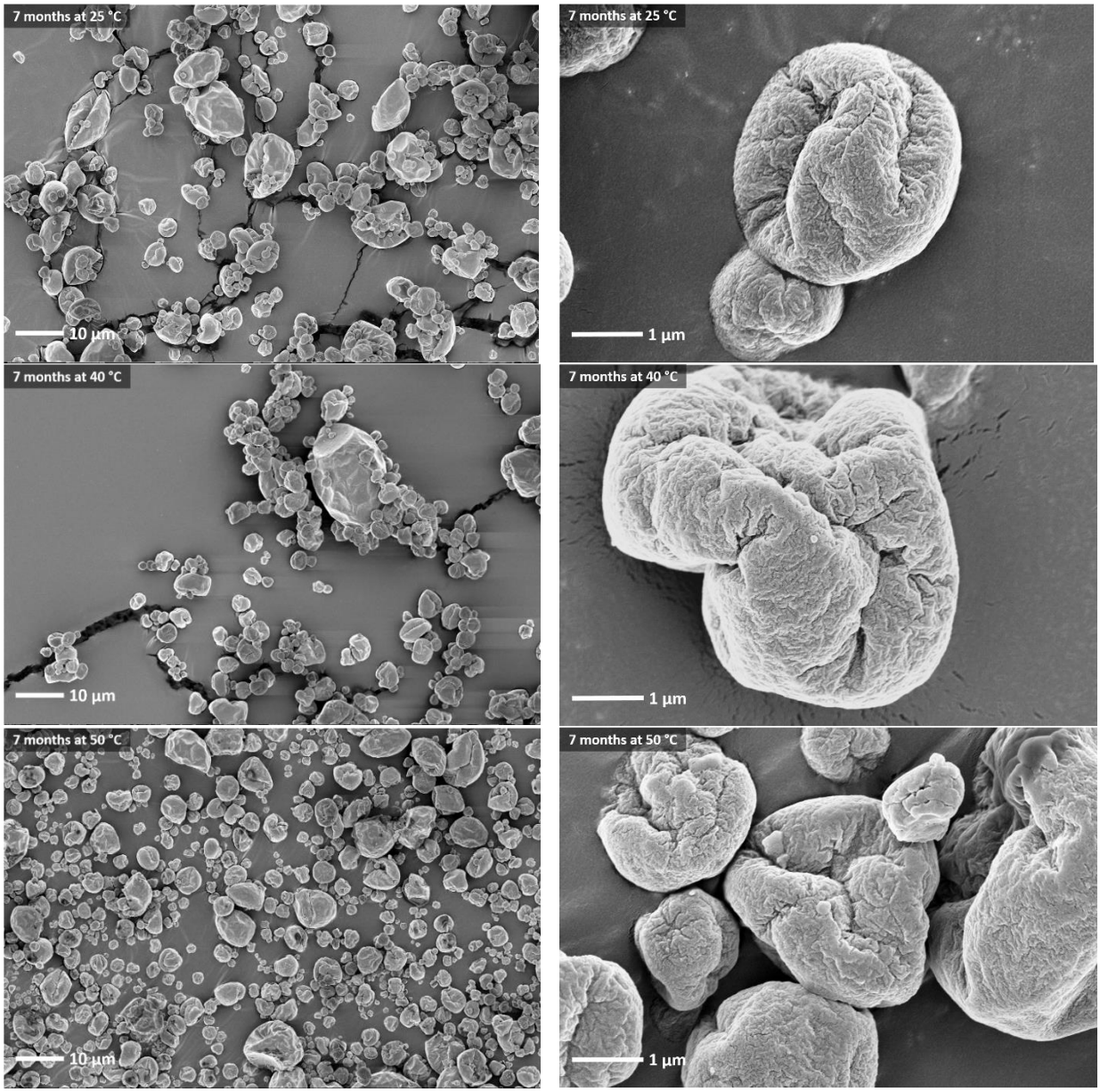

Figure 21 Low magnfication (left) and high magnfication (right) SEM images comparing particle morphology of spray-dried Inhalable Vaccine formulation at timepoint 0 (t0) and after seven months of storage at 5, 25, and 40 °C. Scale bars are indicated on the respective images.

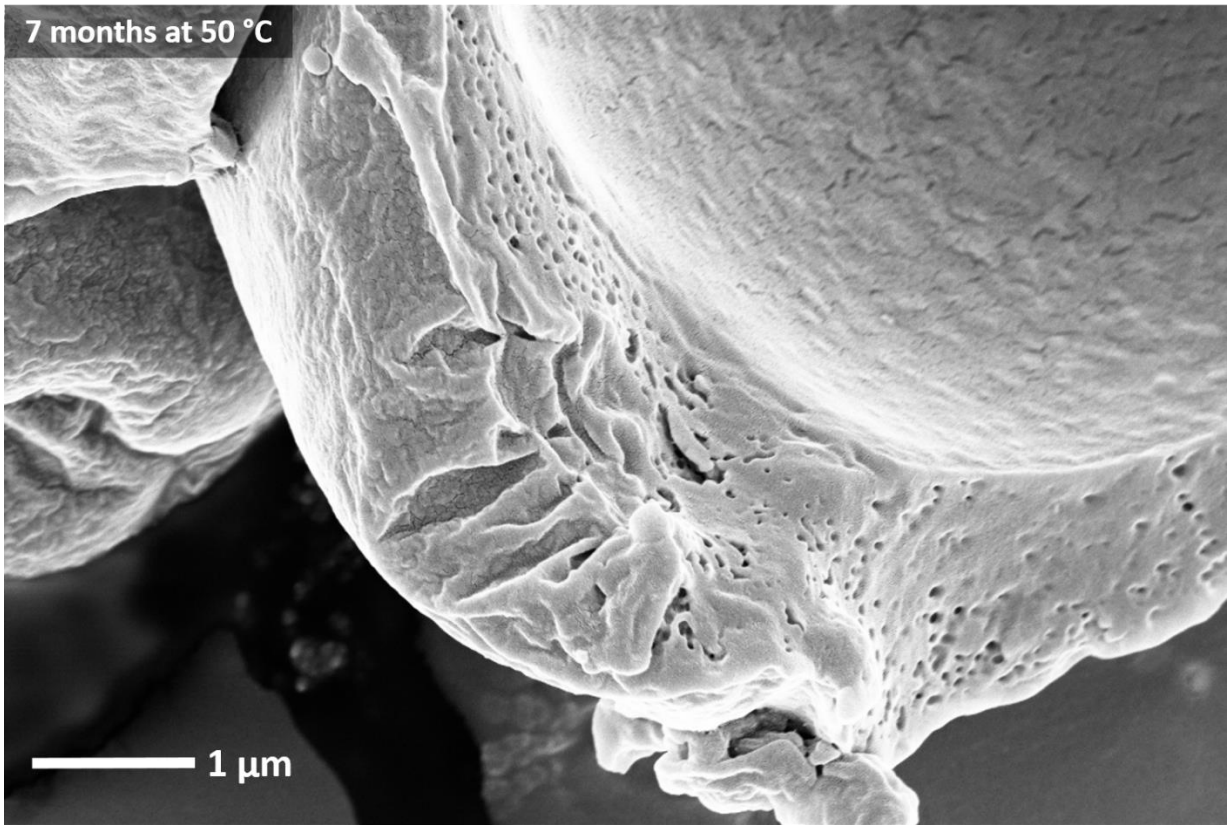

Figure 22 High magnification SEM image of broken Inhalable Vaccine particle showing the interior morphology.

4.3.2. Powder Moisture Content

Powder moisture content over the course of the stability study for both the spray-dried formulations is shown in Figure 23. Moisture content for both the Control and Inhalable Vaccine formulation did not change significantly over seven months, indicating that neither powder experienced moisture uptake. Clearly, the protective packaging method prevented exposure to humidity, thereby preventing moisture sorption by the powders. This packaging system was previously utilized effectively in Chapter 2 to prevent moisture uptake. Prevention of moisture exposure is critical in pharmaceutical powders. Increase in water content of sugars is known to depress the transition glass temperature (Chen, Fowler and Toner 2000). If a powder is stored close to transition temperature, the powder is no longer able to render the encapsulated proteins immobile (Grasmeijer, et al. 2013) which may lead to protein denaturation. Additionally, sugars may crystallize with enough water sorption. Crystallization of the powder will contribute to protein degradation through the loss of hydrogen bonds with the stabilizer. As well, increase in moisture content may lead to capillary forces between particles, decreasing powder dispersibility.

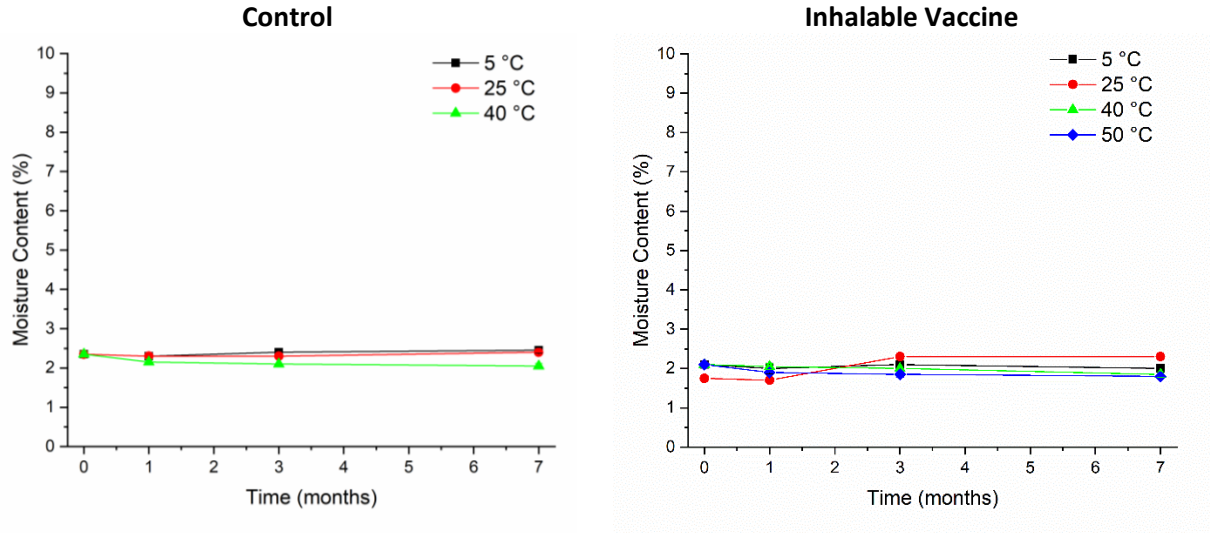

Figure 23 Powder moisture content by wet basis of the Control formulation (left) and the Inhalable Vaccine (right) over seven months. Error bars represent the standard deviation of duplicate measurements.

4.3.3. Solid State Analysis

Raman spectra for the Control and Inhalable Vaccine formulations after seven months of storage are shown in Figure 24 and Figure 25, respectively. The deconvoluted spectra, plotted under the respective sample spectra, were obtained after subtracting reference amorphous trehalose, squalene, and amorphous trileucine spectra. Reference spectra of the components are given in Figure 26. As established in Chapter 3, both formulations are completely amorphous following spray drying. Comparison of the "Batch 1" and "Batch 2" spectra of the Inhalable Vaccine formulation confirm that the solid states are similar. Analysis of the residual spectra after deconvolution shows a relatively straight line for all samples stored for seven months. The lack of substantial peaks in the residual spectra suggests that the solid state of both vaccine powders remains amorphous and has undergone minimal solid-state change compared to timepoint 0, as designed. However, the raw spectra (not shown) of the Control and Inhalable Vaccine powder samples stored at 40 and 50 °C for seven months showed a high degree of background fluorescence, suggesting some level of chemical degradation.

These results show that the intensive packaging procedure utilized in the stability study effectively protected the powders from moisture-induced crystallization. Not only does crystallization of amorphous solids potentially lead to degradation of encapsulated biologics, but it can also impact the aerosolization ability of the powder. Inconsistent dosing due to moisture-induced crystallization has been demonstrated by Shetty et al. (Shetty, Zeng, et al. 2018), where

crystallization of amorphous spray-dried ciprofloxacin powders stored under different humidities led to variable measured emitted dose and fine particle fraction from a DPI.

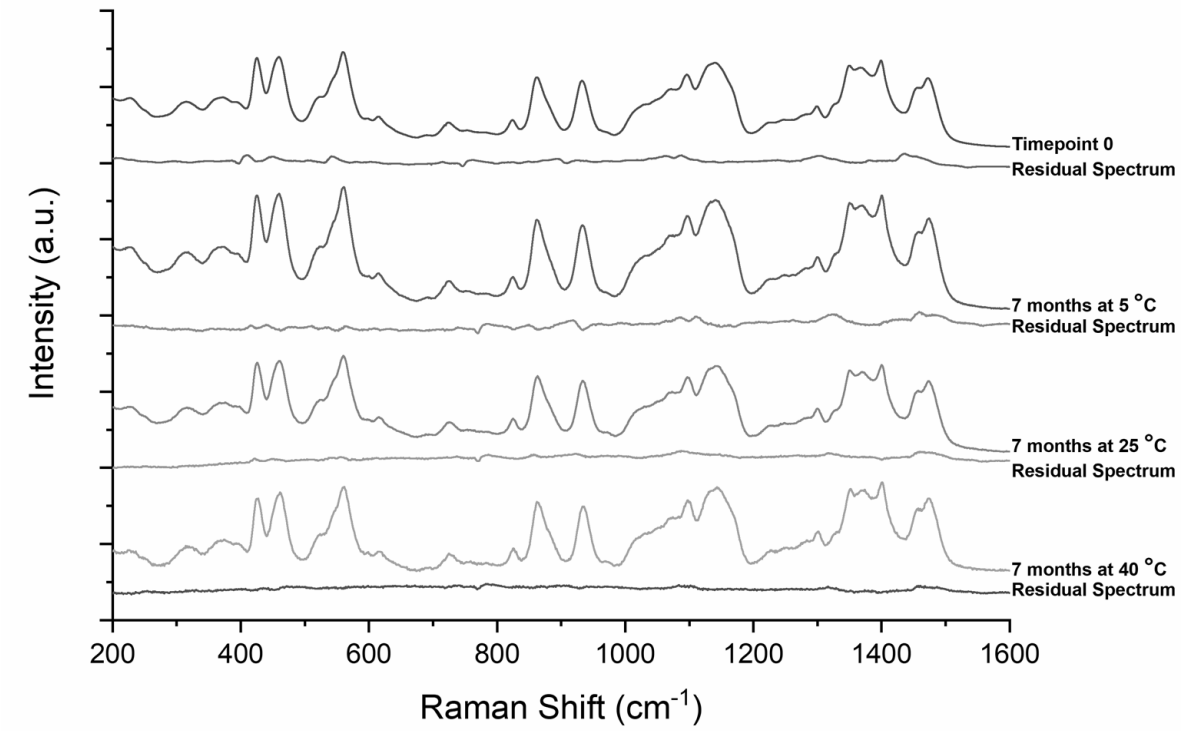

Figure 24 Sample spectra of the Control formulation after spray drying and after seven months of storage at 5, 25, and 40 °C. The residual spectra obtained after deconvolution are given under the respective sample spectra. The low intensity of the residual spectra indicates that the powders have remained amorphous after seven months at all storage temperatures.

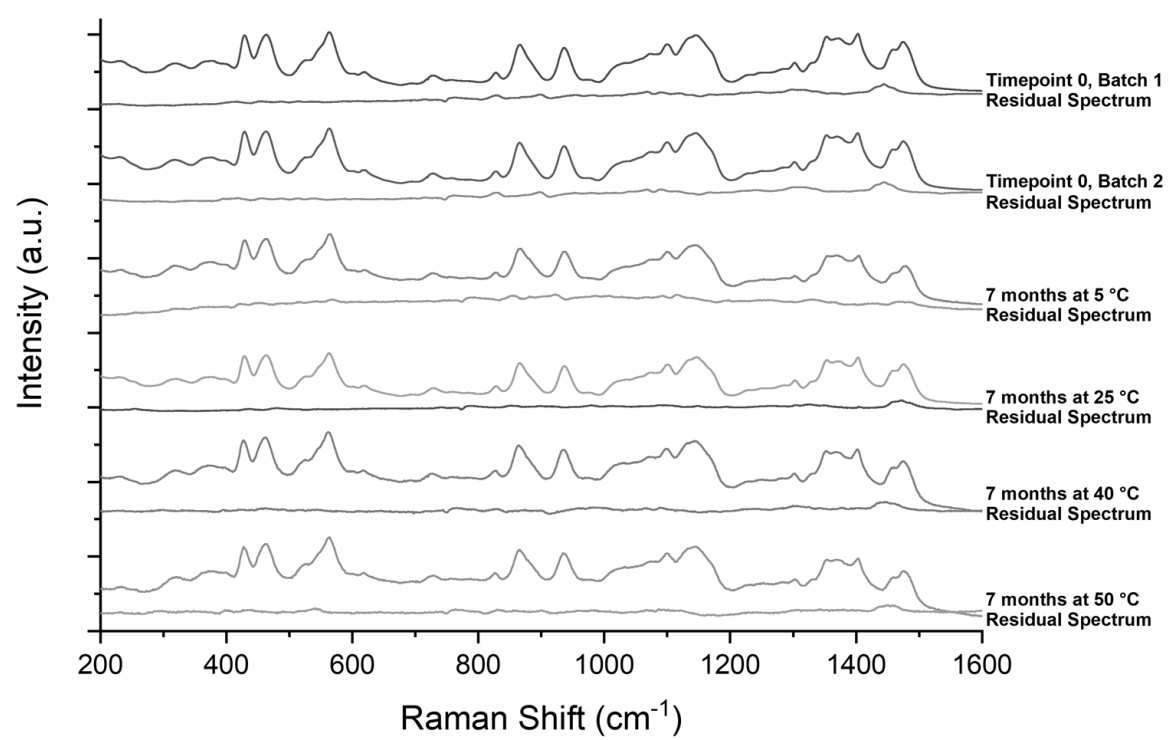

Figure 25 Sample spectra of the Inhalable Vaccine formulation after spray drying and after seven months of storage at 5, 25, 40, and 50 °C. The residual spectra obtained after deconvolution are given under the respective sample spectra. The low intensity of the residual spectra indicates that the powders have remained amorphous after seven months at all storage temperatures.

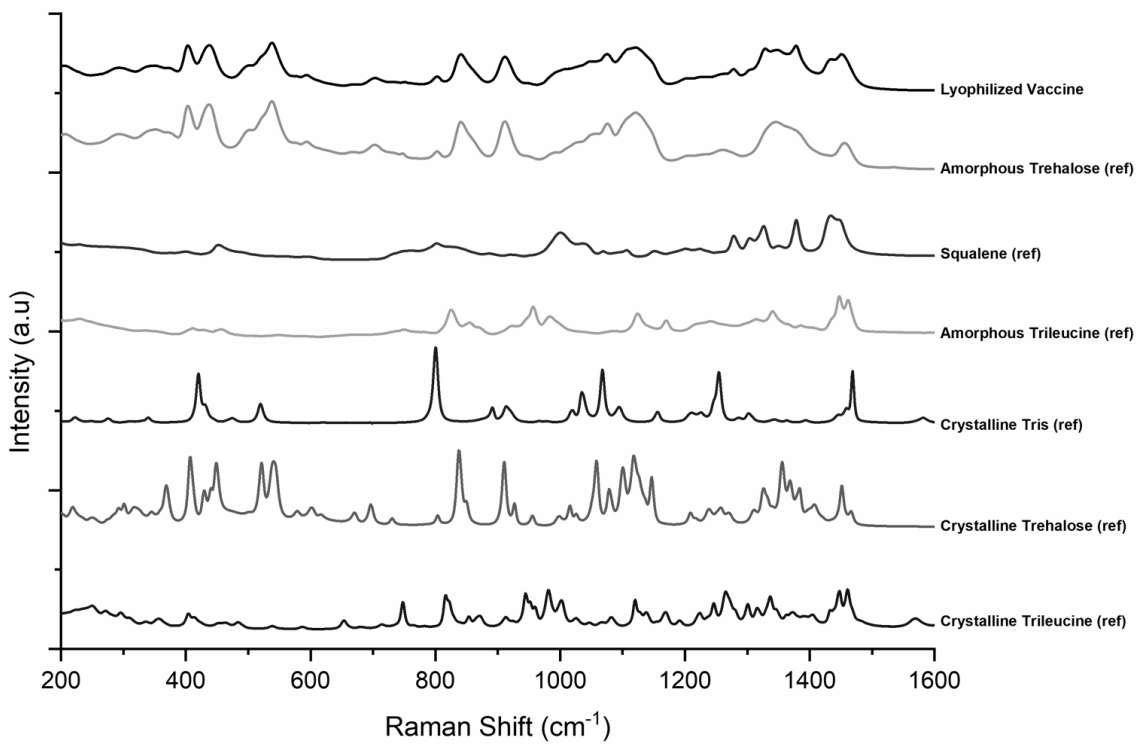

Figure 26 Reference spectra for the main components of the spray-dried Control and the spray-dried Inhalable Vaccine formulation. The spectrum of the lyophlized vaccine has been included for comparison.

4.3.4. Aerosol Performance

The measured emitted dose, total lung dose, and fine particle fraction of the Control and Inhalable Vaccine formulations over the course of the stability study are plotted in Figure 27. Emitted dose for both the Control and the Inhalable Vaccine formulations is relatively high, ranging from 79-98% and 88-104%, respectively throughout the stability study. Previously, *in vitro* NGI experiments on twelve commercial DPIs at flow rates 45-75 L/min showed variable emitted dose of only 15-60%, with an average of 35% (de Boer, et al. 2017). In this context, both of the tested spray-dried vaccine formulations perform very well in terms of emitted dose. These results also suggest that the powders are dispersed from the DPI with relative ease, even after seven months

of storage at high temperatures. The high emitted dose and consistent performance of the vaccine powders suggests reliable administration with a DPI. For comparison, Sibum et al. (Sibum, et al. 2020) spray-dried isoniazid powder with trileucine as a dispersibility enhancer and held the powder for three months at 30 °C and 0% RH. The reported emitted dose of the formulation over the stability study was highly variable (~50-80%).

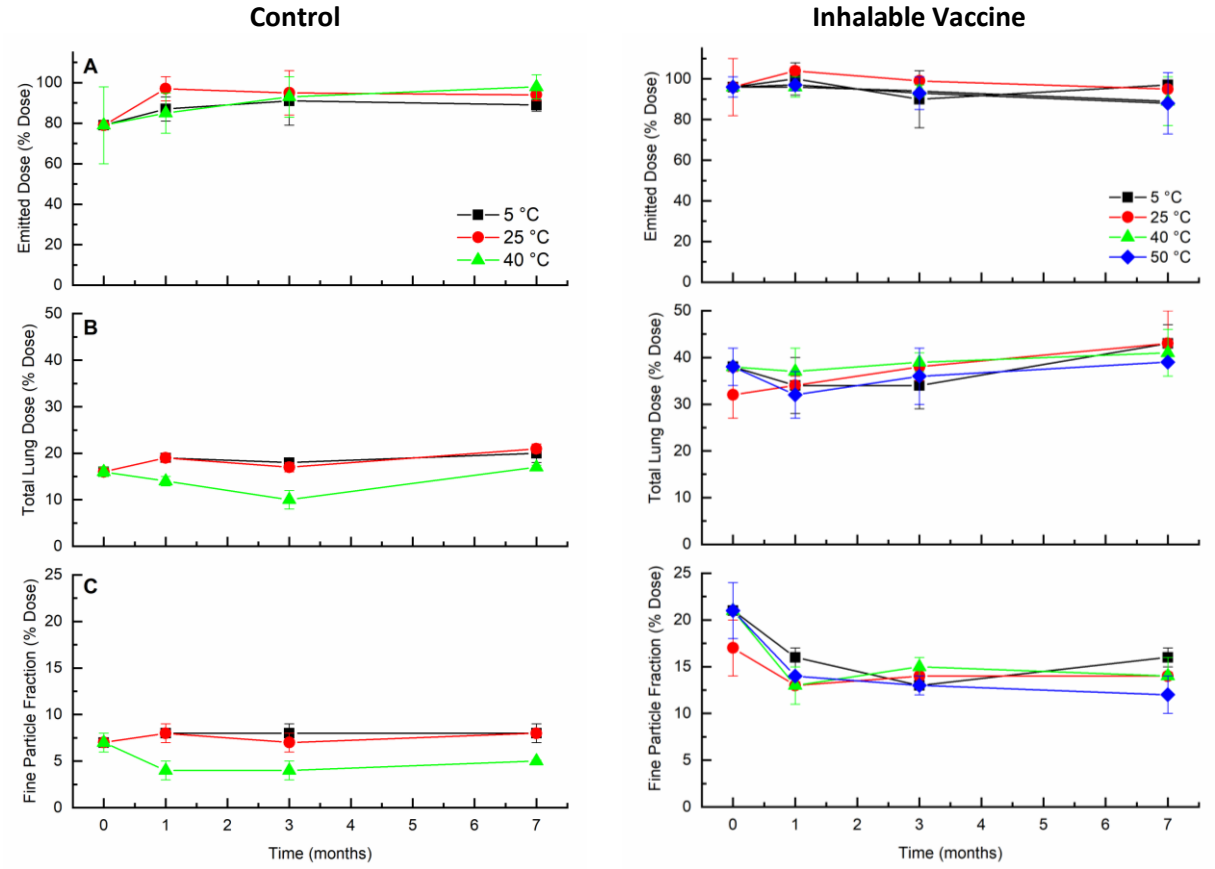

Figure 27 Comparison of aerosol performance for the Control formulation (left) and the Inhalable Vaccine (right) over seven months of storage at various temperatures in terms of A) emitted dose, B) total lung dose, C) and fine particle fraction. Aerosol performance was calculated as percentage of the loaded powder dose. Results shown are the average of triplicate measurements. Error bars represent the standard deviation of triplicate measurements.

Comparison at timepoint 0 indicates that the inclusion of trileucine has doubled total lung dose and fine particle fraction. The improvement of dispersibility due to the addition of trileucine is consistent with the results reported in Chapter 3. The total lung dose and fine particle fraction of the Control formulation after seven months of storage are comparable to initial measurements for powders stored at 5 and 25 °C; however, fine particle fraction is significantly lower for the samples stored at 40 °C. Morphology analysis in Chapter 2 has shown partial fusing among the smaller particles of a similar formulation stored at 40 °C over one year. The fusing of the smaller particles in a polydisperse powder would lead to these aggregates behaving aerodynamically as a large particle. Large particles are expected to deposit prior to the lung, thus decreasing total lung dose and fine particle fraction. Unlike the Control formulation, total lung dose and fine particle fraction was maintained for the Inhalable Vaccine samples throughout the stability study, even for the samples stored at high temperatures. This result suggests that the addition of trileucine not only improves aerosol dispersibility, but also improves physical stability and prevents temperature-related loss of aerosol performance.

The preserved aerosol performance of the Inhalable Vaccine as compared to the Control formulation is due to the presence of trileucine at the surface of the former. Trileucine not only improves the overall dispersibility of the powder, but has also been shown to protect against moisture-related loss of aerosol performance. The preservation of powder dispersibility is due to the hydrophobic nature of trileucine. Trileucine is formed from three leucine residues, and leucine is known to be a highly hydrophobic amino acid due to its hydrocarbon side chains (Glinksi, Chavepeyer and Platten 2000). This hydrophobic nature protects powders against moisture uptake as compared to particles with hydroscopic trehalose at the surface. Sibum et al. (Sibum, et al. 2020)

spray-dried isoniazid with leucine or trileucine at 1-5% mass fractions and assessed the aerosol performance of the powder after storage for up to three months while exposed to 0, 43.5, and 75% RH at 30 °C. Their results found that fine particle fraction for the trileucine-containing formulations was maintained relative to the initial measurement over the stability study for all tested humidities, unlike the leucine-containing formulations. Other studies have shown that storage conditions affect aerosol performance of dry formulations. Arora et al. (Arora, et al. 2016) spray-dried voriconazole with 20% leucine and stored the powder for three months in partially open vials at 25 °C/60% RH and 40 °C/75% RH. The samples stored at 25 °C/60% RH maintained aerosol performance after three months; however, the samples stored at 40 °C/75% RH exhibited a 10% decrease in fine particle fraction.

The mass distribution within the NGI relative to the loaded powder dose after seven months of storage is shown in Figure 28 and Figure 29 for the Control and Inhalable Vaccine formulation, respectively. Distribution of the powders indicates that the Inhalable Vaccine formulation was able to deposit on later stages of the NGI, unlike the Control formulation. The wider distribution of the Inhalable Vaccine powder demonstrated that this formulation is more dispersible than the Control formulation. Additionally, the Inhalable Vaccine powder mass distribution across the stages is similar for all storage temperatures. By contrast, the Control formulation shows that the powder stored at 40 °C had higher deposition on the first stage, with decreasing deposition on progressing stages. This result further demonstrates that the higher storage temperature affected dispersibility of the Control formulation.

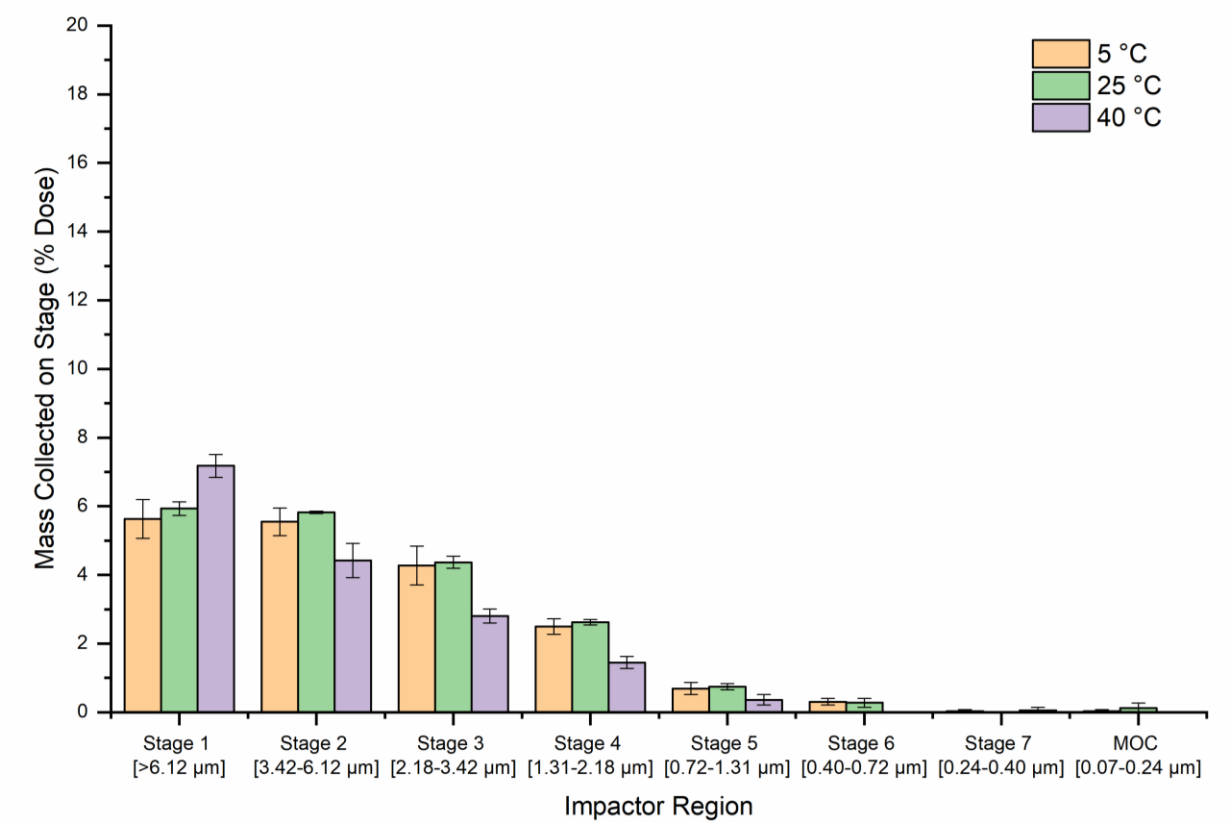

Figure 28 Mass distribution of the Control formulation after seven months of storage at 5, 25, and 40 °C. Results shown represent the average of triplicate measurements. Error bars represent standard deviation.

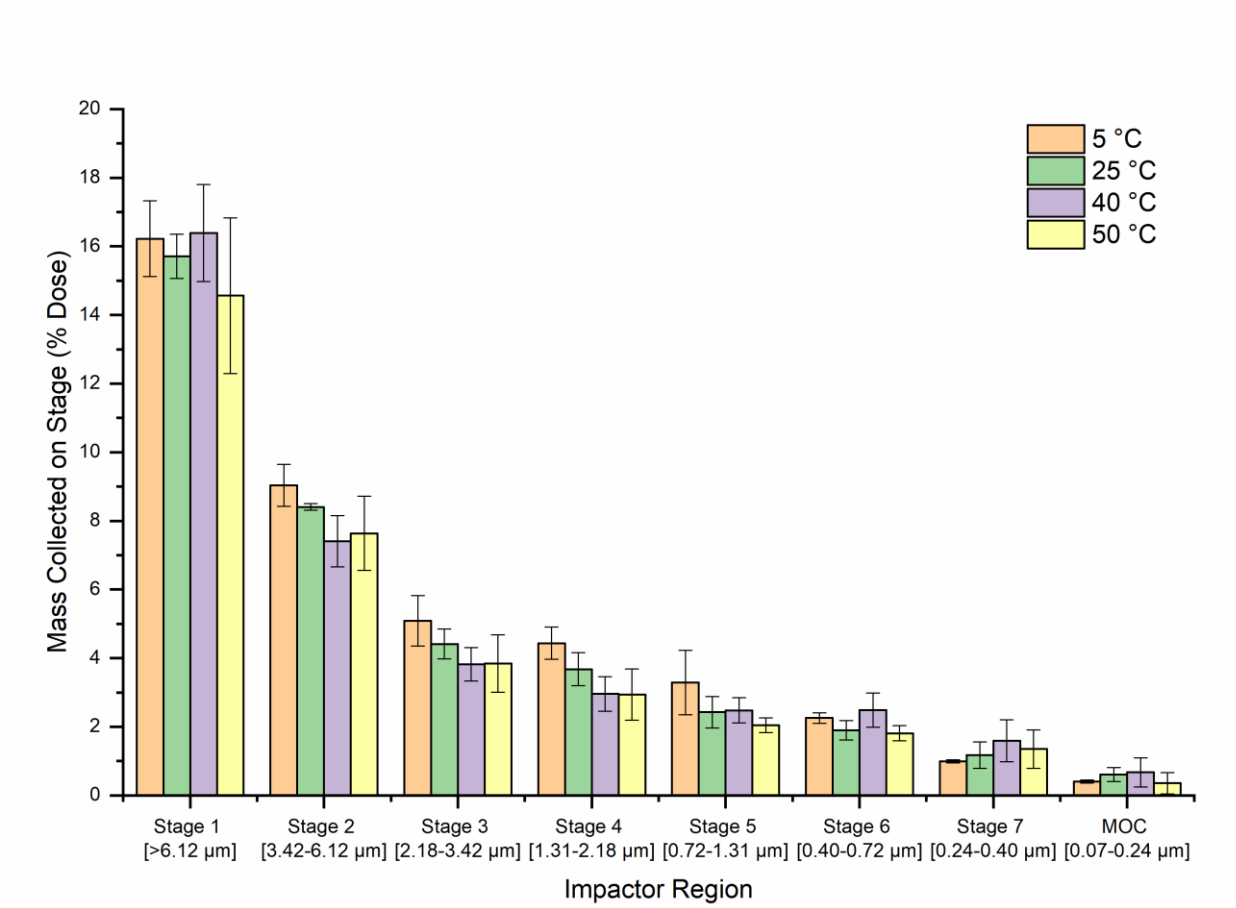

Figure 29 Mass distribution of the Inhalable Vaccine formulation after seven months of storage at 5, 25, 40, and 50 °C. Results shown represent the average of triplicate measurements. Error bars represent standard deviation.

The calculated $d_{a,50}$ and σ_g for the tested formulations are shown in Figure 30. The $d_{a,50}$ of the Control formulation increases for the samples stored at 40 °C, which agrees with the decreased total lung dose and fine particle fraction pattern exhibited by this formulation at 40 °C storage. On the other hand, the $d_{a,50}$ for the Inhalable Vaccine formulation appears to be relatively consistent, which agrees with the reported total lung dose and fine particle fraction consistency over the stability study. The higher σ_g of the Inhalable Vaccine formulation as compared to the Control is indicative of the increased distribution of the former across the NGI impactor stages.

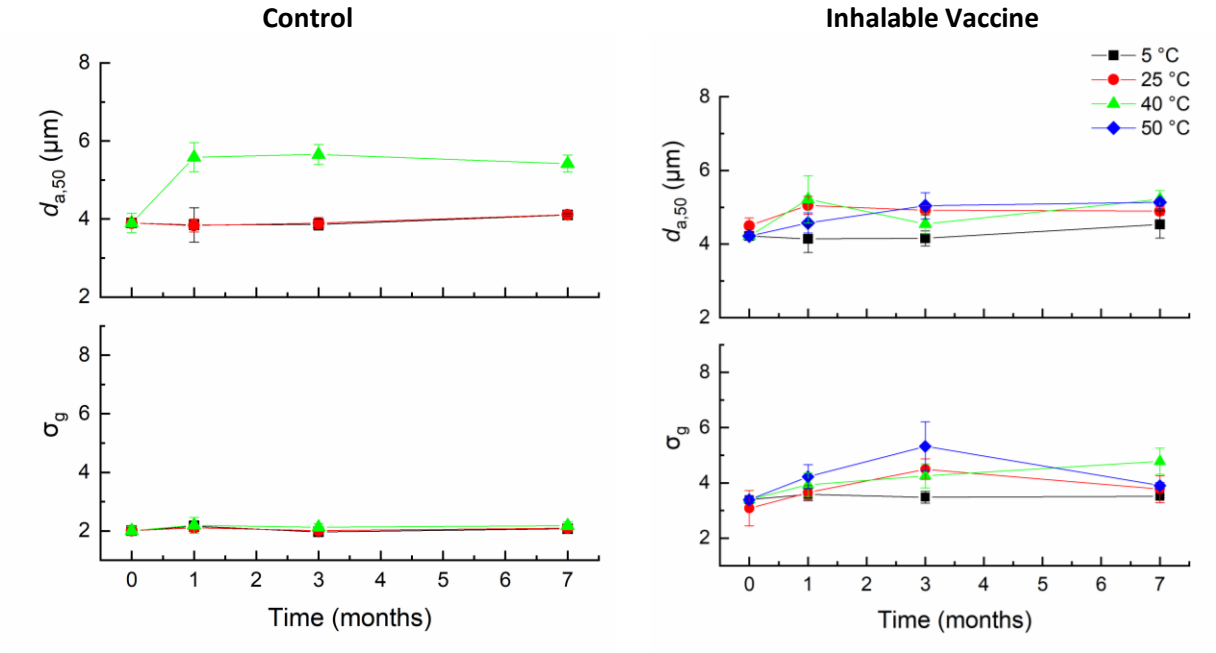

Figure 30 Comparison of size distribution data for the Control formulation (left) and the Inhalable Vaccine formulation (right) over seven months of storage at various temperatures in terms of $d_{a,50}$ (top) and σ_g (bottom). Results are given as the mean of triplicate experiments, with error bars representing the standard deviation.

4.4. Conclusion

This chapter assessed the stability of a spray-dried TB vaccine candidate, ID93+GLA-SE, which was designed for inhalable delivery. This formulation utilized trehalose as a stabilizer and trileucine as a dispersibility enhancing agent. A version of the spray-dried vaccine powder that did not include trileucine was also assessed for comparison. The stability study consisted of powder storage for seven months at multiple temperatures up to 50 °C. The results showed that the particle structure, moisture content, and amorphous solid state were maintained at all investigated temperatures for both formulations. Aerosol performance experiments indicated that both spray-dried vaccine powders exhibited high emitted dose over the course of the stability study. However, inclusion of trileucine was shown to almost double total lung dose and fine particle fraction.

Moreover, total lung dose and fine particle fraction decreased after high temperature storage for the formulation that did not contain trileucine. By contrast, the trileucine-containing vaccine formulation maintained aerosol performance throughout the stability study at all storage temperatures, indicating that the addition of trileucine both improved overall aerosol performance and protected against temperature-dependent dispersibility losses. These results signify that the spray-dried inhalable version of the ID93+GLA-SE vaccine candidate maintains physical stability after seven months of storage at temperatures up to 50 °C. This suggests that the spray-dried powder is physically stable long-term under ambient temperatures, with no negative impact on aerosol performance. Physical stability at high temperatures is highly beneficial for vaccine distribution in regions that lack access to consistent refrigeration. However, chemical analysis of the vaccine must be conducted to determine that chemical stability is also maintained.

Chapter 5. Development of an aerosol delivery system and spray-dried dry powder formulation of tuberculosis vaccine candidate suitable for preclinical mouse inhalation model

5.1. Introduction

A key component of the vaccine development process is *in vivo* preclinical testing to assess safety and immunogenicity prior to testing with humans. Rodents, such as mice, are commonly used for preclinical trials because of their small size, low maintenance cost, and short growth time, all of which allow for many to be tested at one time for statistical validity (Nadithe, et al. 2003, Cryan, Sivadas and Garcia-Contreras 2007). Preclinical trials can also be used to compare routes of administration. A common method of administration is parenteral injection; however, administration due to inhalation has been gaining more attention. There are several benefits to using an inhalable route over parenteral injection, especially for prophylactic or therapeutic treatment of respiratory illnesses. Inhalable routes allow for high-dose targeting at the site of infection while minimizing possible systemic toxic effects (Hickey, et al. 2016). Additionally, immunization studies on mice have shown that administration via intranasal (Aguilo, et al. 2016) and pulmonary (Raeven, et al. 2018) routes conferred greater protection against respiratory diseases than did vaccination via subcutaneous injection. However, the design of inhalation studies to target intranasal and pulmonary deposition is very complex.

Several methods of aerosol delivery have been developed expressly for the mouse respiratory system as it is often not feasible to deliver aerosols to mice using human clinical inhalation devices. The pharmaceutics can be in the form of a liquid or a dry powder. One method that has been used

is the drop method (Aguilo, et al. 2016, Chen, et al. 2004), wherein the liquid product is directly "dropped" into mice nares. For studies seeking to target the pulmonary route only, insufflation (Chang, et al. 2018, Stewart, et al. 2019) or instillation (Raeven, et al. 2018) can be used for either dry powder or liquid products, respectively. This method is highly efficient; however, it requires anesthetization and is not representative of the passive and conscious inhalation typical of humans. An alternative method of aerosol delivery uses exposure systems that allow mice to passively breathe in the aerosolized product. Whole body exposure systems do not require the restraining of animals; however, these systems are inefficient and often result in fur deposition and consequent gastrointestinal deposition via grooming. Instead, nose-only exposure systems can be utilized wherein mice are restrained in tubes against noseports to eliminate additional exposure routes.

Simple, small-scale devices for nose-only delivery of dry powder pharmaceuticals to mice have been used for proof-of-concept single-dose studies, as with the device developed by Kaur et al. (Kaur, et al. 2008). Complex, specialized systems are required to conduct high-dose aerosol delivery to multiple mice through nose-only exposure. These aerosol delivery systems are comprised of two main components: a device to aerosolize the liquid or dry product, and a nose-only exposure system to restrain the mice. The aerosolization of a liquid product can be accomplished via a nebulizer, which generates micron-sized droplets from a solution. The aerosolization of dry products through dispersion of a dry powder can be accomplished through several methods, such as the use of a dust generator. Commercial nose-only exposure systems for various animals are available; however, these commercial devices can be very costly.

As detailed in Chapter 2, the tuberculosis (TB) subunit vaccine candidate ID93+GLA-SE has been successfully stabilized in a dry powder consisting of many microparticles via spray drying.

Initially, the spray-dried ID93+GLA-SE vaccine candidate was designed to be stable long-term at room temperature, with the powder able to be reconstituted as needed prior to administration. Based on the promising results of this candidate, a version of the vaccine suitable for inhalation was developed. Chapter 3 details the investigation of appropriate excipients to confer inhalable characteristics on the spray-dried powder. As detailed in Chapter 4, a stability study on the inhalable version of the powder indicated that the powder was physically stable for seven months, even when held at high temperatures. Despite these promising results, the efficacy of spray-dried ID93+GLA-SE has yet to be tested. Preliminary work was therefore conducted in preparation for preclinical mouse trials to compare the efficacy of the vaccine candidate when administered via injection vs. inhalation.

A critical component in the development process for new drugs and vaccines is the use of preclinical trials to assess safety and immunogenicity. Preclinical trials can be used to compare routes of administration, such as comparing immunization via parenteral injection to mucosal immunization via inhalation. However, if the chosen animal for testing is a mouse, the formulation often has to be adjusted from a human-suitable format due to differences in physiology. Additionally, inhalation studies require specialized equipment to successfully deliver the aerosolized product to the mice. The equipment and the operating parameters have to be optimized prior to conducting the animal studies. In this chapter, the spray-dried inhalable version of the ID93+GLA-SE vaccine was adapted into two forms suitable for inhalation by mice: one targeting nose-only deposition, and the other targeting nose and lung deposition. Additionally, a custom aerosol delivery system was designed, and the system parameters were optimized in preparation for preclinical immunogenicity and protective efficacy trials in mice.

5.2. Materials and Methods

5.2.1. Theory

Respirable Delivery to Mice

Mucosal immunization can be accomplished through intranasal or pulmonary delivery of an aerosol. Two formulations were designed in order to assess both intranasal and pulmonary delivery via inhalation. However, as mice are nose breathers, lung deposition cannot be isolated under passive breathing. As discussed in Chapter 3, particle size is a key indicator of deposition site. Specifically, the aerodynamic diameter, d_a, of an aerosol has been used to predict the site of deposition in different respiratory systems. Kuehl et al. (Kuehl, et al. 2012) conducted a study on deposition of polydisperse aerosols in rodents in which the site of deposition was studied as a function of aerosol d_a. Of the particle sizes investigated in the study, they found that a minimum d_a of 5 μm was required for nose-only deposition and a maximum d_a of 3 μm was required to obtain at least some lung deposition for mice, with lung deposition increasing with decreasing d_a. Based on these findings, the formulation to assess intranasal delivery through nose-only deposition was designed to have a $d_a \approx 5$ μm, and the formulation to assess pulmonary delivery through both nose and lung deposition was designed to have a d_a of 1-2 μm.

Calculation of an optimal aerosol flow rate in an aerosol delivery device requires consideration of several key factors. For instance, the aerosol flow rate must be high enough to sufficiently disperse the spray-dried powder. However, the aerosol flow rate must also be minimized to prevent excessive powder loss due to dilution. In other words, a high aerosol flow rate will lead to greater amounts of aerosol bypassing the mice before they can inhale it. Additionally, the aerosol flow

rate must be greater than the total respiratory minute volume of the mice--the amount of air inhaled per minute--to prevent a hypoxic environment.

The spray-dried powder and aerosol delivery system was designed for preclinical trials involving C56BL/6 mice. The approximate average respiratory minute volume (*RMV*) was calculated to be 22 mL/min per mouse for a similar strain of mice (Carrigy, Larsen, et al. 2019). This value is similar to the generally given respiratory minute volume for laboratory mice (23 mL/min) (Cryan, Sivadas and Garcia-Contreras 2007). Assuming the maximum number of mice in the study is 12, the total respiratory minute volume is 264 mL/min. Including a safety factor of 2, the minimum aerosol flow rate to prevent a hypoxic environment for the mice is 528 mL/min.

The dosing target was chosen to be 0.4 μg of ID93 and 1 μg of GLA delivered to each mouse. Assuming ID93 mass fraction is ~0.003% in the spray-dried lead inhalable ID93+GLA-SE formulation, the targeted powder dose delivered per mouse is approximately 13.3 mg. The delivered dose is defined as the dose available for breathing, as compared to the deposited dose, which is defined as the dose which deposits in the lung. This distinction was made explicit as the deposited dose is expected to be much lower than the delivered dose, with the FDA estimating that only 10% of aerosol delivered to rodents will reach the respiratory system (Tepper, et al. 2016).

Other considerations include the length of time that mice will tolerate being held in the mouse-restraint tubes of the aerosol delivery system without sedation. Mice have been reported to tolerate restraint tubes for less than an hour, even after acclimation to the devices (Phillips, Zhang and Johnston 2017). Retention of the mice in the tubes for longer periods of time may lead to stress-induced breathing pattern changes. For this reason, a duration of exposure limit of 20 minutes was

selected. Another concern was the maximum aerosol concentration that the mice could reasonably tolerate. To limit mouse distress due to high aerosol concentration, a maximum of 3 mg/L of aerosol concentration at the noseports was included as part of the success criteria. The aerosol concentration at the noseports, $C_{\text{noseports}}$, can be calculated using Eq.12, where m_{noseport} refers to the mass of spray-dried powder delivered to the noseports and D is the duration of exposure.

$$C_{\text{noseports}} = \frac{m_{\text{noseport}}}{RMV \times D} \quad \textbf{12}$$

Formulation Development

Particle size is a strong predictor of particle deposition in the appropriate respiratory region. The geometric diameter, d_{g}, of spray-dried spherical particles can be estimated using Eq.13, where c_{F} is the solids concentration of the feedstock, ρ_{P} is particle density, and d_{D} is the diameter of the droplets. If the particles are completely solid and spherical, the geometric diameter is equivalent to the aerodynamic diameter and particle density is equivalent to material density. Based on this equation, it is apparent that the size of particles can be influenced by modifying the feedstock concentration or the processing conditions to change the atomized droplet diameter.

$$d_{\text{g}} = \sqrt[3]{\frac{c_{\text{F}}}{\rho_{\text{P}}}}\, d_{\text{D}} \quad \textbf{13}$$

The density of mixtures can be calculated using Eq.14, where Y_i is the mass fraction of a given component and ρ_i is the component's true density. The density of the spray-dried vaccines can be approximated using the densities of the excipients trehalose, 1580 kg/m^3 (Grasmeijer, Frijlink and Hinrichs 2016), and trileucine, 1250 kg/m^3 (Carrigy, Liang, et al. 2019).

$$\rho_{\mathrm{t,mix}} = \frac{1}{\sum_i \frac{Y_i}{\rho_{\mathrm{t},i}}} \quad \textbf{14}$$

5.2.2. Materials

Trehalose dihydrate with a purity of 98% was used as the primary stabilizing excipient for spray drying (CAS 6138-23-4; Fisher Scientific Ottawa, ON, Canada). Trileucine with a purity of ≥90% (CAS 10329-75-6; Sigma Aldrich, Oakville, ON, Canada) was utilized as a dispersibility enhancing material. Tris(hydroxymethyl)aminomethane (Tris) (CAS 77-86-1; Sigma Aldrich, Oakville, ON, Canada) and hydrochloric acid (CAS 7647-01-0; Sigma Aldrich, Oakville, ON, Canada) were used as a buffer system. Formulations were made using HPLC grade water (CAS 7732-18-5; Fisher Scientific Ottawa, ON, Canada) or deionized water. Manufacture of the ID93 and GLA-SE components has been discussed in Chapter 2.

Three test formulations were developed to assess the feasibility of generating versions of the lead inhalable spray-dried vaccine suitable for mouse inhalation. The test formulations were all designed such that the component mass fractions in the dry powder were equivalent to the mass fractions of the Inhalable Vaccine formulation discussed in Chapter 4. The composition of the formulations prior to spray drying are shown in Table 12. The MV1 formulation was developed to target nose deposition only. For this reason, the formulation was designed to have a feedstock concentration in order to increase particle diameter. The MV2 and MV3 formulations were developed to target nose and lung deposition. The feedstock concentration of these formulations was designed to be relatively low in order to form smaller particles. The two formulations were tested in order to assess if active components were retained in progressively smaller particle sizes.

Table 12 Solution preparation and composition of the three test mouse-inhalable vaccine formulations.

Component	Concentration in Solution			Mass Fraction in Powder
	MV1	MV2	MV3	
Trehalose	100 mg/mL	6.67 mg/mL	1.67 mg/mL	78.5%
Trileucine	3.9 mg/mL	0.26 mg/mL	0.07 mg/mL	3.1%
Tris (buffer)	2.4 mg/mL	0.16 mg/mL	0.04 mg/mL	1.9%
Squalene	17.2 mg/mL	1.15 mg/mL	0.29 mg/mL	13.5%
GLA	10 µg/mL	0.67 µg/mL	0.17 µg/mL	0.008%
ID93	4 µg/mL	0.27 µg/mL	0.07 µg/mL	0.003%
Total Solids Content	123.51 mg/mL	8.24 mg/mL	2.07 mg/mL	N/A

Two versions of the test mouse-inhalable vaccine formulations without the vaccine, formulations C1 and C2, were also produced for testing the aerosol delivery system. These active-free formulations were developed to eliminate the possibility of accidental exposure to the aerosolized vaccine during characterization of the aerosol delivery system. The solution composition of these formulations is shown in Table 13. The C1 and C2 formulations were designed to target nose-only deposition, and nose and lung deposition in mice, respectively. These formulations were also designed to have a trileucine mass fraction of 3%, the same mass fraction as the Inhalable Vaccine formulation and the MV1, MV2, and MV3 formulations. 3% trileucine by mass was added so that the C1 and C2 formulations would be representative of the dispersibility of their vaccine-containing counterparts. The C1 formulation was designed to be representative of the MV1 formulation. Characterization results showed that both the MV2 and MV3 formulations successfully retained the vaccine. As the MV3 formulation produced smaller particles, this formulation is expected to have a higher fraction of lung deposition than the MV2 formulation. However, the MV2 formulation has a more reasonable production time due to its higher feedstock

concentration. The C2 formulation was therefore designed to be between the MV2 and MV3 formulations.

Table 13 Solution preparation and composition of the two formulations used for characterization of the aerosol delivery system. The C1 formulation was designed to target nose-only deposition whereas the C2 formulation was designed to target both nose and lung deposition.

Component	Concentration in Solution		Mass Fraction in Powder
	C1	C2	
Trehalose	100 mg/mL	3.33 mg/mL	94.6%
Trileucine	3.3 mg/mL	0.11 mg/mL	3.1%
Tris (buffer)	2.4 mg/mL	0.08 mg/mL	2.3%
Total Solids Content	105.7 mg/mL	3.52 mg/mL	N/A

5.2.3. Methods

Spray Drying

Spray drying was conducted using a custom research spray dryer and twin fluid atomizer, as previously discussed in Chapter 2. Spray drying parameters were chosen based on several considerations. A necessary parameter for successful delivery of powders to the intended deposition site is the aerodynamic particle size. In the previous section, the feedstock concentration was modified in order to change the predicted particle size. Processing conditions were also calculated in order to produce larger or smaller atomized droplets for production of powders to target nose-only deposition, or nose and lung deposition, respectively. However, due to the interrelated nature of the processing conditions, changing them can affect the ability to successfully stabilize the vaccine.

In order to prevent degradation of the vaccine due to high temperatures, the inlet temperature was limited to a maximum of 70 °C. The outlet temperature was limited to 50 °C since, as has been in shown in Chapter 4, spray-dried particles remain physically stable at this temperature. The outlet RH was also limited to 8% in order to prevent high moisture content in the powders. As previously discussed in Chapter 2, increased moisture content will decrease the T_g of the powder, resulting in powder crystallization at high moisture contents.

To target nose-only deposition, the processing parameters of the MV1 formulation were calculated to maximize the atomized droplet diameter. Conversely, the processing parameters for the MV2 and MV3 formulations were calculated to minimize the atomized droplet diameter to target nose and lung deposition. Additionally, as the MV2 and MV3 formulations had very low feedstock concentration, the liquid feed flow rate was increased to ensure that production time was feasible.

The atomized droplet diameter was predicted based on previous characterization of the droplet diameter as a function of the air-to-liquid ratio (ALR) of the customized atomizer (Hoe, et al. 2014). Due to the interrelated nature of the processing conditions, an energy and balance model (Ivey and Vehring 2010) was utilized iteratively to calculate appropriate processing conditions for each formulation based on the given limitations. The chosen spray drying parameters based on the processing model are shown in Table 14 for the MV1, MV2 and MV3 formulations.

Table 14 Processing parameters used for spray drying the formulations of the three test mouse-inhalable vaccine formulations.

Parameters	MV1	MV2	MV3
Drying Gas Flow Rate (SLPM)	600	600	800
Inlet Temperature (°C)	65	70	70
Atomizing Gas Pressure (psi)	10	70	80
Liquid Feed Flow Rate (mL/min)	2.4	2.7	3.3
Predicted Outlet Temperature (°C)	44	46	49
Predicted Outlet RH (%)	8	8	8
ALR	2	11	10
Theoretical MMD (µm)	5.3	1.5	1.0

Based on the success of the test spray-dried mouse-inhalable vaccine formulations, similar processing parameters were utilized for spray drying the C1 and C2 formulations. Modified parameters from the MV1 formulation were used to spray dry the C1 formulation. The same parameters were used to spray dry the MV3 and C2 formulations, as shown in Table 15.

Table 15 Processing parameters used for spray drying the formualtions for the characterization of the RBG-NOID.

Parameters	C1	C2
Drying Gas Flow Rate (SLPM)	500	800
Inlet Temperature (°C)	70	70
Atomizing Gas Pressure (psi)	10	80
Liquid Feed Flow Rate (mL/min)	1.8	3.3
Predicted Outlet Temperature (°C)	46	49
Predicted Outlet RH (%)	6	8
ALR	3	10
Theoretical MMD (µm)	4.6	1.1

Physicochemical Characterization

Limited analysis was conducted on the reconstituted spray-dried mouse-inhalable vaccine candidates to evaluate vaccine integrity post-spray drying. The powders were reconstituted using an appropriate volume of water to bring the reconstituted solution to the same concentration as the pre-spray-dried feedstock.

The size distribution of the nanoemulsion droplets were characterized using a dynamic light scattering instrument (Zetasizer Nano ZS; Malvern, UK). A similar method as detailed in Chapter 2 and Chapter 3 was utilized to determine whether the average nanoemulsion droplet diameter or polydispersity index of the ID93+GLA-SE vaccine candidate exceeded target values after spray drying for each formulation. Target values were previously given in Chapter 2.

The presence of the antigen ID93 in the samples was assessed through sodium dodecyl sulfate – polyacrylamide gel electrophoresis (SDS-PAGE) on the reconstituted spray-dried test formulations. The procedure has been previously detailed in Chapter 2 and Chapter 3.

Morphology analysis was completed using Field Emission Scanning Electron Microscopy (Zeiss Sigma FE-SEM; Carl Zeiss, Oberkochen, Germany). Samples were prepared by adding the powder to a carbon tape-covered aluminum SEM stub (Product 16111; Ted Pella, Inc.; Redding, CA, USA). The samples were placed in a desiccator connected to an in-house vacuum system for 2-3 days in order to remove exposed nanoemulsion droplets to prevent possible damage to the electron microscope. Then, the samples were sputtered with a gold coating (Denton Vacuum Desk II Sputter Coater; Denton, Moorestown, NJ, USA) to a thickness of approximately 16 nm. Images

ranging from 500-25000× were taken at a working distance of 5.3-6.1 mm using an accelerating voltage of 2.5-3.5 kV.

Aerosol Delivery System Characterization

A rotating brush generator (RBG) (RBG 1000G; Palas, Karlsruhe, Germany) was utilized to disperse the powder into an aerosol. This device has been used in other studies to disperse a dry powder into aerosol for delivery to rodents (Chand, et al. 2016, Cosnier, et al. 2016). The configuration used for this study included a 7 mm diameter feedstock reservoir and dispersion cover type C. All experiments were conducted at the lowest possible system air flow rate, 0.5 m^3/hr (8.33 L/min). The lowest flow rate was chosen to minimize the difference between the mouse inhalation rate and the aerosol flow rate. All experiments were conducted at the maximum brush-rotating speed, 1200 rpm, to maximize the dispersing force. Powder was loaded into the RBG reservoir within a dry environment in order to minimize moisture uptake. The mass of the powder loaded into the reservoir (nominal dose) was recorded as the difference in the powder stock container mass before and after loading powder.

The RBG device was connected to a modified version of a custom-made nose-only inhalation device (NOID), first developed by Nadithe et al. (Nadithe, et al. 2003). This modified version of the NOID was also used in immunogenicity and protective efficacy mouse studies with nebulized bacteriophage (Carrigy, Larsen, et al. 2019). Mouse noseports were plugged for the characterization experiments in this study. Experiments consisted of aerosolizing the C1 or C2 powder using the RBG and determining the delivery efficiency through the NOID. Two feed rates were assessed: ~300 mm/hr and 150 mm/hr. Repeat experiments at ~300 mm/hr were conducted to assess repeatability of the results. An exit filter (VP7100; KEGO Corporation, London, ON,

Canada) was placed at the outlet of the NOID and was measured gravimetrically before and after each experiment to determine powder deposition on the exit filter. Airflow was run for an additional minute after all powder was aerosolized by the RBG in order to allow any remaining aerosol to traverse the system. A simplified schematic of the RBG and NOID system with the exit filter (RBG-NOID) is shown in Figure 31.

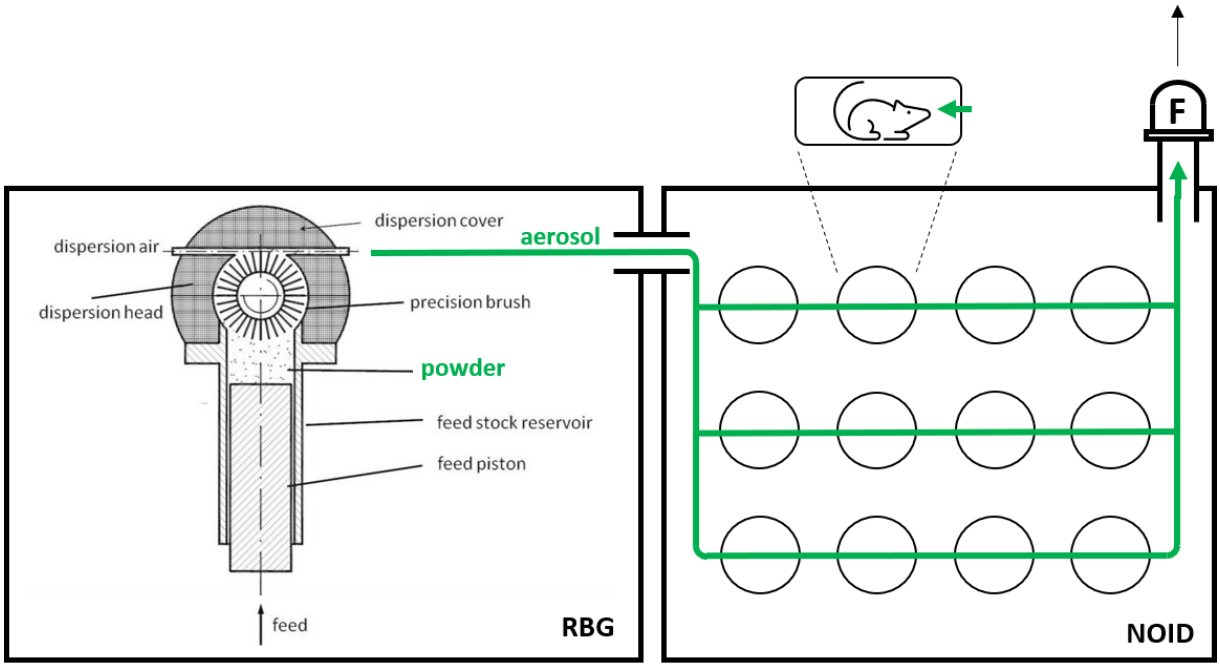

Figure 31 Schematic of the aerosol delivery system, consisting of the RBG (Filtration and Particle Science n.d.) connected to the NOID. Black arrows represent the flow of clean air and green arrows represent the flow of aerosolized powder.

The mass of powder deposited on the exit filter was used to estimate the amount of powder that reached each of the noseports using a ratio of flow rates, as given in Eq.15. In this equation, m_{filter} refers to the measured mass of powder deposited on the exit filter, and Q_{outlet} is the aerosol flow rate at the outlet of the RBG-NOID device, which is 8.33 L/min.

$$\frac{m_{\text{noseport}}}{m_{\text{filter}}} = \frac{RMV}{Q_{\text{outlet}}} \quad \textbf{15}$$

Equipment was completely cleaned and dried between each experiment; however, delivery efficiency is expected to increase for subsequent experiments due to coating of surfaces with powder.

Following the optimization characterization experiments, a feed rate of 150 mm/hr was chosen to assess the dispersing capabilities of both the spray-dried C1 and C2 formulations. The particle size distribution at the outlet of the aerosol delivery system was measured to determine if the tested powder was adequately dispersed to primary particle size by the system. A flexible hose was connected at one end to the outlet of the NOID and connected at the other end to an aerosol diluter (Aerosol Diluter 3302A; TSI, Shoreview, MN, USA) mounted on a time-of-flight aerodynamic particle sizer (APS) (Aerodynamic Particle Sizer Spectrometer 3321; TSI, Shoreview, MN, USA). The aerosol flow rate of the RBG-NOID is 8.33 L/min and the sampling flow rate of the APS is 5 L/min. To prevent pressure buildup within the system, a tee fitting with a filter (VP7100; KEGO Corporation, London, ON, Canada) was attached to the hose prior to the diluter and APS system. A simplified schematic of this sampling setup is shown in Figure 32. Flexible tubing was utilized to avoid sharp changes in flow direction. Gently curved streamlines will mitigate large particle deposition as compared to abrupt changes during aerosol transportation through the tubing.

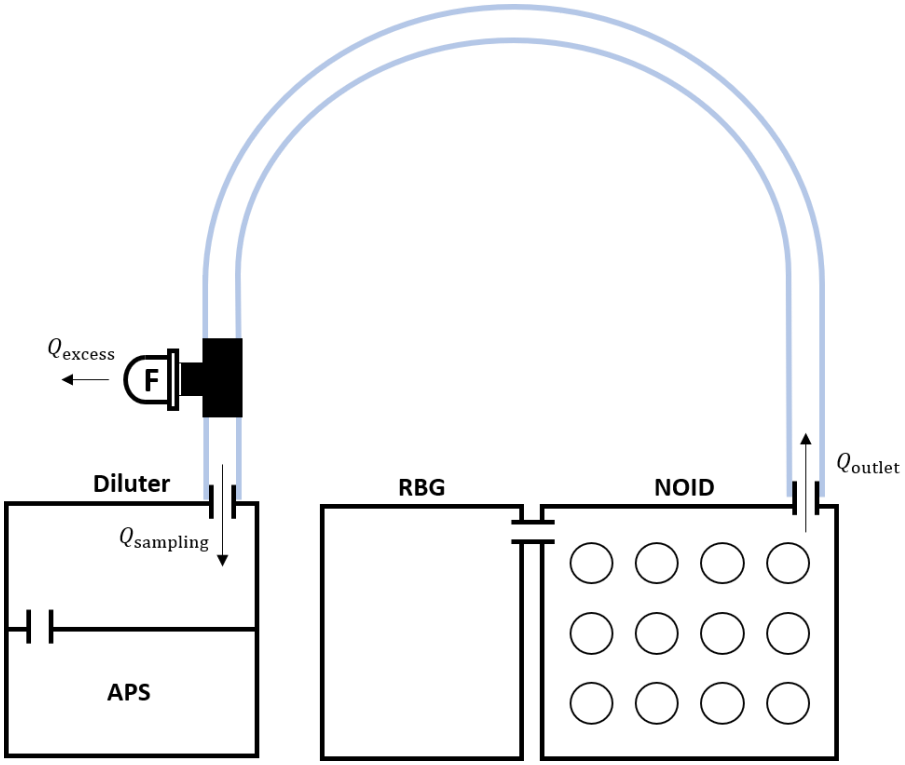

Figure 32 Simplified schematic of the system used to measure the aerosol size distribution at the outlet of the RBG-NOID.

The APS device measures the count median aerodynamic diameter, *CMAD,* and the geometric standard deviation, σ_g. The mass median aerodynamic diameter, $d_{a,50}$, was calculated using the Hatch-Choate equation, as shown in Eq.16. Six and nine recordings were obtained for the C1 and C2 formulations, respectively.

$$d_{a,50} = CMAD \cdot e^{3\ln^2(\sigma_g)} \quad \textbf{16}$$

5.3. Results and Discussion

5.3.1. Emulsion Size Distribution

The average size of the vaccine nanoemulsion droplets before and after spray drying for the test mouse-inhalable formulations MV1, MV2, and MV3 are shown in Figure 33. It is apparent that the emulsion droplet size is preserved over spray drying for all tested formulations. This result is consistent with the preservation of nanoemulsion droplet size of similar formulations, as reported in Chapter 3 and Chapter 4. The maintenance of the nanoemulsion droplet diameter indicates that the processing parameters chosen were suitable for encapsulating the vaccine and stabilizing the nanoemulsion droplet membrane during spray drying.

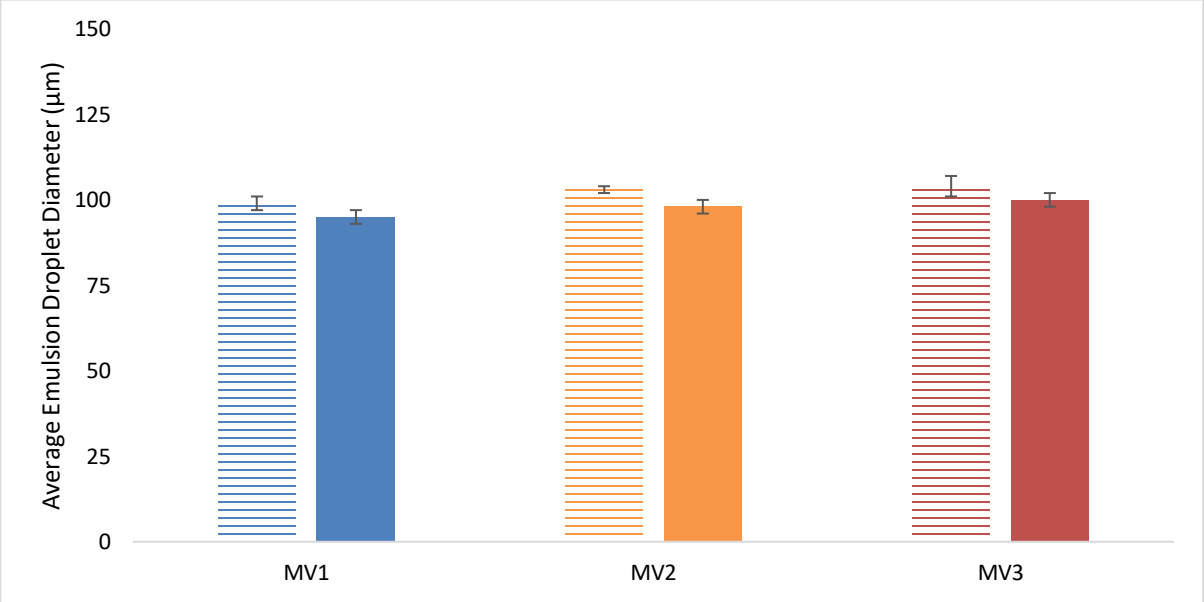

Figure 33 Plot indicating the measured average emulsion droplet diameter of the test mouse-inhalable formulations. Striped bars represent the liquid feedstock and solid bars represent the reconstituted spray-dried powder. Error bars represent the standard deviation.

The polydispersity index of the test mouse-inhalable formulations before and after spray drying are shown in Figure 34. All of the tested formulations had a measured polydispersity index less than 0.2, suggesting a relatively monodisperse distribution. These results further indicate that the chosen processing parameters were appropriate for spray drying the mouse-inhalable vaccine candidates.

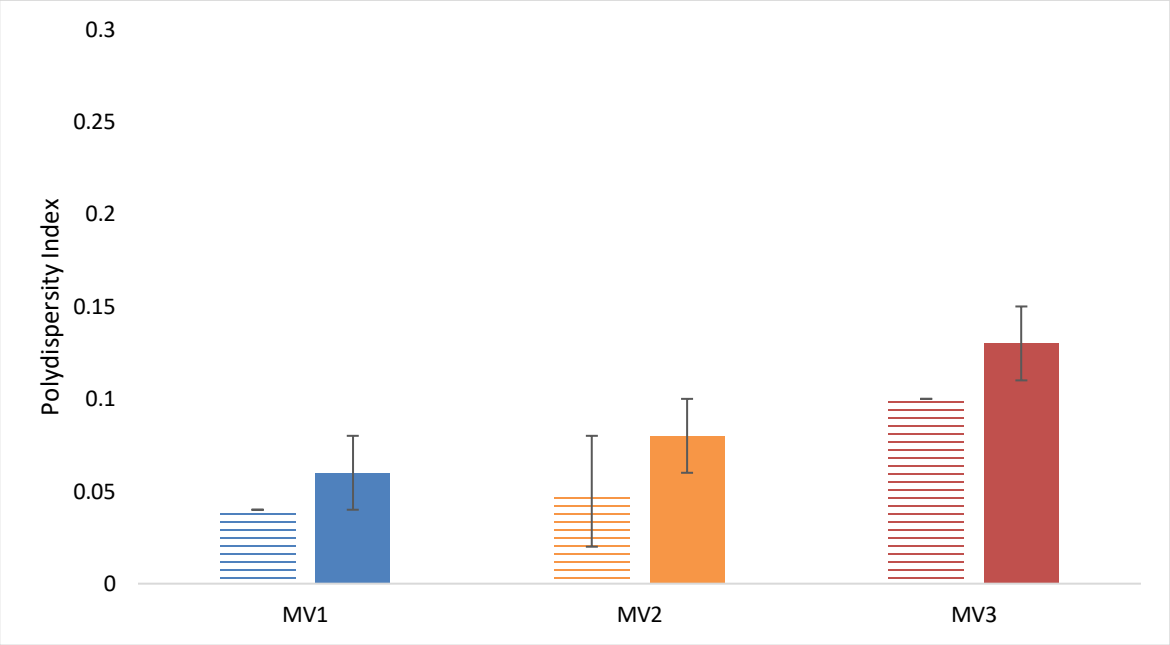

Figure 34 Plot indicating the measured polydispersity index of the test mouse-inhalable formulations. Striped bars represent the liquid feedstock and solid bars represent the reconstituted spray-dried powder. Error bars represent the standard deviation.

5.3.2. Antigen Presence

ID93 antigen presence was determined using SDS-PAGE. An image of the stained gels for the mouse-inhalable vaccine candidates MV1, MV2, and MV3 and a control ID93+GLA-SE formulation is shown in Figure 35. The ID93 band is present for all reconstituted mouse-inhalable vaccine candidates, indicating that the formulation and processing parameters successfully stabilized the ID93 antigen. Both the preservation of nanoemulsion size and the retention of ID93 antigen suggest that all tested mouse-inhalable vaccine candidates successfully encapsulated the ID93+GLA-SE vaccine within particles designed to be suitable for delivery to mice.

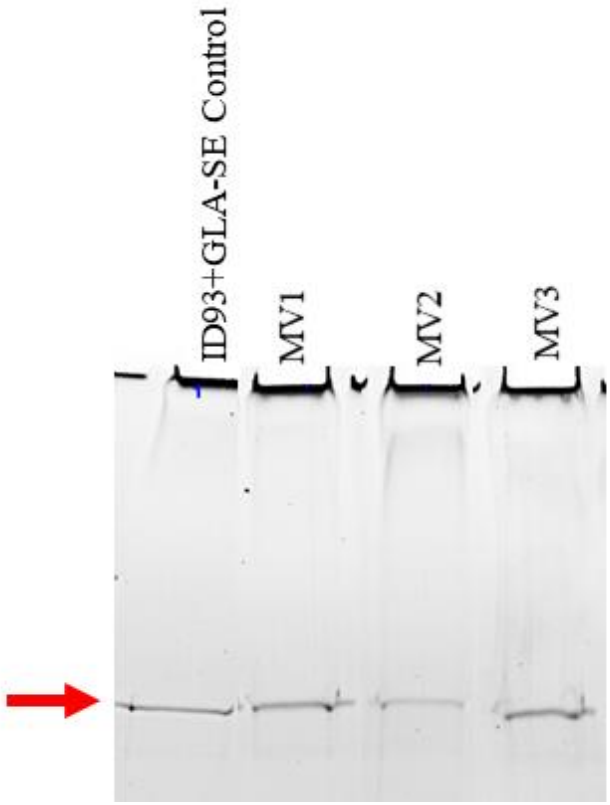

Figure 35 SDS-PAGE analysis for ID93 presence based on existence of antigen band. SDS-PAGE analysis for a control ID93+GLA-SE formulation has been provided for comparison. Analysis completed on the mouse-inhalable vaccine candidates MV1, MV2 and MV3 showed ID93 band is present for all formulations. The red arrow points to the ID93 band.

5.3.3. Particle Morphology

The morphology of the spray-dried mouse-inhalable test powders is shown in Figure 36. It is apparent that the MV1 particles are much larger than the MV2 and MV3 particles, as intended. The MV1 formulation was designed to target nose deposition only, whereas the MV2 and MV3 formulations are designed to target the nose and lungs. The MV3 particles appear to be slightly smaller than the MV2 particles, as designed. The surface particle morphology of all formulations shows some level of roughness. The surface rugosity is due to trileucine surface coverage. As detailed in Chapter 3, excipient investigation has shown that the addition of trileucine enriches the surface and causes folding of the particles. The rough surface morphology was designed in order to improve powder dispersibility. High powder dispersibility is crucial for dry powder delivery as the inability to separate particle aggregates will decrease system delivery efficiency.

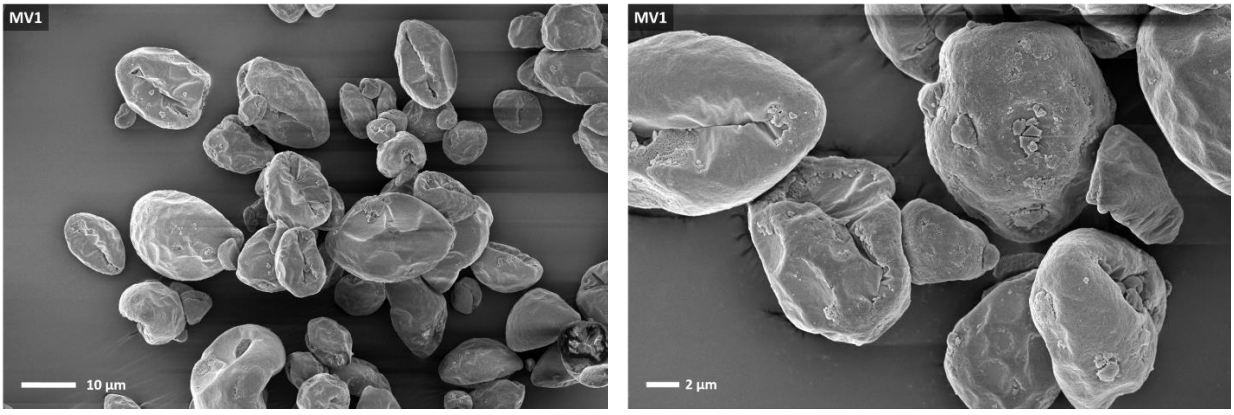

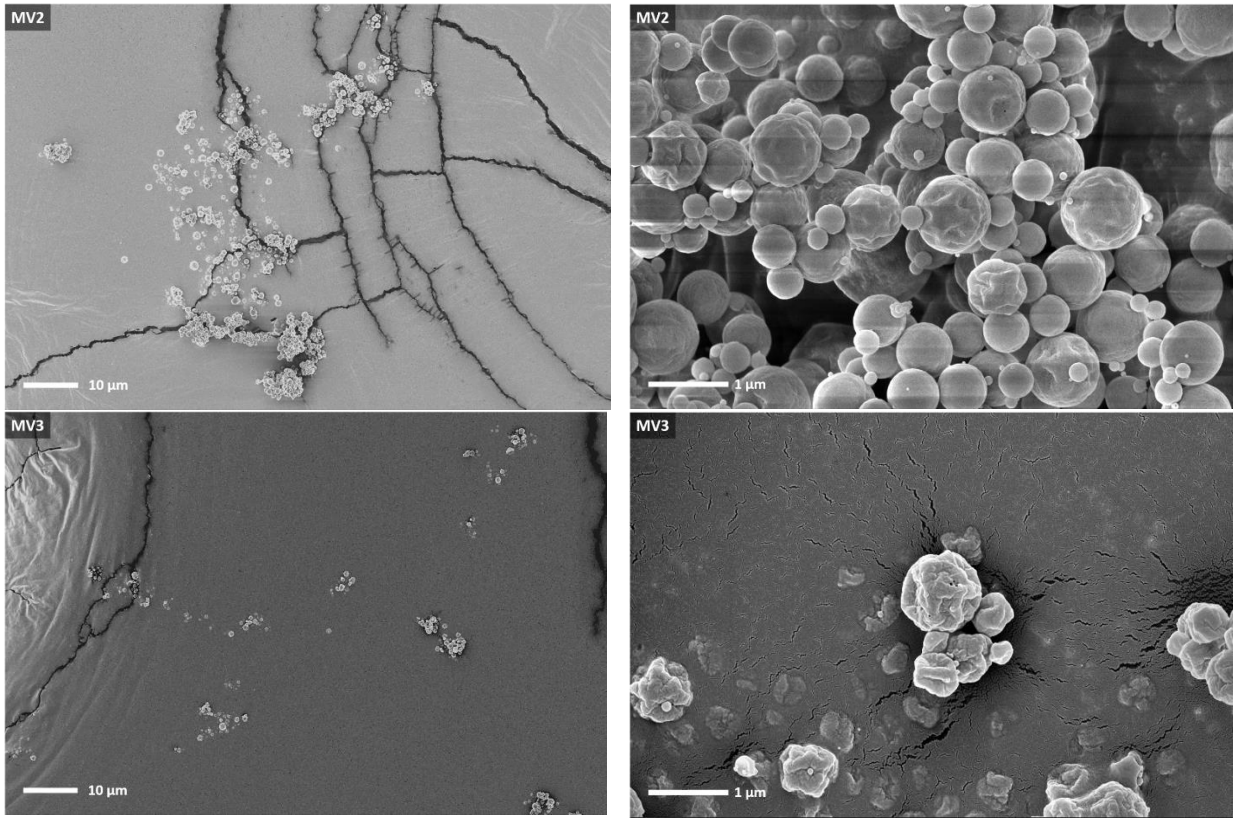

Figure 36 SEM images of the test mouse-inhalable spray-dried formulations MV1, MV2, and MV3. SEM images were captured of each formulation at low (left) and high (right) magnification. The scale bars are shown on the respective images.

SEM images were taken of the C1 and C2 formulations to determine if the morphology was similar to their mouse-inhalable vaccine counterparts. The SEM images of the C1 and C2 formulations are shown in Figure 37. It is apparent that the morphology of the C1 and C2 spray-dried formulations for characterization are similar to the test inhalable mouse formulations MV1, and MV2 and MV3, respectively. The geometric diameters of the MV1 and C1 particles appear to be similar, and both have a similar surface morphology due to the presence of trileucine. Similarly, the geometric diameters and surface morphology of the MV2, MV3 and C2 formulations also appear to be similar. The morphology similarities suggest that the C1 and C2 formulations will provide a reasonable representation of the dispersibility of the test mouse-inhalable candidates.

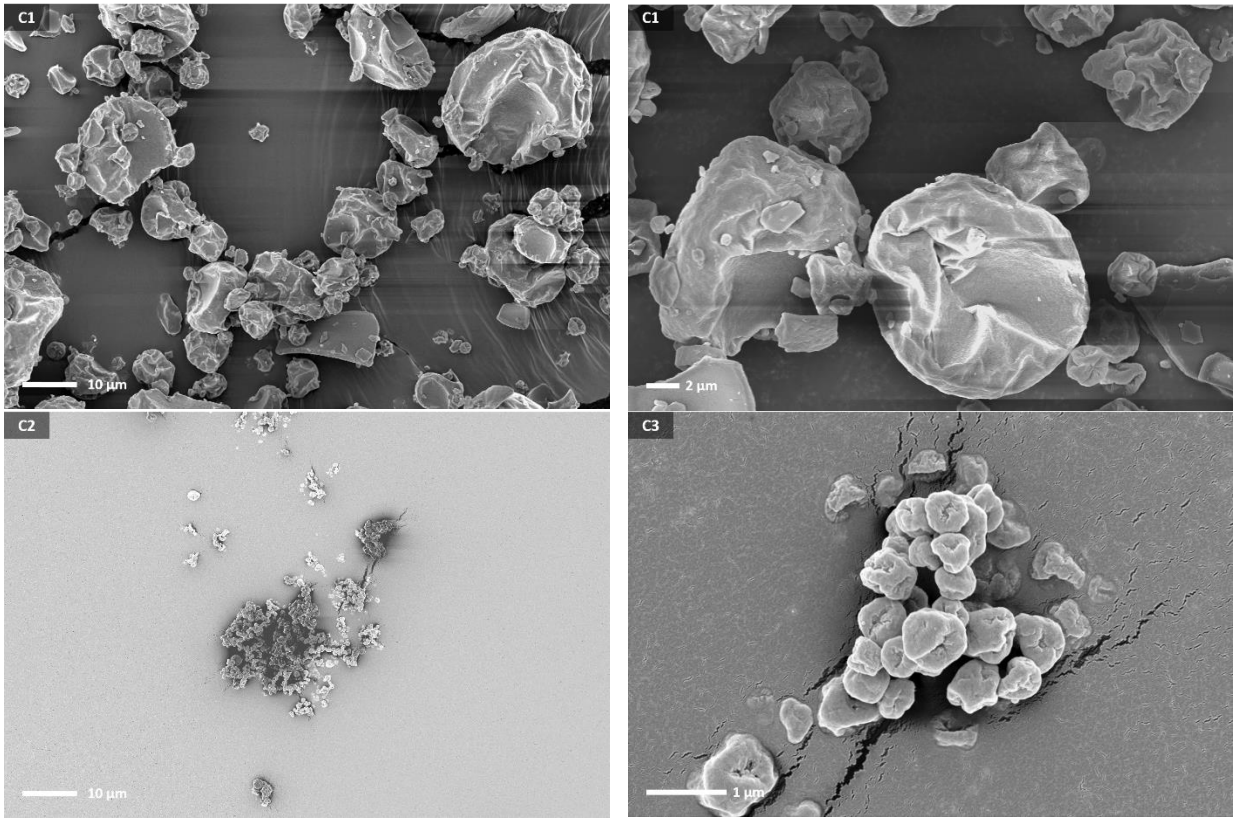

Figure 37 SEM images of the trileucine-containing C1 (top) and C2 (bottom) spray-dried powders at low (left) and high (right) magnification. The scale bars are shown on the respective images.

5.3.4. RBG-NOID Efficiency

A summary of the parameter optimization experiments for the spray-dried C1 formulation is given in Table 9. Tests 1 and 2 were completed at approximately the same feed rate in order to assess the dosing reproducibility; the delivered dose for these tests was 0.013±0.005% nominal dose. Decreasing the feed piston rate increased the efficiency of powder delivery. All tests show that the aerosol concentration at the noseports was less than 3 mg/L, and the duration of exposure was less than the 20-minute limit. Based on these experiments, a feed rate of 150 mm/hr or lower is recommended for maximizing the efficiency of dispersing the spray-dried vaccine powder targeting nose deposition. However, chosen feed rate must not be so low that the duration of exposure is increased to longer than 20 minutes.

A summary of the parameter optimization experiments for the spray-dried C2 formulation is given in Table 17. Tests 4, 5, and 6 were completed at approximately the same feed rate in order to assess the dosing reproducibility. For these tests, a delivered dose of 0.081±0.009 % nominal dose was achieved, indicating a similar level of reproducibility as the C1 formulation. These results show that the C2 formulation is better able than the C1 formulation to reach the noseports of the RBG-NOID system when run under the same parameters. This is to be expected as the C2 formulation was designed to have a smaller aerodynamic particle size than the C1 formulation. As the aerosol traverses the RBG-NOID system, particles are expected to deposit due to inertial impaction or sedimentation. Larger particles are less likely to be able to follow streamlines, and larger particles also have greater inertia, contributing to greater powder deposition within the system prior to reaching the mice.

Table 16 Summary of characterization experiments for the spray-dried C1 formulation.

Test ID	Feed rate (mm/hr)	Nominal Dose (mg)	D (min)	m_{filter} (mg)	$m_{\text{noseports}}$ (mg)	$m_{\text{noseports}}$ (% nominal dose)	$C_{\text{noseports}}$ (mg/L)
1	303	690.1	6.7	22.7	0.06	0.009%	0.41
2	304	711.0	7.3	43.4	0.12	0.016%	0.71
3	150	495.9	11.4	44.3	0.12	0.024%	0.47

The aerosol concentration at the noseports for experiments conducted at ~300 mm/hr feed rate was 3.76±0.97 mg/L, above the set aerosol concentration limit. Reducing the feed rate increased the powder delivery efficiency and decreased the aerosol concentration at the noseports to tolerable levels. Based on these results, a feed rate of 150 mm/hr or lower is recommended for maximizing the delivery efficiency while ensuring tolerable aerosol concentration at the noseports.

As compared to the nominal dose, the delivered dose appears to be low. However, the low percentage of nominal dose reaching the noseports is expected. Due to the difference between aerosol flow rate and the total inhalation rate of the mice, 97% of aerosol available will bypass the mice. Therefore, even in an ideal system with no losses, the maximum dose delivered to each mouse in a 12-mouse experimental set up would be only 0.25% of the nominal dose. At an optimized 150 mm/hr feed rate, approximately 10% and 44% of the maximum possible delivered dose reached the noseports for the C1 and C2 formulations, respectively.

Table 17 Summary of characterization experiments for the spray-dried C2 formulation

Test ID	Feed rate (mm/hr)	Nominal Dose (mg)	D (min)	m_{filter} (mg)	$m_{\text{noseports}}$ (mg)	$m_{\text{noseports}}$ (% nominal dose)	$C_{\text{noseports}}$ (mg/L)
4	306	852.1	8.0	284.6	0.75	0.088%	4.25
5	306	754.1	9.2	203.3	0.54	0.071%	2.65
6	304	754.7	6.6	241.3	0.64	0.084%	4.39
7	150	637.2	13.7	254.8	0.67	0.11%	2.23

For the C1 formulation, 3.3-8.9% of the nominal dose was deposited on the exit filter for the tested feed rates. The system efficiency for the C2 formulation was even higher, with 33.4-40.0% of the nominal dose depositing on the exit filter for the tested feed rates. A recent study delivered nebulized phage-containing droplets to mice using an aerosol system consisting of a vibrating mesh nebulizer and the NOID characterized in this study. Experiments were run with an aerosol flow rate of 500 mL/min (Carrigy, Larsen, et al. 2019). The reported overall system efficiency was much lower than this study, with only 1.50% of the nominal dose measured on the exit filter with optimized processing parameters.

The predicted $m_{\mathrm{noseports}}$ in all experiments indicates that the system was unable to deliver the required 13.3 mg of powder to reach the target dose of ID93 and GLA for either formulation. However, the limits on duration of exposure and concentration at the noseports make the target dose of ID93 and GLA not feasible with the current system and parameters. To address this issue, it is recommended that the ID93 and GLA actives be formulated at higher concentrations to achieve the desired dose.

5.3.5. Particle Size Distribution of the Dispersed Aerosol at the RBG-NOID Outlet

The C1 and C2 powders were aerosolized using the RBG-NOID system, and these aerosols were sized to determine how well the system dispersed the powders. The results of the size distribution measurements are shown in Table 18. As previously discussed, the d_{a} targets were approximately 5 µm and 1-2 µm for the formulations targeting nose-only deposition, and nose and lung deposition in mice, respectively. The measured $d_{\mathrm{a},50}$ of the C1 and the C2 formulations at the outlet of the system was close to these targets. These results suggest that a high brush speed was appropriate to

disperse the powders to primary particle size and that the powder is easily dispersible. The high dispersibility of the C1 and C2 formulations is consistent with the results shown in Chapter 3 and Chapter 4 which indicate that trileucine surface coverage of particles enhances vaccine powder dispersibility.

A gently curved hose was used to connect the RBG-NOID outlet to the APS system in order to minimize deposition of large particles due to inability to follow streamlines at abrupt flow changes and thereby shift the measured size distribution to the lower size. Some deposition was seen within the tubing, indicating that despite precautions there was some particle deposition of the aerosol prior to reaching the APS system. Regardless, the $d_{a,50}$ of the C1 formulation as measured at the outlet of the system is close to target.

The APS device measures the particle size distribution of an aerosol by separating the particle measurements into bins before fitting the data to a lognormal distribution in order to calculate *CMAD* and σ_g. The size range of the APS is 0.5-20 µm, with the lowest bin measuring all particles with aerodynamic particles <0.523 µm. Therefore, the *CMAD* reported by the APS system for the C2 formulation may be higher than the actual *CMAD* of the powder. Regardless, the $d_{a,50}$ of the C2 formulation as measured at the outlet of the system is within the 1-2 µm target.

Table 18 Measured particle size distribution of the dispersed C1 and C2 powders at the outlet of the RBG-NOID. Results shown are the average ± standard deviation of six measurements for the C1 formulation and nine measurements for the C2 formulation.

Formulation	APS Measurement		Calculated $d_{a,50}$ (µm)
	CMAD (µm)	σ_g	
C1	1.9±0.1	1.7±0.1	4.4±0.4
C2	1.1±0.1	1.5±0.1	1.7±0.2

5.4. Conclusion

In this chapter, three spray-dried versions of the ID93+GLA-SE vaccine were designed for delivery to mice through two different routes. The first route targeted nose-only deposition in order to assess administration through the intranasal route. The second route targeted nose and lung deposition in order to assess administration through the pulmonary route. Chemical analysis showed that the nanoemulsion droplet size and the antigen were preserved, suggesting that vaccine integrity was maintained after spray drying for the given processing conditions. Morphology indicated that produced particles were rugose as designed, similar to previously generated formulations. Successful development of a spray-dried ID93+GLA-SE vaccine candidate suitable for delivery to mice via inhalation led to the next phase: design and characterization of an aerosol delivery system.

The aerosol system consisted of two main components: a dust generator to aerosolize the spray-dried vaccine and a nose-only inhalation device to restrain the mice and deliver the aerosolized dry powder vaccine. The aerosol delivery system parameters were optimized using two vaccine-free formulations as a safety precaution: 1) a large particle formulation that would target nose-only deposition and 2) a small particle formulation that would target nose and lung deposition in mice. Experiments with both formulations showed that the designed system outperformed the aerosol delivery efficiency of a similar set up. However, neither formulation was able to achieve the target delivered dose while ensuring that mice would not be under excessive stress. Based on these results, the antigen and agonist relative concentrations within the powder must be increased in order to reach the targeted delivered dose.

Chapter 6. Conclusions and Future Work

The rise of antibiotic resistance is a key motivator for widespread immunization through vaccination. However, global distribution is negatively impacted by the refrigeration requirements of most vaccines. To address this issue, vaccines can be converted through spray drying to dry formats that are suitable for room temperature storage. Particle engineering via spray drying can also be utilized to confer inhalable properties on the dry vaccine. In this thesis, several iterations of spray-dried TB vaccine candidate ID93+GLA-SE were designed for global health applications. The subunit adjuvanted vaccine candidate was formulated as a nano-emulsion; thus successful production required stabilization of all components of the vaccine, that is, the antigen, agonist, and adjuvant system.

In Chapter 2, formulation and spray drying parameters were developed to encapsulate the vaccine candidate within a dry powder composed of many microparticles while preserving the component integrity throughout the spray drying process. The powder was designed for long-term room temperature storage, to be reconstituted as needed. Comparison of the vaccine candidate before and after spray drying indicated that the candidate was successfully protected from desiccation stresses. Then a stability study was conducted on the spray-dried vaccine candidate to assess the long-term stability potential. Results indicated that the dry powder vaccine maintained particle morphology, moisture content, solid state, and emulsion size after one year of storage at temperatures up to 40 °C. The antigen and agonist components showed temperature-dependent degradation over the course of the stability study; however, both were still present after over one year of storage at 40 °C. These results demonstrate the possibility of stabilizing highly complicated formulations such as nanoemulsion and protein systems into a thermostable format via spray

drying. Additionally, unlike lyophilization spray drying allows for the stabilization of freeze-sensitive vaccines. Thermostable presentations reduce costs associated with transport and storage of liquid vaccines and can allow for stockpiling in the event of a pandemic.

The successful development of a thermostable presentation of the TB vaccine candidate prompted the investigation of an inhalable version of the spray-dried vaccine outlined in Chapter 3. Two key inhalable properties were conferred via particle engineering: microparticle size in the human respirable range and increased dispersibility of the spray-dried powder. This was accomplished through the addition of leucine, pullulan, or trileucine as dispersibility enhancing agents and the adjustment of the formulations to produce smaller particles. Characterization of the inhalable vaccine candidates found differences in aerosol performance and preservation of antigen integrity, indicating that the properties of a given vaccine are critical to selecting an appropriate dispersibility-enhancing agent. The trileucine-containing candidates were the only formulations to successfully preserve nanoemulsion size and antigen content and improve aerosol performance. The successful development of an inhalable dry powder presentation of the vaccine candidate opens the door to pulmonary or intranasal administration via inhalation. Needle-free delivery routes bypass a number of issues associated with needles such as injuries, low compliance, and possible transfer of blood-borne illnesses.

Physical stability of the lead trileucine-containing inhalable vaccine candidate was compared to the initial spray-dried vaccine candidate in Chapter 4. The two candidates were stored for seven months at temperatures up to 50 °C. The results showed that inclusion of trileucine in the formulation improved physical stability of the dry powder, with aerosol performance maintained even when stored at 50 °C. This result is consistent with other studies demonstrating that the

inclusion of trileucine improves powder dispersibility and may also improve long term powder stability.

Development of an inhalable version of the spray-dried vaccine showed promising results; however, animal studies need to be conducted in order to assess efficacy. Preliminary work was completed in preparation for animal studies with the lead inhalable vaccine candidate. Two versions of the inhalable spray-dried vaccine candidate were modified for mouse inhalation: one targeting nose deposition only and the other targeting nose and lung deposition. These versions were developed such that intranasal and pulmonary routes of administration, respectively, could be assessed in the animal model. Chemical characterization showed that the inhalable vaccine formulations modified to be suitable for inhalation by mice still retained the antigen and maintained nanoemulsion size after spray drying. In addition to modifying the inhalable vaccine formulation, an aerosol delivery system to house and deliver the vaccine powder to the mice was designed and characterized. The aerosol delivery system operating parameters were optimized to sufficiently disperse the vaccine powder into a fine aerosol and transfer the powder to the mice efficiently. High system efficiencies were obtained; however, results showed that, due to limitations regarding maximum tolerable aerosol concentration for mice, appropriate dosing of the vaccine aerosol would be possible only with increased concentrations of the actives in the powder.

Additional work needs to be completed to assess the long-term stability potential of the inhalable version of the spray-dried vaccine in terms of vaccine integrity. The vaccine has been shown to be physically stable; however, at this point it is unknown if trileucine affects the ability of the formulation to stabilize the vaccine long-term. Furthermore, DPI optimization must be investigated in order to achieve high dosing targets. There are many benefits to needle-free delivery; however,

inhalable delivery is not without its drawbacks. For instance, inhalable delivery of thermostable formulations requires the use of excipients, which decrease the amount of active in every dose. Another issue is that, unlike parenteral injection, it is not easy to confirm the amount of dose delivered to the lung as the airways across different demographics is variable. The risk of exposure to bystanders must also be considered. Preclinical trials must be conducted in order to assess the efficacy of the spray-dried vaccine candidates and determine the best route of administration.

References

Aguilo, Nacho, Samuel Alvarez-Arguedas, Santiago Uranga, Dessislava Marinova, Marta Monzon, Juan Badiola, and Carlos Martin. 2016. "Pulmonary but not subcutaneous delivery of BCG vaccine confers protection to tuberculosis-susceptible mice by an interleukin 17-dependent mechanism." *Journal of Infectious Diseases* 213 (5): 813-839. doi:10.1093/infdis/jiv503.

Andersen, Peter, and Timothy Mark Doherty. 2005. "The success and failure of BCG - implications for a novel tuberculosis vaccine." *Nature Reviews Microbiology* 3: 656-662. doi:10.1038/nrmicro1211.

Anderson, Ryan C., Christopher B. Fox, Timothy S. Dutill, Narek Shaverdian, Tara L. Evers, Garrett R. Poshusta, James Chesko, et al. 2010. "Physicochemical characterization and biological activity of synthetic TLR4 agonist formulations." *Colloids and Surfaces B: Biointerfaces* 75: 123-132.

Argarkhedkar, Sharad, Prasad S. Kulkarni, Scott Winston, Robert Sievers, Rajeev M. Dhere, Bhagwat Gunale, Ken Powell, Paul a. Rota, Mark Papania, and MDVP author group. 2014. "Safety and immunogenicity of dry powder measles vaccine administered by inhalation: A randomized controlled Phase 1 clinical trial." *Vaccine* 32: 6791-6797. doi:10.1016/j.vaccine.2014.09.071.

Arora, Sumit, Mehra Haghi, Paul M. Young, Michael Kappl, Daniela Traini, and Sanyog Jian. 2016. "Highly respirable dry powder inhalable formulation of voriconazole with enhanced pulmonary bioavailability." *Expert Opinion on Drug Delivery* 13 (2): 183-193. doi:10.1517/17425247.2016.1114603 ORIGINAL.

Arpagaus, Cordin, Andreas Collenburg, David Rutti, Elham Assadpour, and Seid Mahdi Jafari. 2018. "Nano spray drying for encapsulation of pharmaceuticals." *International Journal of Pharmaceutics* 546: 194-214. doi:10.1016/j.ijpharm.2018.05.037.

Bahamondez-Canas, Tania F., and Zhengrong Cui. 2018. "Intranasal immunization with dry powder vaccines." *European Journal of Pharmaceutics and Biopharmaceutics* 122: 167-175.

Bakry, Amr M., Zheng Fang, Yingzhou Ni, Hao Cheng, Yong Q. Chen, and Li Liang. 2016. "Stability of tuna oil and tuna oil/peppermint oil blend microencapsulated using whey protein isolate in combination with carboxymethyl cellulose or pullulan." *Food Hydrocolloids* 60: 559-571. doi:10.1016/j.foodhyd.2016.04.026.

Bertholet, Sylvie, Gregory C. Ireton, Diane J. Ordway, Hillarie Plessner Windish, Samuel O. Pine, Maria Kahn, Tony Phan, et al. 2010. "A defined tuberculosis vaccine candidate boosts BCG and protects against multidrug-resistant Mycobaterium tuberculosis." *Science Translational Medicine* 2 (53): 53-74. doi:10.1126/scitranslmed.3001094.

Bertholet, Sylvie, Gregory C. Ireton, Maria Kahn, Jeffrey Guderian, Raodoh Mohamath, Nicole Stride, Elsa M. Laughlin, et al. 2008. "Identification of human T cell antigens for the development of vaccines against Mycobacterium tuberculosis." *Journal of Immunology* 181 (11): 7948-7957. doi:10.4049/jimmunol.181.11.7948.

Boraey, Mohammed A., and Reinhard Vehring. 2014. "Diffusion controlled formation of microparticles." *Journal of Aerosol Science* 67: 131-143.

Brandt, Lise, Joana Feino Cunha, Anja Weinreich Olsen, Ben Chilima, Penny Hirsch, Rui Appelberg, and Peter Andersen. 2002. "Failure of the Mycobacterium bovis BCG vaccine: some species of environmental mycobacteria block multiplication of BCG and induction of protective immunity to tuberculosis." *Infection and Immunity* 70 (2): 672-678. doi:10.1128/IAI.70.2.672–678.2002.

Bringas-Lantigua, Madai, Idalmis Exposito-Molina, Gary A. Reineccius, Orestes Lopez-Hernandez, and Jorge A. Pino. 2011. "Influence of spray-dryer air temperatures on encapsulated mandarin oil." *Drying Technology* 29: 520-526. doi:10.1080/07373937.2010.513780.

Carrigy, Nicholas B. , Lu Liang, Hui Wang, Samuel Kariuki, Tobi E. Nagel, Ian F. Connerton, and Reinhard Vehring. 2019. "Trileucine and pullulan improve anti-Campylobacter bacteriophage stability in engineered spray-dried microparticles." *Annals of Biomedical Engineering* 48: 1169-1180. doi:10.1007/s10439-019-02435-6.

Carrigy, Nicholas B., and Reinhard Vehring. 2019. "Engineering stable spray-dried biologic powder for inhalation." In *Pharmaceutical Inhalation Aerosol Technology (3rd ed.)*, edited by A. J. Hickey and S. da Rocha, 291-326. Boca Raton: CRC Press.

Carrigy, Nicholas B., Mani Ordoubadi, Yushan Liu, Omar Melhem, David Barona, Hui Wang, Leanne Milburn, Conor A. Ruzycki, Warren H. Finlay, and Reinhard Vehring. 2019. "Amorphous pullulan trehalose microparticle platform for respiratory delivery." *International Journal of Pharmaceutics* 563: 156-168. doi:10.1016/j.ijpharm.2019.04.004.

Carrigy, Nicholas B., Sasha E. Larsen, Valerie Reese, Tiffany Pecor, Melissa Harrison, Philip J. Kuehl, Graham F. Hatfull, et al. 2019. "Prophylaxis of Mycobacterium tuberculosis H37Rv infection in preclinical mouse model via inhalation of nebulized bacteriophage D29." *Antimicrobial Agents and Chemotherapy* 63 (12): 1-19. doi:10.1128/AAC.00871-19.

Chan, Michelle Y., Quinton M. Dowling, Sandra J. Sivananthan, and Ryan M. Kramer. 2017. "Particle sizing of nanoparticle adjuvant formulations by dynamic light scattering (DLS) and nanoparticle tracking analysis (NTA)." *Methods in Molecular Biology* 1494: 239-252. doi:10.1007/978-1-4939-6445-1_17.

Chand, Ramesh, Philip J. Kuehl, Peter B. Heifetz, Haim Moskowitz, and Jacob D. McDonald. 2016. "Non-clinical inhalation delivery of a biologic." *Respiratory Drug Delivery 2016* 415-418.

Chang, Rachel Yoon Kyung, Ke Chen, Jiping Wang, Martin Wallin, Warwick Britton, Sandra Morales, Elizabeth Kutter, Jian Li, and Hak-Kim Chan. 2018. "Proof-of-principle study in a murine lung infection model of antipseudomonal activity of phage PEV20 in a dry-powder formulation." *Antimicrobial Agents and Chemotherapy* 62 (2): 1-8. doi:10.1128/AAC.01714-17.

Chen, Lan, Tomoyuki Okuda, Xiang-Yun Lu, and Hak-Kim Chan. 2016. "Amorphous powders for inhalation drug delivery." *Advanced Drug Delivery Reviews* 100: 102-115.

Chen, Lihao, Jun Wang, Anna Zganiacz, and Zhou Xing. 2004. "Single intranasal mucosal Mycobacterium bovis BCG vaccination confers improved protection compared to subcutaneous vaccination against pulmonary tuberculosis." *Infection and Immunity* 72 (1): 238-246. doi:10.1128/IAI.72.1.238–246.2004.

Chen, Liuhua, Lihua Gan, Mingxian Liu, Rong Fan, Zijie Xu, Hao Zhixian, and Longwu Chen. 2011. "Destabilization of artificial biomembrane induced by the penetration of tryptophan." *Applied Surface Science* 257: 5070-5076. doi:10.1016/j.apsusc.2011.01.023.

Chen, Tani, Alex Fowler, and Mehmet Toner. 2000. "Literature review: supplemented phase diagram of the trehalose-water binary mixture." *Cryobiology* 40 (3): 277-282.

Coler, Rhea N., Sylvie Bertholet, Magdalini Moutaftsi, Jeff A. Guderian, Hillarie Plessner Windish, Susan L. Baldwin, Elsa M. Laughlin, et al. 2011. "Development and characterization of synthetic glucopyranosyl lipid adjuvant system as a vaccine adjuvant." *Public Library of Science One* 6 (1): e16333. doi:10.1371/journal.pone.0016333.

Coler, Rhea N., Tracey A. Day, Ruth Ellis, Franco M. Piazza, Anna Marie Beckmann, Julie Vergara, Tom Rolf, et al. 2018. "The TLR-4 agonist adjuvant, GLA-SE, improves magnitude and quality of immune responses elicited by the ID93 tuberculosis vaccine: first-in-human trial." *Nature Partner Journals* 3 (34). doi:10.1038/s41541-018-0057-5.

Cosnier, Frederic, Sebastien Bau, Stephane Grossmann, Herve Nunge, Celine Brochard, Stephane Viton, Raphael Payet, Olivier Witschger, and Laurent Gate. 2016. "Design and characterization of an inhalation system to expose rodents to nanoaerosols." *Aerosol and Air Quality Research* 16 (12): 2989-3000.

Crowe, John H., Folkert A. Hoekstra, and Lois M. Crowe. 1989. "Membrane phase transitions are responsible for imbibitional damage in dry pollen." *Proceedings of the National Academy of Sciences* 2 (520-523): 86.

Crowe, John H., John F. Carpenter, and Lois M. Crowe. 1998. "The role of vitrification in anhydrobiosis." *Annual Review of Physiology* 60 (1): 73-103.

Crowe, Lois M., David S. Reid, and John H. Crowe. 1996. "Is trehalose special for preserving dry biomaterials?" *Biophysical Journal* 71: 2087-2093.

Cryan, Sally-Ann, Neeraj Sivadas, and Lucila Garcia-Contreras. 2007. "In vivo animal models for drug delivery across the lung mucosal barrier." *Advanced Drug Delivery Reviews* 59 (11): 1133-1151.

Darquenne, Chantal. 2012. "Aerosol deposition in health and disease." *Journal of Aerosol Medicine and Pulmonary Drug Delivery* 25 (3): 140-147. doi:10.1089/jamp.2011.0916.

de Boer, A. H., P. Hagedoorn, M. Hoppentocht, F. Buttini, F. Grasmeijer, and H. W. Frijlink. 2017. "Dry powder inhalation: past, present and future." *Expert Opinion on Drug Delivery* 14 (4): 499-512. doi:10.1080/17425247.2016.1224846.

Derrick, Steven C., Kristopher Kolibab, Amy Yang, and Sheldon L. Morris. 2014. "Intranasal administration of Mycobacterium bovis BCG induces superior protection against aerosol infection with Mycobacterium tuberculosis in mice." *Clinical and Vaccine Immunology* 21 (10): 1443-1451.

Dumont, Etienne F., Amanda J. Oliver, Chris Ioannou, Julia Billiard, Jeremy Dennison, Frans van den Berg, Shuying Yang, et al. 2020. "A novel inhaled dry-powder formulation of ribavirin allows for efficient lung delivery in healthy participants and those with chronic obstructive pulmonary disease in a Phase 1 study." *Antimicrobial Agents and Chemotherapy* 64 (5): 1-15.

Ekdawi-Sever, Nancy, and Juan J. de Pablo. 2003. "Diffusion of sucross and a,a-trehalose in aqueous solutions." *Journal of Physical Chemistry A* 107: 936-943. doi:10.1021/jp020187b.

Encina, Cristian, Cristina Vergara, Begona Gimenez, Felipe Oyarzun-Ampuero, and Paz Robert. 2016. "Conventional spray-drying and future trends for the microencapsulation of fish oil." *Trends in Food Science & Technology* 56: 46-60.

Encina, Cristian, Gloria Marquez-Ruiz, Francisca Holgado, Begona Gimenez, Cristina] Vergara, and Paz Robert. 2018. "Effect of spray-drying with organic solvents on the encapsulation, release and stability of fish oil." *Food Chemistry* 263: 283-291. doi:https://doi.org/10.1016/j.foodchem.2018.05.026.

Erickson, Harold P. 2009. "Size and shape of protein molecules at the nanometer level determined by sedimentation, gel filtration, and electron microscopy." *Biological Procedures Online* 11: 32-51. doi:10.1007/s12575-009-9008-x.

Eze, Michael O. 1991. "Phase transitions in phospholipid bilayers: Lateral phase separations play vital roles in biomembranes." *Biochemical Education* 19 (4): 204-208. doi:10.1016/0307-4412(91)90103-F.

Fabio, Karine, Joseph J. Guarneri, Kieran Curley, Marshall L. Grant, and Andrea Leone-Bay. 2018. Heat-stable dry powder pharmaceutical compositions and methods. United States of America Patent 9,925,144 B2. March 27.

Feng, A. L., M. A. Boraey, M. A. Gwin, P. R. Finlay, P. J. Kuehl, and R. Vehring. 2011. "Mechanistic models facilitate efficient development of leucine containing microparticles for pulmonary drug delivery." *International Journal of Pharmaceutics* 409: 156-163.

Filtration and Particle Science. n.d. *Palas RBG 1000 schematic.* Filtration and Particle Science. Accessed 8 June, 2020. https://filterintegrity.com/products/rbg-1000/.

Finlay, Warren H. 2019. *The Mechanics of Inhaled Pharmaceutical Aerosols: An Introduction.* 2nd. Academic Press. doi:10.1016/C2018-0-00116-4.

Flynn, JoAnne L., and John Chan. 2001. "Immunology of Tuberculosis." *Annual Review of Immunology* 19 (1): 93-129.

Flynn, Joanne L., J. Chan, and P. L. Llin. 2011. "Macrophages and control of granulomatous inflammation in tuberculosis." *Mucosal Immunology* 4 (3): 271-278. doi:10.1038/mi.2011.14.

Fox, Christopher B., Ryan C. Anderson, Timothy S. Dutill, Yasuyuki Goto, Steven G. Reed, and Thomas S. Vedvick. 2008. "Monitoring the effects of component structure and source on formulation stability and adjuvant activity of oil-in-water emulsions." *Colloids and Surfaces B; Biointerfaces* 65: 98-105.

Geller, David E. 2005. "Comparing clinical features of the nebulizer, metered-dose inhaler, and dry powder inhaler." *Respiratory Care* 50 (10): 1313-1321.

Gharsallaoui, Adem, Gaelle Roudaut, Odile Chambin, Andree Voilley, and Remi Saurel. 2007. "Applications of spray-drying in microencapsulation of food ingedients: An overview." *Food Research International* 2007: 1107-1121.

Glinksi, Jacek, Guy Chavepeyer, and Jean-Karl Platten. 2000. "Surface properties of aqueous solutions of l-leucine." *Biophysical Chemistry* 84 (2): 99-103. 10.1016/S0301-4622(99)00150-7.

Gordon, Manfred, and James S. Taylor. 1952. "Ideal copolymers and the second-order transitions of synthetic rubbers. i. non-crystalline copolymers." *Journal of Applied Chemistry* 2 (9): 493-500.

Grasmeijer, N., M. Stankovic, H. de Waard, H. W. Frijlink, and W. L. J. Hinrichs. 2013. "Unraveling protein stabilization mechanisms: vitrification and water replacement in a glass transition temperature controlled system." *Biochimica et Biophysica Acta* 1834 (4): 763-769. doi:10.1016/j.bbapap.2013.01.020.

Grasmeijer, Niels, Henderik W. Frijlink, and Wouter L. J. Hinrichs. 2016. "Model to predict inhomogeneous protein-sugar distribution in powders prepared by spray drying." *Journal of Aerosol Science* 101: 22-33. doi:10.1016/j.jaerosci.2016.07.012.

Grasmeijer, Niels, Valeria Tiraboschi, Herman J. Woerdenbag, Henderik W. Frijlink, and Wouter L. J. Hinrichs. 2019. "Identifying critical process steps to protein stability during spray drying using a vibrating mesh or a two-fluid nozzle." *European Journal of Pharmaceutical Sciences* 128: 152-157.

Grgic, Biljana, Warren H. Finlay, and Anthony Heenan. 2004. "Regional aerosol deposition and flow measurements in an idealized mouth and throat." *Journal of Aerosol Science* 35: 21-32.

Hesseling, A. C., L. F. Johnson, H. Jaspan, M. F. Cotton, A. Whitelaw, H. S. Schaaf, P. E. M. Fine, et al. 2009. "Disseminated bacille Calmette-Guerin disease in HIV-infected South African infants." *Bulletin of the World Health Organization* 87: 505-511. doi:doi:10.2471/BLT.08.055657.

Hickey, A. J., P. G. Durham, A. Dharmadhikari, and E. A. Nardell. 2016. "Inhaled drug treatment for tuberculosis: Past progress and future prospects." *Journal of Controlled Release* 240: 127-134.

Hoe, Susan, James W. Ivey, Mohammed A. Boraey, Abouzar Shamsaddini-Shahrbabak, Emadeddin Javaheri, Matinkhoo Sadaf, Warren H. Finlay, and Reinhard Vehring. 2014. "Use of a fundamental approach to spray-drying formulation design to facilitate the development of multi-component dry powder aerosols for respiratory drug delivery." *Pharmaceutical Research* 32 (2): 449-465.

Iglesias, Hector A., Jorge Chirife, and Maria P. Buera. 1999. "Adsorption isotherm of amorphous trehalose." *Journal of the Science of Food and Agriculture* 75 (2): 183-186.

Infectious Disease Research Institute. 2019. "Identifier: NCT03722472, Phase 1 Clinical Trial of Single-Vial ID93 + GLA-SE in Healthy Adults." *U.S. National Library of Medicine Clinical Trials Registry.* September 3. Accessed April 23, 2020. https://clinicaltrials.gov/ct2/show/NCT03722472?term=id93&draw=2&rank=1.

Ingvarsson, Pall Thor, Mingshi Yang, Hanne Morck Nielsen, Jukka Rantanen, and Camilla Foged. 2011. "Stabilization of liposomes during spray drying." *Expert Opinion on Drug Delivery* 8 (3): 375-388. doi:10.1517/17425247.2011.553219.

Ingvarsson, Pall Thor, Signe Tandrup Schmidt, Dennis Christensen, Niels Bent Larsen, Wouter Leonardus Joseph Hindrichs, Peter Andersen, Jukka Rantanen, Hanne Morck Nielson, Mingshi Yang, and Camilla Foged. 2013. "Designing CAF-adjuvanted dry powder vaccines: Spray drying preserves

the adjuvant activity of CAF01." *Journal of Controlled Release* 167: 256-264. doi:10.1016/j.jconrel.2013.01.031.

International Conference On Harmonisation Of Technical Requirements For Registration Of Pharmaceuticals For Human Use. 2003. *ICH Harmonised Tripartite Guideline - Stability Testing of New Drug Substances and Products Q1A(R2).* ICH.

Ivey, James W., and Reinhard Vehring. 2010. "The use of modeling in spray drying of emulsions and suspensions accelerates formulation and process development." *Computers and Chemical Engineering* 34: 1036-1040. doi:10.1016/j.compchemeng.2010.02.031.

Ivey, James, Pallavi Bhambri, David Lewis, Tayna Church, Warren Finlay, and Reinhard Vehring. 2016. "Dried corticosteroid particle formation from evaporating monodisperse propellant solution droplets." *AAPS Annual Meeting and Exposition.* Denver.

Jafari, Seid Mahdi, Elham Assadpoor, Yinghe He, and Bhesh Bhandari. 2008. "Encapsulation efficiency of food flavours and oils during spray drying." *Drying Technology* 26 (7): 816-835.

Jahanshahi-Anbuhi, Sana, Balamurali Kannan, Vincent Leung, Kevin Pennings, Meng Liu, Carmen Carrasquilla, Dawn White, et al. 2016. "Simple and ultrastable all-inclusive pullulan tablets for challenging bioassays." *Chemical Science* 7: 2342-2346. doi:10.1039/c5sc04184h.

Jin, Tom H., Eric Tsao, Jaap Goudsmit, Veerabadran Dheenadhayalan, and Jerald Sadoff. 2010. "Stabilizing formulations for inhalable powders of adenovirus 35-vectored tuberculosis (TB) vaccine (AERAS-402)." *Vaccine* 28: 4639-4375. doi:10.1016/j.vaccine.2010.04.059.

Jones, Jim R., Dominic Prime, Mark C. Leaper, David J. Richardson, Chris D. Rielly, and Andrew G. F. Stapley. 2013. "Effect of processing variables and bulk composition on the surface composition of spray dried powders of a model food system." *Journal of Food Engineering* 118: 19-30.

Jones, R. Mark, Michael Burke, Devon Dubose, Jessica A. Chichester, Slobodanka Manceva, April Horsey, Stephen J. Streatfield, Jeff Breit, and Vidadi Yusibov. 2017. "Stability and pre-formulation development of a plant-produced anthrax vaccine candidate." *Vaccine* 35: 5463-5470. doi:10.1016/j.vaccine.2016.12.009.

Kanojia, Gaurav, Geert-Jan Willems, Henderik W. Frijlink, Gideon F. A. Kersten, Peter C. Soema, and Jean-Pierre Amorij. 2016. "A design of experiment approach to predict product and process parameters for a spray-dried influenza vaccine." *International Journal of Pharmaceutics* 511: 198-1111. doi:10.1016/j.ijpharm.2016.08.022.

Kanojia, Gaurav, Rene H. M. Raeven, Larissa van der Maas, Tim H. E. Bindels , Elly van Riet, Bernard Metz, Peter C. Soema, et al. 2018. "Development of a thermostable spray dried outer membrane vesicle pertussis vaccine for pulmonary immunization." *Journal of Controlled Release* 286: 167-178. doi:10.1016/j.jconrel.2018.07.035.

Kanojia, Gaurav, Rimko ten Have, Peter C. Soema, Henderik Frijlink, Pierre Amorij, and Gideon Kersten. 2017. "Developments in forumulation and delivery of spray dried vaccines." *Human Vaccines & Immunotherapeutics* 13 (10): 2364-2378. doi:10.1080/21645515.2017.1356952.

Kaur, Jatinder, Pavan Muttil, Rahul Kumar Verma, Kaushlendra Kumar, Awadh Bihari Yadav, Rolee Sharma, and Amit Misra. 2008. "A hand-held apparatus for 'nose-only' exposure of mice to inhalable microparticles as a dry powder inhalation targeting lung and airway macrophages." *European Journal of Pharmaceutical Sciences* 34: 56-65.

Koster, V. S., P. F. M. Kuks, R. Lange, and H. Talsma. 1996. "Particle size in parenteral fat emulsions, what are the true limitations?" *International Journal of Pharmaceutics* 134: 235-238.

Kramer, Ryan M., Michelle C. Archer, Natasha Dubois, Natasha Dubois Cauwelaert, Elyse A. Beebe, Po-wei D. Huang, Quinton M. Dowling, et al. 2018. "Development of a thermostable nanoemulsion adjuvanted vaccine against tuberculosis using a design-of-experiments approach." *International Journal of Nanomedicine* 13: 3689-3711.

Krogsgard Nielsen, Christina, Jorgen Kjems, Tina Mygind, Torben Snabe, Karin Schwarz, Yvonne Serfert, and Rikke Louise Meyer. 2016. "Enhancing the antibacterial efficacy of isoeugenol by emulsion encapsulation." *International Journal of Food Microbiology* 229: 7-14.

Kuehl, Philip J., Tamara L. Anderson, Gabriel Candelaria, Benjamin Gershman, Ky Harlin, Jacob Y. Hesterman, Thomas Holmes, et al. 2012. "Regional particle size dependent deposition of inhaled aerosols in rats and mice." *Inhalation Toxicology* 24 (1): 27-35. doi:10.3109/08958378.2011.632787.

Kunda, Nitesh K., Iman M. Alfagih, Eliane N. Miyaji, Douglas B. Figueiredo, Viviane M. Goncalves, Daniela M. Ferreira, Sarah R. Dennison, Satyanarayana Somavarapu, Gillian A. Hutcheon, and Imran Y. Saleem. 2015. "Pulmonary dry powder vaccine of pneumococcal antigen loaded nanoparticles." *International Journal of Pharmaceutics* 495 (2): 903-912. doi:10.1016/j.ijpharm.2015.09.034.

Lambruschini, Cecilia, Annalisa Relini, Andrea Ridi, Lorenzo Cordone, and Alessandra Gliozzi. 2000. "Trehalose interacts with phospholipid polar heads in Langmuir monolayers." *Langmuir* 16: 5467-5470.

Lammert, Amy M., Shelly J. Schmidt, and Gary A. Day. 1998. "Water activity and solubility of trehalose." *Food Chemistry* 61 (1): 139-144.

Langford, Alex, Bakul Bhatnagar, Robert Walters, Serguel Tchessalov, and Satoshi Ohtake. 2018. "Drying technologies for biopharmaceutical applications: Recent developments and future direction." *Drying Technology* 36 (6): 677-687. doi:10.1080/07373937.2017.1355318.

Leathers, T. D. 2003. "Biotechnical production and applications of pullulan." *Applied Microbiology and Biotechnology* 62: 468-473. doi:10.1007/s00253-003-1386-4.

Lechuga-Ballesteros, David, Chatan Charan, Cheryl L.M. Stults, Cynthia L. Stevenson, Danforth P. Miller, Reinhard Vehring, Vathana Tep, and Mei-Chang Kuo. 2008. "Trileucine Improves Aerosol Performance and Stability of Spray-Dried Powders for Inhalation." *Journal of Pharmaceutical Sciences* 97 (1): 287-302. doi:10.1002/jps.21078.

LeClair, Daniel A., Lillian Li, Nausheen Rahman, Emily D. Cranston, Zhou Xing, and Michael R. Thompson. 2019. "Stabilization of HSV-2 viral candidate by spray drying." *International Journal of Pharmaceutics* 569: 1-10. doi:10.1016/j.ijpharm.2019.118615.

Lee, Bruce Y., Brigid E. Cakouros, Tina-Marie Assi, Diana L. Connor, Joel Welling, Souleymane Kone, Ali Djibo, Angela R. Wateska, Lionel Pierre, and Shawn T. Brown. 2012. "The impact of making vaccines thermostable in Niger's vaccine supply chain." *Vaccine* 30 (38): 5637-5643. doi:10.1016/j.vaccine.2012.06.087.

Lee, Bruce Y., Patrick T. Wedlock, Leila A. Haidari, Kate Elder, Julien Potet, Rachel Manring, Diana L. Connor, et al. 2017. "Economic impact of thermostable vaccines." *Vaccine* 35: 3135-3142.

Leung, Sharon S. Y., Thaigarajan Parmasivam, An Nguyen, Thomas Gengenbach, Elizabeth A. Carter, Nicholas B. Carrigy, Hui Wang, et al. 2018. "Effect of storage temperature on the stability of spray dried bacteriophage powders." *European Journal of Pharmaceutics and Biopharmaceutics* 127: 213-222.

Leung, Vincent, Jonathan Mapletoft, Ali Zhang, Amanda Lee, Fatemeh Vahedi, Marianne Chew, Alexandra Szewczyk, et al. 2019. "Thermal stabilization of viral vaccines in low-cost sugar films." *Scientific Reports* 9 (7631).

Li , Q., V. Rudolph, and W. Peukert. 2006. "London-van der Waals adhesiveness of rough particles." *Powder Technology* 161: 248-255.

Li, Lang, Siping Sun, Thaigarajan Parumasivam, John A. Denman, Thomas Gengenbach, Patricia Tang, Shirui Mao, and Hak-Kim Chan. 2016. "L-Leucine as an excipient against moisture on in vitro aerosolization performances of highly hygroscopic spray-dried powders." *European Journal of Pharmaceutics and Biopharmaceutics* 102: 132-141. doi:10.1016/j.ejpb.2016.02.010.

Linke, Annika, Tobias Balke, and Reinhard Kohlus. 2018. "Identification of key factors determining the surface oil concentration of encapsulated lipid particles produced by spray drying." *21st International Drying Symposium.* Valencia, Spain. doi:http://dx.doi.org/10.4995/ids2018.2018.7739.

Lovalenti, Phillip M., Jeff Anderl, Luisa Yee, Van Nguyen, Behnaz Ghavami, Satoshi Ohtake, Atul Saxena, Thomas Voss, and Vu Truong-Le. 2016. "Stabilization of live attenuated influenza vaccines by freeze drying, spray drying, and foam drying." *Pharmaceutical Researach* 33: 1144-1160. doi:10.1007/s11095-016-1860-1.

Marple, Virgil A., Daryl L. Roberts, Francisco J. Romay, Nicholas C. Miller, Keith G. Truman, Michiel Van Oort, Bo Olsson, Michael J. Holroyd, Jolyon P. Mitchell, and Dieter Hochrainer. 2003. "Next Generation Pharmaceutical Impactor (A New Impactor for Pharmaceutical Inhaler Testing) Part 1: Design." *Journal of Aerosol Medicine* 16 (3): 283-299.

McAdams, David, Dexiang Chen, and Debra Kristensen. 2012. "Spray drying and vaccine stabilization." *Expert Review of Vaccines* 11 (10): 1211-1219. doi:10.1586/erv.12.101.

Mensink, Maarten A., Henderik W. Frijlink, Kees van der Voort Maarschalk, and Wouter L. J. Hinrichs. 2017. "How sugars protect proteins in the solid state and during drying (review): Mechanisms of

stabilization in relation to stress conditions." *European Journal of Pharmaceutics and Biopharmaceutics* 114: 288-295.

Mlalila, Nichrous, Hulda Swai, Lonji Kalombo, and Askwar Hilonga. 2014. "Effects of spray-drying on w/o/w multiple emulsions prepared from a stearic acid matrix." *Nanotechnology, Science and Applications* 7: 105-112. doi:10.2147/NSA.S72083.

Munoz-Ibanez, Marta, Christiane Azagoh, Bipro Nath Dubey, Elisabeth Dumoulin, and Christelle Turchiuli. 2015. "Changes in oil-in-water emulsion size distribution during the atomization step in spray-drying encapsulation." *Journal of Food Engineering* 167: 122-132.

Murugappan, Senthil, Harshad P. Patil, Gaurav Kanojia, Wouter ter Veer, Tjarko Meijerhof, Henderik W. Frijlink, Anke Huckriede, and Wouter L. J. Hinrichs. 2013. "Physical and immunogenic stability of spray freeze-dried influenza vaccine powder for pulmonary delivery: Comparison of inulin, dextran, or a mixture of dextran and trehalose as protectants." *European Journal of Pharmacetuics and Biopharmaceutics* 85: 716-725.

Nadithe, Venkatareddy, Muhib Rahamatalla, Warren H. Finlay, John R. Mercer, and John Samuel. 2003. "Evaluation of nose-only aerosol inhalation chamber and comparison of experimental results with mathematical simulation of aerosol deposition in mouse lungs." *Journal of Pharmaceutical Sciences* 92 (5): 1066-1076.

Nakagaki, Masayuki, and Emiko Okamura. 1982. "Penetration leucine and norleucine into lecithin monolayers from underlying aqueous solutions." *Bulletin of the Chemical Society of Japan* 55 (11): 3381-3385. doi:10.1246/bcsj.55.3381.

Ohtake, Satoshi, and John Wang. 2011. "Trehalose: current use and future applications." *Journal of Pharmaceutical Sciences* 100 (6): 2020-2053.

Ohtake, Satoshi, Russell A. Martin, Atul Saxena, David Lechuga-Ballesteros, Araceli E. Santiago, Eileen M. Barry, and Vu Truong-Le. 2011. "Formulation and stabilization of Francisella tularensis live vaccine strain." *Journal of Pharmaceutical Sciences* 100 (8): 3076-3087. doi:10.1002/jps.22563.

Orr, Mark T., Christopher B. Fox, Susan L. Baldwin, Sandra J. Sivananthan, Elyse Lucas, Susan Lin, Tony Phan, et al. 2013. "Adjuvant formulation structure and composition are critical for the development of an effective vaccine against tuberculosis." *Journal of Controlled Release* 172: 190-200.

Orr, Mark T., Ryan M. Kramer, Lucien V. Barnes, Quinton M. Dowling, Anthony L. Desbien, Elyse A. Beebe, John D. Laurance, et al. 2014. "Elimination of the cold-chain dependence of a nanoemulsion adjuvant vaccine against tuberculois by lyophilization." *Journal of Controlled Release* 10 (177): 20-26. doi:10.1016/j.jconrel.2013.12.025.

Pang, Yuqi, Xu Duan, Guangyue Ren, and Wenchao Liu. 2017. "Comparative study on different drying methods of fish oil microcapsules." *Journal of Food Quality* 1-7. doi:10.1155/2017/1612708.

Paramita, V., K. Iida, H. Yoshii, and T. Furuta. 2010. "Effect of additives on the morphoolgy of spray-dried powder." *Drying Technology* 28 (3): 323-329. doi:10.1080/07373931003627098.

Pavkov, Richard, Stefan Mueller, Katrin Fiebich, Dilraj Singh, Frank Stowasser, Giovanni Pignatelli, Benoit Walter, et al. 2010. "Characteristics of a capsule based dry powder inhaler for the delivery of indacterol." *Current Medial Research and Opinion* 26 (11): 2527-2533.

Penn-Nicholson, Adam, Michele Tameris, Erica Smit, Tracey A. Day, Munyaradzi Musvosvi, Lakshmi Jayashankar, Julie Vergara, et al. 2018. "Safety and immunogenicity of the novel tuberculosis vaccine ID93 + GLA-SE in BCG-vaccinated healthy adults in South Africa: a randomised, double-blind, placebo-controlled phase 1 trial." *The Lancet Respiratory Medicine* 6 (4): 287-298. doi:10.1016/S2213-2600(18)30077-8.

Pereira, Cristina S., and Philippe H. Hunenberger. 2006. "Interaction of the sugars trehalose, maltose and glucose with a phospholipid bilayer: a comparative molecular dynamics study." *The Journal of Physical Chemistry* 110 (31): 15572-15581. doi:10.1021/jp060789l.

Phillips, Jonathan E., Xuxia Zhang, and James A. Johnston. 2017. "Dry powder and nebulized aerosol inhalation of pharmaceuticals delivered to mice using a nose-only exposure system." *Journal of Visualized Experiments* (122): 1-10.

Price, Dominique N., Nitesh K. Kunda, Rajaun Ellis, and Pavan Muttil. 2020. "Design and optimization of a temperature-stable dry powder BCG vaccine." *Pharmaceutical Research* 37 (11): 1-14. doi:10.1007/s11095-019-2739-8.

Raeven, R. H. M., J. Brummelman, J. L. A. Pennings, L. van der Maas, K. Helm, W. Tilstra, A. van der Ark, et al. 2018. "Molecular and cellular signatures underlying superior immunity against Bordetella pertussis upon pulmonary vaccination." *Mucosal Immunology* 11 (3): 979-993. doi:10.1038/mi.2017.81.

Raula, Janne, Frank Thielmann, Majid Naderi, Vessa-Pekka Lehto, and Esko I. Kauppinen. 2010. "Investigations on particle surface characteristics vs. dispersion behaviour of L-leucine coated carrier-free inhalable powders." *International Journal of Pharmaceutics* 385: 79-85.

Re, Maria-Ines. 2006. "Formulating Drug Delivery Systems by Spray Drying." *Drying Technology* 24: 433-446.

Reed, Steven G., Sylvie Bertholet, Rhea N. Coler, and Martin Friede. 2009. "New horizons in adjuvants for vaccine development." *Trends in Immunology* 30 (1): 23-32. doi:10.1016/j.it.2008.09.006.

Ribeiro, Roseane Fagundes, Mariana Heldt Motta, Andreia Pisching Garcia Harter, Fernanda Cramer Flores, Ruy Carlos Ruver Beck, Scheila Rezende Schaffazick, and Cristiane de Bona da Silva. 2016. "Spray-dried powders improve the controlled relase of antifungal tioconazole-loaded polymeric nanocapsules compared to with lyophilized products." *Materials Science and Engineering C* 59: 875-884.

Richards, A. B., S. Krakowka, L. B. Dexter, H. Schmid, A. P. M. Wolterbeek, D. H. Waalkens-Berendsen, A. Shigoyuki, and M. Kurimoto. 2002. "Trehalose: a review of properties, history of use and human tolerance, and results of multiple safety studies." *Food and Chemical Toxicology* 40: 871-898.

Roberts, Christopher J. 2006. "Nonnative Protein Aggregation." In *Misbehaving Proteins*, 17-46. New York: Springer. doi:10.1007/978-0-387-36063-8_2.

Roe, K. D., and T. P. Labuza. 2005. "Glass transition and crystallization of amorphous trehalose-sucrose mixtures." *International Journal of Food Properties* 8 (3): 559-574.

Sangon Biotech. 2018. "Safety Data Sheets: Pullulan." February 6. Accessed April 5, 2020. https://www.sangon.com/productImage/SDS/A506209/A506209_EN_S.pdf.

Sarkar, Anwesha, Judith Arfsten, Pierre-Alain Golay, Simone Acquistapace, and Emmanuel Heinrich. 2016. "Microstructure and long-term stability of spray dried emulsions with ultra-high oil content." *Food Hydrocolloids* 52: 857-867.

Schwartz, Alicia M., Michelle Y. Chan, Dawn M. Fedor, and Sandra J. Sivananthan. 2017. "Staining and transfer techniques for SDS-PAGE Gels to minimize oil-in-water emulsion adjuvant interference." In *Vaccine Adjuvants. Methods in Molecular Biology, vol 1494*, 273-283. New York: Humana Press. doi:10.1007/978-1-4939-6445-1_20.

Schwartzbach, Henrik. 2011. "Achieving aseptic drying with spray drying technologies." *Pharmaceutical Technology Europe* 23 (9).

Shang, Yidan, Jingliang Dong, Kiao Inthavong, and Jiyuan Tu. 2015. "Comparative numerical modeling of inhaled micron-sized particle deposition in human and rate nasal cavities." *Inhalation Toxicology* 27 (13): 694-705.

Shetty, Nivedita, David Cipolla, Heejun Park, and Qi T. Zhou. 2020. "Physical stability of dry powder inhaler formulations." *Expert Opinion on Drug Delivery* 17 (1): 77-96. doi:10.1080/17425247.2020.1702643.

Shetty, Nivedita, Lingfei Zeng, Sharad Mangal, Haichen Nie, Matthew R. Rowles, Rui Guo, Youngwoo Han, Joon Hyeong Park, and Qi T. Zhou. 2018. "Effects of moisture-induced crystallization on the aerosol performance of spray dried amorphous Ciprofloxacin powder formulations." *Pharmaceutical Research* 35 (7): 1-13. doi:10.1007/s11095-017-2281-5.

Sibum, Imco, Paul Hagedoorn, Markus P. G. Kluitman, Martijn Kloezen, Henderik W. Frijlink, and Floris Grasmeijer. 2020. "Dispersity and storage stability optimization of high dose isoniazid dry powder inhalation formulations with L-leucine or trileucine." *Pharmaceutics* 12 (24): 1-14. doi:10.3390/pharmaceutics12010024.

Sigma-Aldrich. 2020. "Safety Data Sheet: L-Leucine." January 15. Accessed April 5, 2020. https://www.sigmaaldrich.com/catalog/product/sigma/l8000?lang=en&region=US.

Sou, Tomas, David A. V. Morton, Mark Williamson, Els N. Meeusen, Lisa M. Kaminskas, and Michelle P. McIntosh. 2015. "Spray-dried influenza antigen with trehalose and leucine produces an aerosolizable powder vaccine formulation that induces strong systemic and mucosal immunity after pulmonary administration." *Journal of Aerosol Medicine and Pulmonary Drug Delivery* 28 (5): 361-371. doi:10.1089/jamp.2014.1176.

Stewart, Ian E., Pradeep B. Lukka, Jiuyu Liu, Bernd Meibohm, Mercedes Gonzalez-Juarrero, Miriam S. Braunstein, Richard E. Lee, and Anthony J. Hickey. 2019. "Development and characterization of a dry powder formulation for anti-tuberculosis drug spectinamide 1599." *Pharmaceutical Research* 36 (136): 1-13. doi:10.1007/s11095-019-2666-8.

Teekamp, Naomi, Yu Tian, Carolina Visser, Peter Olinga, Henderik W. Frijlink, Herman J. Woerdenbag, and Wouter L. J. Hinrichs. 2017. "Addition of pullulan to trehalose glasses improves the stability of beta-galactosidase at high moisture conditions." *Carbohydrate Polymers* 176: 374-380.

Tepper, Jeffrey S., Philip J. Kuehl, Stuart Cracknell, Kristen J. Nikula, Luqi Pei, and James D. Blanchard. 2016. "Symposium Summary: "Breathe In, Breathe Out, Its [sic] Easy: What You Need to Know about Developing Inhaled Drugs"." *International Journal of Toxicology* 35 (4): 376-392.

Thakur, Aneesh, Pall Thor Ingvarsson, Signe Tandrup Schmidt, Fabrice Rose, Peter Andersen, Dennis Christensen, and Camilla Foged. 2018. "Immnological and physical evaluation of the multistage tuberculosis subunit vaccine candidate H56/CAF01 formulated as a spray dried powder." *Vaccine* 36: 3331-3339. doi:10.1016/j.vaccine.2018.04.055.

Toniolo, Steven P., Sam Afkhami, Ahmad Mahmood, Cecile Fradin, Brian D. Lichty, Matthew S. Miller, Zhou Xing, Emily D. Cranston, and Michael R. Thompson. 2019. "Excipient selection for thermally stable enveloped and non-enveloped viral vaccine platforms in dry powders." *International Journal of Pharmaceutics* 561: 66-73. doi:10.1016/j.ijpharm.2019.02.035.

Tonnis, W. F., M. A. Mensink, A. de Jager, K. van der Voort Maarschalk, H. W. Frijlink, and W. L. Hinrichs. 2015. "Size and molecular flexibility of sugars determine the storage stability of freeze-dried proteins." *Molecular Pharmaceutics* 12: 684-694. doi:10.1021/mp500423z.

United States Pharmacopeia. 2017. "<601> Aerosols, nasal sprays, metered-dose inhalers, and dry powder inhalers."

Usmani, Omar S., Martyn S. Biddiscombe, and Peter J. Barnes. 2005. "Regional lung deposition and bronchodilator response as a function of beta2-agonist particle size." *American Journal of Respiratory and Critical Care Medicine* 172 (12): 1497-1504.

Vandenheuvel, Dieter, Joke Meesus, Rob Lavigne, and Guy Van den Mooter. 2014. "Instability of bacteriophages in spray-dried trehalose powders is caused by crystallization of the matrix." *International Journal of Pharmaceutics* 472: 202-205.

Vehring, Reinhard. 2008. "Pharmaceutical Particle Engineering via Spray Drying." *Pharmaceutical Research* 25 (5): 999-1022. doi:10.1007/s11095-007-9475-1.

Vehring, Reinhard. 2005. "Red-excitation dispersive Raman spectroscopy is a suitable technique for solid-state analysis of respirable pharmaceutical powders." *Applied Spectroscopy* 59 (3): 286-292.

Vehring, Reinhard, Willard R. Foss, and David Lechuga-Ballesteros. 2007. "Particle formation in spray drying." *Aerosol Science* 38: 728-746.

Verreck, Frank A. W., Elma Z. Tchilian, Richard A.W. Vervenne, Claudia C. Sombroek, Ivanela Kondova, Okke A. Eissen, Vinod Sommandas, et al. 2017. "Variable BCG efficacy in rhesus populations: pulmonary BCG provides protection where standard intradermal vaccination fails." *Tuberculosis* 104: 46-57.

Wang, Hui, David Barona, Sulayman Oladepo, Lisa Williams, Susan Hoe, David Lechuga-Ballesteros, and Reinhard Vehring. 2017. "Macro-Raman spectroscopy for bulk composition and homogeneity

analysis of multi-component pharmaceutical powders." *Journal of Pharmaceutical and Biomedical Analysis* 141: 180-191.

Wang, Hui, David S. Nobes, and Reinhard Vehring. 2019. "Particle Surface Roughness Improves Colloidal Stability of Pressured Pharmaceutical Suspensions." *Pharmaceutical Research* 36 (43). doi:https://doi.org/10.1007/s11095-019-2572-0.

Wang, Yang, Liming Che, Nan Fu, Xiao Dong Chen, and Cordelia Selomulya. 2015. "Surface formation phenomena of DHA-containing emulsion during convective droplet drying." *Journal of Food Engineering* 150: 50-61.

Wang, Yang, Wenjie Liu, Xiao Dong Chen, and Cordelia Selomulya. 2019. "Micro-encapsulation and stabilization of DHA containing fish oil in protein-based emulsion through mono-disperse droplet spray dryer." *Journal of Food Engineering* 175: 74-84.

Waterman, Kenneth C., and Bruce C. MacDonald. 2010. "Package selection for moisture protection for solid, oral drug products." *Journal of Pharmaceutical Sciences* 99 (11): 4437-4452. doi:10.1002/jps.22161.

World Health Organization (WHO). 2006. "Temperature sensitivity of vaccines." August. Accessed April 17, 2020. doi:WHO/IVB/06.10.

World Health Organization. 2019. "Global Health Observatory data: Immunization Coverage." December 6. Accessed May 4, 2020. https://www.who.int/en/news-room/fact-sheets/detail/immunization-coverage.

World Health Organization. 2019. *Global Tuberculosis Report.* Geneva: World Health Organization. https://www.who.int/tb/publications/global_report/en/.

World Health Organization. 2005. *Monitoring vaccine wastage at country level: guidelines for programme managers.* Geneva: World Health Organization. https://apps.who.int/iris/handle/10665/68463.

World Health Organization. 2018. *WHO Preferred Product Characteristics for New Tuberculosis Vaccines.* Geneva: World Health Organization.

Yu, Lian. 2016. "Surface mobility of molecular glasses and its importance in physical stability." *Advanced Drug Delivery Reviews* 100: 3-9.

Zhang, Yu, Kyle Gilbertson, and Warren H. Finlay. 2007. "In vivo-in vitro comparison of deposition in three mouth-throat models with Qvar and Turbuhaler inhalers." *Journal of Aerosol Medicine* 20: 227-235. doi:10.1089/jam.2007.0584.

Zhou, Deliang, Geoff G.Z. Zhang, Devalina Law, David J.W. Grant, and Eric A. Schmitt. 2000. "Physical stability of amorphous pharmaceuticals: Importance of configurational thermodynamic quantities and molecular mobility." *Journal of Pharmaceutical Sciences* 91 (8): 1863-1872.

Zhou, Yue, Jajie Sun, and Yung-Sung Cheng. 2011. "Comparison of deposition in the USP and physical mouth-throat models with solid and liquid particles." *Journal of Aerosol Medicine and Pulmonary Drug Delivery* 24 (6): 277-284. doi:10.1089/jamp.2011.0882.

Zhu, Changcheng, Yoko Shoji, Michael Burke, Caitlin E. Hartman, Jessica A. Chichester, Jeff Breit, Vidadi Yusibov, Dexiang Chen, and Manjari Lal. 2014. "Stabilization of HAC1 Influenza Vaccine by Spray Drying." *Pharmaceutical Research* 31: 3006-3018. doi:10.1007/s11095-014-1394-3.

Ziaee, Ahmad, Ahmad B. Albadarin, Luis Padrela, Tim Femmer, Emmet O'Reilly, and Gavin Walker. 2019. "Spray drying of pharmaceuticals and biopharmaceuticals: Critical parameters and experimental process optimization approaches." *European Journal of Pharmaceutical Sciences* 127: 300-318.

Appendix A. Supplementary data from the stability study on the spray-dried vaccine designed for reconstituted injectable delivery

Analysis was completed at multiple timepoints throughout the stability study on the SD-TG and SD-TGI powders, as discussed in Chapter 2. Data relevant to Chapter 2 that was excluded for the sake of brevity are instead given in this appendix.

Initially, an additional temperature storage arm at 50 °C was planned for the stability study. However, near the beginning of the stability study, a temperature excursion occurred on the samples set aside for chemical analysis at 50 °C. The samples set aside for physical stability analysis did not undergo this temperature excursion. Due to this discrepancy, data from the 50 °C arm was excluded from the manuscript as the temperature excursion prevented comparison of the chemical and physical stability. For the sake of completeness, the physical stability data for the SD-TGI powders stored at 50 °C are shown here.

A.1. Particle Morphology

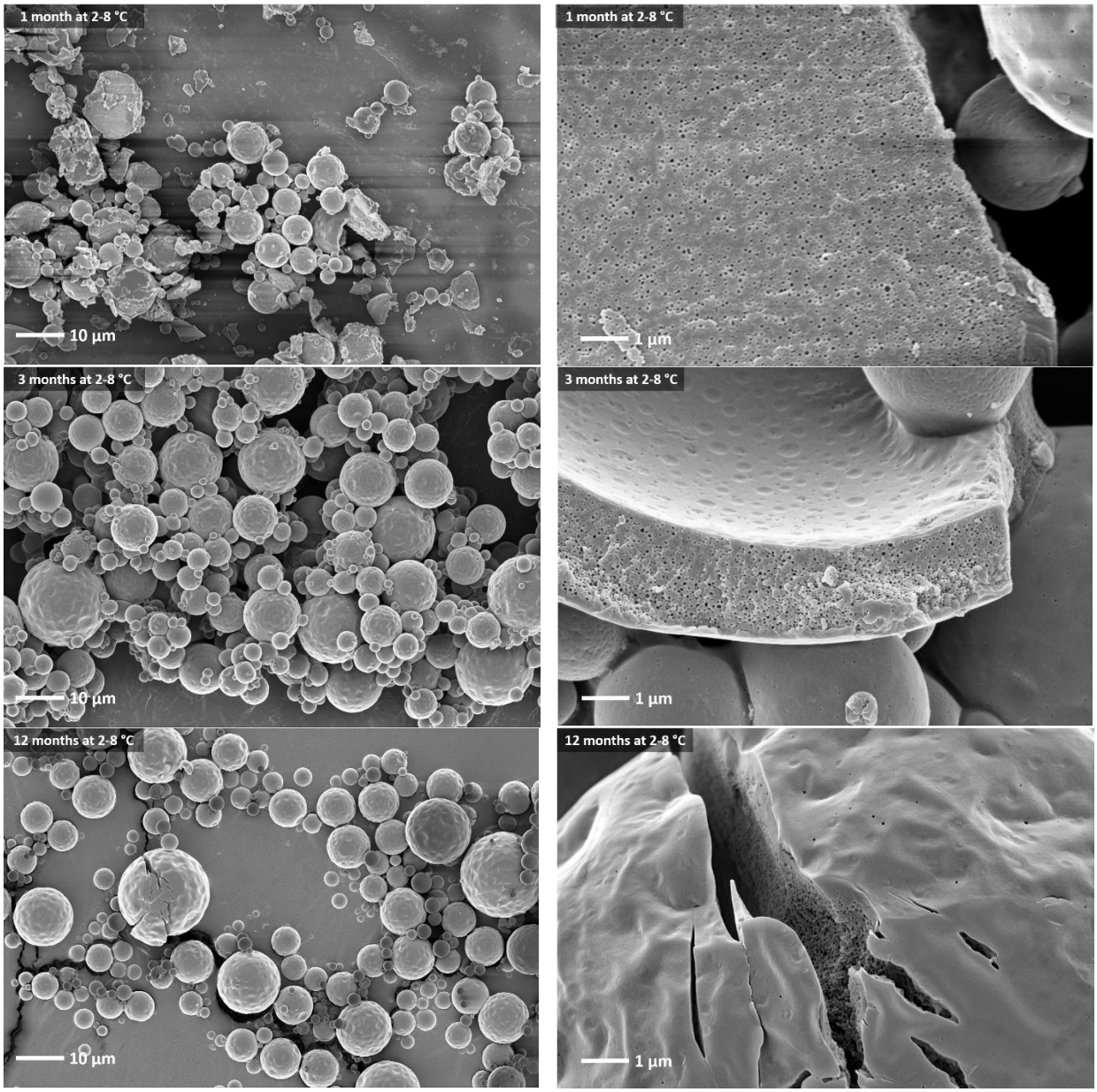

Figure A1 SEM images of exterior (left) and interior (right) particle morphology of the SD-TGI formulation after storage at 2-8 °C for one month, three months, and twelve months. Preservation of the morphology indicates that the formulation does not undergo any significant changes in particle structure when stored at 2-8 °C for up to twelve months.

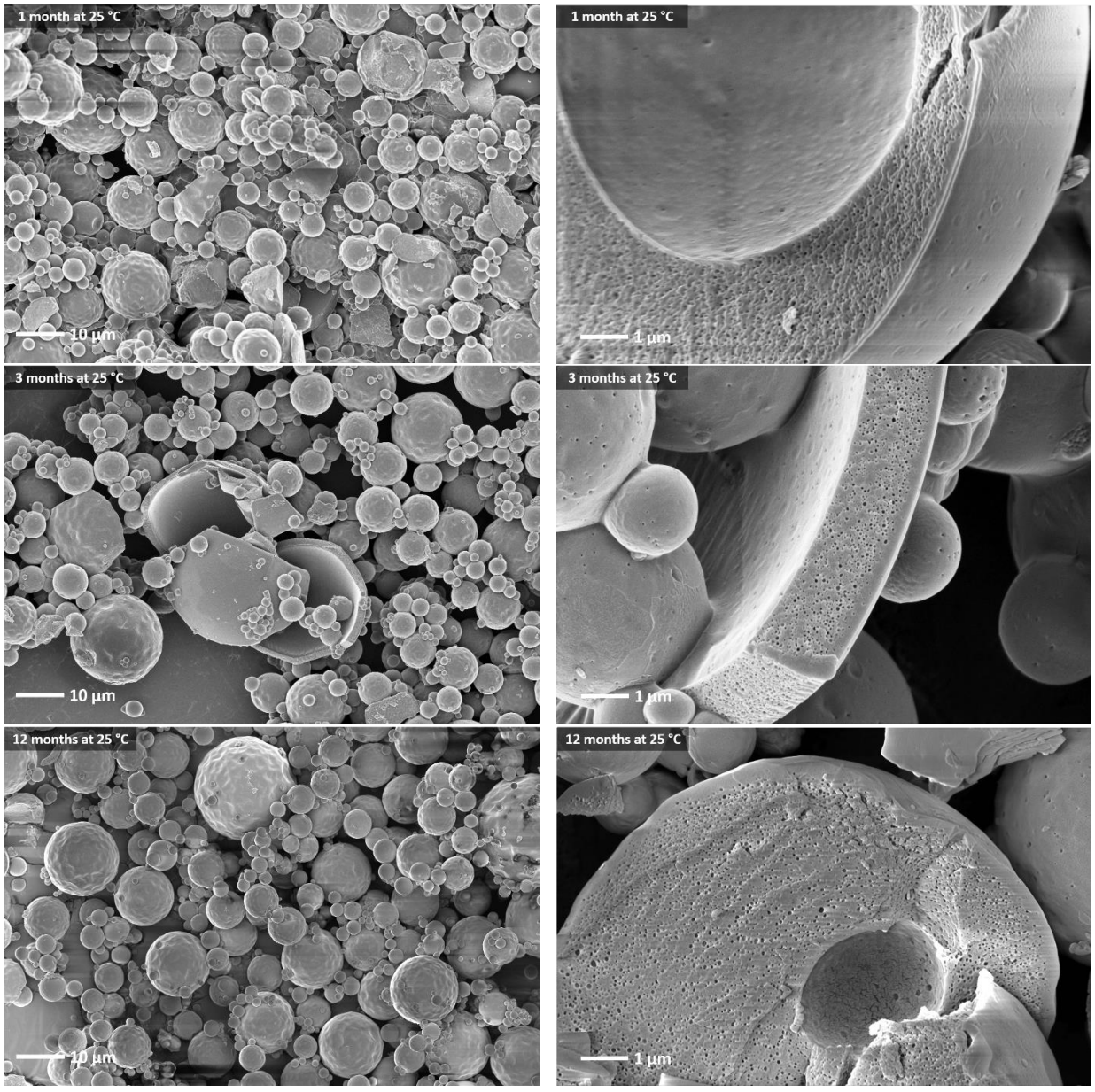

Figure A2 SEM images of exterior (left) and interior (right) particle morphology of the SD-TGI formulation after storage at 25 °C for one month, three months, and twelve months. Preservation of the morphology indicates that the formulation does not undergo any significant changes in particle structure when stored at 25 °C for up to twelve months.

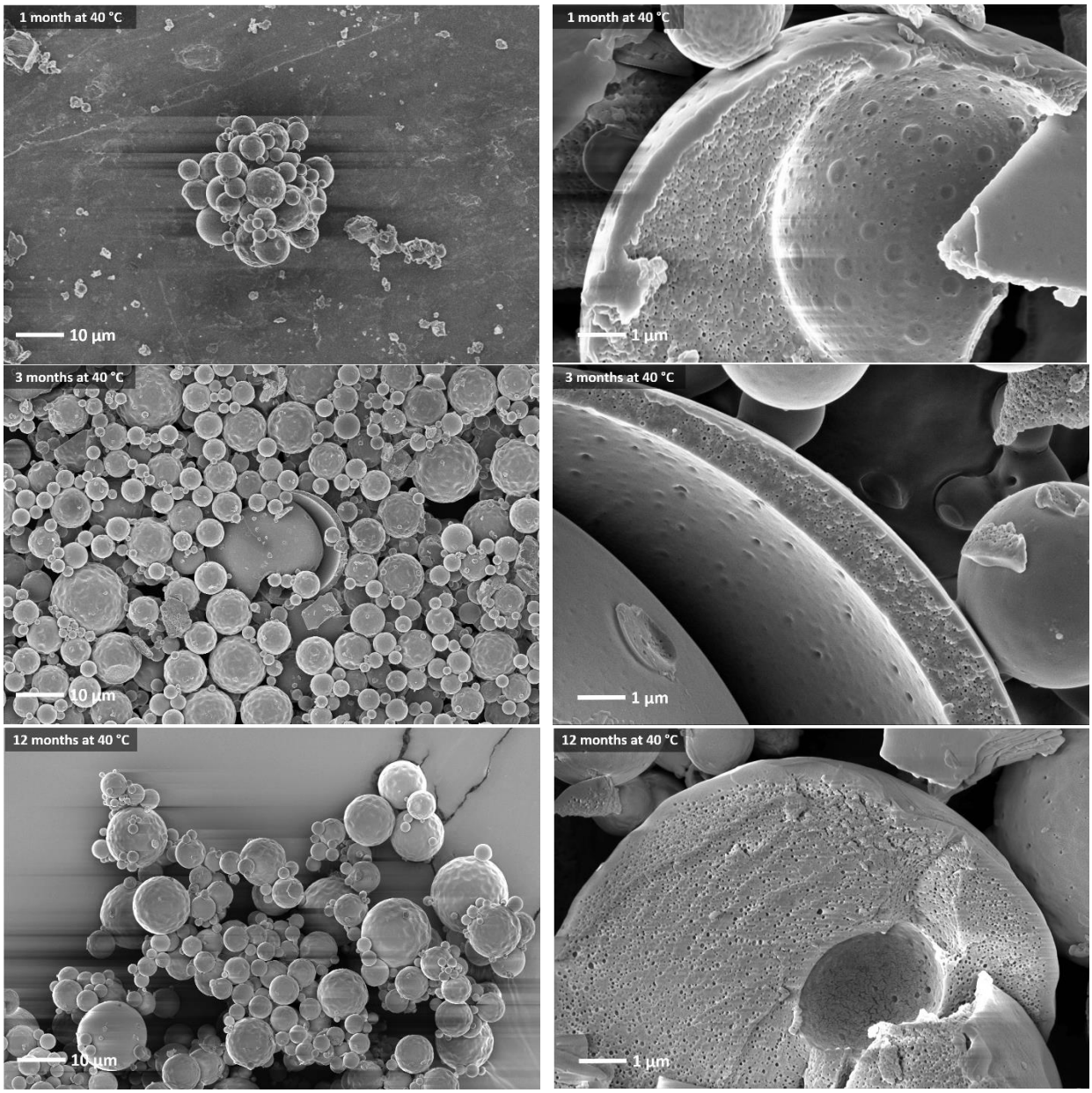

Figure A3 SEM images of exterior (left) and interior (right) particle morphology of the SD-TGI formulation after storage at 40 °C for one month, three months, and twelve months. Comparison of the morphology indicates that the formulation maintains interior particle structure when stored at 40 °C for up to twelve months. Exterior structure is preserved at the three-month timepoint; however, the smaller particles may be affixed to the larger particles after twelve months of storage.

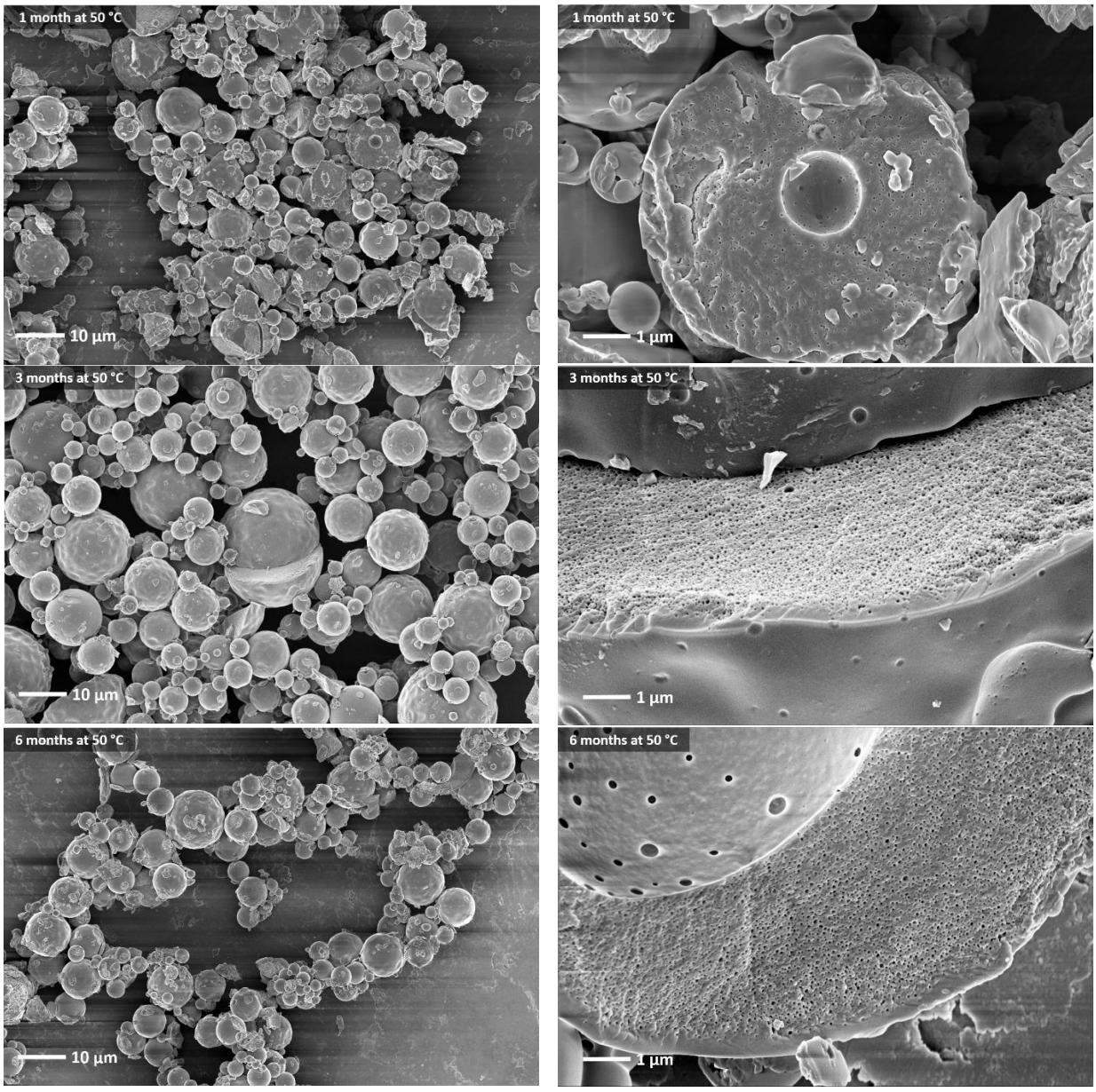

Figure A4 SEM images of exterior (left) and interior (right) particle morphology of the SD-TGI formulation after storage at 50 °C for one month, three months, and six months. Comparison of the morphology indicates that the general particle shape is still maintained after six months of storage. Interior particle structure is also preserved even after six months of storage.

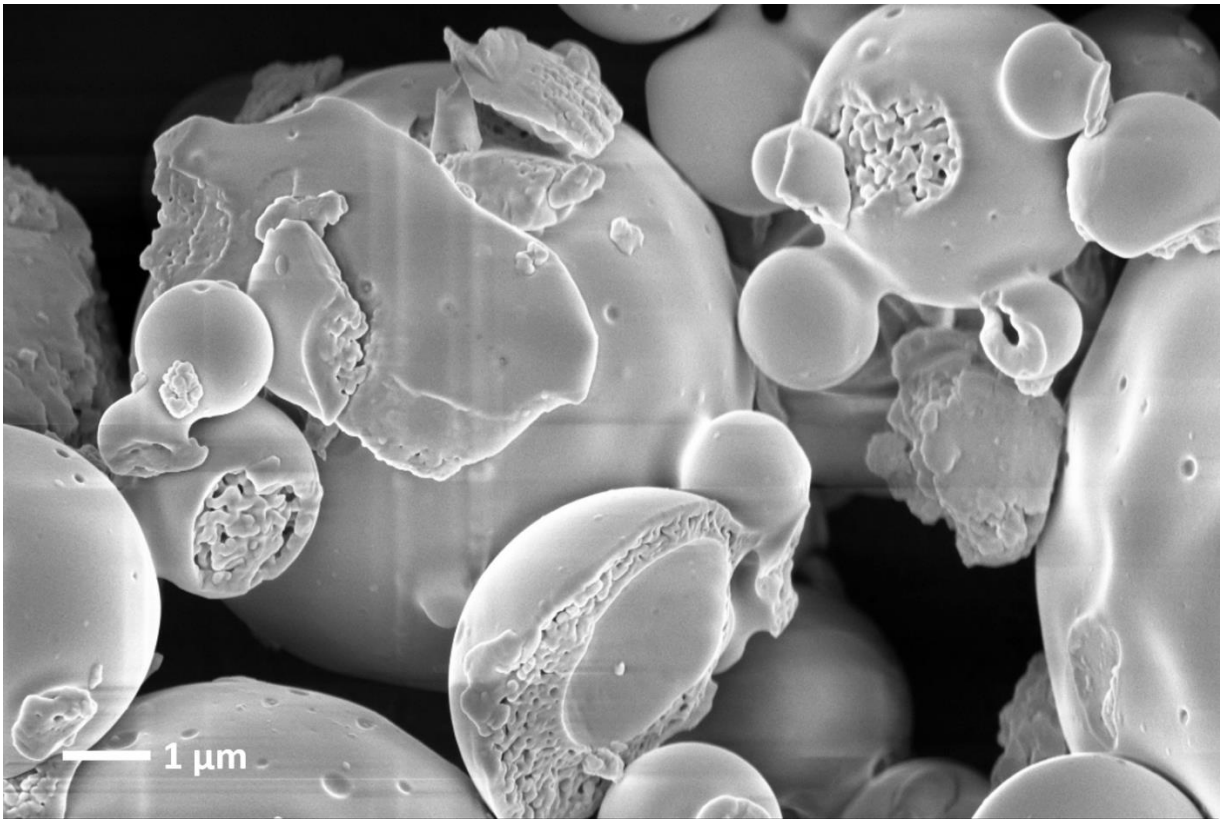

Figure A5 High magnification SEM image of the smaller SD-TGI particles after six months of storage at 50 °C. It is apparent that the smaller particles experience some bridging at this timepoint. This result is expected as the powder formulation and spray drying parameters were designed for stability at storage temperatures 40 °C and below.

A2. Solid State Analysis

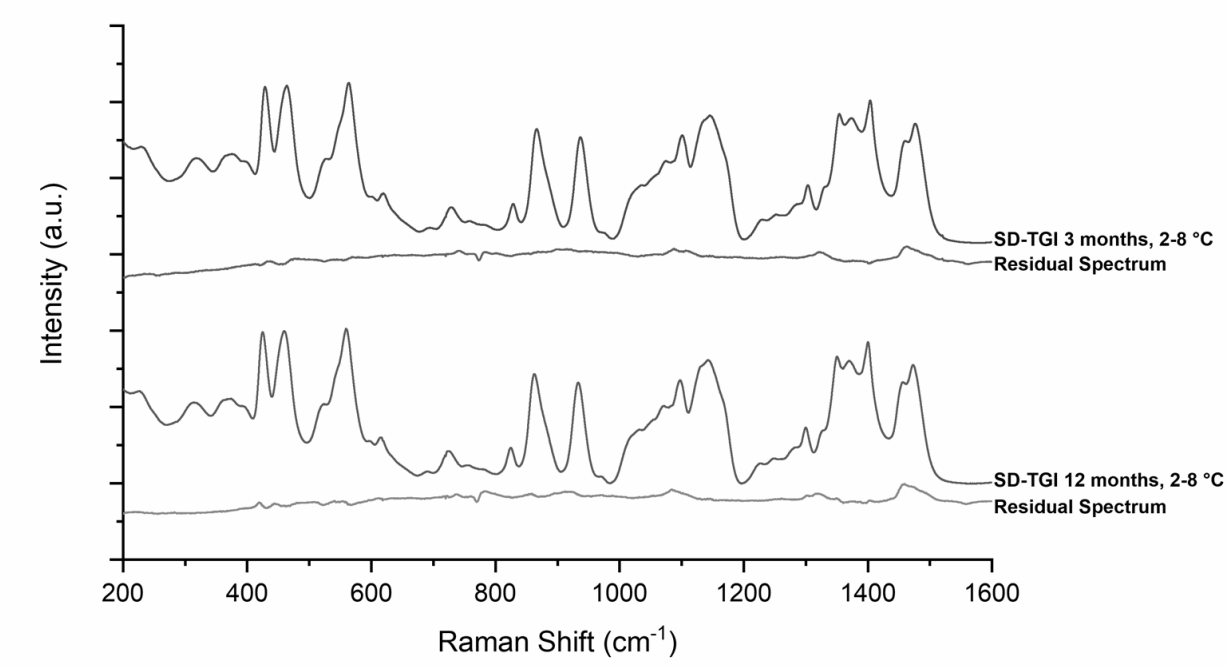

Figure A6 Normalized Raman spectra of the SD-TGI powder formulation, shown after three and twelve months of storage at 2-8 °C. Also shown is the respective residual spectrum obtained from deconvolution. The low residual spectra indicate that the powder remains amorphous when stored at 2-8 °C for up to twelve months.

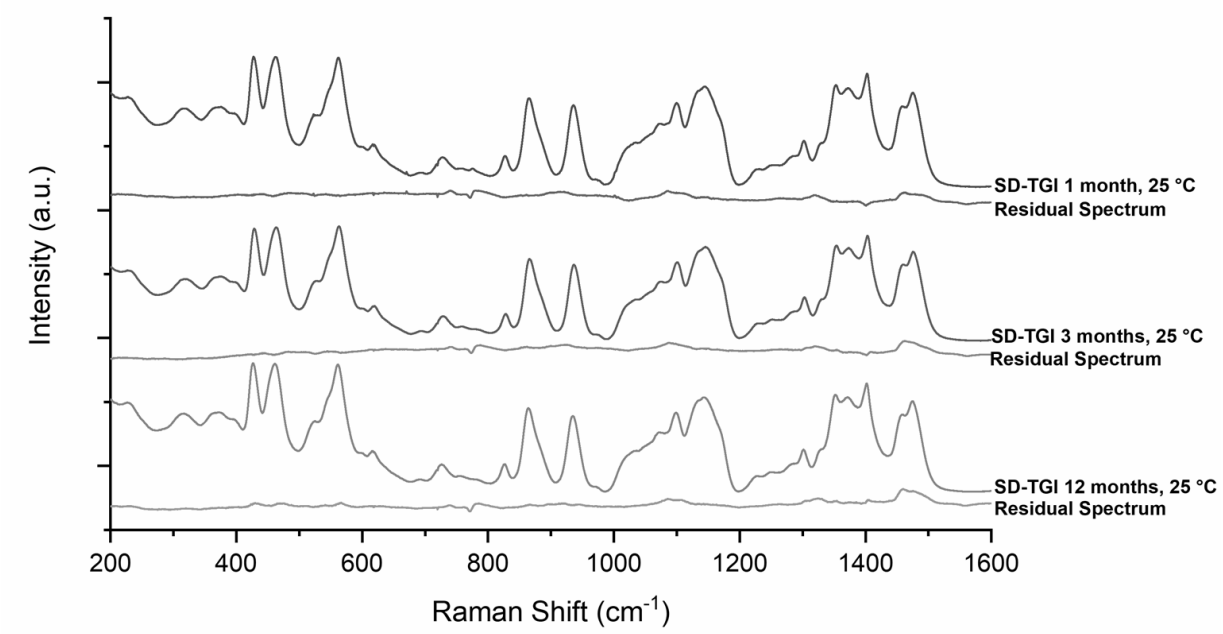

Figure A7 Normalized Raman spectra of the SD-TGI powder formulation, shown after one, three, and twelve months of storage at 25 °C. Also shown is the respective residual spectrum obtained from deconvolution. The low residual spectra indicate that the powder remains amorphous when stored at 25 °C for up to twelve months.

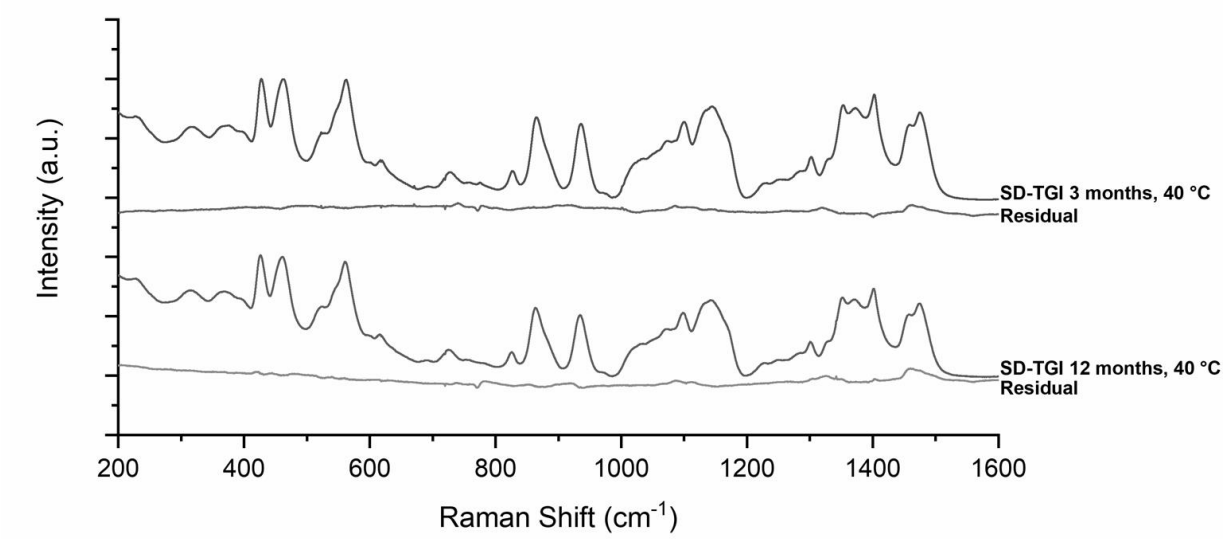

Figure A8 Normalized Raman spectra of the SD-TGI powder formulation, shown after three and twelve months of storage at 40 °C. Also shown is the respective residual spectrum obtained from deconvolution. The low residual spectra indicate that the powder remains amorphous when stored at 40 °C for up to twelve months.

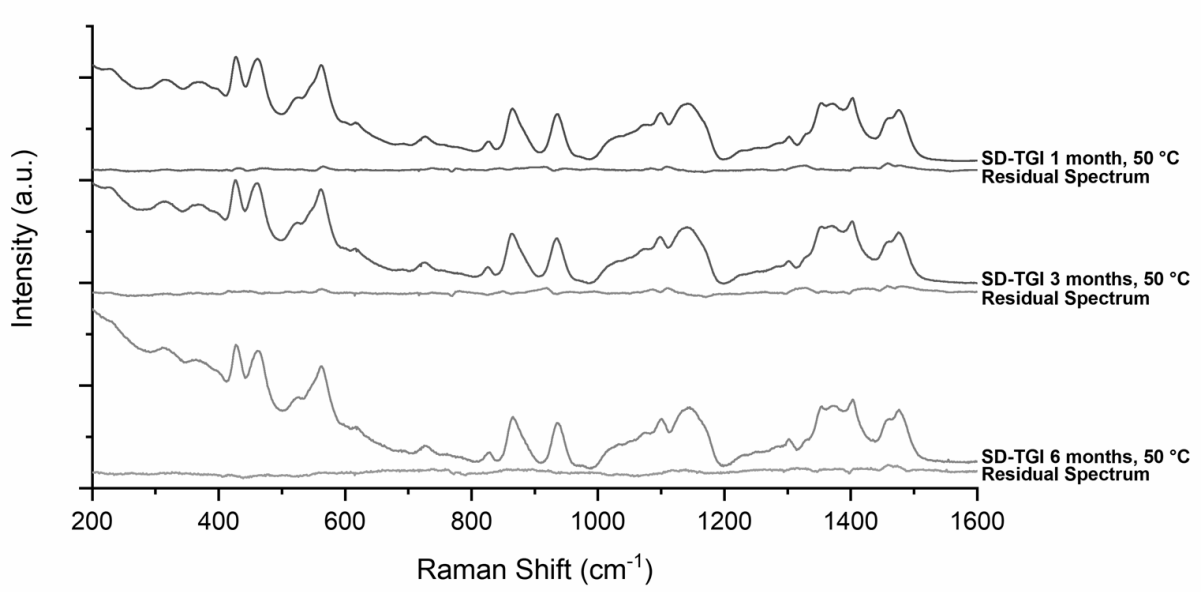

Figure A9 Normalized Raman spectra of the SD-TGI powder formulation, shown after one, three, and six months of storage at 50 °C. Also shown is the respective residual spectrum obtained from deconvolution. The low residual spectra indicate that the powder remains amorphous when stored at 50 °C for up to six months. Increasing background fluorescence over time suggests that the powder experiences some chemical degradation at 50 °C, however, the level of degradation cannot be quantified with this method.

A3. Powder Cohesiveness

Experiments were conducted on the SD-TG and SD-TGI powders to assess powder cohesiveness over the course of the stability study as part of the physical stability analysis. The method consisted of using a small-scale powder disperser (Model 3433; TSI, Shoreview, MN, USA) to aerosolize powder samples into a time-of-flight aerodynamic particle sizer (APS) (Aerodynamic Particle Sizer Spectrometer 3321; TSI, Shoreview, MN, USA). The APS device subsequently measured the particle size of the dispersed powder. However, results found that the disperser was unable to sufficiently disperse the powder into primary particles. Instead, partially dispersed particle aggregates were measured by the APS device. Increase in measured particle aggregate size would indicate that the powder was fusing together. Results indicate that the aggregate size remains similar over the course of the study.

Table A1 Measured $d_{a,50}$ of the SD-TG and SD-TGI formulation after partial dispersion at different timepoints throughout the stability study. Results shown are the average of five measurements ± standard deviation.

Measured $d_{a,50}$ of Aggregates (µm)					
Timepoint (Months)	**SD-TG**	**SD-TGI**			
	25 °C	**5 °C**	**25 °C**	**40 °C**	**50 °C**
0	8.8 ± 0.6	10.1 ± 0.6	10.1 ± 0.6	10.1 ± 0.6	10.1 ± 0.6
1	8.6 ± 0.4	N/A	N/A	N/A	N/A
3	N/A	10.2 ± 0.4	10.2 ± 0.2	10.6 ± 0.1	11.1 ± 0.3
6	N/A	N/A	N/A	N/A	10.9 ± 0.2
12	N/A	10.7 ± 0.3	10.8 ± 0.2	11.6 ± 0.6	N/A

Appendix B. Supplementary data from the stability study on the spray-dried vaccine designed for inhalable delivery

B1. Particle morphology

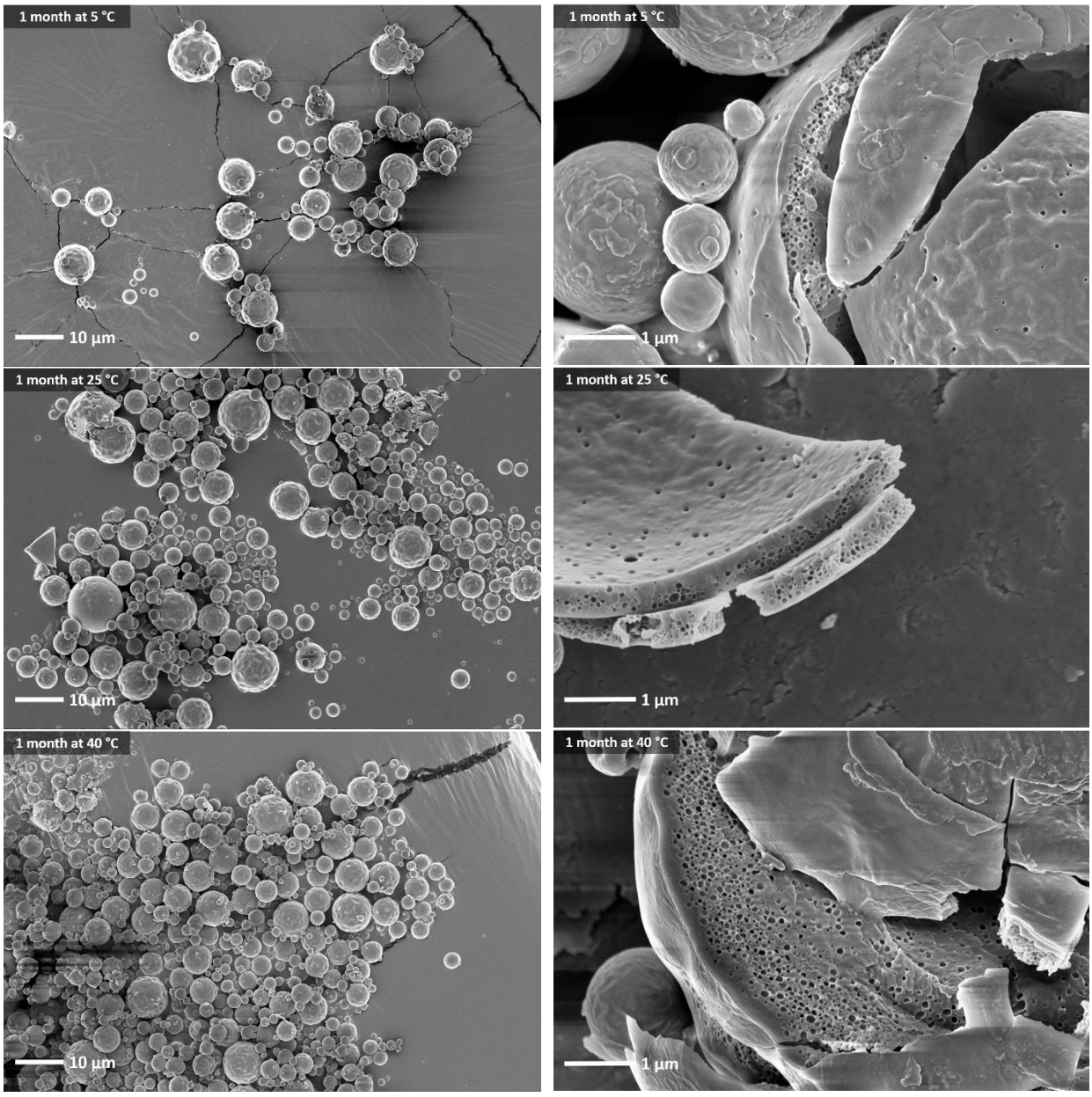

Figure B1 Low (left) and high (right) magnification SEM images of the Control formulation after one month of storage at 5, 25, and 40 °C. There is no discernible difference in particle morphologies at

the different temperatures, suggesting that after one month of storage the Control formulation's particle structure is maintained at all storage temperatures.

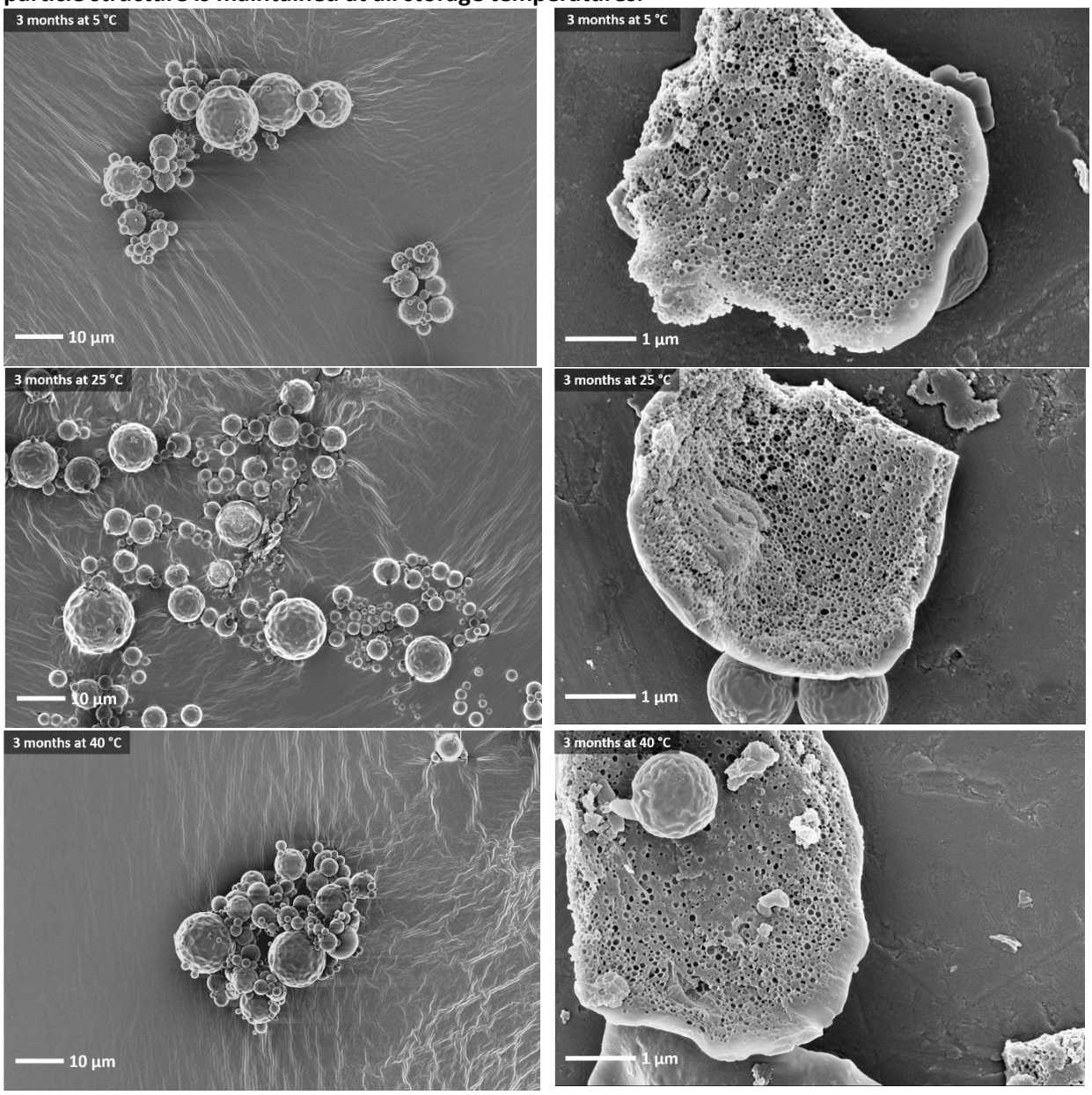

Figure B2 Low (left) and high (right) magnification SEM images of the Control formulation after three months of storage at 5, 25, and 40 °C. There is no discernible difference in particle morphologies at the different temperatures, suggesting that after three months of storage the Control formulation's particle structure is maintained at all storage temperatures.

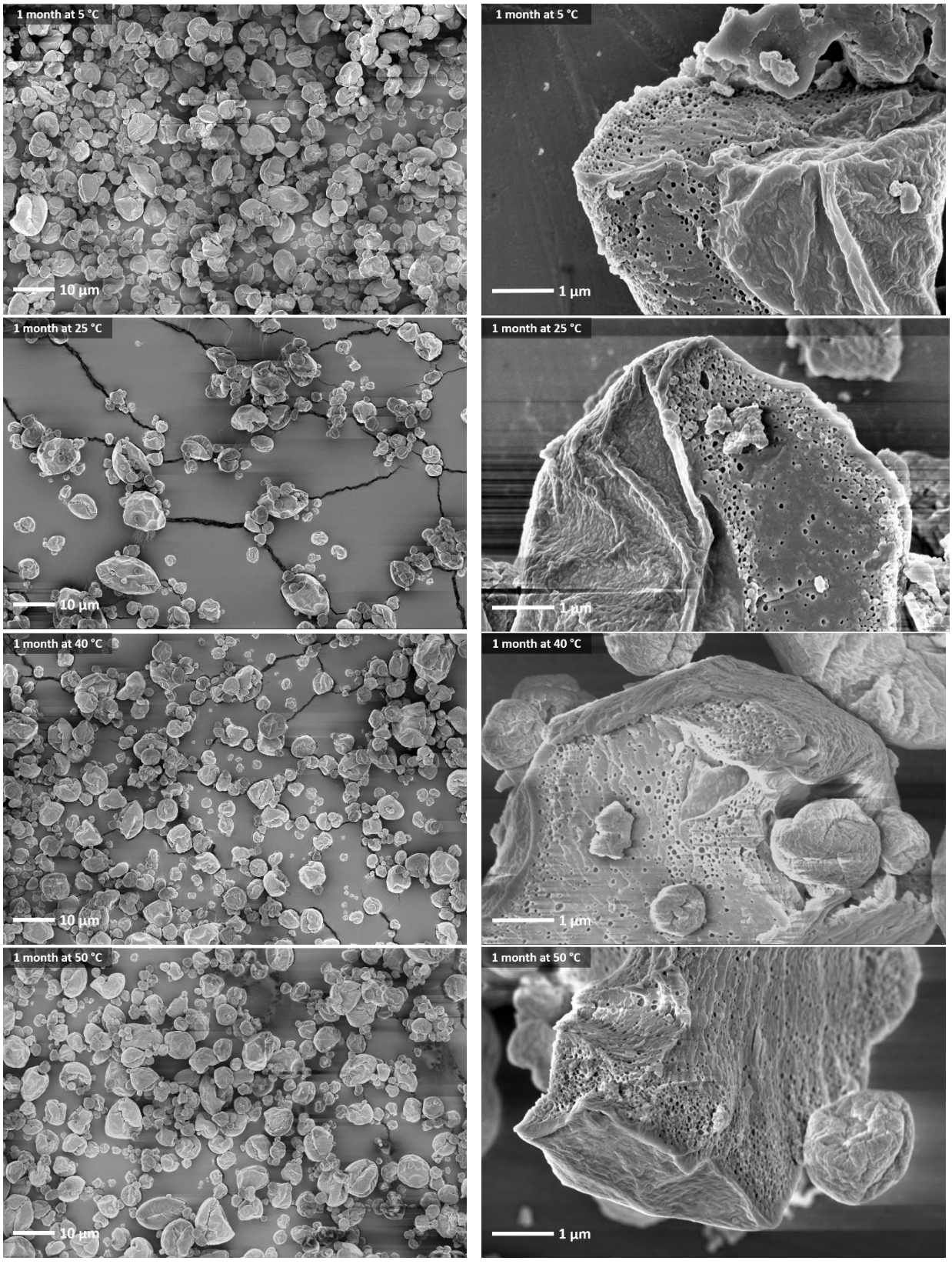
1 month at 5 °C
10 µm
1 month at 5 °C
1 µm
1 month at 25 °C
10 µm
1 month at 25 °C
1 µm
1 month at 40 °C
10 µm
1 month at 40 °C
1 µm
1 month at 50 °C
10 µm
1 month at 50 °C
1 µm

Figure B3 Low (left) and high (right) magnification SEM images of the Inhalable Vaccine formulation after one month of storage at 5, 25, 40, and 50 °C. There is no discernible difference in particle morphologies at the different temperatures, suggesting that after one month of storage the Inhalable Vaccine formulation's particle structure is maintained at all storage temperatures.

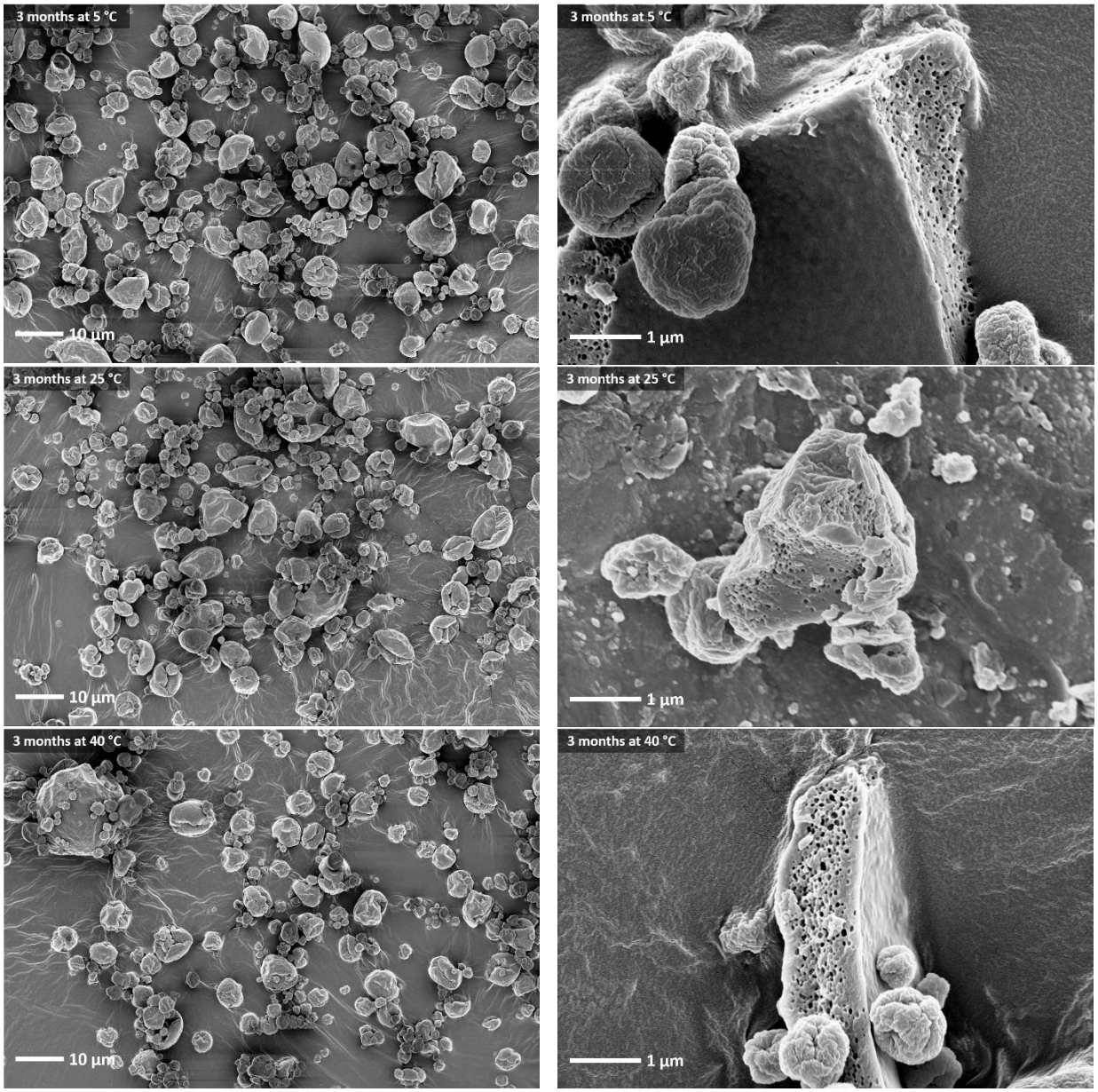

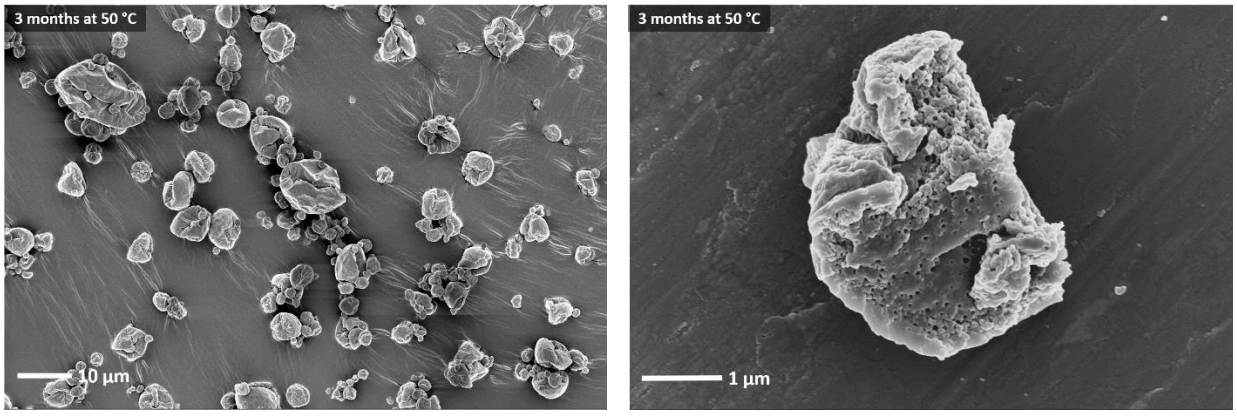

Figure B4 Low (left) and high (right) magnification SEM images of the Inhalable Vaccine formulation after three months of storage at 5, 25, 40 and 50 °C. There is no discernible difference in particle morphologies at the different temperatures, suggesting that after three months of storage the Inhalable Vaccine formulation's particle structure is maintained at all storage temperatures.

B2. Solid State Analysis

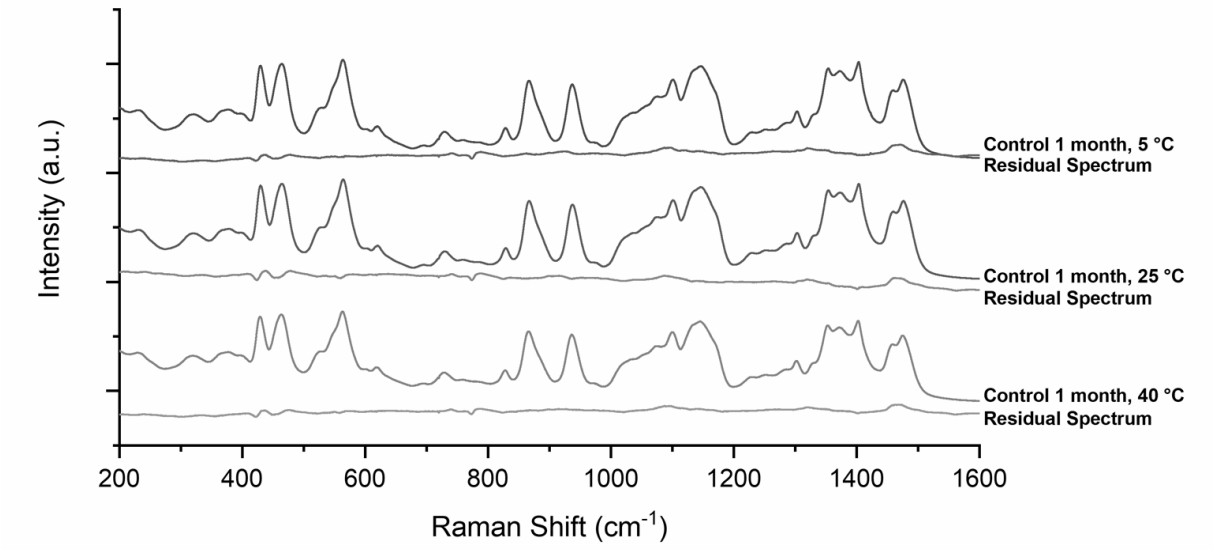

Figure B5 Sample spectra of the Control formulation after one month of storage at 5, 25, and 40 °C. The residual spectra obtained after deconvolution are given under the respective sample spectra. The low residual spectra indicate that the Control formulation remains amorphous at all storage temperatures after one month.

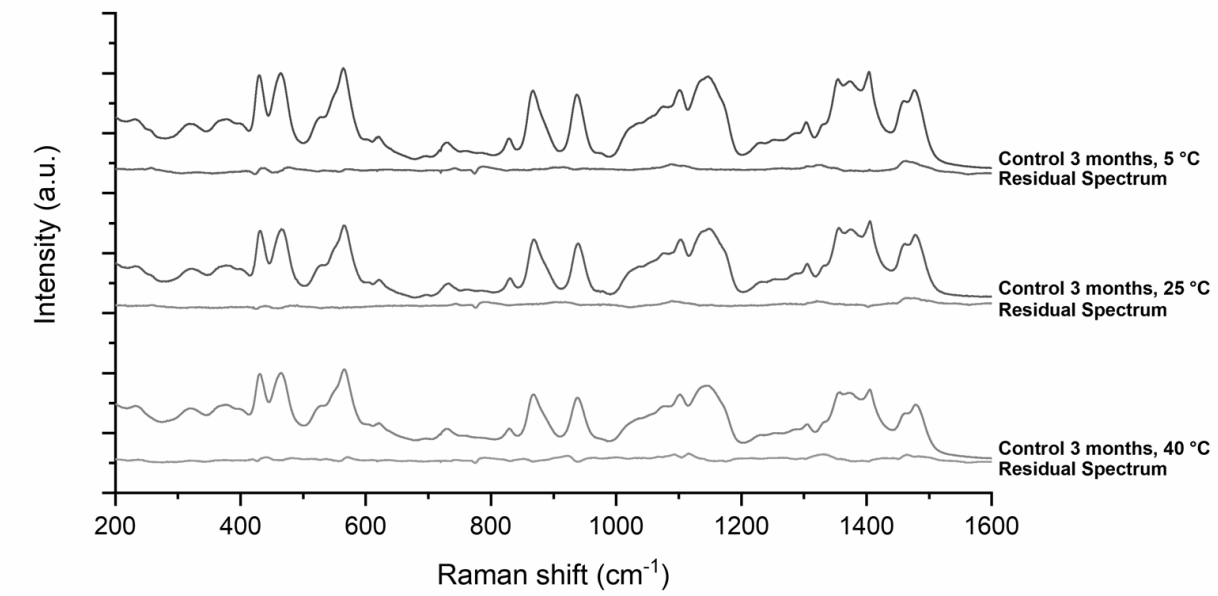

Figure B6 Sample spectra of the Control formulation after three months of storage at 5, 25, and 40 °C. The residual spectra obtained after deconvolution are given under the respective sample spectra. The low residual spectra indicates that the Control formulation remains amorphous at all storage temperatures after three months.

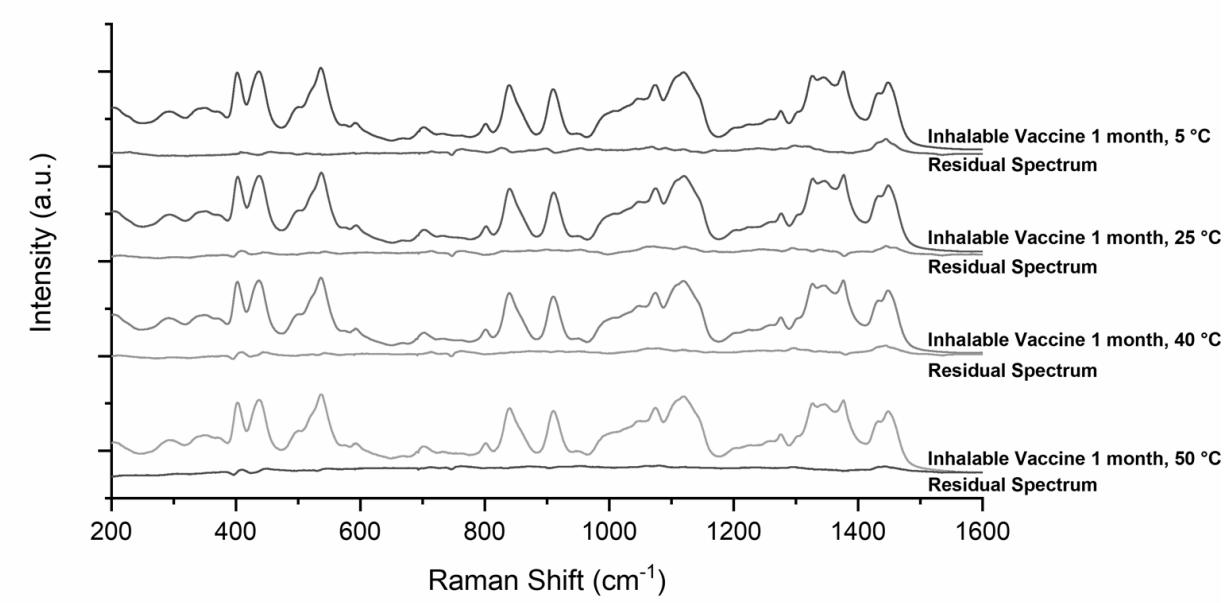

Figure B7 Sample spectra of the Inhalable Vaccine formulation after one month of storage at 5, 25, 40 and 50 °C. The residual spectra obtained after deconvolution are given under the respective sample spectra. The low residual spectra indicate that the Inhalable Vaccine formulation remains amorphous at all storage temperatures after one month.

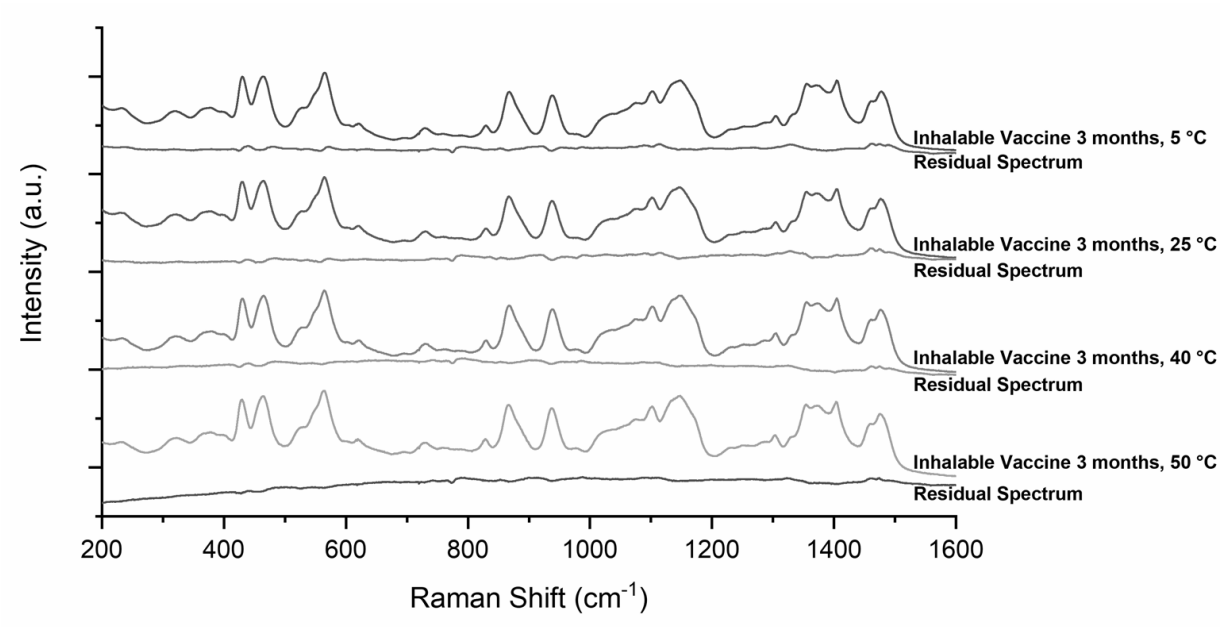

Figure B8 Sample spectra of the Inhalable Vaccine formulation after three months of storage at 5, 25, 40 and 50 °C. The residual spectra obtained after deconvolution are given under the respective sample spectra. The low residual spectra indicate that the Inhalable Vaccine formulation remains amorphous at all storage temperatures after three months.

B3. Powder Size Distribution

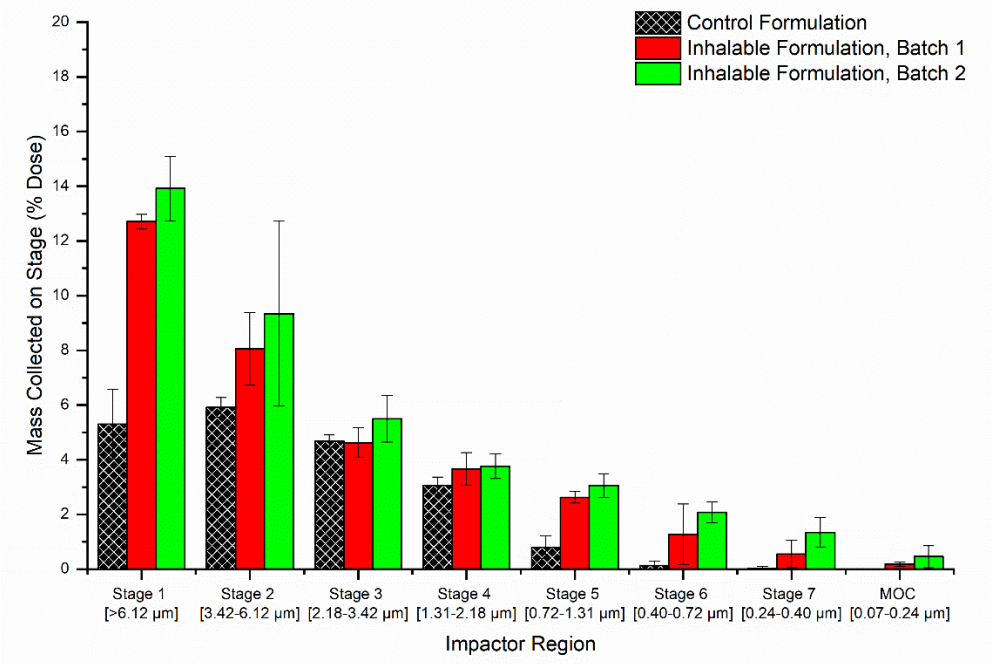

Figure B9 Mass distribution of the Control and Inhalable Vaccine formulations at timepoint 0. Greater overall stage deposition of the Inhalable Formulation demonstrates that trilueince improves aerosol performance. Similarity of Batch 1 and Batch 2 aerosol performance suggests that production of the Inhalable Vaccine is reproducible. Results shown represent the average of triplicate measurements. Error bars represent standard deviation.

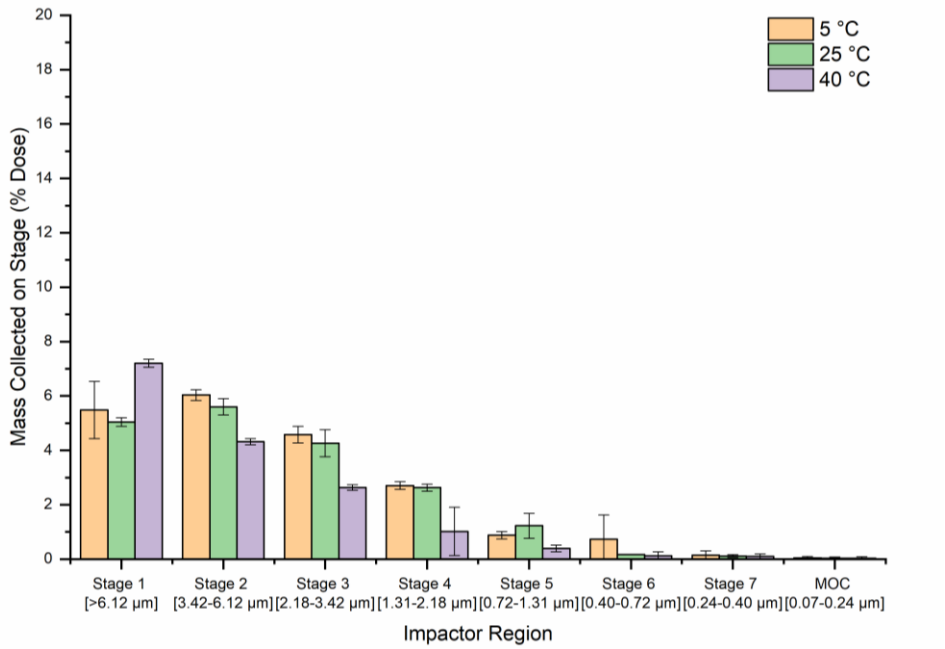

Figure B10 Mass distribution of the Control formulation after one month of storage at 5, 25, and 40 °C. After one month, the sample stored at 40 °C show decreased depositon with progressing stages. Results shown represent the average of triplicate measurements. Error bars represent standard deviation.

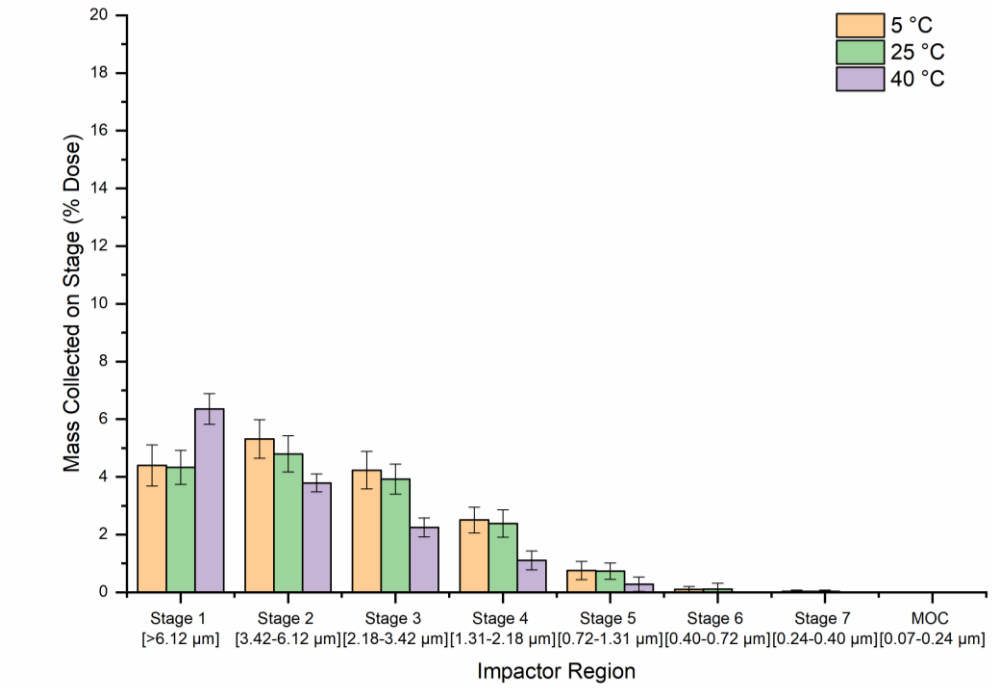

Figure B11 Mass distribution of the Control formulation after three months of storage at 5, 25, and 40 °C. After three months, the sample stored at 40 °C show decreased depositon with progressing

stages. Results shown represent the average of triplicate measurements. Error bars represent standard deviation.

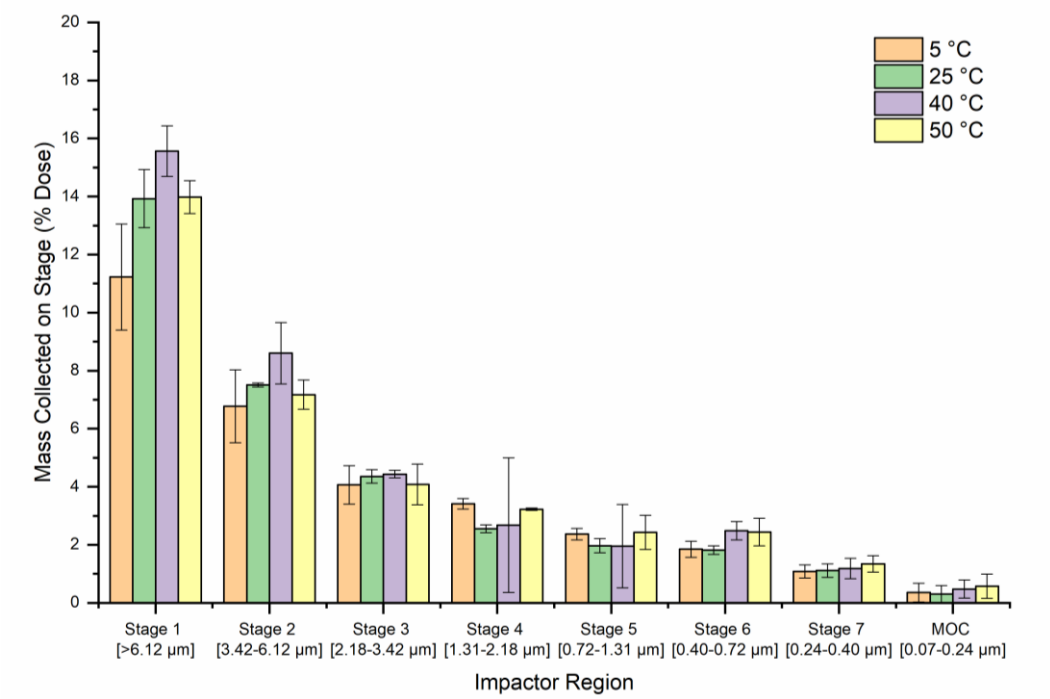

Figure B12 Mass distribution of the Inhalable Vaccine formulation after one month of storage at 5, 25, 40, and 50 °C. Similar stage deposition shown for all storage temepratures. Results shown represent the average of triplicate measurements. Error bars represent standard deviation.

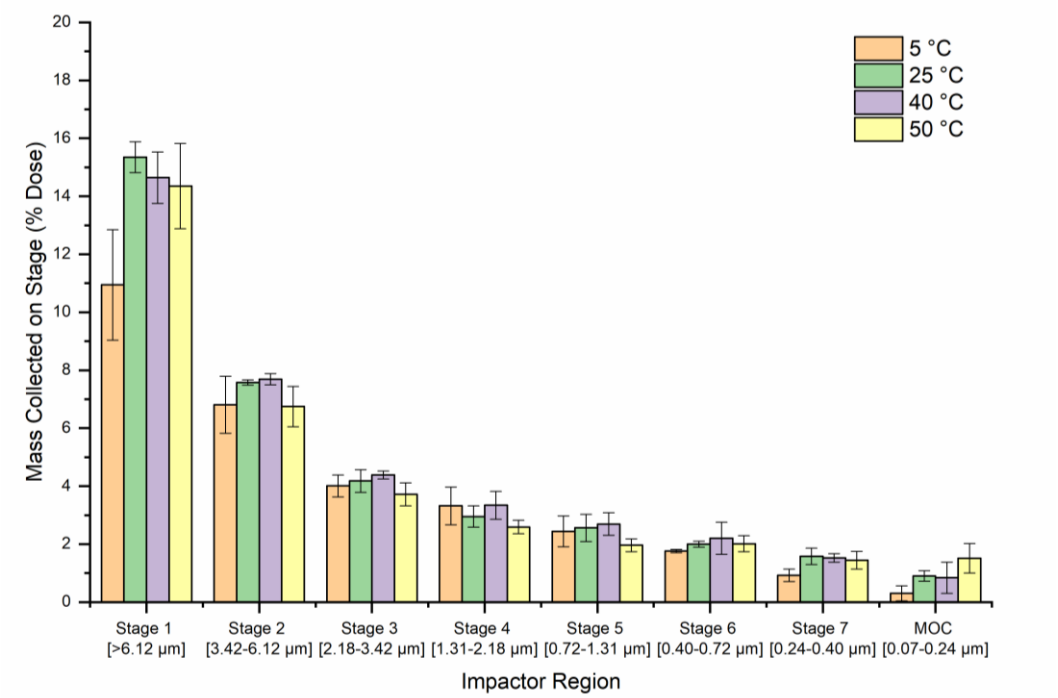

Figure B13 Mass distribution of the Inhalable Vaccine formulation after three months of storage at 5, 25, 40, and 50 °C. Similar stage deposition shown for all storage temepratures. Results shown represent the average of triplicate measurements. Error bars represent standard deviation.